DRAFT FOR COMMENT

DRAFT UCID

THE FINAL PROGRESS REPORT FOR THE SAN ONOFRE NUCLEAR GENERATING STATION UNIT 1 AUXILIARY FEEDWATER SYSTEM PROJECT

SEISMIC SAFETY MARGINS RESEARCH PROGRAM

T. Y. Chuang
L. E. Cover
B. J. Benda*
D. L. Bernreuter
J. C. Chen
J. J. Johnson*
D. A. Lappa
O. R. Maslenikov*
J. B. Savy
L. C. Shieh
S. N. Shukla
J. E. Wells

June 18, 1982

*Structural Mechanics Associates (SMA)

DRAFT FOR COMMENT

ABSTRACT

This final progress report describes the accomplishments of the San Onofre Nuclear Generating Station Unit 1 (SONGS-1) Auxiliary Feedwater System (AFWS) Project of the Seismic Safety Margins Research Program (SSMRP). The project was started on May 1, 1981 and terminated by the Nuclear Regulatory Commission (NRC) on January 29, 1982. This report also briefly presents the progress of this project.

The development of the structural and piping models for SONGS-1 was almost completed. Piping fragility data generation and fault tree development for the AFWS were completed. The synthetic time histories targeted to three spectra: the SONGS-1 seismic reevaluation spectra; SONGS Units 2 and 3 design spectra, and the average of the two, were generated. The SSMRP methodology was utilized to compute the seismic responses of the reactor building complex using these time histories as the seismic excitation. The seismic responses have been compared with the SONGS-1 seismic reevaluation results provided by the Southern California Edison Company (SCEC)/Bechtel Power Corporation. In general, the SCEC/Bechtel results enveloped the Lawrence Livermore National Laboratory's (LLNL's) results due to all three target spectra mentioned above. The only exception appears in the in-structure response spectra of several selected points in the reactor building. The LLNL's spectral accelerations in the low frequency range of these spectra due to SONGS Units 2 & 3 design spectra exceeded the SONGS-1 seismic reevaluation results. This effect may be interpreted as a result of the strong motions in the low frequency range of the SONGS Unit 2 & 3 design spectra. Significant progress toward the development of a seismic hazard curve for the SONGS site and the time histories (associated with this hazard curve) required for the probabilistic study of the SONGS-1 has been made. Substantial progress has also been made toward the generation of structural fragility curves. All the design data and drawings obtained from SCEC and the computer files generated by LLNL and its subcontractors are stored in a retrievable manner.

TABLE OF CONTENTS

DRAFT FOR COMMENT

DRAFT FOR COMMENT

ACKNOWLEDGMENTS

We would like to express our appreciation to the Southern California Edison Company (SCEC) and Bechtel Power Corporation for providing the necessary design data and drawings, as well as the opportunities to visit the San Onofre site. We especially extend our thanks to Mr. R. C. Blaschke, Project Engineer of SCEC for his efforts to coordinate the project with Bechtel Power Corporation, SCEC, and the Lawrence Livermore National Laboratory (LLNL) staff and its subcontractors.

We extend special thanks to Dr. P. D. Smith, Associate Program Leader of Seismic and Structural Safety of LLNL's Nuclear Systems Safety Program, Dr. M. P. Bohn, Program Manager of the Seismic Safety Margins Research Program, and Dr. R. T. Langland, Section Leader of the Engineering Mechanics Section, Nuclear Test Engineering Division of LLNL's Mechanical Engineering Department, for their helpful critical review of the report. We are grateful to Dr. D. H. Chung for his contribution to the development of the earthquake occurrence and ground motion models (Appendix C), and to Mr. S. M. Pratuch for his assistance in developing the auxiliary feedmeter (AFW) piping models. We appreciate the support of the LLNL Nuclear Safety Systems Program Office, Mechanical Engineering Department, Nuclear Test Engineering Division, Engineering Mechanics Section, Methods Development Group and Statistics and Probability Group.

Over the course of our work, our secretaries, Ms. Sue Aubuchon, Ms. Virge Jaramillo, Ms. Terry Patters, Ms. Marilynn Govenor, and Ms. Claudia Ambrose, and Director's Office Correspondence Center's Word Processing Specialist, Sandy Auguadro were indispensable and their efforts are deeply appreciated. We also wish to acknowledge the effort of LLNL technical information specialist, Ms. Carol Meier, who has helped with the editing of this report and produced the draft in a timely and orderly fashion.

The LLNL's Project Manager is Dr. T. Y. Chuang who has the full responsibility for managing the project and would like to thank the project staff and LLNL's subcontractors. Finally, we wish to thank our NRC Project Manager, Mr. Roger M. Kenneally, and the office of Nuclear Reactor Regulatory (NRR) Technical Monitor, Mr. K. S. Herring, who provided guidance and support to this project.

This work was supported by the United States Nuclear Regulatory Commission under a Memorandum of Understanding with the United States Department of Energy.

SECTION 1: INTRODUCTION

The seismic qualification requirements for the auxiliary feedwater systems (AFWS) of Pressurized Water Reactors (PWR's) were developed over a number of years. These requirements are formalized in the publication, General Design Criteria, Appendix A to Title 10 of the Code of Federal Regulation (CFR) Part 50. Guidance for the implementation of these requirements was published in 1972 as Regulatory Guide 1.26 (Quality Group Classifications and Standards for Water, Steam, and Radioactive Waste Containing Components of Nuclear Power Plants) and as Regulatory Guide 1.29 (Seismic Design Classification). Although both guides identified that the AFWS is important to safety and required protection against a seismic event, the full recognition of the AFWS as an engineered safety feature (ESF) did not occur until publication of the Standard Review Plan (SRP) in 1975. Efforts to determine how to backfit seismic requirements to earlier PWR plants have been undertaken primarily in the Systematic Evaluation Program (SEP) for a limited number of operating PWR's.

The Three Mile Island Unit 2 (TMI-2) accident in 1979 further focused attention on the importance of decay heat removal systems in general, and on the AFWS in particular. The Nuclear Regulatory Commission's (NRC's) Office of Nuclear Reactor Regulation (NRR) has developed and implemented several short-term improvements related to the AFWS, via the Bulletins and Orders Task Force, Lessons Learned Task Force, through the Division of Licensing. In the course of the development of the TMI-2 Action Plan it was concluded that these short-term changes were sufficient until a comprehensive, three-year study of decay heat removal system requirements was completed (TMI-2 Action Plan Items II.E.3.1, II.E.3.2, II.E.3.3, and II.E.3.4). However, the seismic qualification of the AFWS was not directly addressed by the above Task Forces, and thus this area remained a potential safety issue for the PWR plant operation during the period of time needed to complete the Action Plan studies and any subsequent modifications. In July, 1980, the NRC staff completed a brief risk study[1] of seismically induced loss-of-decay heat removal for plants without a seismically qualified AFWS. The review[2] of this risk study was completed by the Lawrence Livermore National Laboratory (LLNL) and concluded that a more detailed study should be conducted. Based on the results of this brief study and until a more detailed study is available, NRC decided to permit continued operation of PWR plants without the AFWS qualified for current standards (i.e., R.G. 1.26, R.G. 1.29, R.G. 1.60 and etc.). This decision reflects, in part, the consideration to preserve the continuity of the SEP and the TMI-2 Action Plan which may call for changes in the area of decay heat removal. It is not desirable to implement unnecessary or marginally necessary changes while these more comprehensive programs are underway.

In December, 1980, the Office of Nuclear Reactor Research (RES) requested[3] that LLNL develop a work plan[4] for a probabilistic study on the AFWS and its related systems for the San Onofre Nuclear Generating Station Unit 1 (SONGS-1) utilizing the tools developed by the Seismic Safety Margins Research Program (SSMRP).[5] Hereafter, the "AFWS" may be loosely referred to as the AFWS and its related systems: condensate storage system; electric power; auxiliary steam supply; and service water and fire protection system. The work plan was approved by NRC on May 1, 1981, and the SONGS-1 AFWS Project was formally established.

The SONGS-1 is a three-loop PWR plant and the net electric output is 436 MWe. The nuclear steam supply system (NSSS) was provided by the Westinghouse Corporation. The plant is jointly owned by the Southern California Edison Company (SCEC) and the San Diego Gas and Electric Company. It was designed and constructed by Bechtel Power Corporation in the 1960's, and located at San Onofre (about halfway between Los Angeles and San Diego), California. The operation of the plant began in January, 1968. The original seismic design criteria was based on a 0.5 g Housner spectra for the design basis earthquake (DBE). The plant is included in the SEP study and has been reevaluated for a criteria based on a 0.67 g modified Housner spectra.

The objectives of the SONGS-1 AFWS project were as follows:

- To evaluate the conservatism in the SCEC/Bechtel seismic reevaluation program.

- o To provide input to NRC licensing decisions on SONGS Unit 1 for the Balance of Plant Seismic Reevaluation Program (BOPSRP).
- o To assist the NRC in addressing the generic issue of the seismic qualification requirements for AFWS.

In order to accomplish these objectives, the following approaches are taken as part of the SSMRP:

- o Compare the seismic responses of structures and piping systems of the AFWS due to different target spectra and the SONGS-1 seismic reevaluation values provided by SCEC/Bechtel.
- o Identify the weak links of the AFWS of SONGS Unit 1.
- o Compare the probability of failure of the AFWS of Zion Unit 1 with SONGS Unit 1.

A parallel NRR effort which will determine the seismic qualification level of the AFWS of all operating PWR's, is currently being conducted at LLNL. This effort is a part of NRC Multiplant Action Plan C-14 whose goals are:

- o Identify deficiencies amenable to simple remedial actions.
- o Survey the plants to determine the extent and areas where significant improvements may be needed.
- o Complete re-analysis and/or modifications for those plants that do not have an AFWS with demonstrated reasonable assurance of functioning following a safe shutdown earthquake (SSE).

The SSMRP methodology was to be applied to the Zion Unit 1 and SONGS Unit 1 auxiliary feedwater systems in the same level of detail. Steps in the methodology can be broadly outlined as follows:

- o Definition of the earthquake hazard and generation of time histories.
- o Calculation of plant response by the SMACS (Seismic Methodology Chain with Statistic) program[6], which entails calculation of soil-structure interaction (SSI), the responses of structures, and the responses of subsystems, e.g. piping systems.
- o Evaluation of failure, which requires definition of the fragilities of structures, components, and systems, and a description of the operation and interaction of components within the AFWS.

DRAFT FOR COMMENT

One of the basic assumptions of the work plan was to utilize the SONGS-1 seismic design modifications existing at the time the work plan was prepared. As the work progressed, however, new modifications to the turbine and fuel storage building and their foundations were identified, and were also incorporated in accordance with an NRC request during the site visit in June, 1981. This caused a significant delay in completing the project.

On January 29, 1982, the analysis effort was terminated by NRC, because it became only marginally cost-effective to complete the analysis due to constraints imposed by NRC licensing schedules.

This report documents the accomplishments of the project at the time that the analysis was terminated. The format used in this report closely follows that of the quarterly progress reports issued throughout the project.

This report contains four sections. In addition to Section 1 which contains the introductory material, Section 2 briefly describes the individual tasks which comprise the SONGS-1 AFWS project. Section 3 contains information regarding the accomplishments under each task, and Section 4 includes milestone charts and descriptions. Three appendices have also been employed to provide detailed results documenting the various task accomplishments. Appendix A describes in detail the structural response comparison of the containment sphere and reactor building. Appendix B detailed the fault tree development effort. Finally, the remaining incomplete tasks are elaborated in Appendix C which provides the development of piping models, earthquake occurence model, ground motion model, beta-factor for pipe component and structural fragilities.

SECTION 2: TASK DESCRIPTIONS

Seven major tasks, designated I through VII, were identified for the SONGS-1 AFWS Project. Each of these tasks is described in the following:

Task I—Develop the Models for Response Computation

Task I develops the models for soil, structures, soil-structure interacton (SSI) and auxiliary feedwater (AFW) piping systems. Existing models furnished by SCEC will be carefully studied to evaluate their efficiency. If it is determined to be too inefficient to use the existing models due to, for instance, the differences in computer programs, new models will be developed. For the portion for which SCEC does not have existing models, new models will have to be developed. There are four subtasks, which are described below.

Task I.1—Develop Soil Model

Obtain and evaluate soil data for SONGS Unit 1. Equivalent linear soil properties for system analysis will be estimated.

Task I.2—Develop Structural Models

Obtain, evaluate, and rerun the structural models furnished by SCEC/Bechtel. The structural models for the SMACS analysis will be prepared. The structural models will then be benchmarked against the models developed by SCEC/Bechtel. Fixed-base eigenvalue analysis will be performed for model comparison.

Task I.3—Develop Soil-Structure Interaction Models

The impedances and scattering matrices for soil conditions in the coupled soil-structure system analysis will be generated. The SSI models for SMACS analysis will then be prepared.

Task I.4—Develop the Models of the AFWS Piping System

Obtain the piping models for the AFWS from SCEC. Evaluate and rerun these models. Create new models if necessary, e.g., the portion of the AFWS not recently modified, since the SCEC may not have existing models for this portion. Identify the support points in the structures of these models in order to provide the input motions to the AFW piping systems.

Task II—Compare the Seismic Responses of Structures and Piping Systems of the SONGS-1 AFWS with the Seismic Reevaluation Results

Task II is to compare the seismic responses of structures and piping systems of the AFWS due to three different target spectra and the seismic reevaluation results furnished by SCEC. The three target spectra are:

1. SONGS Unit 1 seismic reevaluation (modified Housner) spectra.
2. The design (modified Newmark & Hall) spectra for SONGS Units 2 and 3.
3. An average spectra of the above two.

A set of synthetic time histories for each spectra will be generated. The analyses of soil-structure interaction (SSI) analysis, structure housing the AFWS, and the AFW piping systems will be performed using SMACS. The seismic responses of the structure and piping systems will then be computed. These results will be compared with the seismic reevaluation results furnished by SCEC. This task has four subtasks, which are described below.

Task II.1—Develop Seismic Input Time Histories for Different Target Spectra

A set of time histories will be generated for each target spectra as mentioned above. The response spectra of the time history will envelop their target spectra, respectively.

Task II.2—Compute Seismic Responses of Structures due to Different Target Spectra

The seismic responses of structures will be computed for each target spectra as described above. The input motions for the AFW piping support locations will also be computed.

Task II.3—Compute Seismic Responses of the AFW Piping Systems due to Different Target Spectra

The input motions from the structures supporting the auxiliary feedwater (AFW) piping systems will be imposed on the AFW piping models. The multisupport time history analysis techniques will then be utilized to compute the seismic responses of the AFW piping systems for each input target spectra as described above.

DRAFT FOR COMMENT

Task II.4--Compare the SMACS Results of Structures and Piping Systems with Seismic Reevaluation Results

The results computed in Tasks II.2 and II.3 will be compared with the seismic reevaluation results furnished by SCEC/Bechtel. This comparison will estimate the conservatism in the reevaluation analysis which was based on the 0.67 g modified Housner spectra.

Task III--Develop the SONGS Site Specific Seismic Hazard Curves, Spectra and Time Histories

In this task, the seismic input required for both the systems analysis (SEISIM) and structural analysis program (SMACS) will be developed. SEISIM, Seismic Evaluation of Important Safety Importance Measure, requires (as one of its inputs) the annual exceedance probability of any level of peak ground acceleration at the SONGS site. SMACS, Seismic Methodology Analysis Chain with Statistics, requires (as input) sets of time histories which are correlated with the hazard curve used in SEISIM. To develop this required input, it is necessary to first develop an earthquake occurrence model which gives the locations of the earthquake relative to the SONGS site and rate of occurrence of various magnitude earthquakes. Along with the earthquake occurrence model, a ground motion model is also required to predict the ground motion at the SONGS site from an earthquake of a specific magnitude located at a specific distance from the site. The earthquake occurrence model and ground motion model are then incorporated into the hazard analysis program (HAZARD) to generate the required input for SEISIM and SMACS. Three subtasks are defined and outlined below.

Task III.1--Develop the Earthquake Occurrence Model for the SONGS Site

A range of earthquake occurrence models will be developed using both the extensive geologic and seismological investigation carried out by SCEC. The SCEC investigations will provide the basic zonation. Also a brief literature review will be conducted to develop a range of alternative models. Rates of occurrence will be estimated using both LLNL and SCEC data. Largest earthquakes will be estimated using several approaches based on fault length, strain rate, and so on.

Task III.2--Develop the Ground Motion Model for the SONGS Site

Ground motion models will be developed to account for the saturation of the magnitude scale based on such parameters as seismic moment, stress drop, and surface wave magnitude. In addition to source modeling, statistical analysis will be performed to establish reasonable bounds for correction factors. These will then be applied to generic ground motion models to account for focusing of seismic energy from nearby earthquakes. The models will represent an extension of a project underway at LLNL for RES and an analysis of near source ground motion. In addition to these model other ground motion models will also be used.

Task III.3—Develop Hazard Curves and Time Histories for the SONGS Site

The HAZARD program developed in Phase I of the SSMRP will be used to develop the seismic hazard and spectra at the SONGS site using the earthquake occurrence and ground motion models. Sensitivity studies will be carried out to determine which faults contribute most to the seismic hazard. This information will be used to improve the model and reduce the uncertainty in the estimates. Time histories will be generated from the spectra developed from the improved model using the SIMQKE[7] program developed by the Massachusett Institute of Technology (MIT).

Task IV--Develop the AFWS Fault Tree

Task IV generates the fault tree for the AFWS of SONGS Unit 1. This task will also modify the AFWS Fault tree of Zion Unit 1 to be comparable to SONGS Unit 1. The fault tree of the Zion-1 AFWS was trimmed down considerably due to the size limitation of the SEISIM program, because there were other systems (e.g., residual heat removal, safety injection, and etc.) included in the systems analysis. Since the AFWS is the only system considered in this project, the level of the details of the Zion-1 AFWS fault tree could be expanded. There are two subtasks for this task.

Task IV.1—Develop Fault Tree of SONGS-1 AFWS

The fault tree for the AFWS, including water supply to AFW pumps, electric power buses, AFW pump discharge to steam generators, and the auxiliary steam supply to AFW pump turbine will be generated. The fault tree will be analyzed to minimize the cut sets. The human and maintenance failure data, and fragility related basic event listings will also be generated.

Task IV.2—Modify the Fault Tree of the AFWS of Zion Unit 1

The AFWS fault tree for Zion Unit 1 will be modified to be comparable to the one for SONGS Unit 1. The fault tree of the auxiliary steam supply to the AFW pump turbine will be developed. These fault trees will be analyzed for the input to SEISIM program.

Task V—Develop Fragility Data and Coordinate with Fault Tree

Task V develops the fragility curves of the structures and the beta-factors of the specific pipe sizes for the SONGS Unit 1 AFWS. The fragility data for electrical and mechanical components of Phase I of the SSMRP (which are generic in nature) will be used to the maximum extent. The fault tree will be coordinated with the responses of the electrical and mechanical components and the AFW piping systems. There are four subtasks as described below.

Task V.1—Develop the Fragility Curves for the Structures Housing the AFWS

Using loads computed in the structures as part of Task II.2, the load paths, critical wall shear loads and collapse mechanisms will be examined to determine the most likely modes of failure and corresponding fragility curves. These curves will include inelastic energy absorption through consideration of ductility factors. The building design specifications will also be examined for any potential local failures which might affect critical AFWS components.

DRAFT FOR COMMENT

Task V.2—Develop the Beta-factor for the Pipe Components of the AFWS

Piping failure probability is determined by scaling the computed (SMACS) response appropriately and then compared with a single master fragility curve. These scale factors (the beta-factors) must be determined for all pipe sizes. A large number of these factors have already been derived for those pipes in the Zion Unit 1. However, some additional factors will have to be developed for pipe sizes in SONGS-1 which were not needed in the Zion Unit 1 analysis.

Task V.3—Coordinate the Electrical and Mechanical Components of the AFWS with Fault Tree and Structure Responses

The location of the components (or groups of components) for each basic event identified on the fault trees developed in Task IV.1 will be determined from either piping and instrumentation diagrams (P & ID's) or plant inspection, and then a table correlating all these components with their locations and fragility categories will be prepared. The minimum set of responses sufficient to provide the necessary SEISIM input for all the basic events will be identified and correlated with the components on the fault trees.

Task V.4—Coordinate the Responses and Fault Tree of the Songs-1 AFWS

Coordinate the seismic responses and fault tree of the Songs-1 AFWS. The beta-factor technique developed in Phase I of the SSMRP will be used to normalize the responses, i.e., resultant moments of pipes. Only those valves or pipe components identified in the fault tree of the AFWS will be analyzed.

Task VI—Identify the Weak Links of the AFWS

Task VI computes the probabilities of failure of the AFWS of SONGS Unit 1. The responses of structures and AFW piping systems will be computed by SMACS. The probabilities of failure of the AFWS will be computed by the SEISIM program. The weak links of AFWS will then be identified. There are two subtasks, as described below.

Task VI.1—Compute the Seismic Responses of Structures and Piping Systems of the AFWS

The responses of structures and AFW piping systems will be computed over a range of earthquake time histories developed in Task III.3. These responses will be coordinated with the basic events of the fault tree of the AFWS. SMACS will be used to generate the response corresponding to its basic event as an input to SEISIM.

Task VI.2—Compute the Probabilities of Failure of AFWS and Identify the Weak Links

The hazard curves, SMACS's responses, fragility data and fault tree will be incorporated into the SEISIM program. The probabilities of failure of the SONGS-1 AFWS will be computed. The initial dominance ranking will be produced, and additional dominance measures will be generated. The risk contributors to the failure of the AFWS will be ranked to identify the weak links of the AFWS of SONGS Unit 1.

Task VII—Compare the Probabilities of Failure of the AFWS Between SONGS-1 and Zion-1

The probabilities of failure of the AFWS of Zion Unit 1 will be computed. The initial dominance ranking will be produced and additional dominance measures will be generated. The risk contributors to the failure of the AFWS will be ranked to identify the weak links of the AFWS of Zion Unit 1. These results will be compared to the results for SONGS Unit 1.

SECTION 3: TASK ACCOMPLISHMENTS

PROJECT MANAGEMENT AND DATA RETENTION

The LLNL staff was instructed by NRC to terminate the analytical effort related to the SONGS Unit 1 AFWS at the end of January, 1982. All pertinent information was filed in a retrievable manner. The following controls have been employed to assure that efficient retrieval can be accomplished:

1. All published documents are retained in the LLNL Technical Information Department Library.

2. Aperture cards of the design drawings obtained from Southern California Edison Company and Bechtel Power Corporation are retained in the LLNL Mechanical Engineering Department Library in a permanent print file.

3. Essential computer program and data files are being retained in an indexed tape library file at the LLNL Computer Center.

4. History and correspondence files are being retained in storage at the LLNL Forms and Records Office.

The accomplishments for each subtask (until the project was terminated) are summarized, with supportive details either referenced in published documents or included in the appendices of this report, as follows.

TASK I.1 - SOIL MODEL DEVELOPMENT

The purpose of this task was to obtain and evaluate soil data for SONGS-1. Nominal soil properties (shear modulus and material damping) and their variability were estimated. Major effort was concentrated on the 0.67 g excitation level. The 0.67 g excitation level was of interest for two reasons: to compare seismic responses of structures and AFW piping systems with the seismic reevaluation result; and as one excitation level for the probabilities analysis of the SONGS-1 AFWS. The results of the 0.67 g excitation level, in conjunction with selected analyses at other excitation levels, were extrapolated to estimate soil properties over the entire range of excitations for the risk analysis. A number of sensitivity studies were performed (e.g., variation in soil material damping with bearing pressure, shear modulus degradation with increasing strain level, etc.). The soil properties were used to develop the SSI models. Appendix A provides more details on the development of soil models.

TASK I.2 - STRUCTURAL MODELS DEVELOPMENT

Structural models development proceeded in several steps beginning with the initial examination of the structural drawings, proceeding to coding and debugging of the model, eigenvalue extraction of the fixed-base structure, preliminary stress analysis for fragility assessment, independent review and ending with a benchmark comparison of the model with SCEC/Bechtel results. Output requirements for later fragility, system, and subsystem analysis must be specified. Details of the SONGS-1 structure model development are given in Appendix A. A summary of the work follows.

1. Reactor Building Complex

The reactor building complex includes sphere enclosure building, containment sphere and reactor building. Each structure was modeled separately in accordance with the input requirements of SMACS. The sphere enclosure building model is completed through eigenvalue extraction of the fixed-base modes (as required for the SMACS analysis). The containment sphere model, including generation of preliminary stress information for assessing structural fragility, was completed. The reactor building model was completed through the stage of preliminary stress analysis for fragility assessment. Benchmarking the reactor building model with SCEC/Bechtel required extensive effort. The modeling details of the reactor building by SCEC/Bechtel were compared as closely as possible to permit a valid model comparison. The resulting fixed-base frequencies were compared and significant frequencies were within 15% of each other. Remaining differences in modal analysis results were attributed to differences in the modeling approach.

2. Turbine Building Complex

This building complex includes five separate structures, i.e., turbine pedestal, north and south turbine building extensions, and east and west feedwater heater platforms. They are interconnected on five foundations which also interconnect with the foundation of the fuel storage building. Three of these five structures, the turbine pedestal, the north turbine building extension, and the west feedwater heater platform, are of interest because they house a portion of the AFWS. Detailed models of these structures and the south turbine building extension were developed. The dynamic characteristics of the east feedwater heater platform are similar to the west feedwater heater platform, and the same model was used. These models reflect the latest design configurations at the time the project was terminated. The equipment loadings were specified by SCEC/Bechtel. All models were completed through the eigenvalue extraction stage.

DRAFT FOR COMMENT

3. Fuel Storage Building

Initially, a model reflecting the proposed design modifications to the fuel storage building was constructed and a modal (eigenvalue) analysis completed. However, further modification from SCEC/Bechtel required additional changes. These changes were incorporated into the model, but no modal analysis was performed. Finally, SCEC/Bechtel returned to the unmodified configuration. The information for roof decking of the fuel storage building will be required in order to change the modal to its unmodified configuration. Therefore, no progress on modal analysis was accomplished at the time the project was terminated.

4. Control-administration Building

The control-administration building model incorporated the latest set of floor and equipment loads supplied by SCEC/Bechtel. The model was completed through the eigenvalue extraction stage. An initial comparison was made with frequencies provided by SCEC/Bechtel; however, no progress was accomplished to reconcile the observed differences before the project was terminated.

TASK I.3 - SSI MODEL DEVELOPMENT

SONGS-1 soil-structure interaction (SSI) model development proceeded as follows.

1. Reactor Building/Containment Sphere

These two structures are supported on a partially embedded spherical foundation. Preliminary SSI models (impedances and scattering matrices) were generated for the 0.67 g excitation level. Evaluation of these preliminary results proceeded along several paths. The methodology was benchmarked against known analytical and finite element solutions of a full hemispherical foundation in a uniform half-space. Simpler cases were analyzed (e.g., rigid circular disk on a layered half-space and approximate solution procedures), and the results compared. A sensitivity study of the effects of soil layer discretization on the variation in impedances was made prior to selecting the final soil profile and discretization used. Final impedances and scattering matrices for the 0.67 g excitation reflect a finer soil discretization and frequency interval than the preliminary results. The preliminary values were smoothed to better match variations expected due to smooth soil variability. The results were used to compute the seismic responses of structures due to different target spectra.

2. Other Buildings

The remaining SONGS-1 structures of interest (except the control-administration building) are supported by a complicated, interconnected foundation. Although they are not connected through their super-structure, the five structures of the turbine building complex and the fuel storage building share portions of foundations resulting in a complex structural system. SSI models were developed for the turbine pedestal foundation, both anchor blocks, the fuel storage pool, and several column footings. Sensitivity studies of the spatial discretization of the foundation impedance models were conducted. Selection of the final model configurations was based on these studies. Appendix A describes in detail the work associated with this task.

TASK I.4 - AFWS PIPING MODELS DEVELOPMENT

This task was concerned with the development of models of the AFW piping systems. Fourteen dynamic piping models were developed. They are: nine models for the discharge piping of the auxiliary feedwater (AFW) pumps; one for the suction piping of the AFW pumps; two for auxiliary steam supply piping; and two for service water and fire protection piping. The natural frequencies and mode shapes for these fourteen piping models were computed. The support locations for the fourteen models were identified and coordinated with their location in the structure models in order to provide input motions to piping systems. These piping models and the analytical methods used are described in Appendix C.

TASK II.1 - SEISMIC INPUT TIME HISTORIES DEVELOPMENT

The goal of this task was to generate time histories for each of three target spectra: the SONGS Unit 1 seismic reevaluation spectra, the SONGS Units 2 & 3 design spectra, and the average of the two. Thirty sets of time histories (consisting of two horizontal components and a vertical component) were generated for these three target spectra. They are all anchored at 0.67 g zero period acceleration (ZPA) in the horizontal directions and 0.45 g ZPA in the vertical direction. Refer to Appendix A for details.

TASK II.2 - COMPUTATION OF SEISMIC RESPONSES OF STRUCTURES DUE TO DIFFERENT INPUT SPECTRA

The seismic responses of the structures were computed for the three target spectra described in Task II.1. Using the dynamic characteristics of the reactor building and containment sphere, and the impedance and scattering matrices for the partial spherical foundation; response analyses were performed for three cases of the free-field ground motion. The three cases corresponded to the three specified target spectra for the SONGS site. In each case, thirty sets of time histories defined the input motion. The time histories were targeted to the SONGS Unit 1 seismic reevaluation spectra, the SONGS Units 2 and 3 design response spectra, and the average of the two. In-structure response spectra at selected points were generated for comparison with SCEC/Bechtel seismic reevaluation results. Details of the response analyses are given in Appendix A.

DRAFT FOR COMMENT

TASK II.3 - COMPUTATION OF SEISMIC RESPONSES OF AFW PIPING SYSTEMS

This task had not been initiated at the time the project was terminated, because the piping systems are interconnected with different buildings and the structural and SSI models were not all completed.

TASK II.4 - COMPARISON OF THE SEISMIC RESPONSES OF STRUCTURES AND AFW PIPING SYSTEMS WITH THE SEISMIC REEVALUATION

The results of the SMACS analyses were compared with data generated by SCEC/Bechtel from a deterministic analysis. The latter used procedures and parameter values selected for seismic reevaluation. It was performed by SCEC/Bechtel with the SONGS Unit 1 seismic reevaluation spectra anchored to 0.67 g ZPA.

Comparison with the SMACS analyses using time histories whose spectra were targeted to the SONGS Unit 1 seismic reevaluation spectra, shows that the SCEC/Bechtel seismic reevaluation results envelop those of SMACS over the entire frequency range. The SCEC/Bechtel results also envelop and are significantly larger than the SMACS results computed using both the SONGS Units 2 and 3 design response spectra and the average spectra of SONGS-1 and SONGS 2 & 3 as seismic input definitions in the amplified frequency range. The exception only occurs in the lower frequency range where the SMACS results due to the SONGS Units 2 and 3 design spectra exceeded the SCEC/Bechtel SONGS Unit 1 seismic reevaluation results. Details of the comparison appear in Appendix A.

TASK III.1 - EARTHQUAKE OCCURRENCE MODEL DEVELOPMENT

Considerable progress was made on this task. A report on the assessment of active faults and maximum earthquakes of the Southern California-Northern Baja region that adjoins the SONGS site[8] has been completed. A study of the seismic activity rates using the earthquake history indicated that activity rates would have to be determined from estimates of the geological slip rate for the various faults. The required slip rates and the zones for the hazard assessment model were developed. Details of the earthquake occurrence model development are described in Appendix C.

TASK III.2 - GROUND MOTION MODEL DEVELOPMENT

To obtain improved estimates of the ground motion in the near-field, the effect of various schemes of weighting the near-field data were explored. Various scaling schemes were found and led to significant differences in the ground motion estimates, particularly for larger magnitude earthquakes. Several models will be used in the hazard analysis, since it was difficult to choose one model over another. Details of the development of the ground motion model are described in Appendix C.

TASK III.3 - HAZARD CURVES AND TIME HISTORIES DEVELOPMENT

Preliminary work on the task of incorporating the ground motion models, developed in Task III.1 into the computer model was underway at the time the project was terminated. No hazard curves or time histories were obtained.

TASK IV.1 - SONGS-1 AFWS FAULT TREE DEVELOPMENT

The objective of this task was to generate a fault tree for the SONGS AFWS, including the water supply to AFW pumps, electric power buses, AFW pump discharge to steam generators, and the auxiliary steam supply to AFW pump turbine. A fault tree for the SONGS Unit 1 AFWS was developed. Appendix B contains the top levels of the fault tree. The remaining data are stored in the files at LLNL. The model includes the AFWS as well as those portions of other systems (condensate storage, auxiliary steam supply, electric power, service water and fire protection) which relate to the AFWS. This work has been documented in the report on fault tree modeling of AFWS.[9]

The fault trees were drawn down to the component level, i.e., valves, pumps, pipe segments, etc. The different failure modes of such components were considered to be primary events of the fault tree. The top event was chosen to be: "Insufficient cooling of the steam generators during required operation of the AFWS."

The fault tree was analyzed using the WAMCUT and FTAP programs.[10] The doubles, i.e., cut sets that contain two basic events, generated by this analysis are shown in Appendix B. The basic event coding scheme is described in Appendix E of the Phase I final report of SSMRP. The remaining minimum cut sets are on file at LLNL.

TASK IV.2 - ZION UNIT 1 AFWS FAULT TREE MODIFICATION

Modifications were performed on the Zion Unit 1 AFWS fault tree to make it comparable to the SONGS Unit 1.[9] The modified fault tree covers all the AFWS components plus the headers of the service water system (SWS), which connect to the suction of the AFW pumps, up to the common SWS main header. The fault tree for the auxiliary steam supply to AFW pump turbine was also generated. These fault trees were prepared for analysis with the FTAP program.

TASK V.1 - STRUCTURAL FRAGILITY CURVES DEVELOPMENT

The SONGS Unit 1 structures evaluated in this study included the reactor building, containment sphere, sphere enclosure building, control-, administration building, diesel generator building, turbine pedestal, north turbine building extension, west feedwater heater platform, and the fuel storage building. Structural failure is defined as occurring when inelastic deformations are of sufficient magnitude to potentially interfere with the operability of attached equipment. When complete these analytical fragility relations provide the correlation between earthquake input and structural failure.

The methods used in the structural fragility development and the results are described in the report on seismic structural fragility investigation on the SONGS-1.[12] Only fragilities (median structure strengths and variabilities) which were completed are described. These median strengths are based on median material properties estimated from actual plant specific test data, where available, or by comparison to other data bases. Predictive models derived from actual test data were used whenever possible, to eliminate design conservatism normally associated with building code requirements. Refer to Appendix C for more details.

DRAFT FOR COMMENT

TASK V.2 - AFWS PIPE COMPONENT BETA-FACTORS DEVELOPMENT

Only one fragility description is provided to SEISIM to describe the fragility of all pipe components, and the pipe component fragilities are related to a master (i.e., reference) pipe component fragility by a load scale factor (beta-factor). This factor is defined as:

$$\text{Beta-factor} = \frac{\text{Capacity of reference pipe component}}{\text{Capacity of pipe component under consideration}} \ .$$

A large number of these factors were developed in Phase I of the SSMRP. A complete discussion of the methodology used in their development is contained in Section 4.2 of a the report on subsystem fragilities.[13] The factors developed for Zion-1 did not, however, include all of those needed for the SONGS-1 AFWS analysis. Hence, a sufficient number of additional factors were calculated to permit interpolating over a wide range of parameters. This has the twofold benefit of providing the needed factors for the SONGS-1 AFWS while also providing a wide range of factors for other future applications.

The Zion-1 factors were plotted as functions of both temperature and pipe schedule to determine which data points were missing and which would be needed to allow interpolation. Missing data were then calculated by scaling from existing data. The basis for scaling of different pipe schedules was section modulus, and scaling from one material to another was based on yield strength. This is consistent with the methodology described in the report[13] as mentioned above.

Appendix C contains the tables of the resulting beta-factors for different sizes of carbon and stainless steel pipe. For each pipe size, the beta-factors for different schedules (10, 40, 60, 80, 120, and 160) are shown. Factors are also shown for butt welds, elbows, and straight pipes at different temperatures (100°F, 300°F, and 500°F). As indicated in the subsystem fragilities report,[13] the beta-factors for butt welds can be used for reinforced branches, and the beta-factors for elbows can be used for unreinforced branches.

DRAFT FOR COMMENT

TASK V.3 - AFWS ELECTRICAL AND MECHANICAL COMPONENTS, FAULT TREE AND STRUCTURAL RESPONSES COORDINATION

The locations of nearly all of the electrical and mechanical components were determined. The locations of the few remaining components will have to be determined by on-site inspection. Once established, these locations determine the appropriate SMACS response to use for each component in the failure and risk analysis. This effort was not completed at the time the project was terminated.

TASK V.4 - AFWS PIPING RESPONSES AND FAULT TREE COORDINATION

Critical pipe components (such as tees, nozzles, elbows/pipe bends, etc.) were identified for all fourteen piping models as described in Task I.4. However, the data preparation effort for only seven of these fourteen piping models was completed. They are identified in Appendix C. No effort on coordination between critical pipe components and basic event of fault tree was initiated at the time the project was terminated.

TASK VI.1 - COMPUTATION OF THE SEISMIC RESPONSES OF STRUCTURES AND AFWS PIPING

Since the time histories development for the SONGS site was not completed at the time the project was terminated, only preliminary set-up for the SMACS analysis was accomplished.

TASK VI.2. - COMPUTATION OF THE PROBABILITIES OF FAILURE OF THE AFWS AND IDENTIFICATION OF WEAK LINKS

The fault trees for both SONGS-1 and Zion-1 AFWS were solved, and the cut sets were generated in a form suitable for SEISIM.[14] No SEISIM runs were initiated at the time the project was terminated.

SECTION 4: MILESTONE CHARTS AND DESCRIPTIONS

In Section 4, milestone charts and descriptions are given for each of the tasks in the SONGS-1 AFWS project. Milestone dates include the original target dates, the revised target dates, and the completed dates. All tasks were terminated in accordance with NRC request.

DRAFT FOR COMMENT

SONGS-1 AFWS Project Milestone Charts*

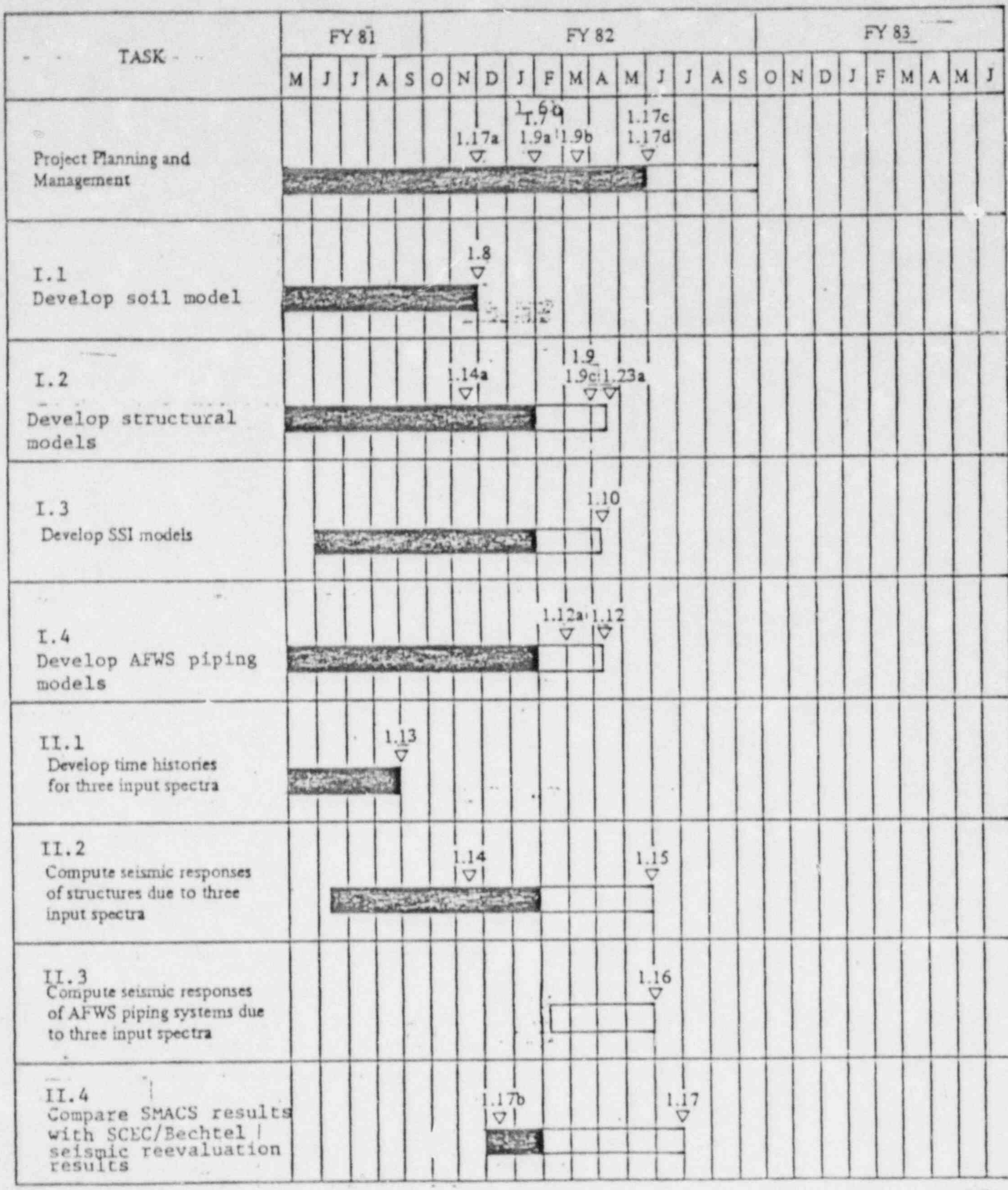

*All tasks were terminated by NRC on January 29, 1982.

DRAFT FOR COMMENT

SONGS-1 AFWS Project Milestone Charts*
(continued)

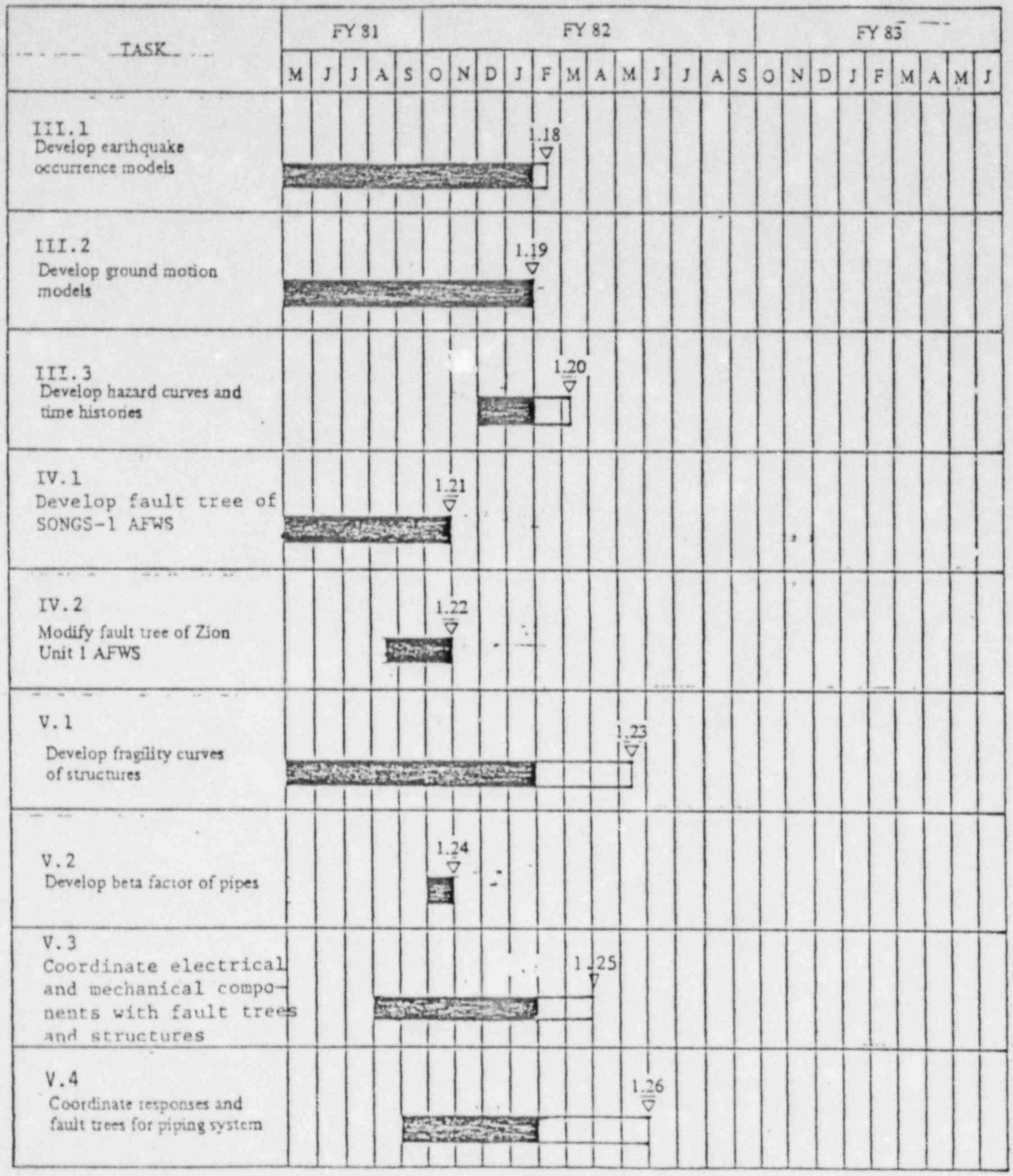

*All tasks were terminated by NRC on January 29, 1982.

DRAFT FOR COMMENT

SONGS-1 AFWS Project Milestone Charts*
(continued)

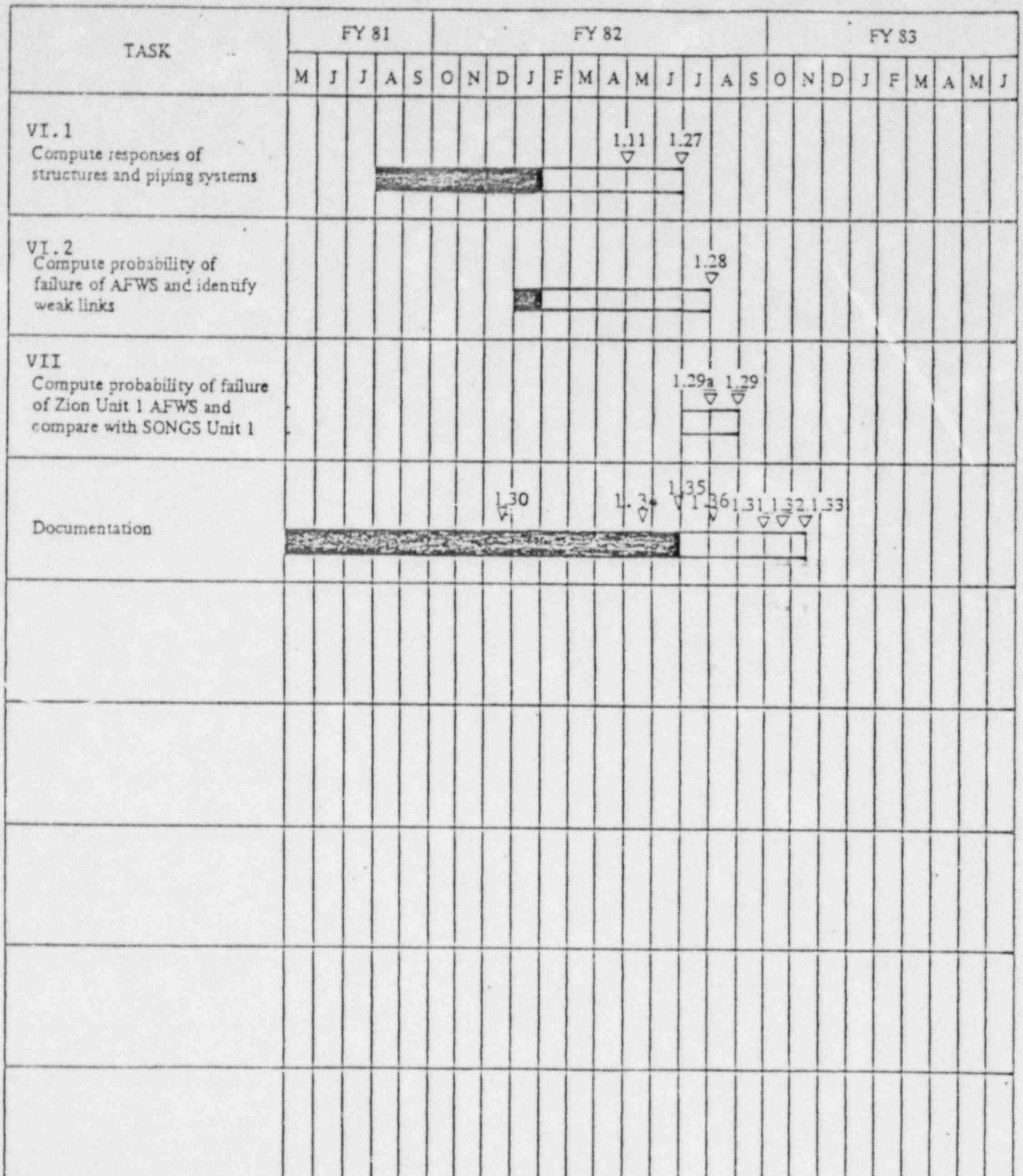

*All tasks were terminated by NRC on January 29, 1982.

DRAFT FOR COMMENT

SONGS-1 AFWS Project Milestone Dates**

	Milestone	Original Target Date	Revised Target Date	Completed Date
1.1	Kickoff meeting	11-21-80		11-21-80
1.2	SONGS site visit	11-24-80		11-25-80
1.3	NRC-LLNL meeting	12-18-80		12-18-80
1.4	Proposed work plan completed	1-15-81		1-22-81
1.5	Proposed work plan revised	2-6-81		2-6-81
1.6	Proposed work plan finalized	2-24-81		2-24-81
1.6a	Final work plan approved by NRC			5-1-81
1.6b	Project terminated by NRC	NA***		1-29-82
1.7	All necessary data and models obtained from SCEC	7-3-81	1-29-82	
1.8	Soil model developed	7-3-81	12-1-81	12-1-81
1.9	All structural models developed	10-23-81	4-5-82	
1.9a	Modification of turbine and fuel storage building obtained	1-29-82		
1.9b	SCEC/Bechtel fixed-base results of all structures obtained	3-19-82		
1.9c	All LLNL fixed base structure models compared with SCEC/Bechtel	4-5-82		
1.10	All SSI models developed	10-23-81	4-5-82	
1.11	SMACS test runs completed	12-4-81	5-1-82	
1.12	AFW piping models developed	10-23-81	4-5-82	
1.12a	AFW pipe supports location in the structural models identified	3-1-82		
1.13	Time histories for the three target spectra developed	7-3-81	7-15-81	8-31-81
1.14	Reactor building responses due to the three target spectra computed	8-14-81	11-24-81	11-24-81

**All tasks were terminated by NRC on January 29, 1982.
***NA = not applicable

DRAFT FOR COMMENT

SONGS-1 AFWS Project Milestone Dates **
(continued)

	Milestone	Original Target Date	Revised Target Date	Completed Date
1.14a	Reactor building model compared with SCEC/Bechtel	11-15-81		11-15-81
1.15	All structural responses due to the three target spectra computed	1-8-82	6-1-82	
1.16	AFWS piping responses due to the three target spectra computed	1-8-82	6-1-82	
1.17	SCEC/Bechtel seismic reevaluation results and SMACS results compared	2-5-82	7-1-82	
1.17a	SCEC/Bechtel seismic reevaluation results of reactor building obtained	11-30-81		
1.17b	SCEC/Bechtel seismic reevaluation results of reactor building compared	12-15-81		12-15-81
1.17c	SCEC/Bechtel seismic reevaluation results of all structures obtained	6-1-82		
1.17d	SCEC/Bechtel seismic reevaluation results of AFW piping systems obtained	6-1-82		
1.18	Earthquake occurrence model developed	9-18-81	2-15-82	
1.19	Ground motion model developed	9-4-81	2-1-82	
1.20	Hazard curves and time histories developed	11-20-81	3-5-82	
1.21	Fault tree of SONGS-1 AFWS developed	9-18-81	10-31-81	10-31-81
1.22	Fault tree of Zion Unit 1 AFWS modified	6-12-81	10-31-81	10-31-81
1.23	Fragility curves for structures developed	11-6-81	5-15-82	
1.23a	Preliminary stress analysis of structures for input to fragilities completed	4-15-82		
1.24	Beta-factor for AFW pipe components developed	10-16-81	10-31-81	10-31-81
1.25	AFWS components, fault tree, and structure coordinated	1-15-82	3-31-82	
1.26	Responses and fault tree of piping systems coordinated	12-18-81	6-1-82	

**All tasks were terminated by NRC on January 29, 1982.

DRAFT FOR COMMENT

SONGS-1 AFWS Project Milestone Dates**
(continued)

	Milestone	Original Target Date	Revised Target Date	Completed Date
1.27	Seismic responses of structures and AFW piping systems due to the time histories generated by Task III.3 computed	2-15-82	7-1-82	
1.28	Probabilities of failure of SONGS-1 AFWS computed	3-19-82	8-1-82	
1.29	Probabilities of failure of Zion-1 compared with SONGS-1 result	4-16-82	9-1-82	
1.29a	Probabilities of failure of Zion-1 AFWS computed	8-1-82		
1.30	Documentation of AFWS fault trees development	12-31-81		12-15-81
1.31	Draft report of the SONGS-1 AFWS project transmitted to NRC	10-1-82		
1.32	NRC comments on the draft report of SONGS-1 AFWS project received	10-15-82		
1.33	Camera-ready copy of the final report of SONGS-1 AFWS project transmitted to NRC	11-15-82		
1.34	Preliminary final progress report of the SONGS-1 AFWS project transmitted to NRC and SCEC for comment	4-30-82	6-28-82	
1.35	NRC and SCEC comment on draft final progress report of the SONGS-1 AFWS project received	7-19-82		
1.36	Final progress report of the SONGS-1 AFWS Project transmitted to NRC	8-15-82		

*All tasks were terminated by NRC on January 29, 1982.

DRAFT FOR COMMENT

REFERENCES

1. R. W. Mattson, Director of Safety Technology, NRR, U.S. Nuclear Regulatory Commission, memorandum to D. G. Eisenhut, Director of Licensing, NRR, Analysis and Recommendations Related to Plants without Seismically Qualified Auxiliary Feedwater Systems, (August 8, 1980).
2. P. D. Smith, D. L. Bernreuter, M. P. Bohn, T. Y. Chuang, G. E. Cummings, R. G. Dong, J. J. Johnson, R. W. Mensing and J. W. Wells, A Review of a Seismic Risk Analysis of the Decay Heat Removal Capability of Nuclear Power Plants, Lawrence Livermore National Laboratory, Livermore, CA., UCID-18692, (1980).
3. J. E. Richardson, U.S. Nuclear Regulatory Commission, telegraphic message to P. D. Smith, LLNL , "Use of SSMRP for San Onofre AFWS," (December 19, 1980).
4. T. Y. Chuang, P. D. Smith, R. G. Dong, D. L. Bernreuter, M. P. Bohn, G. E. Cummings, and J. E. Wells, Seismic Safety Margins Research Program, Project I, SONGS-1 AFWS Project, Lawrence Livermore National Laboratory, Livermore, CA., UCID-18959, (February 24, 1981).
5. P. D. Smith, R. G. Dong, D. L. Bernreuter, M. P. Bohn, T. Y. Chuang, G. E. Cummings, J. J. Johnson, R. W. Mensing, J. E. Wells, Seismic Safety Margins Research Program: Phase I Final Report-Overview, Lawrence Livermore National Laboratory, Livermore, CA., UCRL-53021, NUREG/CR-2015, Vol. 1, (April, 1981).
6. J. J. Johnson, G. L. Goudreau, S. E. Bumpus, O. R. Maslenikov, Seismic Safety Margins Research Program Phase I Final Report - SMACS - Seismic Methodology Analysis Chain with Statistics (Project VIII), Lawrence Livermore National Laboratory, Livermore, CA., UCRL-53021, NUREG/CR2015, Vol. 9, (July, 1981).
7. D. Gasparini and E. H. Vanmarcke, Simulated Earthquake Motions Compatible with Prescribed Response Spectra, Report 2 or Evaluation of Seismic Safety of Buildings, Department of Civil Engineering, Massachussetts Institute of Technology, Cambridge, Massachussetts, Pub. No. R76-4, (January, 1976).
8. D. B. Slemmons, P. Omalley, R. A. Whitney, D. H. Chung, and D. L. Bernreuter, Assessment of Active Faults for Maximum Credible Earthquakes of the Southern California - Northern Baja Region, Lawrence Livermore National Laboratory Livermore, CA., UCID-19125, (1982).

9. B. Najafi and S. Eide, San Onofre/Zion Auxiliary Feedwater System Seismic Fault Tree Modeling, Seismic Safety Margins Research Program, Lawrence Livermore Laboratory, Livermore, CA, UCRL-in print, (1982).

10. R. R. Willie, Computer-Aided Fault Tree Analysis, Operations Research Center, University of California, Berkeley, CA, ORC78-14, (1978).

11. J. Wells, L. George and G. Cummings, SSMRP Phase I Final Report - Systems Analysis (Project VII), Seismic Safety Margins Research Program, Lawrence Livermore National Laboratory, Livermore, CA., UCRL-53021, NUREG/CR-2015, Vol. 8, (1982).

12. D. A. Wesley and P. S. Hashimoto, Seismic Structural Fragility Investigation for the San Onofre Nuclear Generating Station Unit 1, Seismic Safety Margins Research Program, Lawrence Livermore National Laboratory, Livermore, CA., UCRL-in print, (1982).

13. R. P. Kennedy, R. C. Campbell, G. Hardy and H. Banon, Seismic Safety Margins Research Program (Phase I) Subsystem Fragility, Structural Mechanics Associates, Newport Beach, CA., UCRL-15407, NUREG/CR-2405 (February, 1982).

14. J. M. Hudson, J. D. Gasca and B. Kennedy, SEISIM Option 1, User's Manual, (Revision 1), J. H. Wiggins Company Technical Report No. 80-1366-2, J. H. Wiggins, Redondo Beach, CA. (1980).

DRAFT FOR COMMENT

APPENDIX A

STRUCTURAL RESPONSE COMPARISON

A1 INTRODUCTION

One of the major objectives of the San Onofre Nuclear Generating Station Unit 1 (SONGS-1) Auxiliary Feedwater System (AFWS) Project was to assess the conservatism in the SCEC/Bechtel Balance of Plant Seismic Reevaluation Program (BOPSRP). Meeting this objective required the development of seismic input time histories, soil properties and soil models of the San Onofre site, and mathematical models of the structures and piping systems affecting the response of the AFWS. The computer program, SMACS, Seismic Methodology Analysis Chain with Statistics calculates the seismic response of structures, systems, and components.

The program SMACS links the seismic input with soil-structure interaction (SSI), structural response, and piping response calculations. Seismic input is defined by ensembles of acceleration time histories for three orthogonal directions (two horizontal and a vertical) on the surface of the soil. SSI and detailed structural response are determined simultaneously by the substructure approach to SSI. This approach analyzes the coupled soil-structure system in a series of steps, i.e., determination of the foundation input motion, calculation of the foundation impedances, and analysis of the coupled system. The result of this approach is structural responses in the form of peak values and time histories of accelerations, displacements, and forces. Using these results, SMACS then calculates time history responses of piping systems through a multisupport time history analysis technique.

Throughout these computations, uncertainties are accounted for probabilistically. The largest source of variability in seismic input is acknowledged by using ensembles of time histories; in the SSI link, the shear modulus and damping in the soil are varied; in the computation of structural and piping responses, variation in the natural frequencies and modal damping ratios account for uncertainties. This appendix describes both this developmental effort and the results of the subsequent design comparison analyses performed on the SONGS Unit 1 reactor building complex.

Section A2 describes the seismic input time histories which is comprised of three elements: generation of artificial time histories which match the three target spectra (SONGS Unit 1 seismic reevaluation spectra, SONGS Units 2 and 3 design spectra, and the average of the two). Section A3 contains the development of best estimate equivalent linear soil properties and their variability. It also describes the SONGS Unit 1 structures that influence the seismic response of the AFWS, the SSI and structural models that defined the dynamic characteristics of these buildings. Finally, a comparison of dynamic characteristics with the SCEC/Bechtel model of reactor building is also included in Section A4.

A2 SEISMIC INPUT TIME HISTORIES

Thirty sets of (two horizontal and a vertical) time histories were generated for the three target spectra: the SONGS Unit 1 seismic reevaluation spectra, the SONGS Units 2 and 3 design spectra, and the average of the two. All spectra were anchored at 0.67 g zero period acceleration (ZPA) for the horizontal components and 0.45 g for the vertical component. A sensitivity study calculating mean response using 90 sets of input time histories varied little from the mean results obtained using 30 time history sets. This study confirmed the adequacy of using 30 sets in subsequent response analyses.

All time histories were generated using the computer program, SIMQKE.[1] The time histories were generated at a time step of 0.01 seconds (s). All time histories were 18 s in duration and generated for a target spectrum with 2% damping. Figure 1 shows a comparison between the mean of the thirty spectra and the target spectrum for the three target spectra as mentioned above.

SIMQKE generates statistically independent artificial acceleration time histories which match a specified response spectrum, and it refines the spectral match through an iterative procedure. It also performs a baseline correction on the generated motion to ensure zero final ground velocity; and, of course, it calculates response spectra with the time histories as input.

DRAFT FOR COMMENT

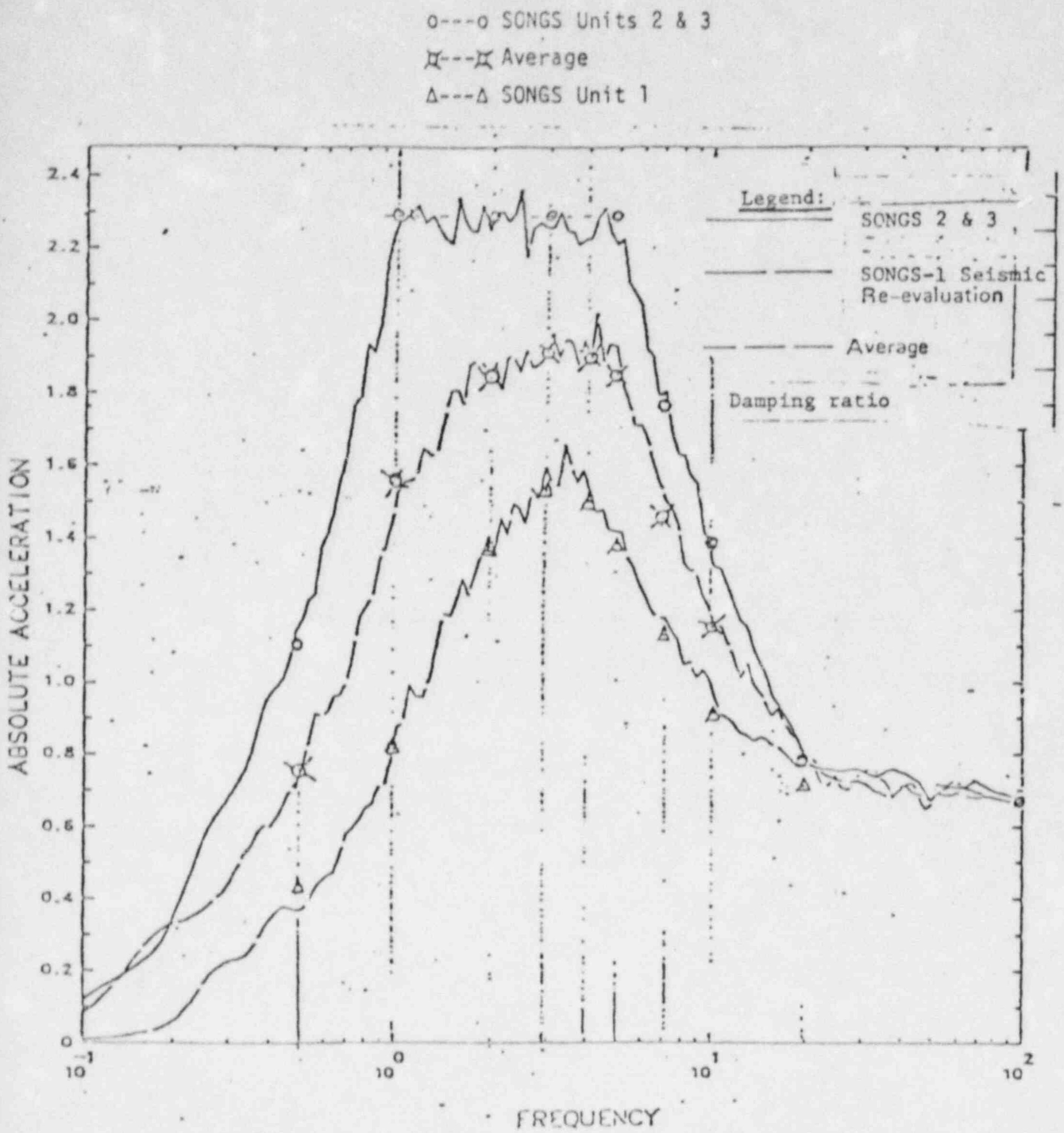

Figure 1. Comparison of target spectra with the mean of each set.

The method used by the program for artificial motion generation is superposition of sinusoids having random phase angles and amplitudes derived from a stationary power spectral density function of the motion. To simulate the transient character of real earthquakes, an envelope function, $I(t)$, is used. The final simulated motion, $z(t)$, then becomes:

$$z(t) = I(t)\,\Sigma A_n \sin(\omega_n t - \phi_n).$$

It is stationary in frequency content with a peak acceleration close to the target peak acceleration. In order to introduce variability consistent with real time histories only one iteration for each generated time history was allowed. This led to a coefficient of variation (COV) of about 0.10 - 0.15 for frequencies higher than 2 Hz and about 0.15 - 0.20 for frequencies higher than 0.2 Hz but lower than 2 Hz. For the set of real time histories used to generate Regulatory Guide 1.60 design spectra (all scaled to 1.0 g), the COV is over a factor of 2 to 3 times larger than for the sets of time histories that were generated. However, unlike the set of real time histories, the spectrum of each time history as generated is a "reasonable" match to the target spectrum. Figure 2 shows a typical example.

DRAFT FOR COMMENT

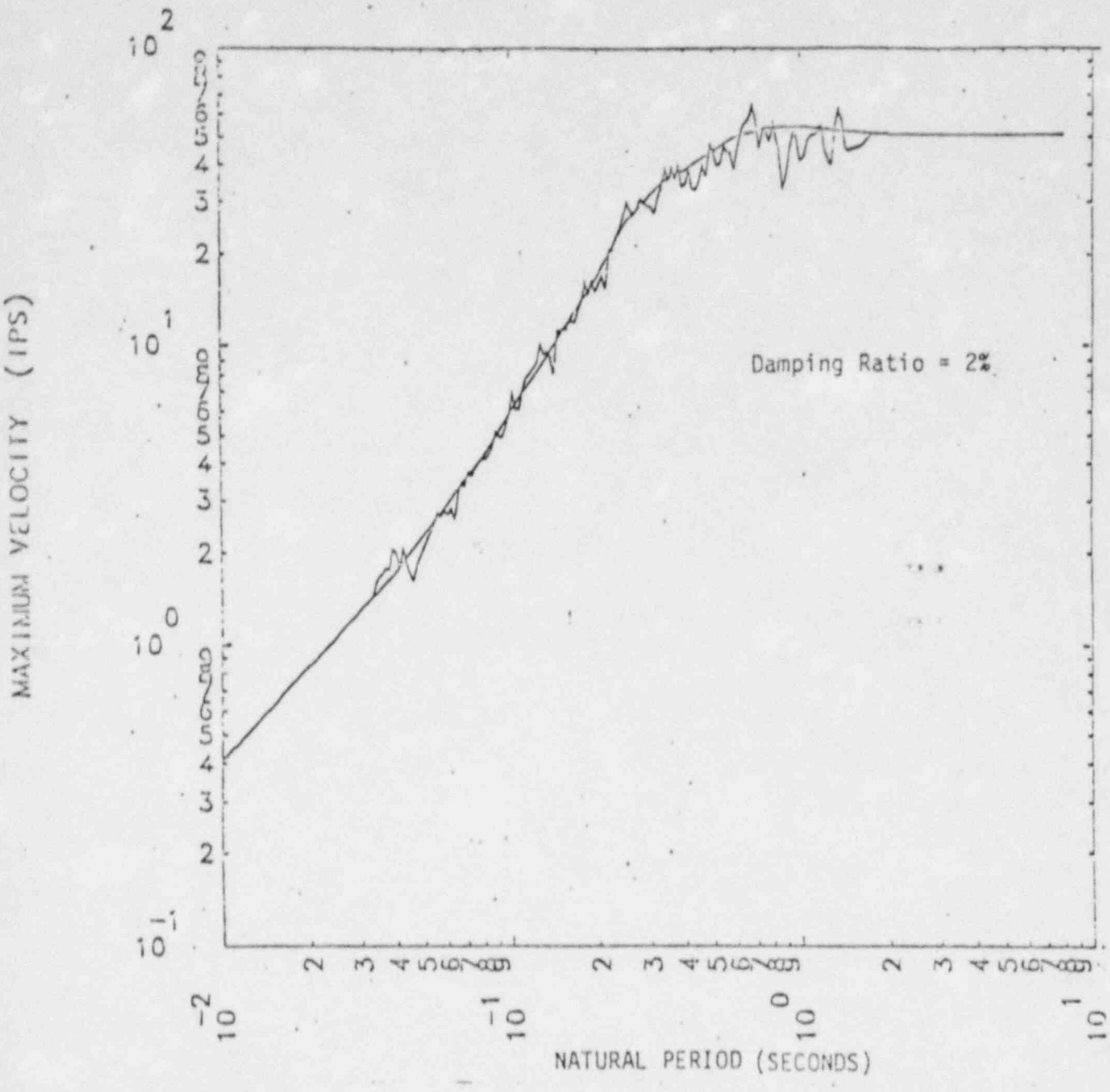

Figure 2. Comparison of a typical response spectrum computed from generated time history to the SONGS-1 target spectrum.

A3 SOIL, SSI AND STRUCTURAL MODELS

The soil model of the SONGS site and the soil-structure interaction (SSI), and structural models the SONGS-1 structures housing the AFWS are described below.

A3.1 Methodology

A potentially large source of uncertainty in the soil-structure interaction (SSI) analysis is associated with the determination of soil properties to be used in the analysis. This process involves selecting a mathematical model to represent soil stress-strain behavior, measuring properties for this model in the laboratory and relating them to the properties in situ and determining the variation of these properties at a constant strain level, and for increasing levels of strain corresponding to higher levels of seismic excitation.

The stress-strain behavior of soil was modeled on the basis of a linear viscoelastic theory. The parameters defining the model are two elastic constants, i.e., shear modulus and Poisson's ratio, and a material damping factor. The nonlinear behavior of soil was taken into account by equivalent linear techniques, i.e., values of the material constants (shear modulus and material damping) were selected on the basis of average strain levels expected in the soil as a result of the earthquake. An iterative linear analysis was then performed to estimate the final soil properties.

SSI and detailed structural response are determined by simultaneously using the substructure approach to SSI. The substructure approach divides the problem into a series of simpler problems, solves each independently, then superposes the results. Typically, these simpler problems are: determination of the foundation input motion; determination of the foundation impedances; and analysis of the coupled soil-structure system. This process culminates in a prediction of the response of the soil-structure system. The CLASSI family of computer programs, an implementation of the substructure approach, forms the basis of the SSI and structural response calculations in SMACS.[2] CLASSI is organized according to the steps of the substructure approach. The set of continuum linear analysis (CLA) codes solves the first two steps, i.e., foundation input motion and impedances, then the SSIN code analyzes the coupled soil-structure system. SSIN forms the core of the SSI and major structure response calculation in SMACS. Some general comments concerning the procedure are in order.

DRAFT FOR COMMENT

Several general features characterized the solution of the SSI problems as formulated in CLASSI. The basic formulation is in the frequency domain, which permits modeling the behavior of the soil by frequency-dependent impedances and scattering matrices. Fourier transform techniques are applied to obtain the time history of response.

The mathematical model selected to represent the stress-strain behavior of soil is based on a linear viscoelastic theory. The parameters defining the model produce constant hysteretic-type (i.e., frequency-independent) damping and consist of two elastic constants (typically, shear modulus and Poisson's ratio) and a material damping factor. The nonlinear behavior of soil was taken into account by equivalent linear techniques. Equivalent linear soil properties were determined by an iterative process that estimates material constants as a function of an average strain level over the duration of the excitation. The process and results for the SONGS-1 site are described in subsection A3.2. Note that one-dimensional wave propagation analysis was performed to determine the properties. Only the "primary nonlinearity," i.e., the nonlinear behavior induced in the free-field by the earthquake itself, was treated. Best estimate values of the material constants for differing excitation levels were estimated along with the expected variability in these values.

The three steps of the substructure approach are shown schematically in Fig. 3. Specification of the free-field ground motion (i.e., the control point, frequency characteristics of the control motion, and the spatial variations of the motion) is a preliminary step which was discussed in Section A2. Each of the three steps is briefly described as follows.

1. Determination of the Foundation Input Motion

The foundation input motion differs from the free-field ground motion in all cases, except for surface foundations subjected to vertically propagating waves. The motions differ primarily for two reasons. First, waves are scattered from the soil-foundation interface. Second, points on the foundation are constrained to move according to the geometry and stiffness of the foundation. This constraint leads to a reduction in the total number of degrees of freedom necessary to define the motion of the foundation. When the effective stiffness of the foundation is large compared to the soil, rigid

DRAFT FOR COMMENT

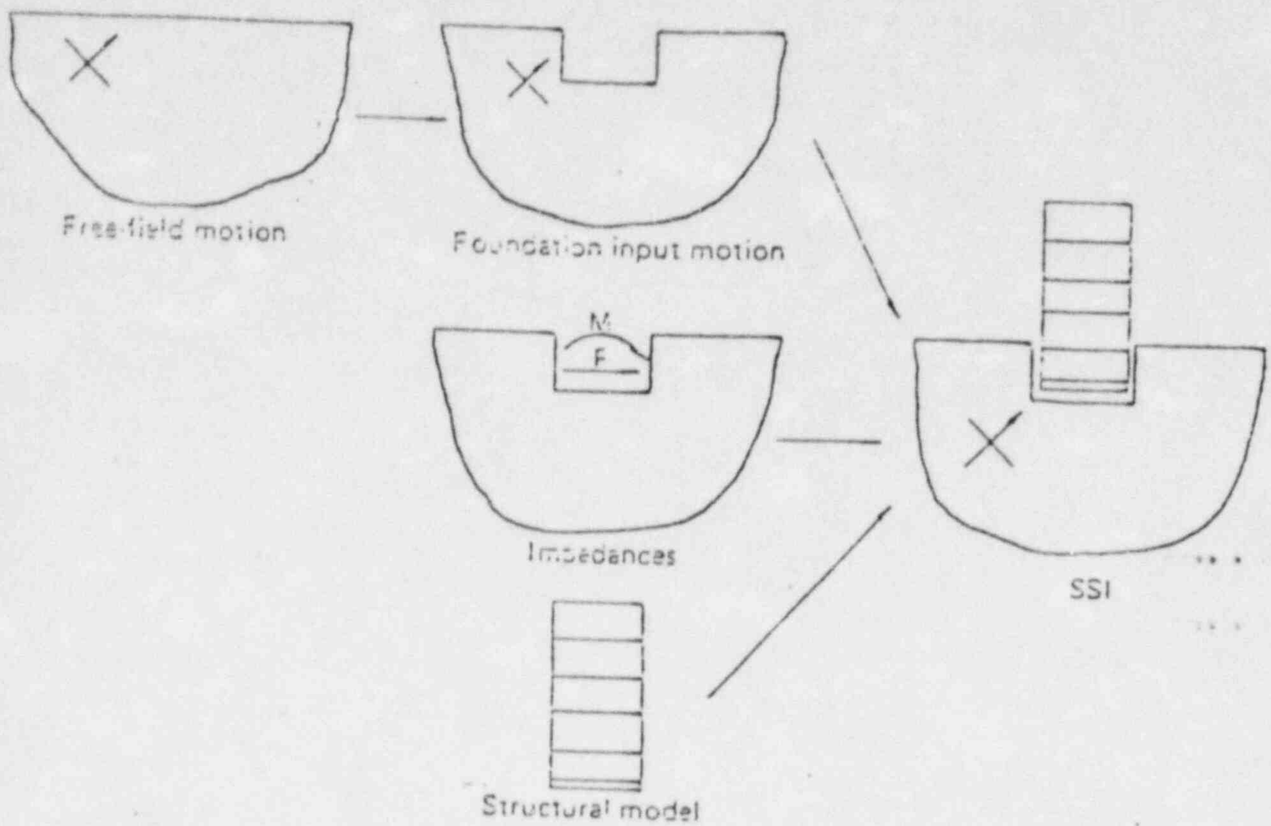

Figure 3. A schematic representation of the elements of the substructure approach to soil-structure interaction analysis.

behavior is assumed, and the motion of the foundation is uniquely defined by six rigid-body degrees of freedom, i.e., three translations and three rotations.

The foundation input motion, $\{U^*\}$, is related to the free-field ground motion by means of a transformation defined by a scattering matrix, $[S(\omega)]$, which is complex-valued and frequency dependent:

$$\{U^*(\omega)\} = [S(\omega)]\,\{f(\omega)\}\ ,$$

where the vector, $\{f(\omega)\}$, is the complex Fourier transform of the free-field ground motion, which contains a complete description of the free-field motion. For a particular frequency, ω, each complex number in the vector corresponds to the amplitude and phase of an assumed wave component of the free-field motion. Each column of $[S(\omega)]$ represents the response of a massless rigid foundation to a given incident wave of unit amplitude. The response is frequency-dependent, because the incident wavelength, and in some cases the apparent velocity of the wave front, varies with frequency. There can be numerous columns in $[S(\omega)]$ because incoming seismic waves may be assumed to contain many surface modes, each having a different phase velocity. In addition to its dependence on the composition of the free-field motion in terms of the different types of waves, $[S(\omega)]$ depends on the geometry of the foundation and the characteristics of the soil, i.e., its material properties and configuration. The matrix product, $[S(\omega)]\{f(\omega)\}$, is therefore the response of the rigid, massless foundation to a particular seismic event.

Of the SONGS Unit 1 structures to be analyzed, only the reactor building/containment sphere is embedded to a significant extent. The fuel storage building foundation is slightly embedded. In addition, for SONGS Unit 1 analyses completed to date, vertically propagating waves were assumed. Hence, the scattering matrix, $[S(\omega)]$ reduces to its simplest form (i.e., unity for translational components, zero for all others, and constant over the frequency range) for all foundations except the reactor building/containment sphere.

DRAFT FOR COMMENT

2. Determination of Foundation Impedances

The second step in the substructure approach is determining the force-displacement characteristics of the soil. The relationship is typically presented in the form of impedances, $[K_s(\omega)]$. Foundation impedances depend on soil configuration and material behavior, the frequency of the excitation, and the geometry of the foundation. The SONGS-1 analysis assumed rigid foundations for which the force-displacement characteristics are uniquely defined by a 6 x 6 matrix relating a resultant set of forces and moments to the six rigid-body degrees of freedom.

In general, for a linear elastic or viscoelastic material and a uniform or horizontally stratified soil deposit, each element of the impedance matrix is complex-valued and frequency dependent. Each complex element of the matrix, $[K_s(\omega)]$, can be thought of as a pair of functions: the real part representing the stiffness of the soil, and the imaginary part the damping.

3. Solution of the Coupled Soil-Structure System

The final step in the substructure approach is performing the actual SSI analysis. The results of the first two steps are combined with a dynamic model of the structure to solve the equations of motion of the coupled soil-structure system. The solution procedure in SMACS for completing this step is quite powerful. The structure is modeled by its fixed-base eigensystem and modal damping factors. The structure dynamic characteristics are projected in the form of modal participation factors to a reference point on the foundation at which SSI response of the foundation is determined. This projection reduces the characterization of structural dynamic effects to a size dependent only on the number of modes and the number of foundation degrees-of-freedom. This permits the use of extremely complicated structural models. For a single foundation, the SSI response computation requires solution of, at most, six simultaneous equations. In-structure response is determined with a similar size reduction.

DRAFT FOR COMMENT

A3.2 SOIL MODEL

The soil model for the SONGS site is described below.

A3.2.1 Soil Conditions

The subsurface soil conditions were investigated by drilling exploratory borings around the site. The site stratigraphic column for SONGS Unit 1 as published in the SONGS Unite 1 Final Safety Analysis Report (FSAR)[3] is shown in Fig. 4. For SONGS Units 2 and 3,[4] a detailed geophysical investigation, consisting of seismic refraction surveys, seismic velocity surveys, micromotion and borehole surveys was performed by Dames and Moore.[5] The measured and computed data are presented in Fig. 5.

The site is underlain by terrace deposits, consisting of approximately 30 - 45 ft of sands, silts, and clays with layers of gravel and cobbles. These soils are generally dry, and some are cemented. Measured compressional and shear wave velocities for the terrace deposits range from 1000 to 3100 feet per second (fps), and 300 to 1250 fps, respectively. The Poisson's ratio for this material ranges from 0.40 to 0.44. The unit weight varies from 120 to 130 pounds per cubic foot (pcf).

DRAFT FOR COMMENT

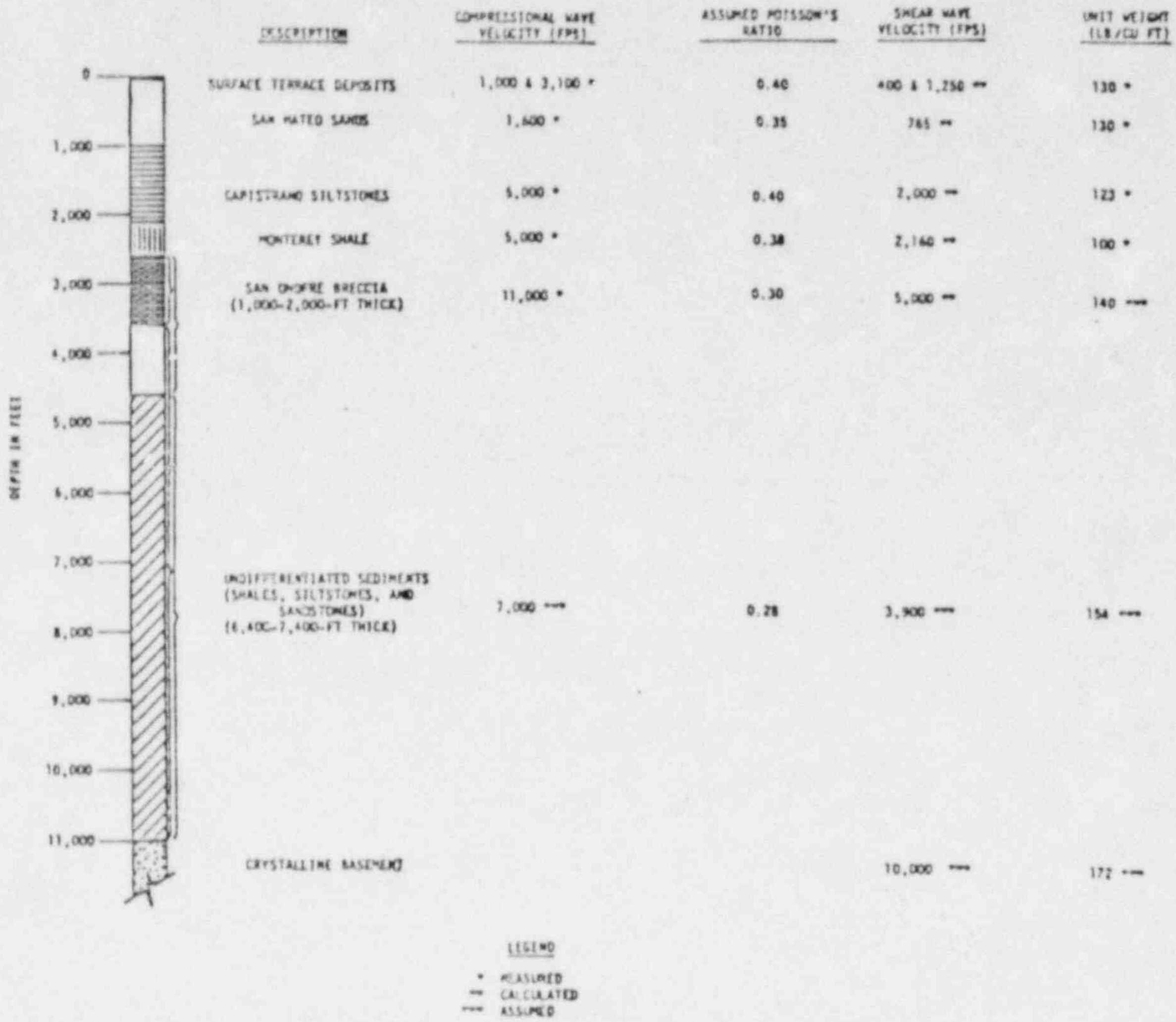

Figure 4. Subsurface profile of SONGS Unit 1 (extracted from SONGS Unit 1 FSAR[3]).

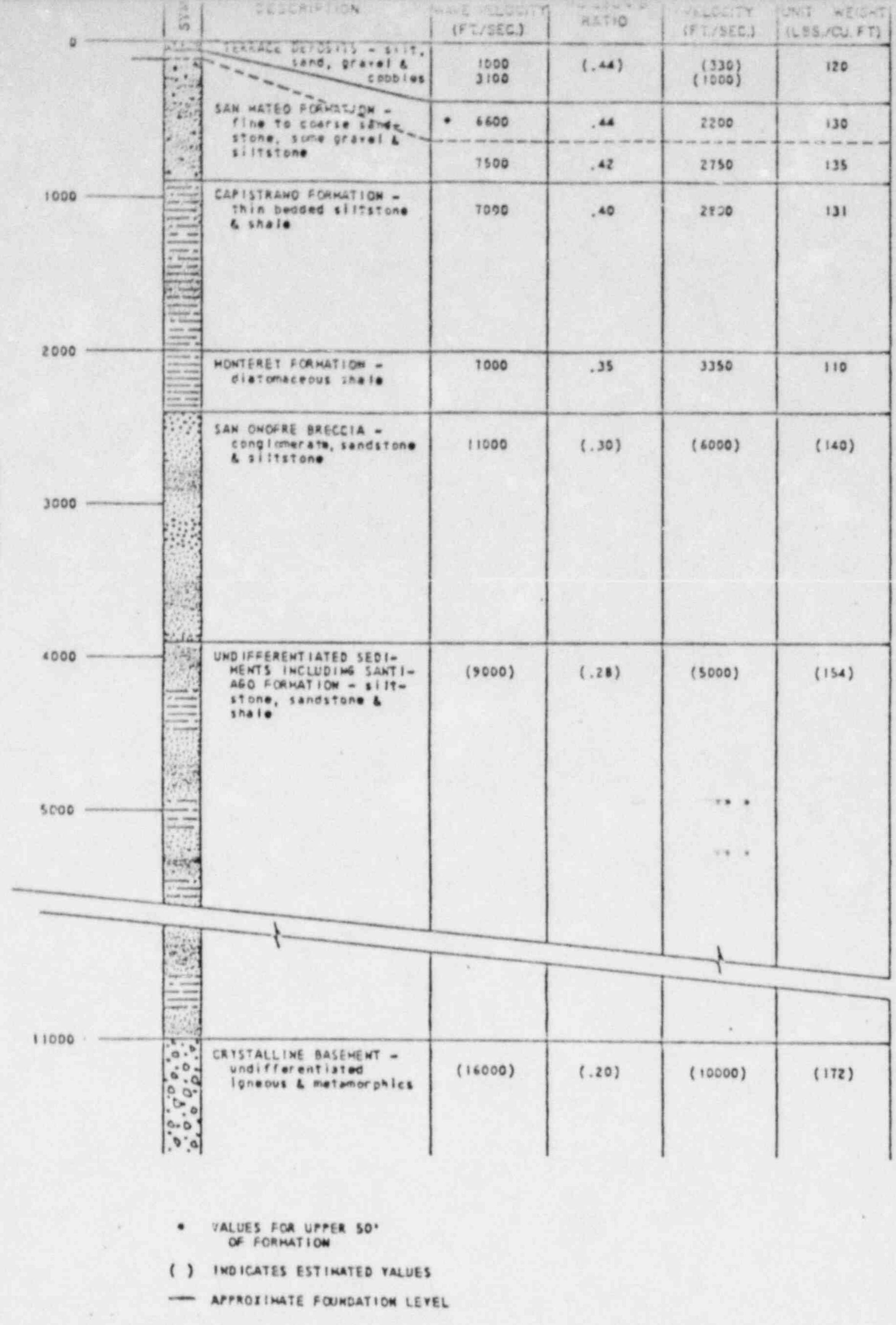

Figure 5. Stratigraphic column showing geophysical data (extracted from SONGS Units 2 and 3 FSAR[4]).

DRAFT FOR COMMENT

The terrace deposits are underlain by a deep deposit of fine-to-coarse well-graded and slightly cemented sands, termed San Mateo formation. The San Mateo sands extend approximately 940 ft below the existing ground surface. The unit weight varies from 130 to 135 pcf. The average dry unit weight ranges from 119 to 127 pcf with an average of about 123 pcf. The relative density was estimated to be close to 100%. The measured compressional and shear wave velocities range from 3000 to 7000 fps, and 1000 to 2750 fps, respectively. The Poisson's ratio based on these measured wave velocities ranges from 0.40 to 0.45. The average elevation of the ground water table was approximately 5 ft above mean lower low water (MLLW). MLLW describes an average height over a 19 year period of the lower of the two low waters of all tidal days.

A3.2.2 Dynamic Material Properties

In order to conduct site response analyses, dynamic material properties of the subsurface soils must be assigned. For analysis of the San Onofre site, only the properties of San Mateo sand need be considered. Dynamic properties generally refer to the low-strain shear modulus, strain-dependent shear modulus, and damping ratio.

The low-strain shear modulus (G_{max}) of the San Mateo sand was based on laboratory and in-situ tests that determined the shear wave velocity as a function of depth. The range of the measured shear wave velocities is shown in Fig. 6. The low-strain shear modulus can then be computed from the equation:

$$G_{max} = \rho V_s^2 ,$$

where ρ = mass density, and V_s = shear wave velocity. The range of G_{max} based on measured shear wave velocities are shown in Table 1.

DRAFT FOR COMMENT

Site Depth	Shear Wave Velocity (V_s, fps)	Low-strain Shear Modulus (G_{max}, ksf)
upper 50 ft.	1000 - 2200	4037 - 19540
below 50 ft.	1900 - 2750	15135 - 31706

Table 1. Ranges of shear wave velocity and G_{max}.

The shear modulus of San Mateo sands was also calculated from an empirical equation. Using parametric values recommended by Woodward-McNeill[6], the equation for low-strain shear modulus is:

$$G_{max} = 59\ (\sigma_m)^{2/3} \quad ,$$

where σ_m = the mean effective stress in units of pounds per square foot (psf), while G_{max} is measured in units of kips per square foot (ksf). Computed shear wave velocities at different depths based on this equations are also shown in Fig. 6. A comparison between the measured and calculated values for V_s indicates a variation that ranges from 18% to 37%. This range implies that the values for G_{max} as a function of depth could vary by approximately as much as 50% of the mean values.

The nominal strain-dependent shear modulus and damping ratio curves are recommended by Woodward-McNeill[6] on the basis of the field seismic tests and laboratory tests. The average value of Poisson's ratio, 0.42, was used to convert major principal strains to shear strains. As shown in Fig. 7, the shear modulus of San Mateo sand decreases rapidly with increased strain levels.

DRAFT FOR COMMENT

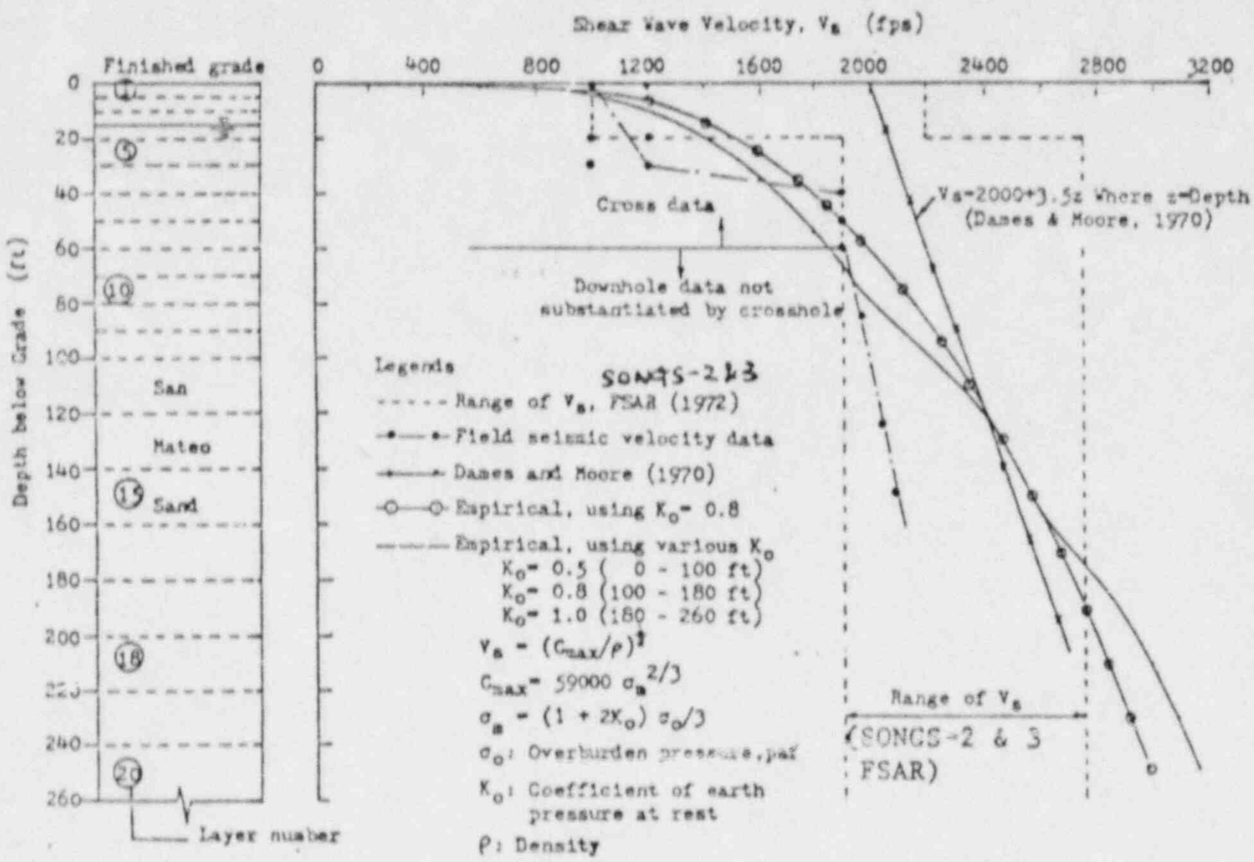

Figure 6. Variation of shear wave velocity with depth.

DRAFT FOR COMMENT

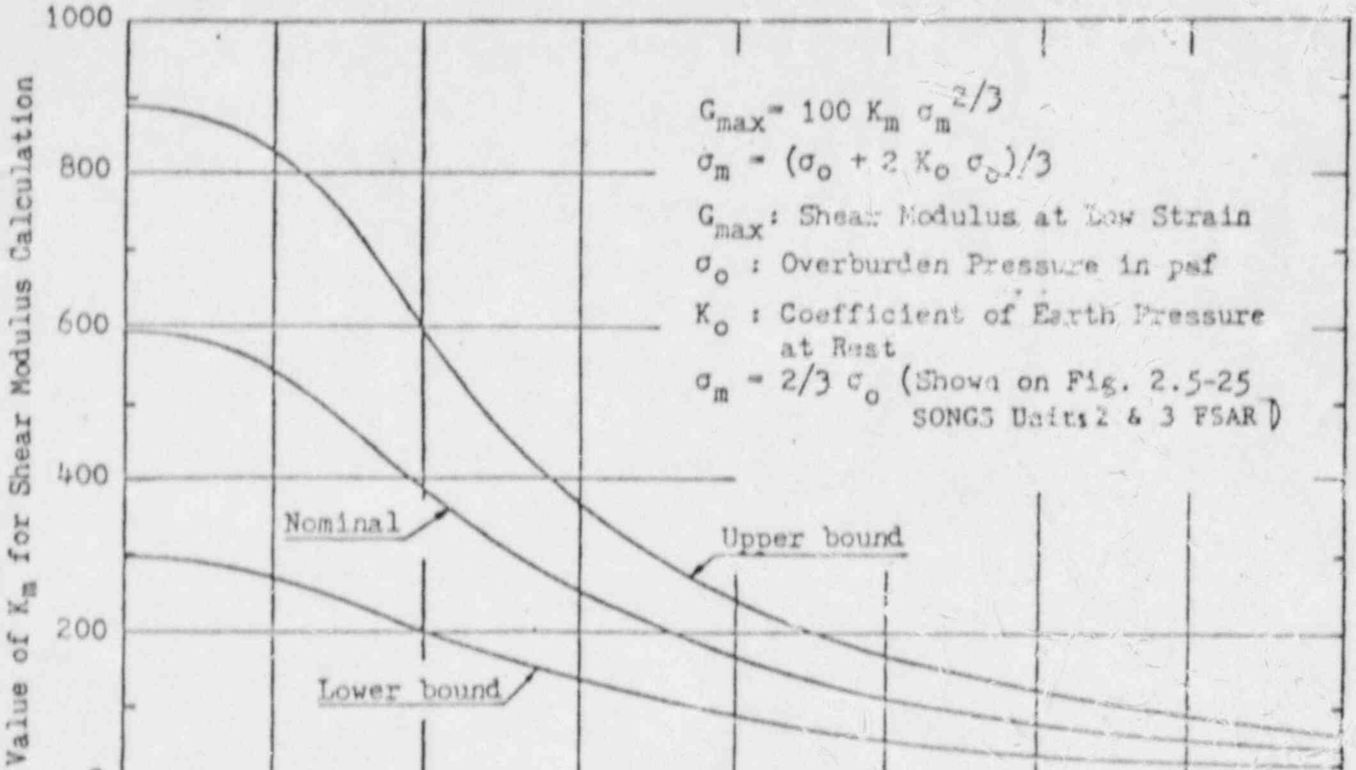

Figure 7. Variaton of shear modulus with shear strain for San Mateo sand.

DRAFT FOR COMMENT

In order to estimate the variation in soil properties at different strain levels, strain-controlled dynamic triaxial tests were performed on samples taken from exploratory borings at the site. The variation in the modulus of elasticity and damping was obtained by testing seven samples at each of three confining pressures. The greatest scatter of data for Young's modulus was found at the lowest confining pressure. The deviation was about 25% at low strain and 51% at high strain levels. On the basis of this scattering and uncertainties associated with calculated values of G_{max} described previously, it is reasonable to assume values of $\pm$ 50% of nominal as the upper and lower bounds for shear modulus over the entire strain range. The variation is illustrated in Fig. 7.

The dynamic triaxial tests also provided the basis for determining the nominal values and the scatter of damping ratios (β). The data scatter shows a variation of 80% of the nominal value at low shear strain and a variation of 42% at high strain. The estimated range is shown in Fig. 8.

A3.2.3 Development of Equivalent Linear Soil Models

Equivalent linear soil characteristics were evaluated by one-dimensional wave propagation analysis. Computer program, SHAKE,[7] was used for this study. Soil properties described in earlier paragraphs were used in the SHAKE analyses. For each acceleration level, sets of synthetic time histories developed to represent variability in design motion were used. Variations in three input parameters, low-strain shear modulus, shear modulus r[illegible] [illegible]th strain level, and damping with strain level, were considered. The parameter values were selected according to a simulated experimental scheme that covered the parameter spaces. For each acceleration level, iterative, linear analyses were performed until the calculated soil properties were compatible with the average calculated shear strain in each soil layer. Since subsequent structural response calculations were performed at a ground acceleration of 0.67 g, emphasis was given to determining the parameter values at this input level.

DRAFT FOR COMMENT

63

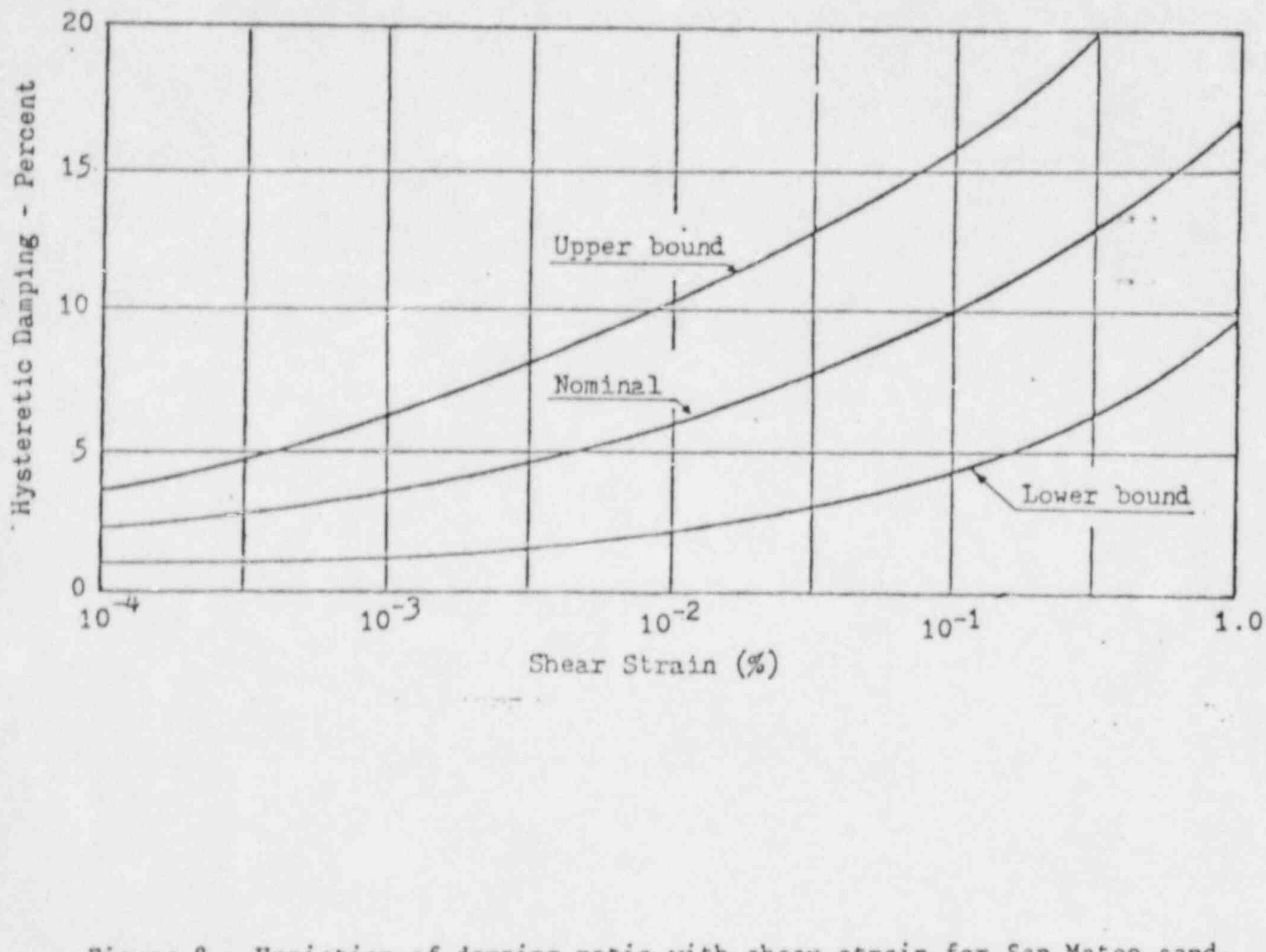

Figure 8. Variation of damping ratio with shear strain for San Mateo sand.

DRAFT FOR COMMENT

1. Generalized Soil Profile

The SONGS site is underlain by approximately 40 ft of terrace deposit and about 900 ft of San Mateo sand. The terrace deposit was excavated and all structures were founded below the finished plant grade at an elevation of 20 ft in San Mateo sand. The finished grade will be referred to as the free-field ground surface of the idealized soil profile used for the SSI model.

Since the main purpose of using equivalent linear soil properties in SSI analysis is to approximately account for non-linear soil effects due to seismic wave motions, it is not necessary to define the soil model to the bottom of San Mateo formation. The selection of a rigid base in a deep soil site is dependent not only on the size of the foundation but also on the justification of the existing soil properties in the soil profile. It has been customary to assume the rigid base exists at a certain depth where the low-strain shear wave velocity is 2500 fps or greater.

Based on the dimension of the reactor building, as well as the relationships between shear wave velocity and the depth at the SONGS site recommended by Dames and Moore[5], the rigid base was initially selected at a depth of 260 ft below the finished grade. To assure the adequacy of the rigid base location, simplified analyses to simulate SSI effects were conducted for several cases with the base located at three different depths. Input motion was specified at ground surface in order to compute the motion at different elevations. For all cases, the response spectra at the same elevation were compared and the differences in response shape at a depth of 260 ft or greater are negligible as shown in Fig. 9. Therefore, the location of the artificial rigid base at 260 ft is adequate. The idealized soil profile used for SHAKE analysis is shown earlier in Fig. 6.

2. Nominal Soil Properties for 0.67 g

Two sets of synthetic motions were used as input in the analysis to determine soil properties at 0.67 g. One set was targeted to a the SONGS Units 2 and 3 design response spectrum of 2% damping, the other set was

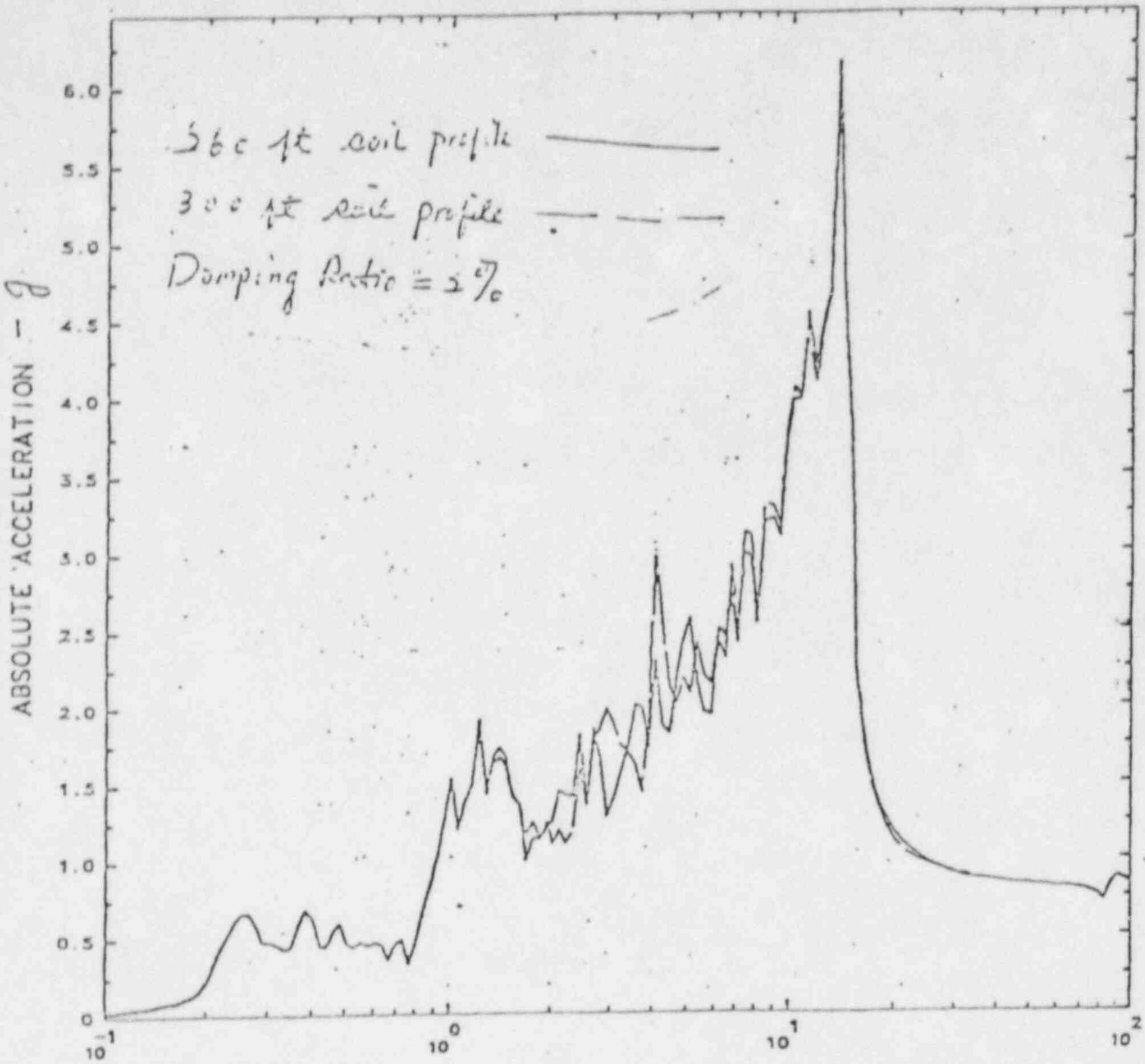

Figure 9. Comparison of response spectra of computed motions at the depth of 260 ft for two soil profiles with different elevation of rigid base.

based on the SONGS Unit 1 seismic reevaluation spectrum of 2% damping. Four time histories comprised each set. Their mean spectra are shown in Fig. 10. The frequency content of the two spectra is significantly different at levels below 9 Hz. This difference may contribute to variations in the soil properties.

Having established the input motion and the generalized soil profile, the analyses to determine the nominal equivalent soil properties were conducted. Iteration on soil properties uses the curves of strain-dependent moduli and damping shown earlier in Fig. 8. Two cases using different empirical formulations defining the low-strain shear modulus were considered. The nominal values given by each case for shear modulus and damping were plotted in Fig. 11. Small differences are seen between the two cases at depths less than 100 ft, and it is believed that the overall effect on generated impedance and scattering matrices due to these differences is insignificant.

3. Uncertainty of Strain-Compatible Soil Properties

The uncertainty of strain compatible soil properties is a function of the variation in the soil parameters, G_{max}, G/G_{max}, β (where G is the shear modulus and β is the damping ratio) and the characteristics of the input motion. To assess the variability, multiple analyses were conducted with SHAKE. The soil parameters were modeled as three random variables. For each analysis, the values of the soil parameters were chosen by a Latin hypercube sampling technique.[8] Two sets of synthetic motions, each consisting of four time histories and targeted to the specified spectra, were employed to provide the variability attributed to seismic input. Twenty-nine sets of property combinations were combined with eight control motions to define 232 SHAKE analyses. A second simulation was performed treating G_{max} as a dependent variable. This served to reduce the variability of soil properties. The difference in the coefficient of variation (COV) of the equivalent linear soil properties due to the two different simulation schemes was negligible. The results of these analyses are shown in Figs. 12, 13 and Table 2. Figure 12 concentrates on the soil properties calculated at 0.67 g. The mean and the one-plus and minus standard deviation values are plotted for both shear modulus and damping ratio. Figure 13 shows the mean values as a function of soil depth for each of four acceleration levels. The variations in G and β are listed in Table 2.

Table 2. Mean values and coefficient of variations (COV) of G and β for each g level.

Acc. Level	0.204 g				0.460 g				0.670 g				0.890 g			
	G (ksf)		β (%)		G (ksf)		β (%)		G (ksf)		β (%)		G (ksf)		β (%)	
Layer No.	Mean	COV	Mean	COV	Mean	COV	Mean	COV	Mean	COV	Mean	COV	Mean	COV	Mean	COV
1	757	.478	7.09	.491	485	.482	10.32	.476	393	.481	11.66	.452	338	.471	12.80	.438
2	1319	.488	7.43	.493	857	.485	9.67	.468	699	.472	10.92	.445	610	.479	11.98	.433
3	1721	.484	7.10	.475	1139	.486	9.18	.269	940	.481	10.37	.449	817	.481	11.39	.436
4	1922	.477	7.03	.495	1297	.486	9.03	.470	1076	.486	10.21	.452	934	.480	11.23	.434
5	2053	.472	7.10	.472	1413	.487	9.05	.467	1172	.489	10.26	.450	1024	.478	11.27	.430
6	2271	.474	7.02	.488	1595	.494	8.89	.471	1320	.472	10.09	.450	1160	.482	11.07	.427
7	2508	.477	6.88	.488	1785	.504	8.67	.474	1473	.496	7.86	.450	1278	.487	10.83	.427
8	2751	.482	6.72	.490	1975	.512	8.44	.477	1629	.502	9.61	.451	1435	.495	10.56	.427
9	2998	.488	6.55	.492	2163	.518	8.21	.480	1780	.504	9.36	.453	1570	.501	10.30	.431
10	3240	.493	6.39	.494	2343	.519	8.00	.482	1930	.508	9.13	.456	1703	.506	10.05	.432
11	3478	.496	6.25	.495	2528	.524	7.80	.485	2078	.511	8.91	.458	1833	.511	9.81	.435
12	3712	.499	6.10	.476	2708	.531	7.62	.487	2220	.514	8.71	.459	1960	.516	9.59	.436
13	5317	.508	5.57	.505	3858	.542	6.98	.498	3138	.533	7.99	.472	2755	.537	8.83	.452
14	5894	.513	5.37	.507	4272	.551	6.73	.500	3471	.543	7.70	.473	3043	.549	8.52	.452
15	6454	.516	5.18	.508	4681	.563	6.50	.501	3777	.543	7.44	.474	3308	.550	8.24	.452
16	6990	.519	5.01	.509	5071	.568	6.29	.502	4083	.546	7.20	.474	3574	.551	7.97	.453
17	8691	.521	4.71	.513	6294	.572	5.91	.508	5054	.554	6.78	.481	4393	.556	7.50	.461
18	9255	.523	4.58	.512	6725	.576	5.74	.509	5394	.554	6.58	.482	4682	.554	7.29	.462
19	9815	.524	4.46	.512	7159	.579	5.58	.511	5727	.554	6.40	.483	4976	.557	7.09	.464
20	10368	.524	4.24	.513	7584	.580	5.43	.512	6067	.556	6.23	.484	5274	.560	6.89	.466

DRAFT FOR COMMENT

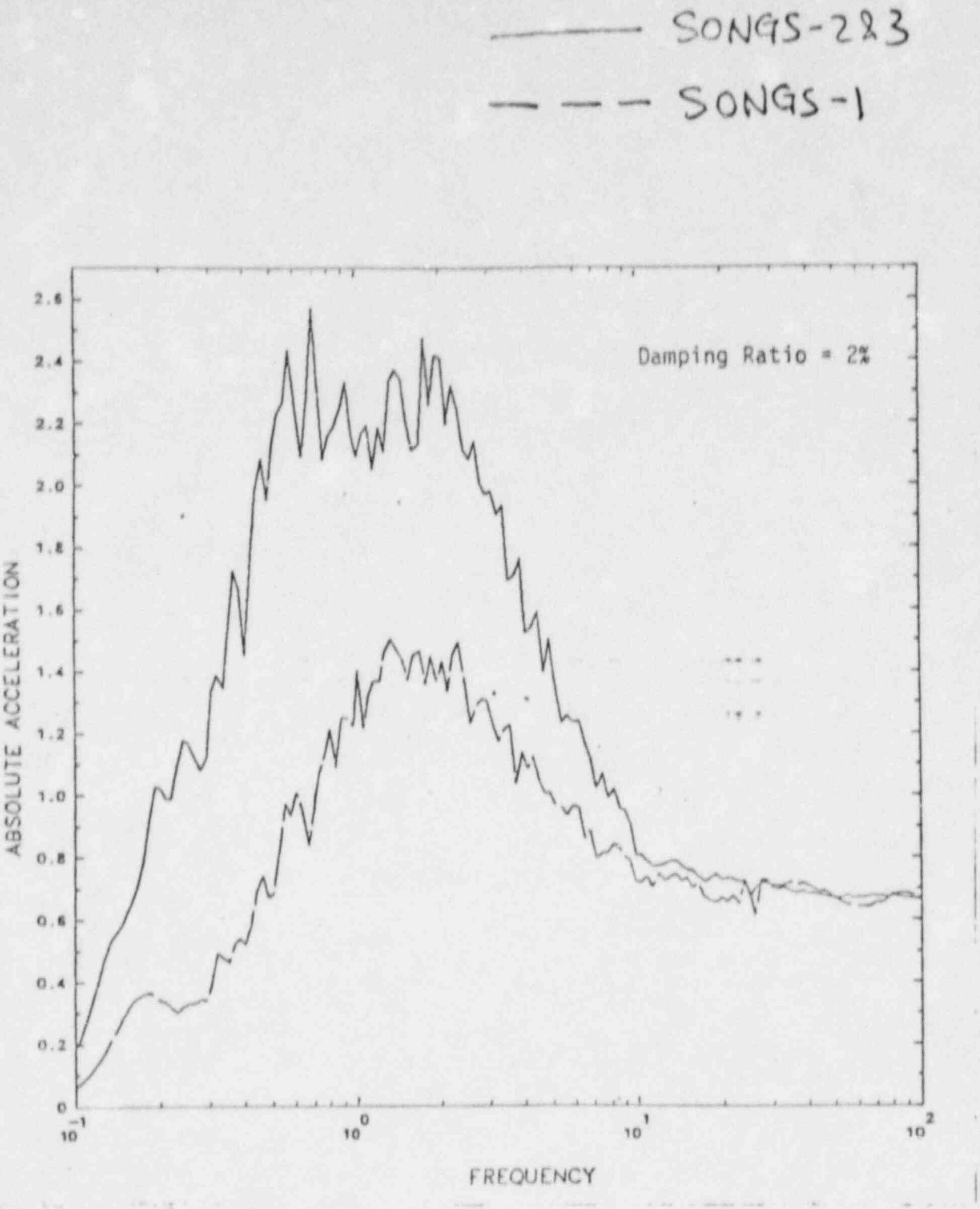

Figure 10. Mean input spectra targeted to the SONGS Unit 1 seismic reevaluaton spectra and the SONGS Units 2 & 3 design spectra.

DRAFT FOR COMMENT

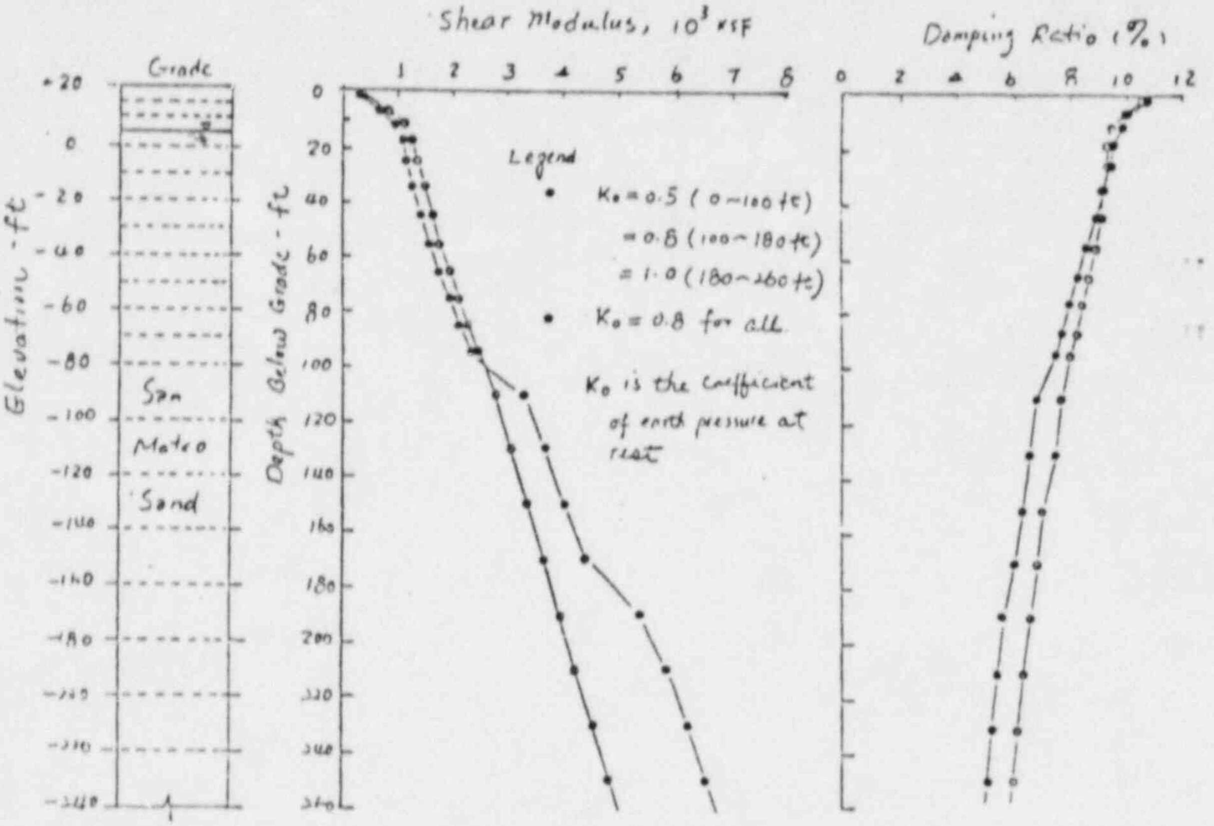

Figure 11. Nominal strain compatible soil properties, based on 8 design motions specified at ground surface.

DRAFT FOR COMMENT

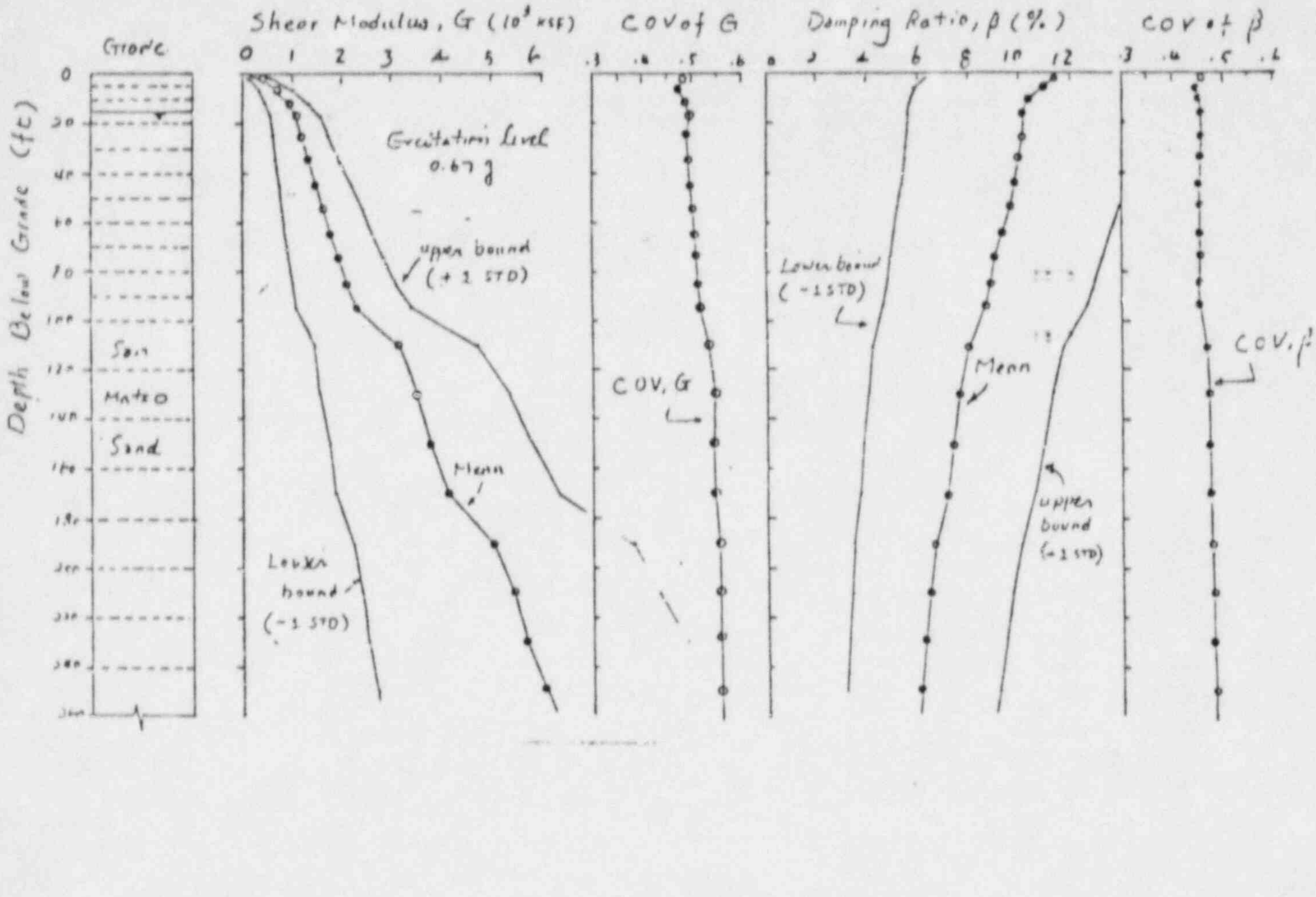

Figure 12. Variation of strain compatible soil properties at 0.67 g level based on simulation experiment and 8 design motions specified at ground surface.

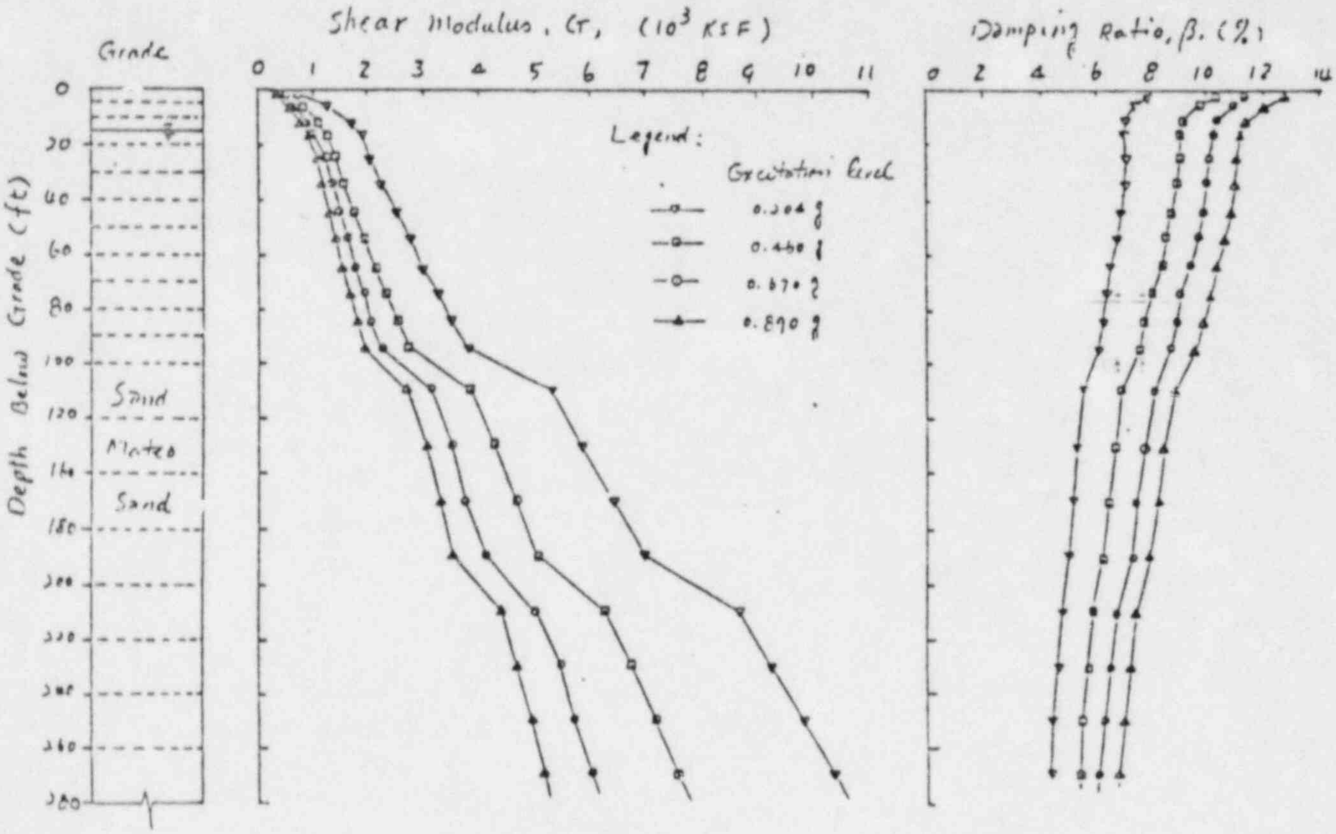

Figure 13. Strain compatible soil properties for different acceleration levels based on simulation experiment and 8 design motion specified at ground surface.

DRAFT FOR COMMENT

A3.3 SSI AND STRUCTURAL MODELS

Determination of the dynamic response of structures housing (or supporting) the auxiliary feedwater system (AFWS) components is needed to provide input motion to the AFWS models. Figure 14 shows a plan view of the San Onofre Unit 1 and schematically illustrates the location of the auxiliary feedwater system. The west feedwater heater platform houses the auxiliary feedwater pumps. Piping system is supported within the heater platform, along the fuel storage building, and within the north turbine building extension before joining the main feedwater lines that penetrate the containment sphere. The main feedwater lines then connect to the steam generators inside the reactor building. Foundation impedance and scattering matrices were obtained and detailed finite element models were constructed for each of these structures. In addition, detailed soil and structural models were made for the turbine pedestal, the south turbine extension, and the control administration building. Although these structures do not house the auxiliary feedwater system itself, they all influence its response and houses its related systems, e.g. electric power, and etc.

A3.3.1 Reactor Building Complex

The SONGS-1 reactor building complex consists of three basic structures. The reactor building is a massive, reinforced concrete structure which is housed inside a spherical steel containment shell. Both the reactor building and the containment sphere are supported on a common foundation whose external surface, which is in contact with the soil, has the shape of a spherical segment. The geometry of this foundation is shown in Fig. 15. Above the foundation the containment sphere and reactor building are isolated from each other. Immediately surrounding the reactor building and containment sphere is the cylindrical sphere enclosure building which is supported on a segmented circular strip footing.

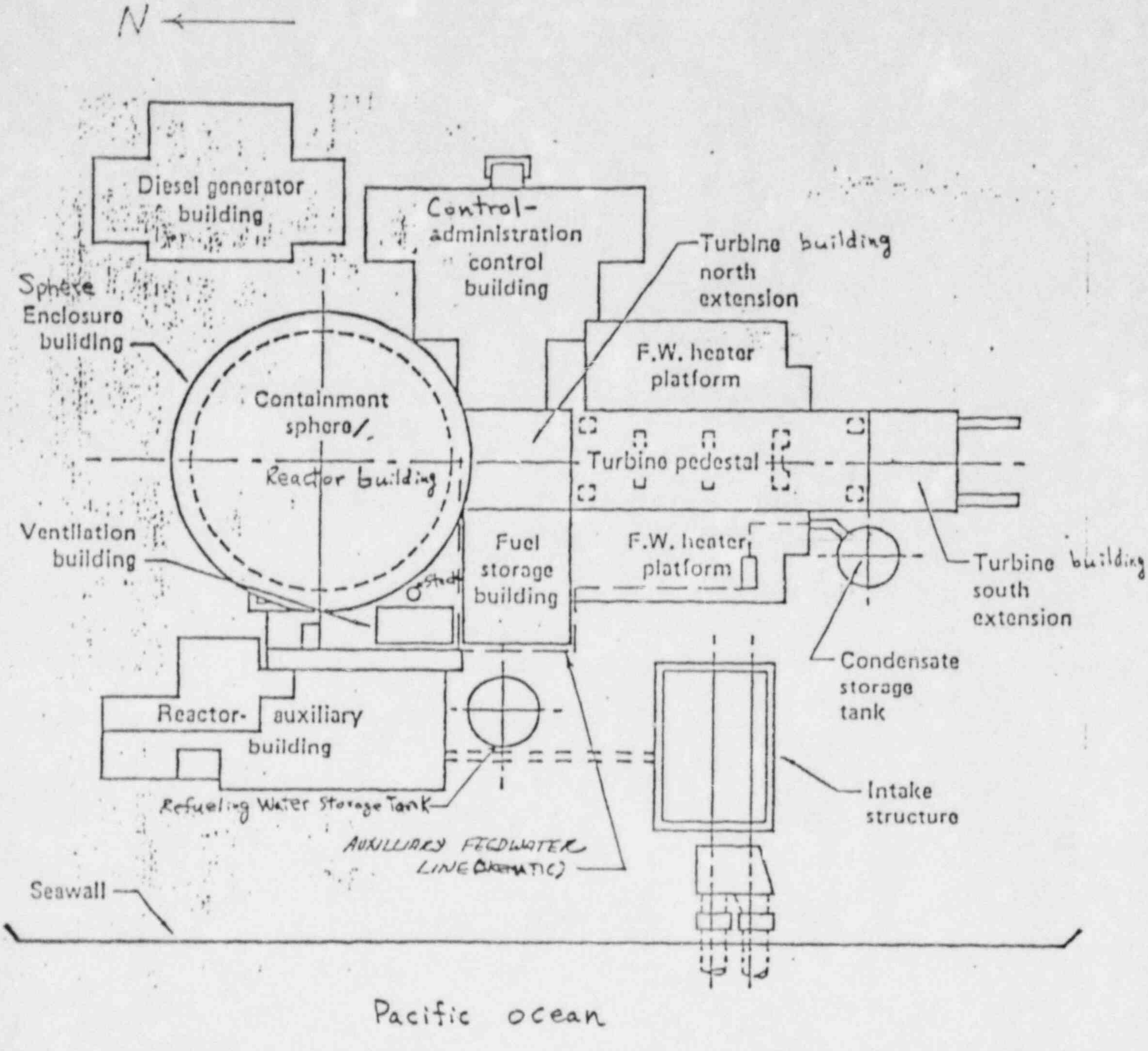

Figure 14. SONGS-1 site plan.

DRAFT FOR COMMENT

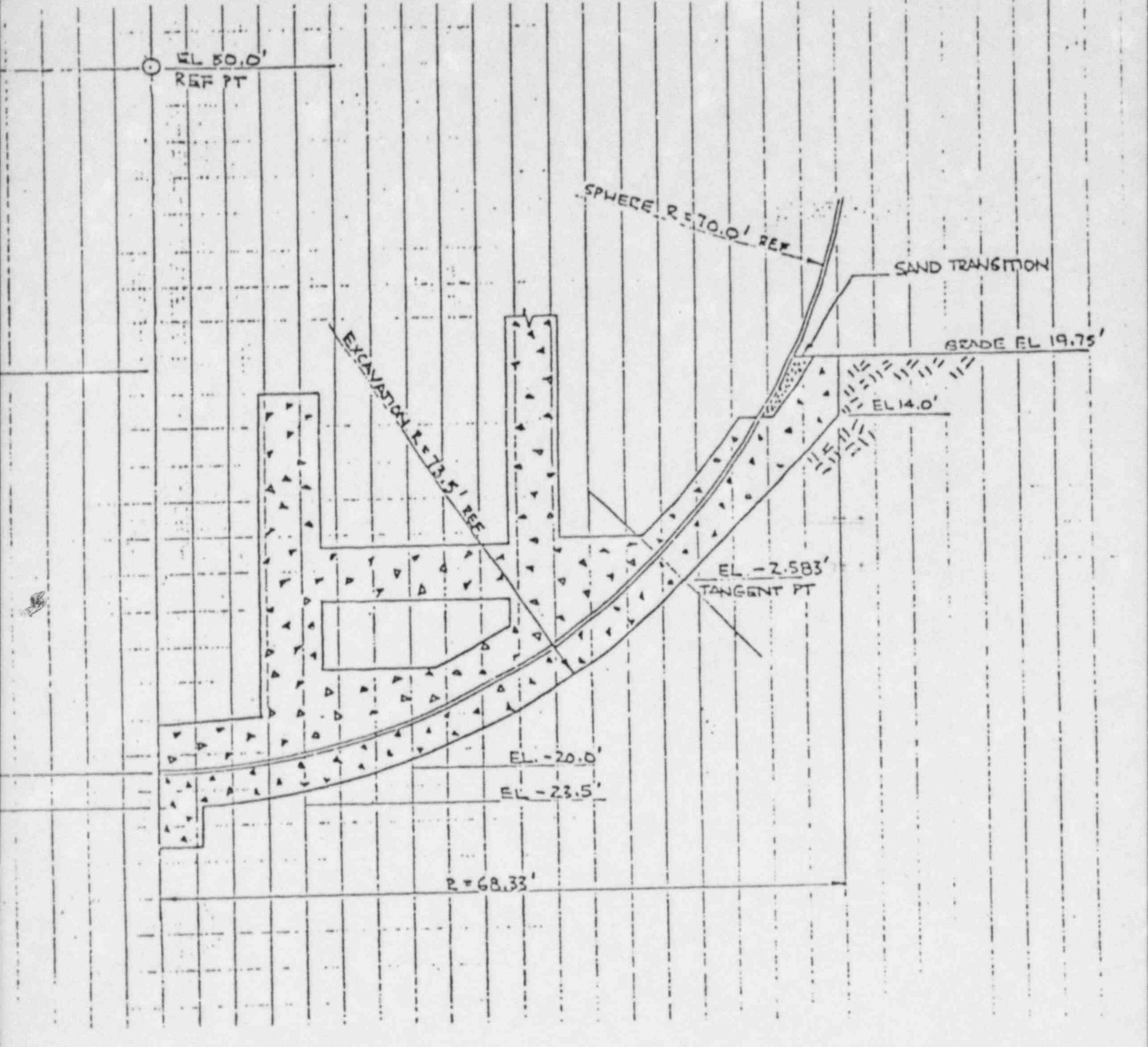

Figure 15. Containment sphere foundaton geometry.

DRAFT FOR COMMENT

A3.3.1.1 Soil Impedance and Scattering Matrices for the Reactor Building Complex

For the initial studies of the reactor building foundation, the foundation of the reactor building is modeled as an isolated, rigid sphere of radius 75.6 ft, embedded in the soil 19.75 ft. The impedance and scattering matrices for the idealized foundation geometry were computed by Prof. J. E. Luco, University of California, San Diego. Typical impedance and scattering components are shown in Figs. 16 and 17, respectively. Similar calculations were performed for a circular surface foundation for comparison purposes. An equivalent circular foundation of radius 68.33 ft and founded 30 ft below the ground surface was analyzed. The size of the foundation corresponds to the projected area of the spherical foundation. It was asusmed to be founded with properties corresponding to those of the SONGS-1 site beginning 30 ft below the free surface—the average depth of the spherical foundation below grade. Two different soil profiles were assumed: the first was the same as that used by Prof. Luco; the second was a uniform halfspace with the same properties as were used by Bechtel in their earlier design calculations. A comparison of the impedances from the three calculations shows reasonably good agreement between results. Differences can be explained by differences in embedment conditions, in soil properties in the immediate vicinity of the foundation and in assumed Poisson's ratios.

Comparisons of static impedance values from these analyses with those obtained from simplified methods (as suggested by Woodward-Clyde and by Roesset) and with values used by Bechtel in their design calculations were also performed. With the exception of the horizontal and rocking impedances (K_{HH} and K_{RR}) for Bechtel design springs and the horizontal impedance (K_{HH}) from Woodward-Clyde formulas, the results appear to be in reasonable agreement when differences in embedment and soil property assumptions are considered. The high value for K_{HH} from the Woodward-Clyde formulas is a result of their assumptions of the correction factor for embedment. The differences in Bechtel springs, K_{HH} and K_{RR}, have not yet been reconciled completely.

DRAFT FOR COMMENT

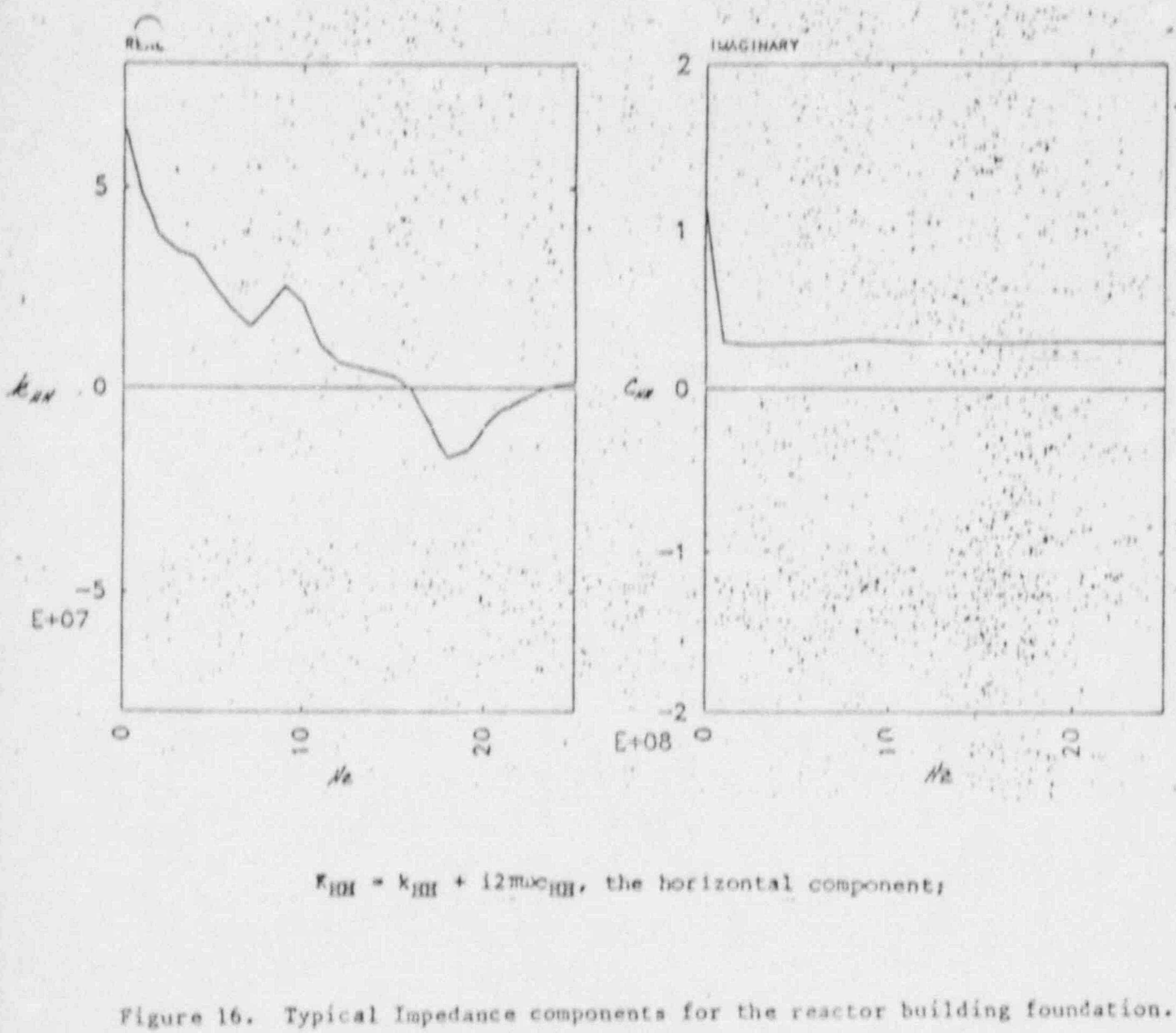

$K_{HH} = k_{HH} + i2\pi\omega c_{HH}$, the horizontal component;

Figure 16. Typical Impedance components for the reactor building foundation.

DRAFT FOR COMMENT

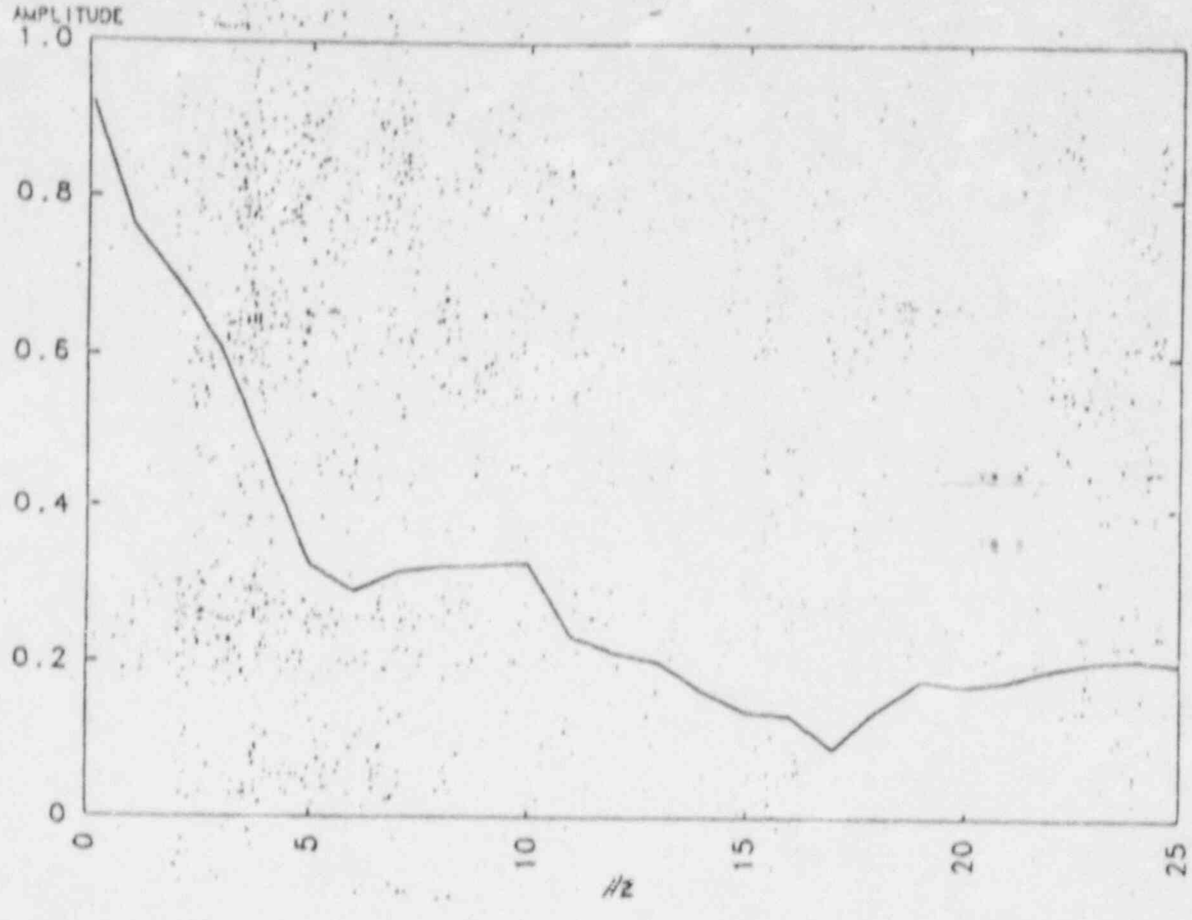

Typical
Figure 17. Scattering component for the reactor building foundation.

DRAFT FOR COMMENT

A.3.3.1.2 Structural Model of the Reactor Building Complex

The structural model of the reactor building complex is described below.

1. Reactor Building

The reactor building is a massive, reinforced concrete structure located within the containment sphere that supports and protects the components of a three-loop nuclear steam supply system (NSSS). The principal elements of the reactor building are the primary and secondary radiation shields, the operating deck, refueling pool and steam generator compartments. The primary shield is a 6 ft thick cylinder that surrounds the reactor pressure vessel. The secondary shield is a 5 ft thick wall, rectangular in plan, that essentially forms the outer perimeter of the reactor building. The refueling pool sits atop the primary shield and, along with the secondary shield, supports the operating deck. The steam generator compartments extend above the deck to act as missile shields for the three steam generators and the pressurizer. Both the reactor building and containment sphere are supported on a partial-spherical foundation.

The finite element model of the reactor building employed 3-D thin plate and shell elements to define the concrete slabs while beam elements defined structural steel frames. Frames included in the model were the operating deck extension on the south side of the secondary shield and the gantry crane support structure. The NSSS and its support were modeled by the reduced mass and stiffness matrices provided by Bechtel/Westinghouse.[9] In all, approximately 650 nodes and 630 elements were used to define the model (Fig. 18).

The nominal strength and density values for both concrete and steel used in the reactor building model are shown in Table 3:

	Modulus of elasticity (psi)	Poisson's ratio	Mass density $lb\text{-}sec^2/in^4$
Concrete	4.40×10^6	0.17	2.25×10^{-4}
Steel	29.0×10^6	0.30	7.34×10^{-4}

Table 3. Material properties of the reactor building model.

DRAFT FOR COMMENT

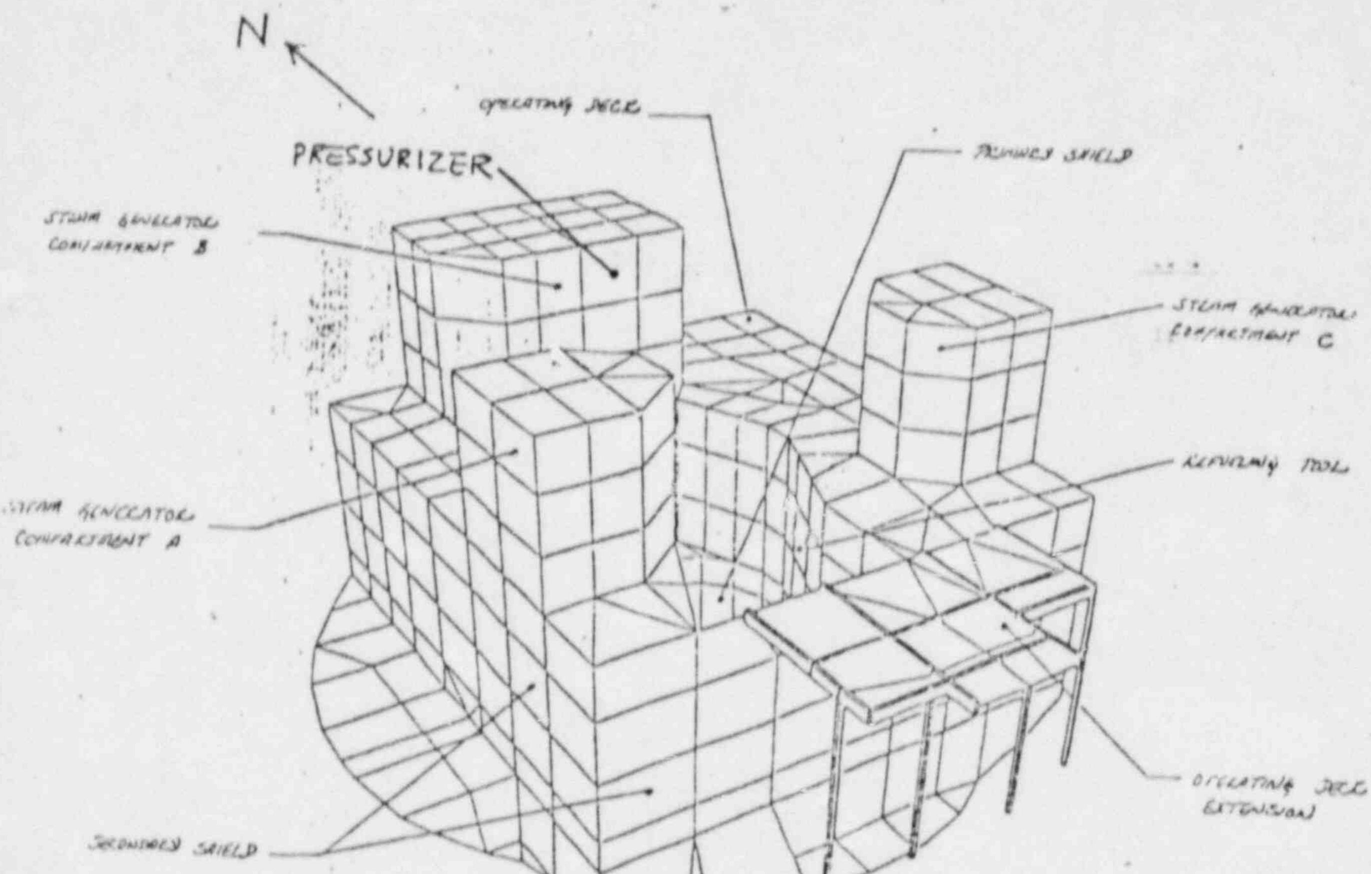

Figure 18. Reactor building model.

DRAFT FOR COMMENT

Considerable effort was made to benchmark the LLNL modal results of the reactor building model with those computed by SCEC/Bechtel. Some differences were found and resolved by refining the reactor building model and exercising engineering judgement. Finally, a version of the reactor building model for subsequent response analyses was eventually established. Differences in the modal frequencies as given by this model and those of SCEC/Bechtel reflect acceptable differences in modeling approaches.

Table 4 lists the major modes of the LLNL reactor building model. The structural response in the y-coordinate (east) direction is dominated by a single mode at 13.3 Hz, while several modes in the range from 13.5 Hz to 20.6 Hz contribute to response in the x-coordinate (south) direction.

Mode Number	Frequency (Hz)	Mass Participation Fraction X	Y	Z
29	13.34	0.4	30.8	0.0
40	16.15	9.2	0.0	0.4
43	17.45	7.8	0.4	0.1
44	18.10	6.7	0.0	0.0
48	20.61	10.5	0.0	2.1
68	33.71	0.9	0.8	9.2
69	34.47	1.5	0.6	11.2
	Mass sum of all modes	77.9	79.3	59.1

Note: First 20 modes are mainly for NSSS and the steel frames for gantry crane.

Table 4. Significant modes of the reactor building model.

2. Containment Sphere

The containment sphere is a stainless steel sphere of 140 ft in diameter and is slightly greater than one inch thick. The upper portion is free-standing, extending 100 ft above finished grade at elevation 19 ft to an approximate elevation of 120 ft. The lower portion is embedded in a concrete foundation previously described (Fig. 19).

The containment sphere is modeled with isoparametric shell of revolution elements as found in the MODSAP program.[10] The axisymmetric model is assumed to be fixed at the point where the sphere becomes encased by the concrete foundation. Consequently, only a partial sphere is modeled. The sand transition area is defined by axisymmetric solid of revolution elements.

A nonuniform grid of elements was used. In those areas where significant spatial variation in stress was expected, a fine discretization of elements were employed. In the free-standing portion of the sphere, a coarser grid was used. One hundred and ten nodes, 83 shell elements and 24 sand elements defined the model. The material properties of the containment sphere are listed in Table 5:

	Modulus of elasticity (psi)	Poisson's ratio	Mass density ($lb\text{-}sec^2/in^4$)
Steel shell	2.9×10^7 lb/in^2	0.30	7.34×10^{-4}
Sand	4.86×10^4 lb/in^2	0.35	not applicable

Table 5. Material properties of the containment sphere model.

DRAFT FOR COMMENT

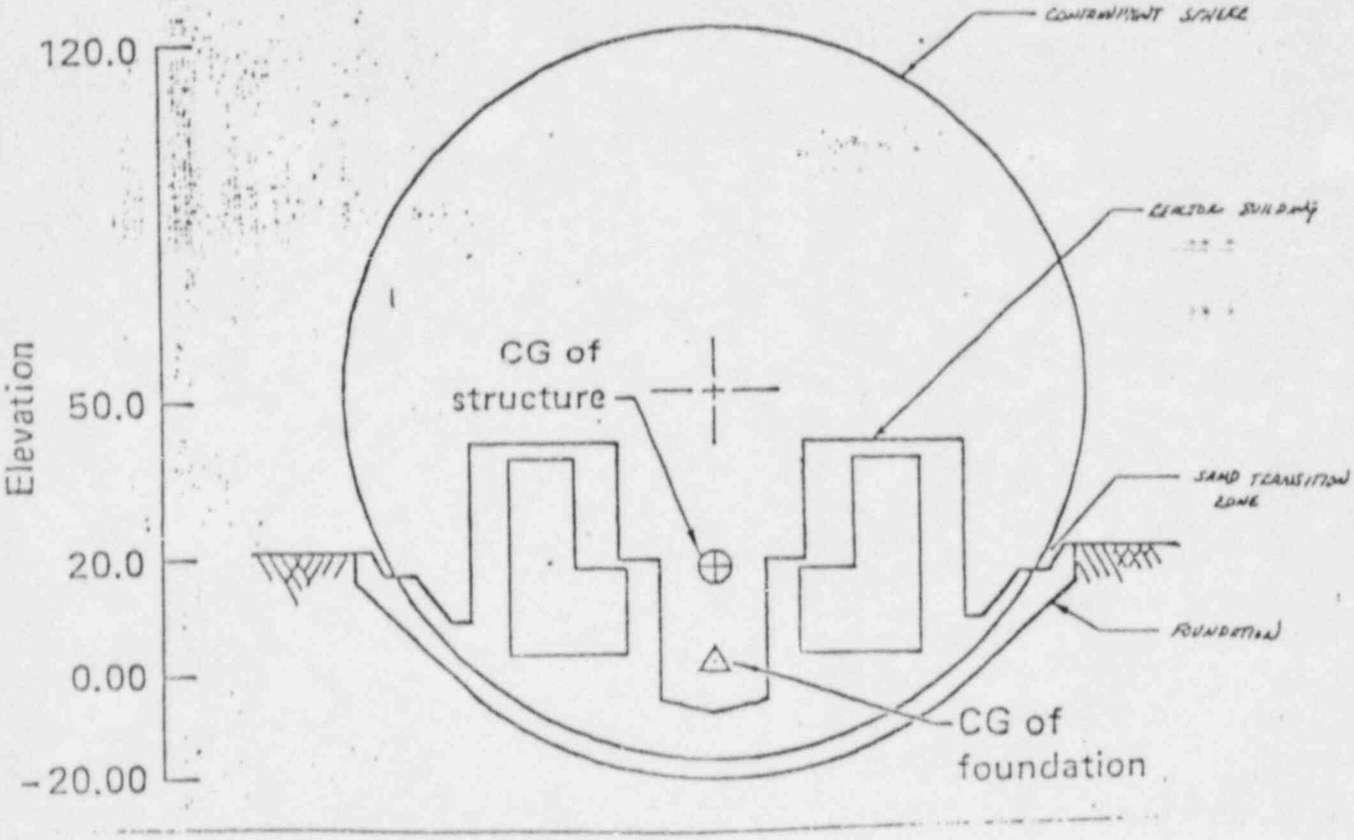

Figure 19. Containment sphere diagram.

The results of two eigenvalue analyses were combined to define the dynamic characteristics of the containment sphere. First, modes corresponding to Fourier harmonic, n = 0, were determined. Then, modes corresponding to n = 1 were found. A total of thirty modes were used in subsequent response analyses of the sphere. Table 6 lists the modal frequencies and mass fractions of major modes where it shows that the first three modes dominate the structural response in the three coordinate directions.

Mode Number	Frequency (Hz)	Mass Participation Fraction X	Y	Z
1	11.42	75.1	0.0	0.0
2	11.42	0.0	75.1	0.0
3	21.31	0.0	0.0	65.3
Mass sum of all nodes		76.4	76.4	68.0

Table 6. Significant modes of the containment sphere model.

DRAFT FOR COMMENT

3. Sphere Enclosure Building

As its name implies, the sphere enclosure building surrounds the containment sphere and reactor building. It is independent of the other structures in that it rests on strip footings that are separate from the reactor building foundation. The enclosure building consists of a cylindrical wall approximately 3-ft thick that supports a conical roof. The cylindrical section has major cut-out openings to accommodate the turbine deck and the piping penetrations. Smaller cut-outs provide for cables, piping and hatches.

The conical roof consists of sloping steel beams forming a composite section with the concrete roof slab. A ring girder supports the roof at its intersection with the cylindrical wall.

The finite element model of the sphere enclosure building is shown in Fig. 20. The cut-out that accommodates the turbine deck is evident. Beam elements combined with thin plate and shell elements were used to model the roof while thin plate and shell elements alone defined the cylindrical wall. A total of 463 nodes, 549 shell elements and 160 beam elements were used to produce the fixed-base model. The material properties of sphere enclosure building are described in Table 7.

	Modulus of elasticity (psi)	Poisson's ratio	Mass density ($lb\text{-}sec^2/in^4$)
Steel beams	29×10^6	0.30	7.34×10^{-4}
Concrete shell	3.834×10^6	0.17	2.25×10^{-4}

Table 7. Material properties of the sphere enclosure building model.

Modal analysis results for the sphere enclosure building are listed in Table 8.

Mode Number	Frequency (Hz)	Mass Participation Fraction X	Y	Z
1	3.54	48.5	0.2	0.0
3	6.33	1.8	54.1	1.5
4	7.34	0.5	0.5	19.5
7	7.83	9.4	7.5	0.2
25	14.68	0.0	6.8	9.8
Mass sum of all nodes		90.1	90.3	46.8

Table 8. Significant modes of the sphere enclosure building model.

DRAFT FOR COMMENT

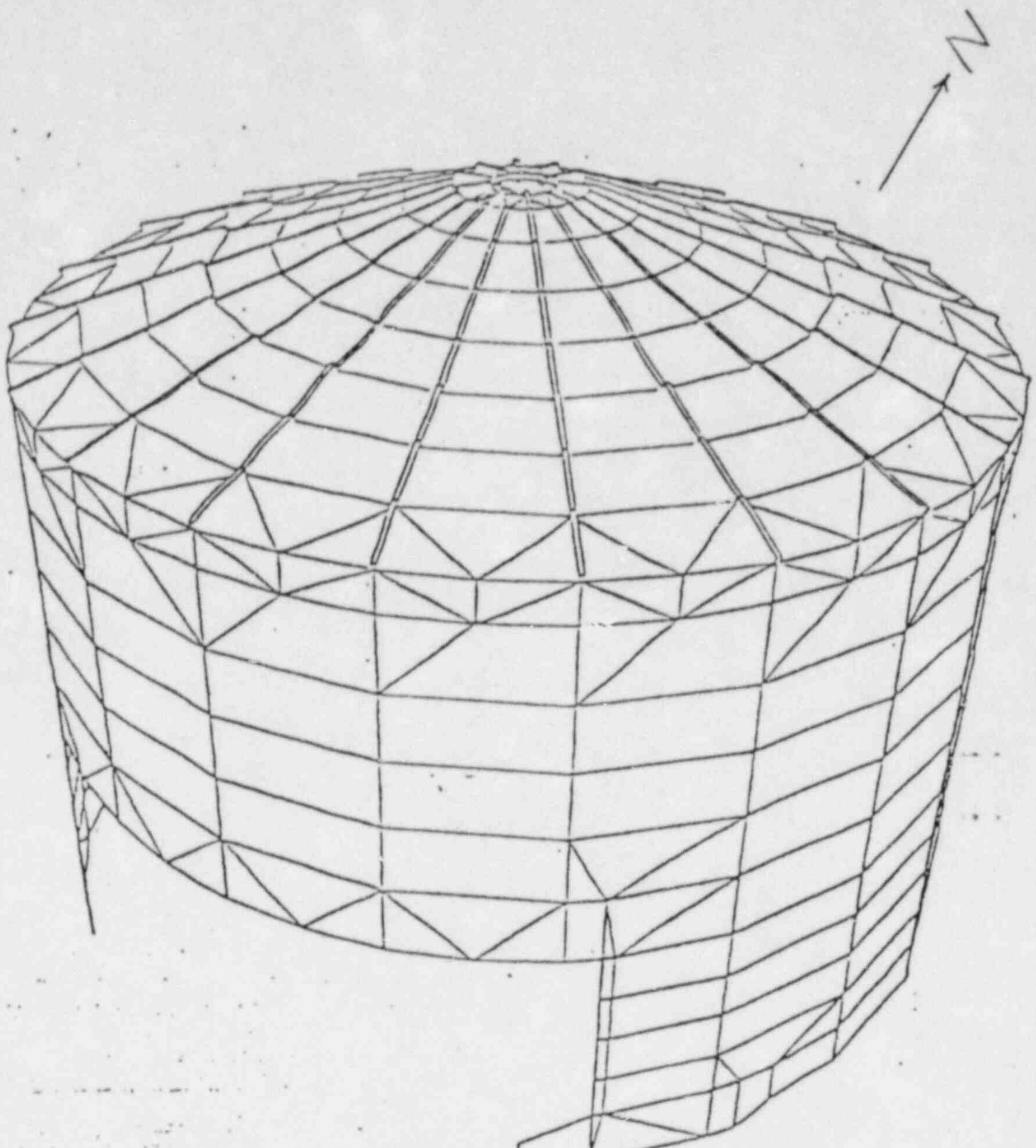

Figure 20. Sphere enclosure building model.

DRAFT FOR COMMENT

A3.3.2 Turbine Building Complex

The turbine building is comprised of five structures: the turbine pedestal; the north and south turbine building extensions; and the east and west feedwater heater platforms. These areas and their foundations are shown in Fig. 21. Each of these areas is enclosed by a structure which is physically separated from its adjacent structures above the foundation. However, most of these structures are supported on a combination of isolated and combined column footings and/or large basemats. Furthermore, every structure shares at least one common foundation mat or combined footing with another structure. This structure/foundation configuration greatly complicates the SSI analysis of the turbine building because it means that the foundations will interact not only through the soil, but also through the structures which they support. The SSI problem should be treated for this case by first developing impedance functions and foundation input motions which include the effects of interaction between foundations through the soil. Once these properties are developed, the SSI response of the structures can be calculated using an algorithm which includes the effects of multiple foundations supporting each structure.

Our SSI work on the turbine building proceeded as far as the development of preliminary models of the major foundations, calculation of impedance functions for these models, and in some cases, the performance of sensitivity studies to investigate the effect of the refinement of the spatial discretization of the models. The foundations which have been modeled are: the turbine-generator pedestal foundation mat; Anchor Block No. 1 (West feedwater heater platform); Anchor Block No. 2 (east feedwater heater platform); fuel storage pool; and a typical isolated footing, 5 ft x 12 ft in dimension, supporting a single column.

The studies of impedances for these foundations consisted of calculations assuming isolated foundations. Foundation shapes which have not yet been studied include the combined footings which support three columns spaced about 20 ft apart and the square or near-square footings of differing sizes. These studies are briefly summarized below.

DRAFT FOR COMMENT

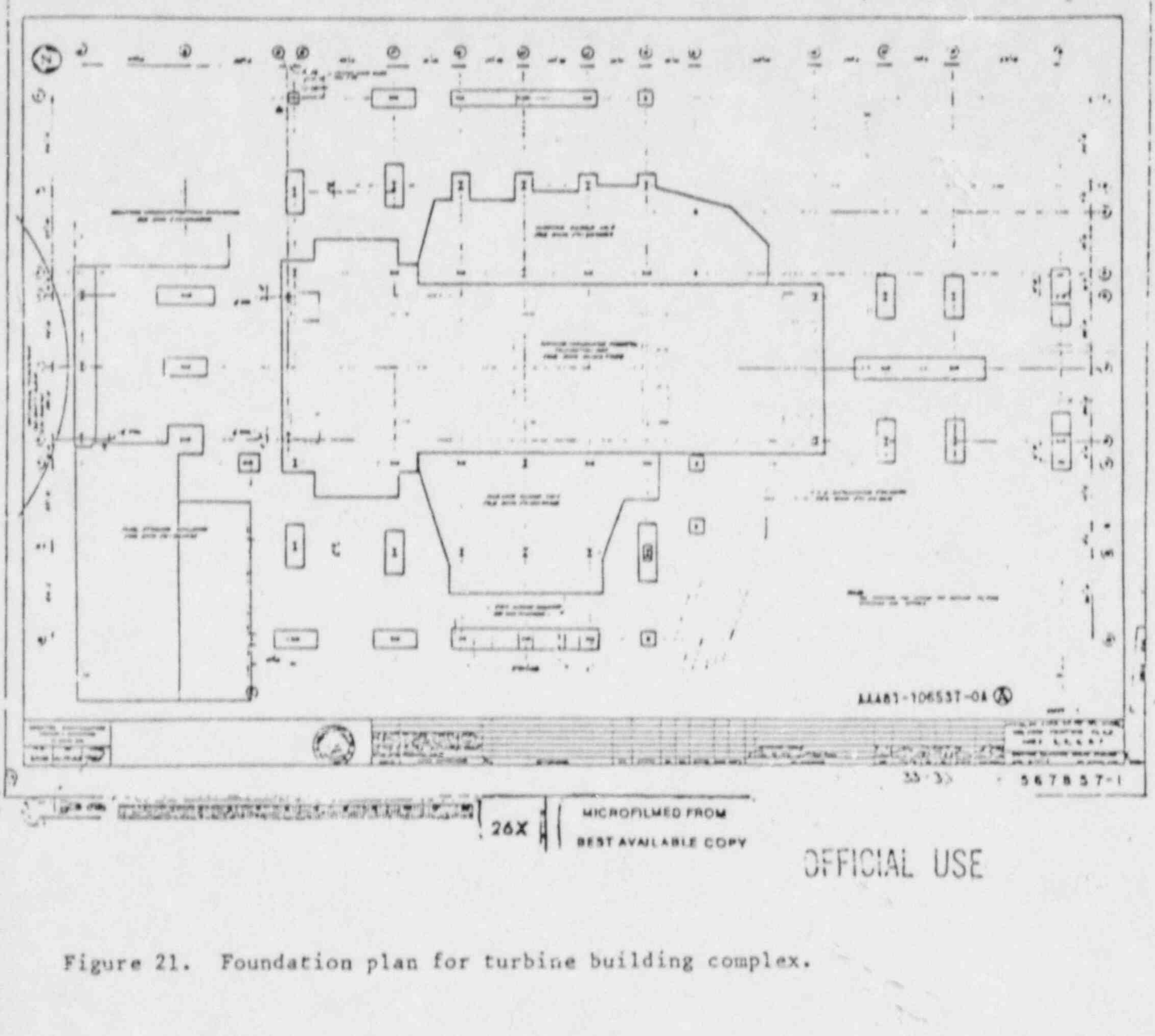

26X MICROFILMED FROM BEST AVAILABLE COPY

OFFICIAL USE

Figure 21. Foundation plan for turbine building complex.

DRAFT FOR COMMENT

A3.3.2.1 Impedance and Scattering Matrices

The impedance and scattering matrices for the turbine building complex are described below.

1. Turbine Pedestal Foundation Mat

This foundation is the largest of all the foundations associated with the turbine building. It extends about 150 ft from north to south and is about 50 ft wide. The foundation mat is 5 ft thick over most of its extent. In addition to supporting the turbine generator pedestal, the foundation mat also provides support to several columns belonging to adjacent structures: the turbine building northern and southern extensions, and the east and west feedwater heater platforms.

A fairly detailed model was constructed to describe the shape of the turbine generator pedestal foundation mat. The discretization is shown in Fig. 22. The foundation impedances for this model were computed by using the soil profile described previously. A representative impedance is shown in Fig. 23. The foundation reference point (origin of coordinate system of the model) was chosen close to the centroid of the foundation shape in an effort to minimize coupling between east-west translation and torsion and between vertical translation and north-south rocking. Minimizing this coupling helps to isolate different SSI effects and makes it easier to understand the dynamic behavior of the soil/structure system.

The impedances appear to be reasonable by comparing them to impedances published by Wong and Luco[11] for an equivalent rectangular foundation on a uniform viscoelastic halfspace. Considering the perfect symmetry of the retangular foundation, differences in material damping (Wong and Luco used 5%, while the material damping in the layered halfspace was nearly 10% near the surface), and differences between behavior of uniform and layered halfspaces, the two sets of impedances agree well.

2. Isolated and Combined Column Footings

A number of isolated column footings are located in the turbine building area. These vary in size from 3 ft x 3 ft to 5 ft x 16 ft. Several combined footings, each supporting three columns of a single structure and spaced at 18 to 20 feet, also exist in this area. A 5 ft x 6 ft spread footing exists near the location where the turbine pedestal foundation mat, the north turbine building extension, the fuel storage building and the west feedwater heater platform meet. This footing supports two closely situated columns, one of which belongs to the fuel storage building, the other to the west feedwater heater platform.

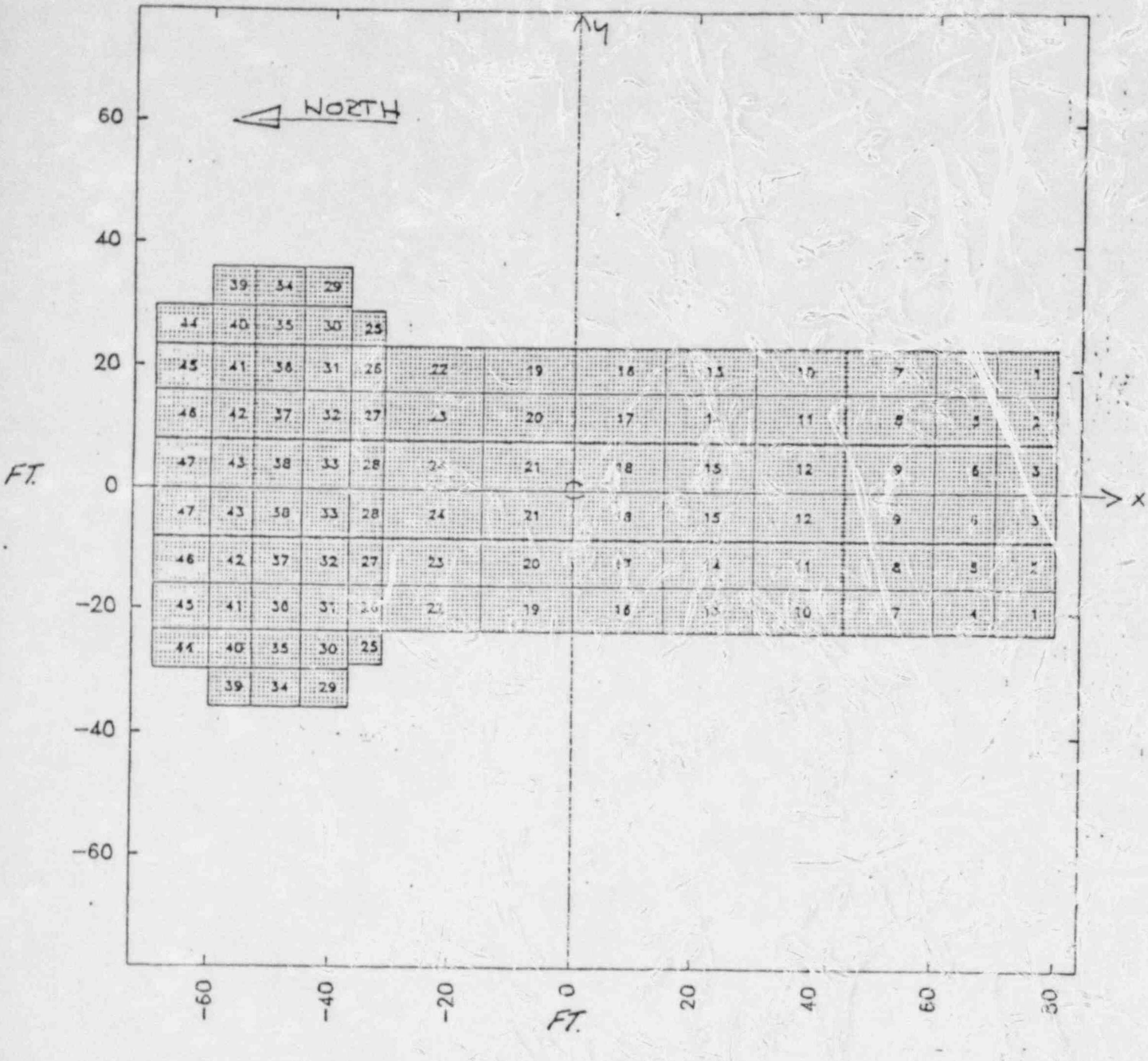

Figure 22. Turbine pedestal foundation model.

DRAFT FOR COMMENT

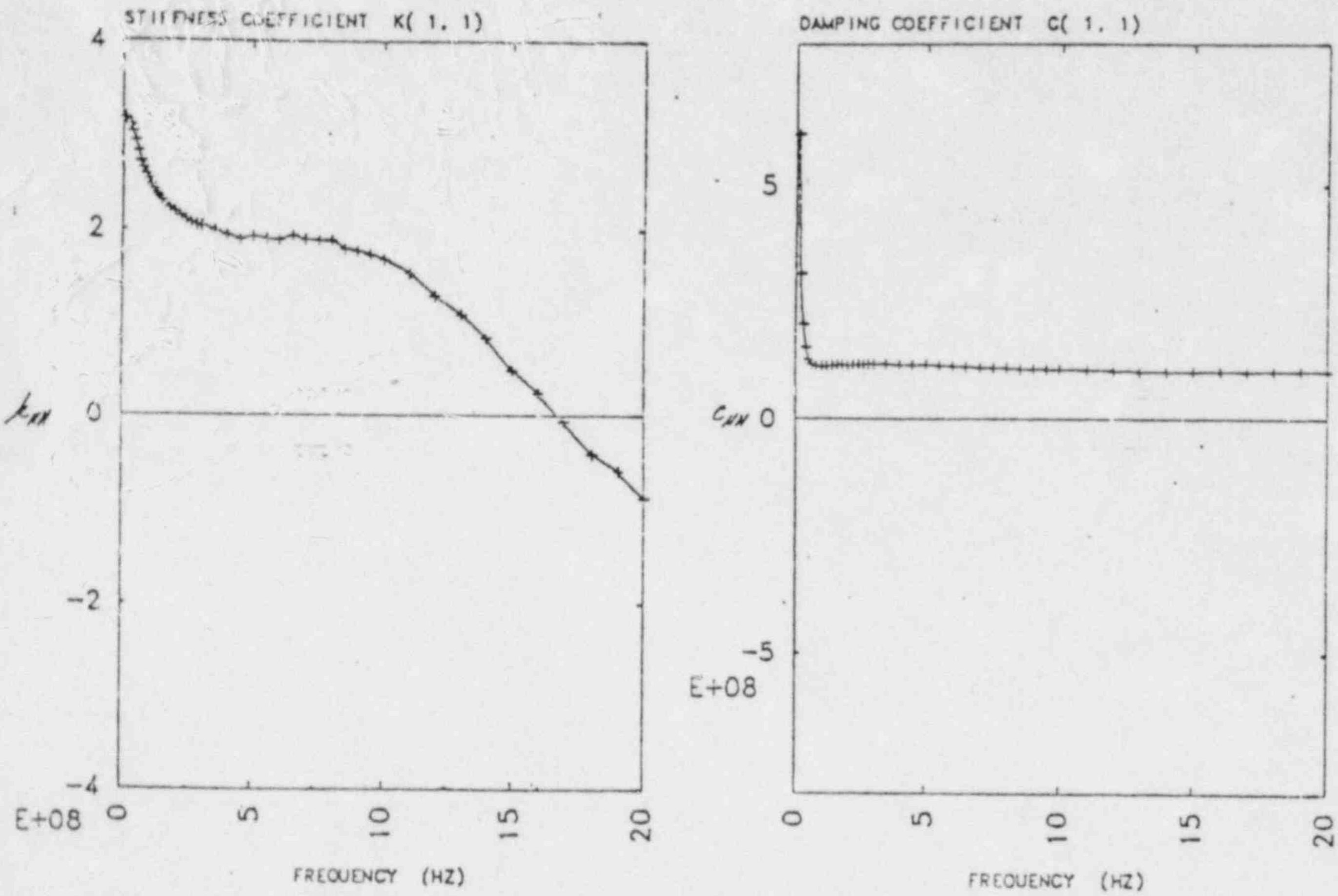

Figure 23. Typical impedance component for the turbine pedestal foundation model.

DRAFT FOR COMMENT

Two models of a typical isolated footing were compared to see the effect of spatial discretization on the impedance functions. Their dimensions are both 5 ft by 12 ft. Most of the impedance terms compared fairly closely, being within 10% of each other. However, for the rocking term about the long axis (K_{44}), the coarse model was 20% softer than the refined one. The significance of the difference that would be introduced by use of the coarse model depends on the importance of the columns being supported.

3. Anchor Block No. 1, West Feedwater Heater Platform

Anchor Block No. 1 is a concrete slab about 60 ft long, 40 ft wide and 12.5 ft thick. It is immediately adjacent to the turbine generator pedestal foundation mat on the west side and is separated from it by one inch Flexcell. Four tunnels approximately 6 ft in diameter are located in the anchor block which provide cooling water to the turbine generator.

We constructed a fairly refined model to describe the geometry of the anchor block. The model is shown in Fig. 24. The foundation reference point was selected near the centroid of the foundation shape to minimize coupling between the foundation degrees of freedom. Figure 25 shows a typical impedance computed for the isolated foundation. As might be expected, weak coupling exists between the horizontal translations and torsional impedance and between rocking and vertical translation, since the foundation is not symmetric in either direction.

4. Anchor Block No. 2, East Feedwater Heater Platform

Anchor Block No. 2 is a concrete slab about 100 ft long, 30 ft wide and 14.5 ft thick. It is immediately adjacent to the turbine generator pedestal foundation mat and is separated from it by one inch Flexcell. Four six feet diameter tunnels are located in the slab. These tunnels carry the turbine's cooling water to a 9 ft discharge culvert originating in the anchor block and running its full length and passing into the turbine pedestal foundation mat.

Two foundation models of Anchor Block No. 2 were constructed in order to study the effects of spatial discretization on the computed impedances. The models are shown in Figs. 26 and 27. Model A is the coarser of the two; the

DRAFT FOR COMMENT

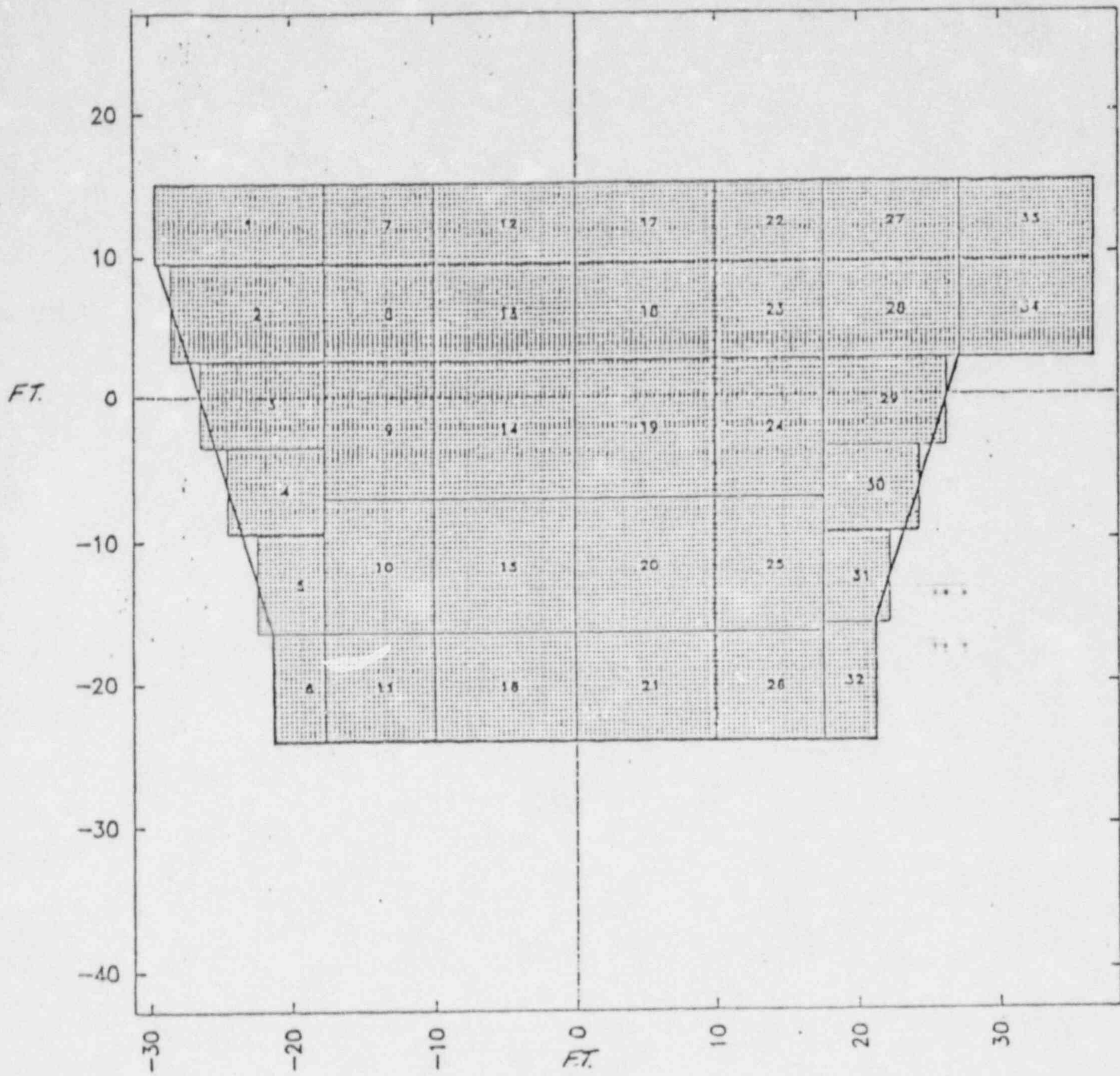

Figure 24. Anchor block number 1 foundation model.

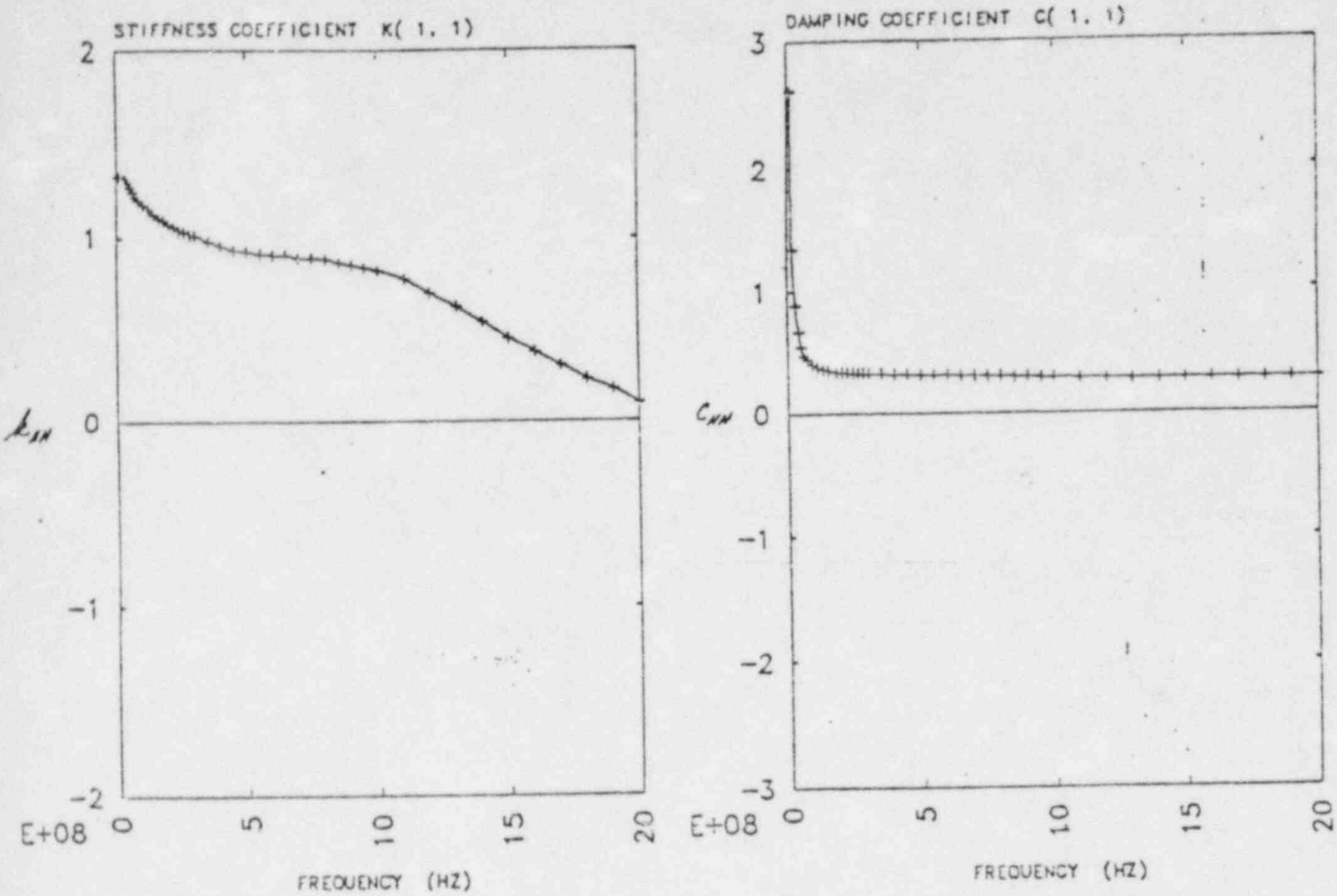

Figure 25. Typical impedance component for anchor block number 1 foundation model.

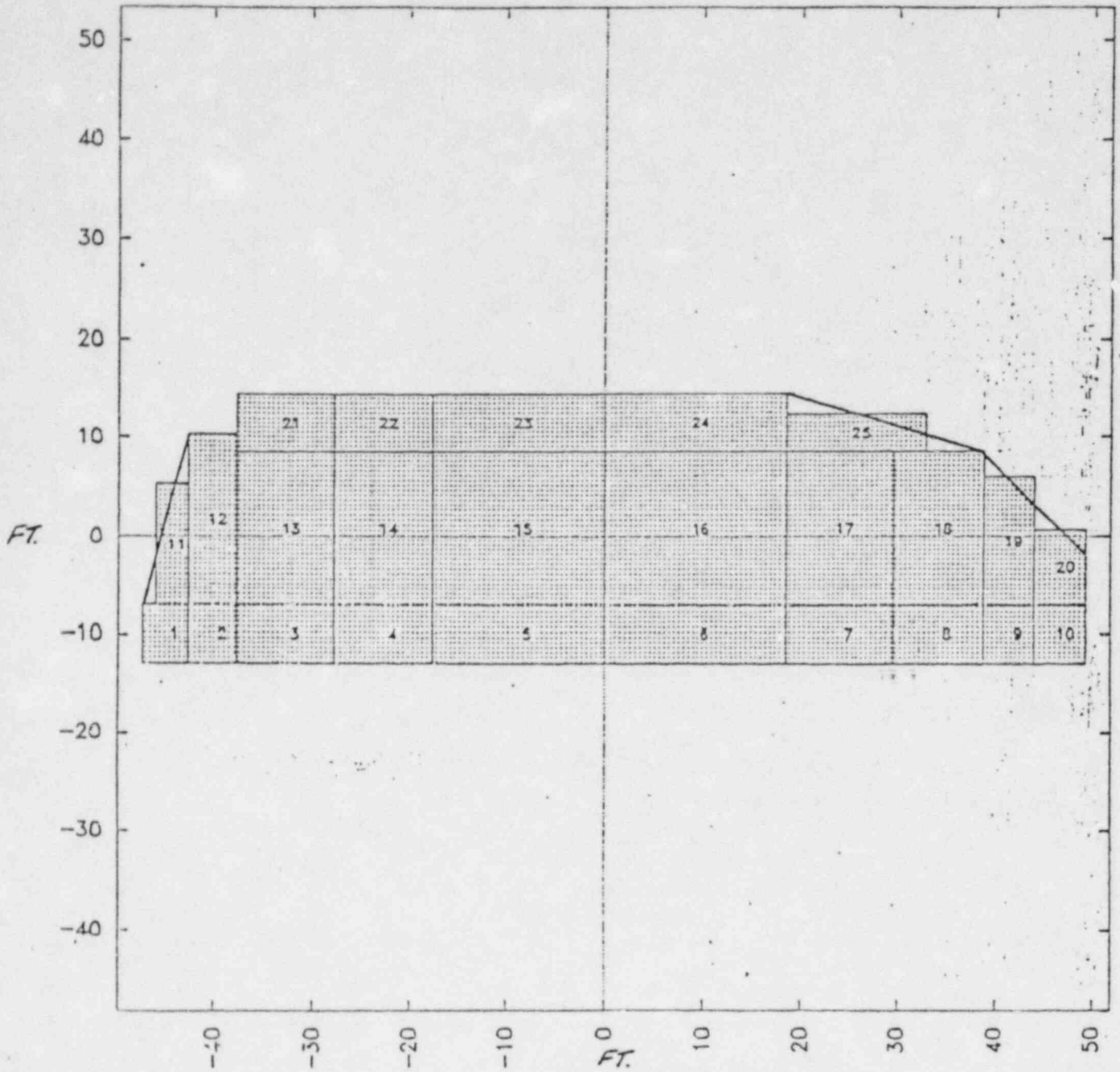

Figure 26. Anchor block number 2 foundation model A.

DRAFT FOR COMMENT

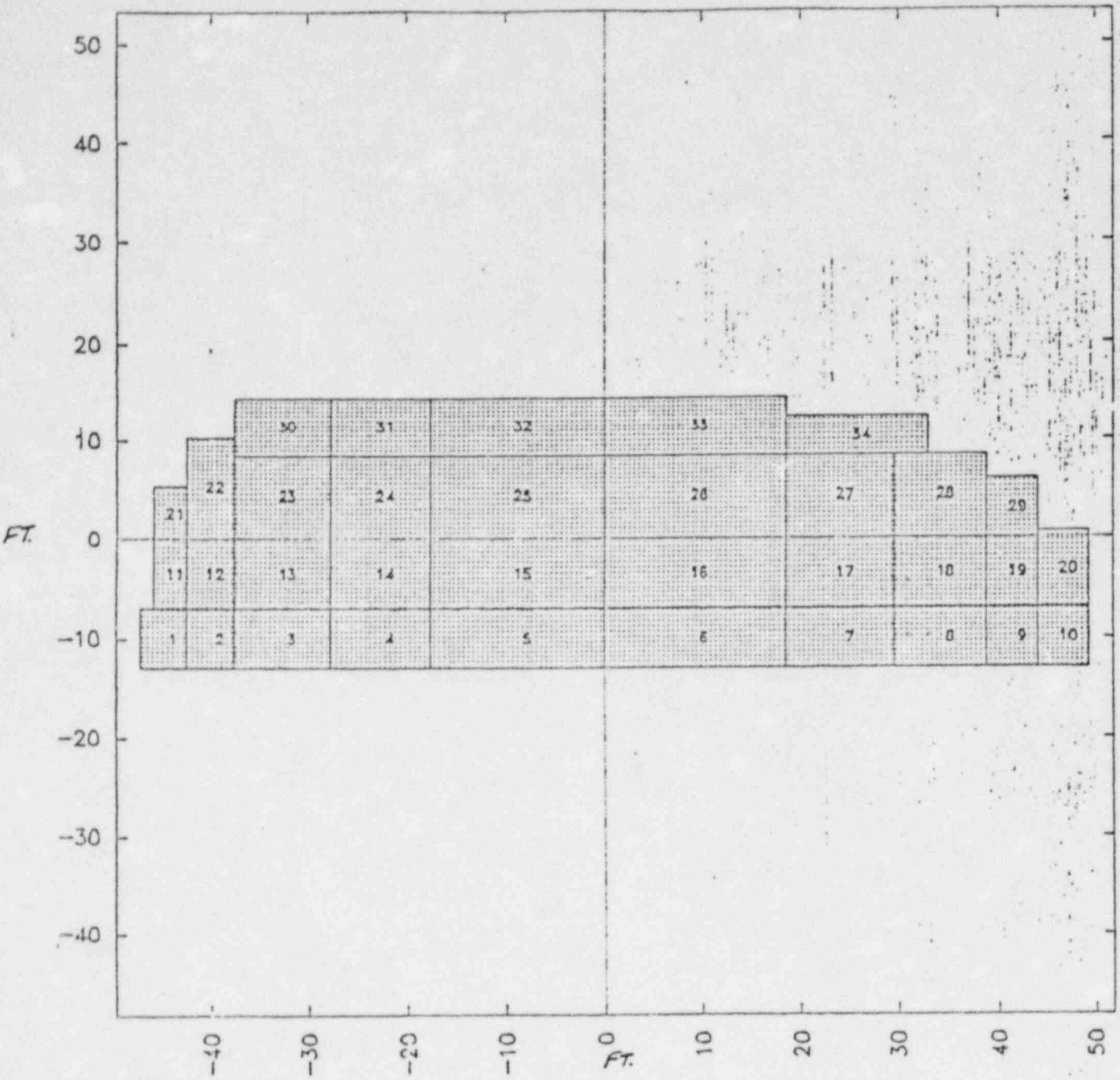

Figure 27. Anchor block number 2 foundation model B.

DRAFT FOR COMMENT

subregions in Model B are either the same as those in Model A, (e.g. along the extreme east & west sides) or are subdivisions of them (e.g. along the x-axis of the model). In order to minimize the coupling effects, the reference point was chosen to be close to the centroid of the foundation shape. Figure 28 shows a comparison of a typical impedance term computed for the two models. For all terms, the impedances compare quite well at frequencies below 10 Hz. The only terms where significant differences occur above 10 Hz are east-west rocking (K_{44}), rocking/vertical translation coupling (K_{34} and K_{35}), and east-west translation (rocking coupling K_{24}). For a detailed SSI analysis of the West Heater Bay area where the auxiliary feedwater system is located, we would expect that these differences would have little effect, and that the coarser Model A would be adequate.

DRAFT FOR COMMENT

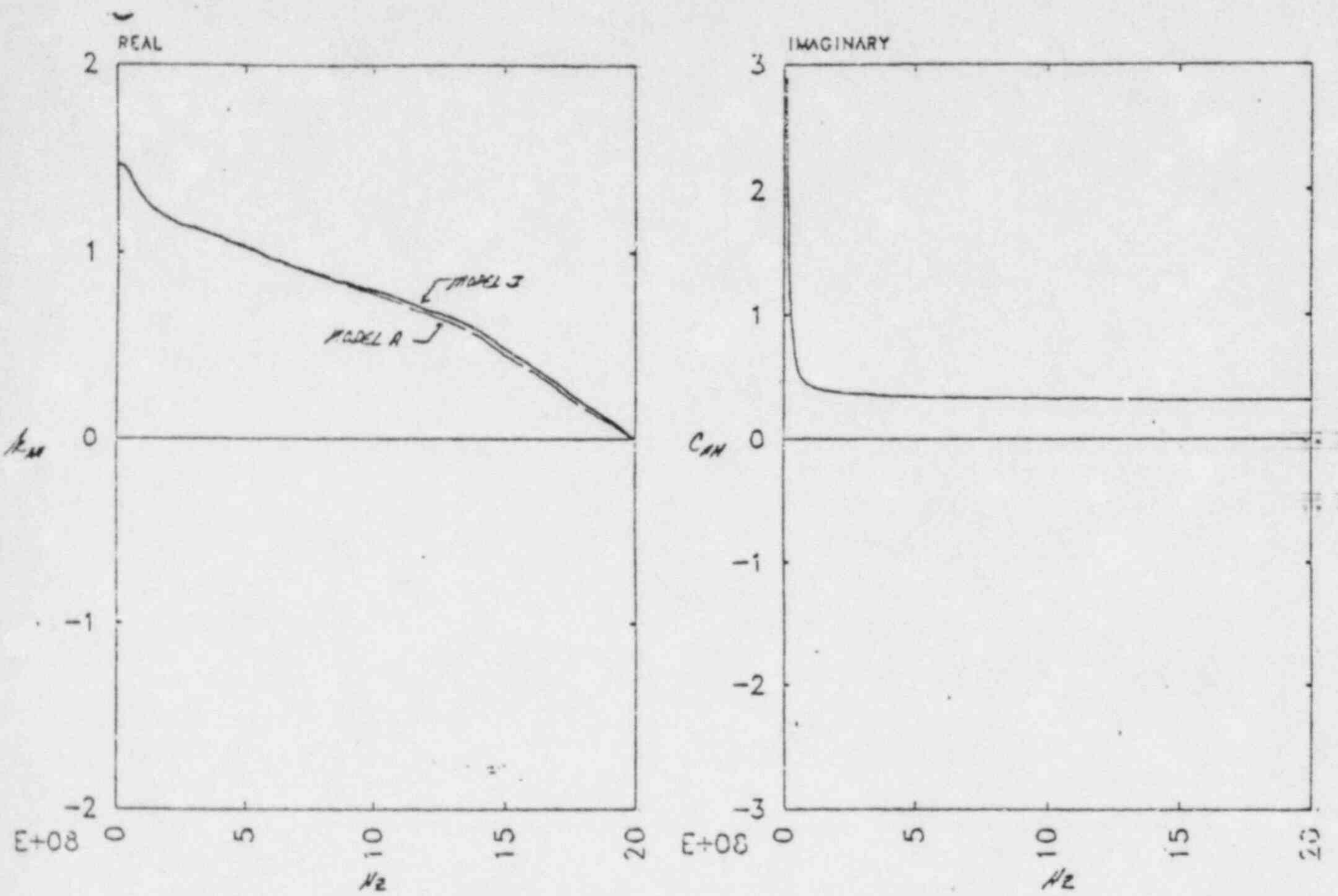

Figure 28. Typical impedance component in the comparison of the two anchor block models.

A3.3.2.2 Structural Model

The structural models for the turbine building complex are described below.

1. Turbine Pedestal

The turbine pedestal is a massive, reinforced concrete space frame. The structure consists of an 8 ft thick, reinforced concrete roof supported by two end rectangular frames and three intermediate pedestals. The frames and the pedestals rest on a 5 ft thick concrete foundation mat.

The finite element model of the turbine pedestal consists of variable-node, thick shell and three-dimensional solid elements for the roof, columns and pedestals (Fig. 29). One hundred eight elements connect 414 nodes. Equipment loading specified for the turbine pedestal is included by increasing the densities of appropriate elements.

The results of a fixed-base eigenvalue analysis are listed in Table 9.

Mode Number	Frequency (Hz)	Mass Participation Fraction X	Y	Z
1	7.97	90.9	0.0	0.0
2	9.86	0.0	15.8	0.0
3	11.22	0.0	60.3	0.0
6	20.95	0.0	0.0	13.4
12	26.67	0.0	0.0	18.0
13	27.12	0.0	0.0	15.4
15	30.55	0.0	11.2	0.0
16	30.81	0.0	0.0	13.2
	Mass sum of all nodes	90.0	89.6	64.4

Table 9. Significant modes of the turbine pedestal model.

DRAFT FOR COMMENT

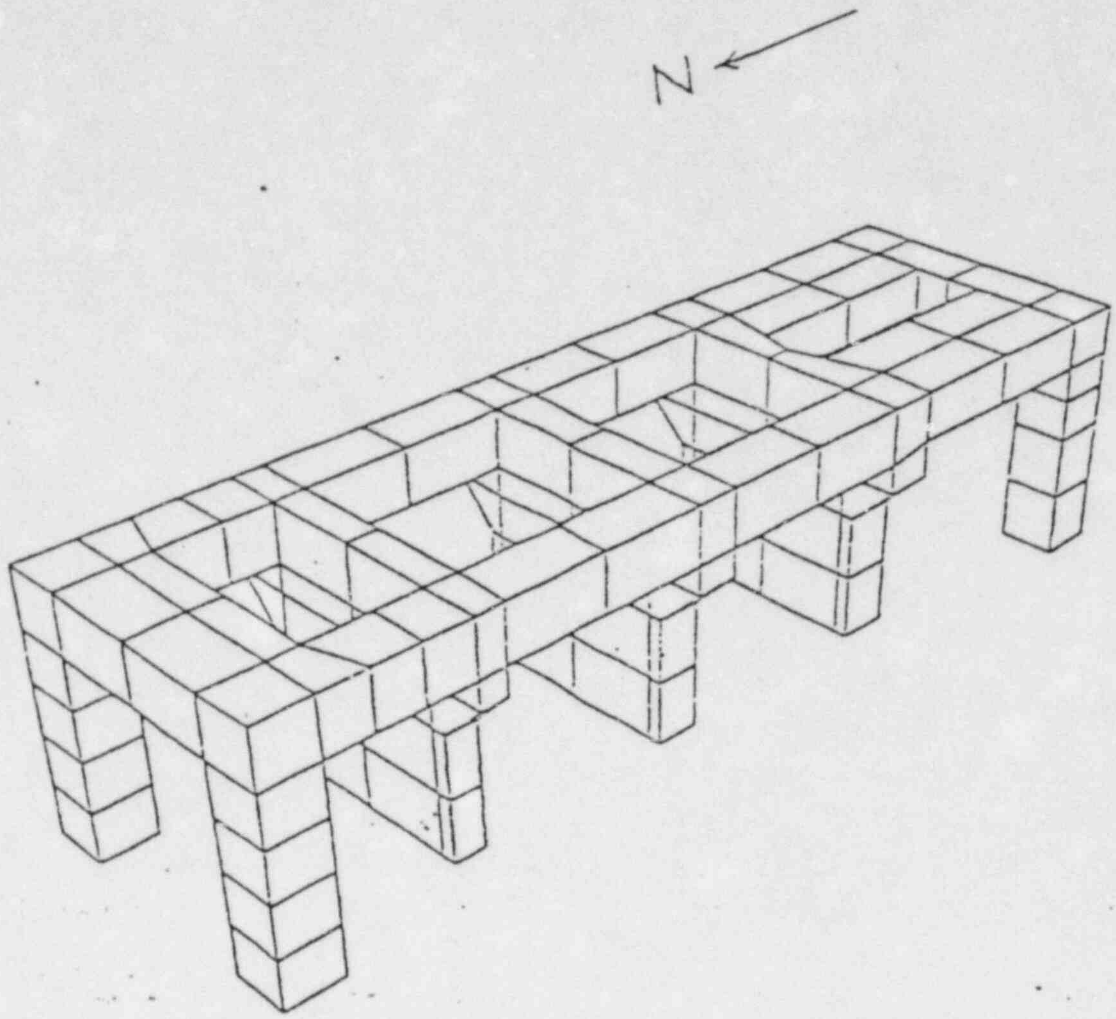

Figure 29. Turbine pedestal model.

DRAFT FOR COMMENT

2. North and South Turbine Building Extension

The north and south turbine building extensions are rectangular structures located ou either end of the turbine pedestal. They both consist of prestressed concrete deck at elevation 42 ft supported by steel framing. The columns supporting the roof slabs rest on individual or combined footings.

The finite element models of both structures employed thin plate and shell elements to define the concrete deck, while beam elements modeled the structural steel frames. Where adequate shear anchors exist, composite section properties were calculated for steel roof beams and the concrete deck.

The north turbine building extension model consisted of 95 nodes, 114 beam element and 50 shell elements. Figure 30 illustrates the model, while Table 10 lists the results of a fixed-base eigenvalue analysis.

Mode Number	Frequency (Hz)	Mass Participation Fraction X	Y	Z
1	4.30	36.6	13.3	0.2
2	4.65	4.3	83.7	0.0
3	5.23	55.3	0.2	0.0
7	7.61	0.0	0.1	13.6
8	8.78	0.2	0.0	26.2
	Mass of all modes	98.0	97.5	79.6

Table 10. Significant modes of the north turbine building extension model.

In a fashion similar to the north extension, the deck and support frame of the south turbine building extension were modeled with thin plate and beam elements, respectively. Concrete block walls that surround the structure on three sides made use of beam elements to define the out-of-plane behavior of the walls and plane-stress elements to model their in-plane behavior. These elements use

DRAFT FOR COMMENT

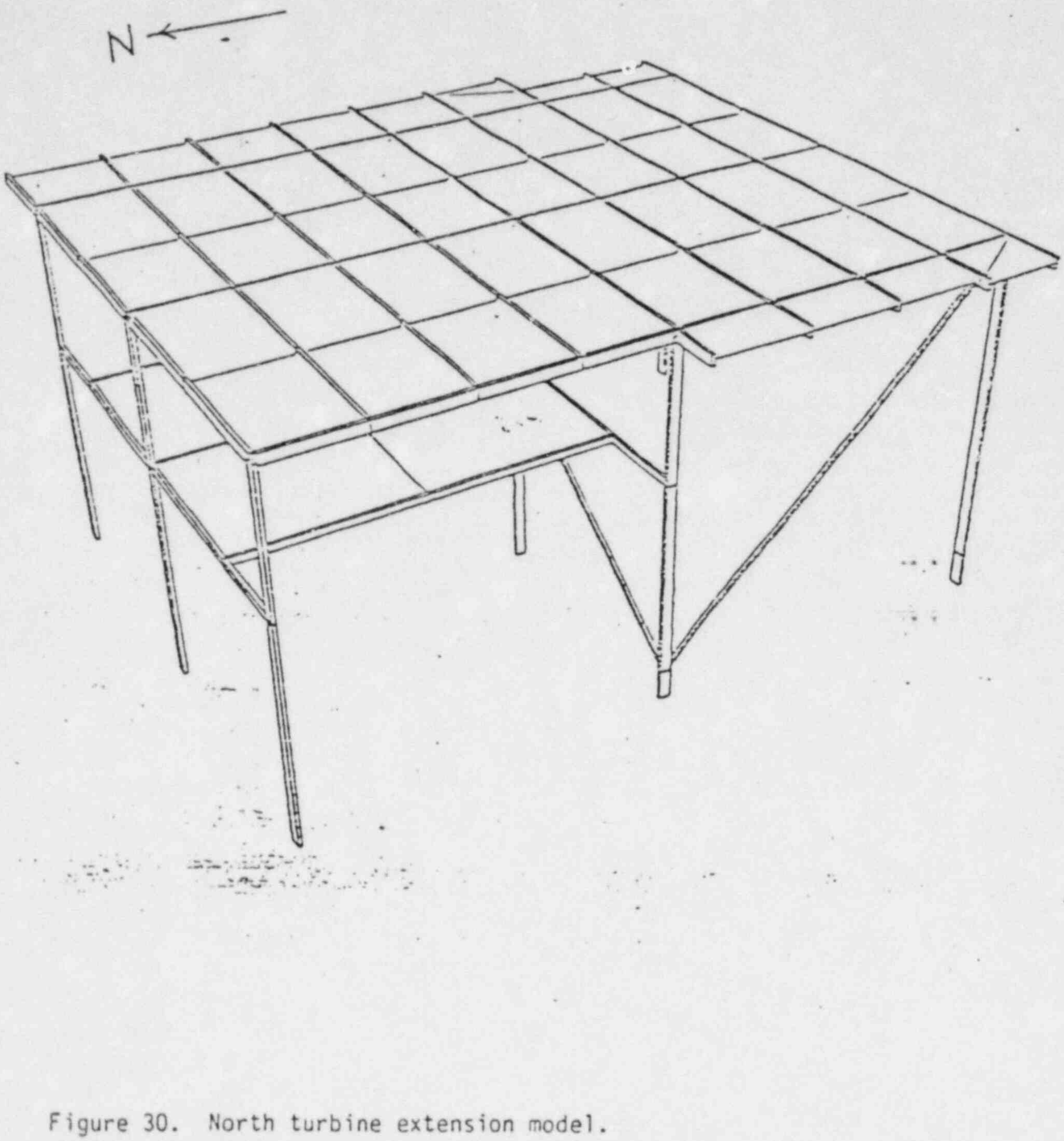

Figure 30. North turbine extension model.

DRAFT FOR COMMENT

properties recommended by the SCEC/Bechtel.[12] The model is shown in Fig. 31. Modal frequencies and mass fractions are listed in Table 11.

Mode Number	Frequency (Hz)	Mass Participation Fraction X	Y	Z
2	1.18	24.1	0.0	0.0
3	1.51	12.3	0.0	0.0
4	1.81	0.0	46.0	0.0
5	7.71	24.4	0.0	0.5
6	8.45	29.0	0.0	0.0
7	8.85	0.0	25.1	0.9
8	10.44	0.0	23.9	0.0
13	17.10	0.0	0.0	23.0
15	17.80	0.0	0.0	14.0
20	23.66	0.4	0.0	11.3
23	25.28	0.0	0.1	17.4
Mass sum of all nodes		98.9	97.7	92.3

Table 11. Significant modes of the south turbine building extension model.

DRAFT FOR COMMENT

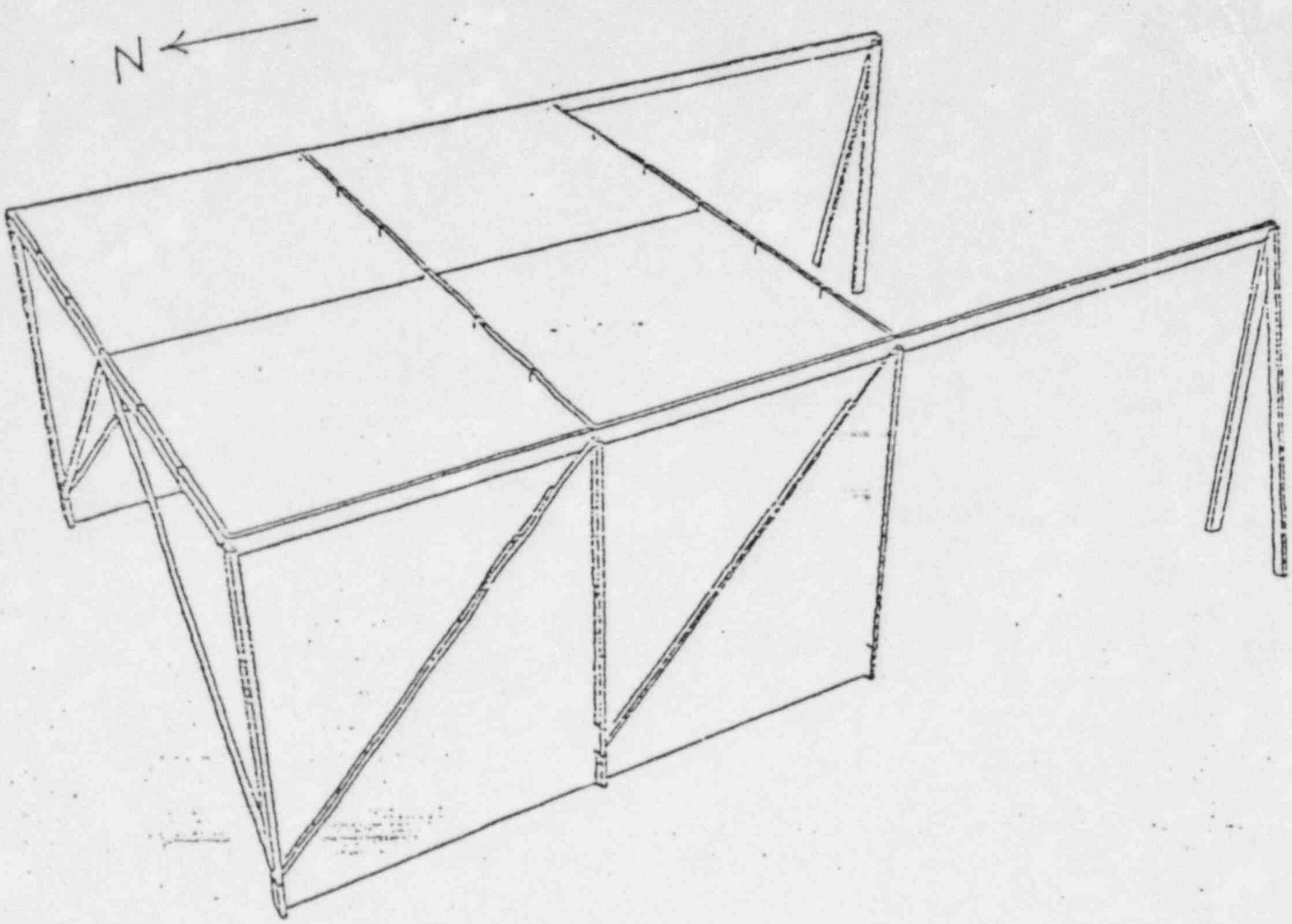

Figure 31. South turbine building extension model.

3. West Feedwater Heater Platform

The west feedwater heater platform is located on the west side of the turbine pedestal. It is a rectangular structure, approximately 120 ft long and 50 ft wide, consisting of a prestressed concrete deck at elevation 35 ft supported by structural steel framing. Steel support columns extend down to individual or combined footings. Concrete block walls attach to the steel framing on the south, west, and north sides of the building. The entire structure rests on a massive, concrete mat. The west feedwater heater platform is of particular interest, since it houses portions of the AFWS.

The finite element model of the west platform shown in Fig. 32 defined the dynamic characteristics of the roof, steel frames and block walls. Shell and beam elements modeled the deck while beam elements model the support frame.

Same as the south turbine building extension, the behavior of the masonry walls within the feedwater heater platforms was modeled with a combination of beam and plane stress elements. Various equipment loads were included in the structure model by proportionally increasing the mass density of affected elements.

The frequency and mass fraction of all modes with frequencies less than 33.0 Hz are listed in Table 12.

Mode Number	Frequency (Hz)	Mass Participation Fraction X	Y	Z
5	3.89	16.3	43.5	0.0
10	7.24	0.1	0.0	13.3
11	8.03	44.4	42.2	1.2
12	8.94	1.9	1.4	14.1
16	12.19	30.3	8.9	0.0
Mass sum of all modes		98.4	98.4	79.2

Table 12. Significant modes of the west feedwater heater platform.

DRAFT FOR COMMENT

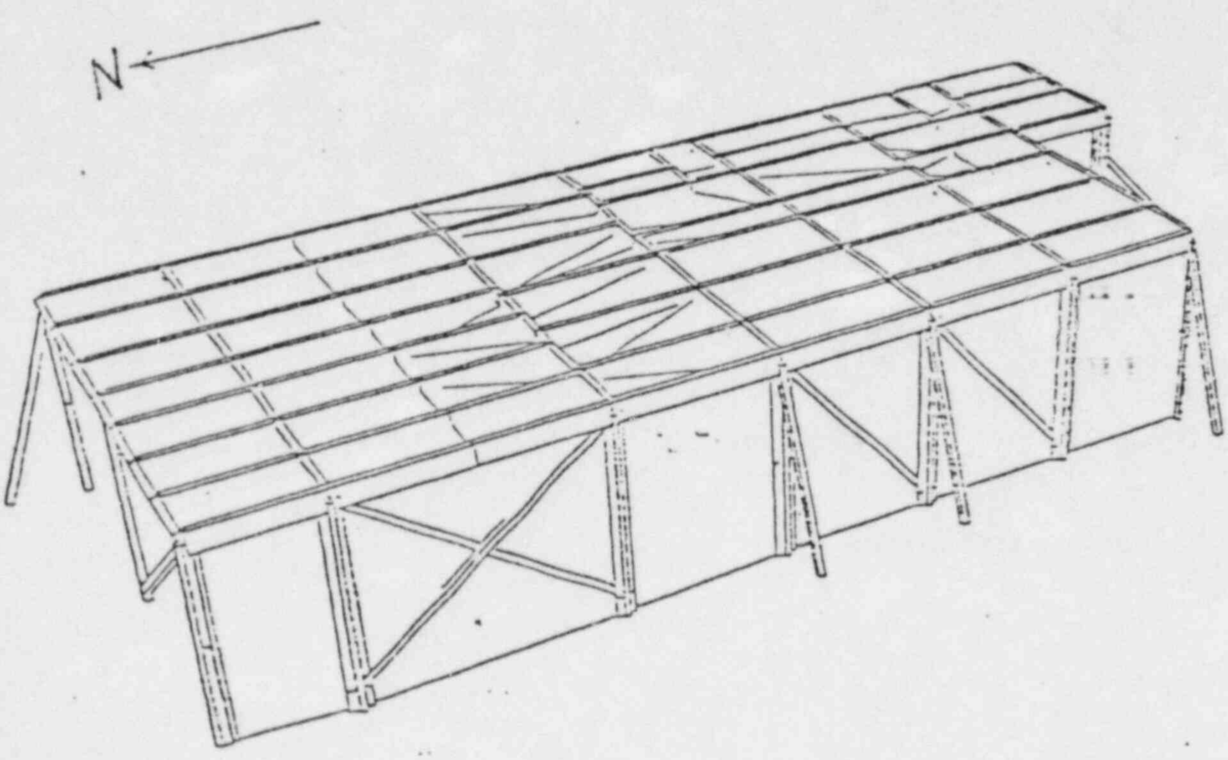

Figure 32. West Feedwater Heater Platform Model.

4. East Feedwater Heater Platform

The dynamic characteristics of the east feedwater heater platform are similar to the west feedwater heater platform and the same model would be used.

A.3.3 Fuel Storage Building

The fuel storage building lies between the west feedwater heater platform and the sphere enclosure building. It consists in part of a massive, reinforced concrete fuel pool. The surrounding structure is steel framing that supports concrete block walls. The soil-supported mat that forms the bottom of the fuel pool is approximately 5 ft thick. Four foot thick concrete walls form the sides of the pool. The pool is embedded such that the top of the mat is an average of 14 ft below grade. The pool stores both new and spent-fuel assemblies.

On the south side of the structure, concrete block walls and steel frames extend down to strip footings at elevation 14 ft. On the north side, the frames and wall sit atop the refueling pool. The building is covered by a prefabricated deck roof at elevation 64 ft. This portion of the fuel storage building houses the switchgear room and other equipment.

A3.3.1 Impedance and Scattering matrices for the Fuel Storage Pool

The fuel storage pool is a reinforced concrete box-like structure about 75 ft long in east-west direction, 30 ft wide and embedded about 14 ft below the level of adjacent foundations. Its walls are between 4 ft and 5 ft thick. To the south side of the pool lies the remainder of the Fuel Storage Building which consists of concrete block walls supported on a 1.5 ft wide by 8 in. strip footing. Located at intervals along this footing are 4 foot square footings about 1.5 ft thick which support columns for the fuel handling building and for the west heater bay. Because of the flexibility of the strip footings, the column footings must be considered to be isolated from each other except in the axial direction of the strip footing.

Two foundation models of the spent fuel pool were constructed. Model A (Fig. 33) was more refined than Model B (Fig. 34) and included the shape of the column footing located in the southeast corner of the pool. The reference point was chosen near the centroid of the rectangular portion of the foundation. Figure 35 shows a comparison of a typical impedance term calculated for both models. The eccentricity of the column footing in Model A caused some additional coupling between horizontal translation and torsion (K_{16} and K_{26}) and between vertical translation and rocking (K_{34} and K_{35}). However, this is not considered to be a significant effect, especially since the footing in Model A is actually cast into the wall of the pool at the elevation of the strip footing and is not level with the bottom of the foundation.

A3.3.2 Structural Model of the Fuel Storage Building

Initially, a model reflecting the proposed design modifications to the fuel storage building was constructed and a modal (eigenvalue) analysis completed. However, further modification from SCEC/Bechtel required additional changes. These changes were incorporated into the model, but no modal anaysis was performed. Finally, SCEC/Bechtel returned to the unmodified configuration. The information for the roof decking of fuel storage building will be required in order to change the model to its unmodified configuration. Therefore, no progress on model analysis was accomplished at the time the project was terminated.

A.3.4 Control-administration Building

The control-administration building is the structure housing the control room and the battery room. The building also houses various laboratories; heating, ventilation and air-conditioning (HVAC) equipment; and locker facilities. The main load-bearing elements of the building are reinforced concrete and concrete-block shear walls. The walls extend to strip footings. Ground-floor slabs at elevations 14 ft, 20 ft and 21 ft are soil-supported. In the administration area, partial floors exists between the ground slab and the roof at elevation 37 ft. In the control room bay, floor slabs are at grade and elevation 42 ft. A grid of steel framing at elevation 37 ft supports cable trays that run under the control room floor. The elevation of the roof is approximately 55 ft.

DRAFT FOR COMMENT

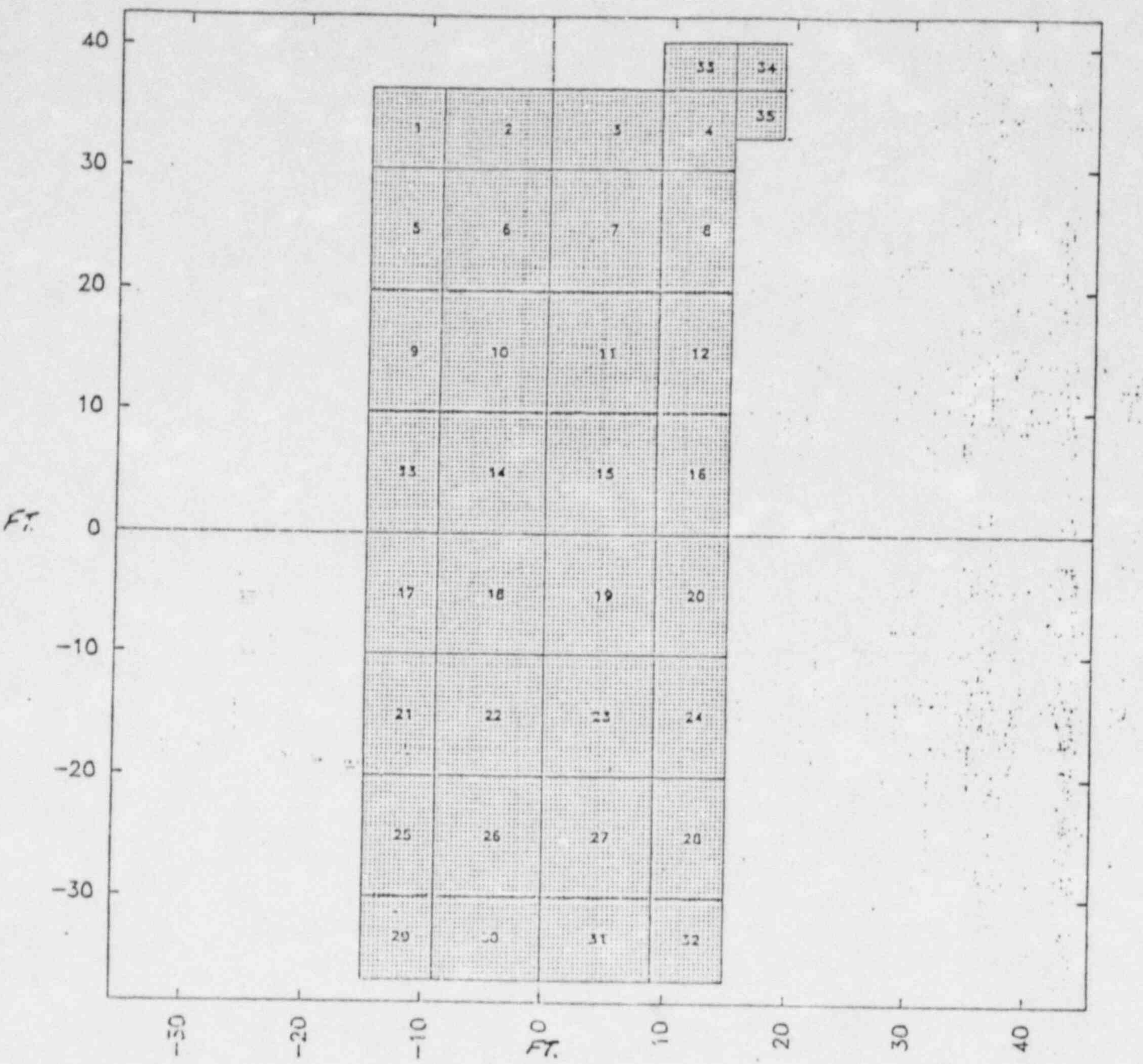

Figure 33. Fuel storage building foundation model A.

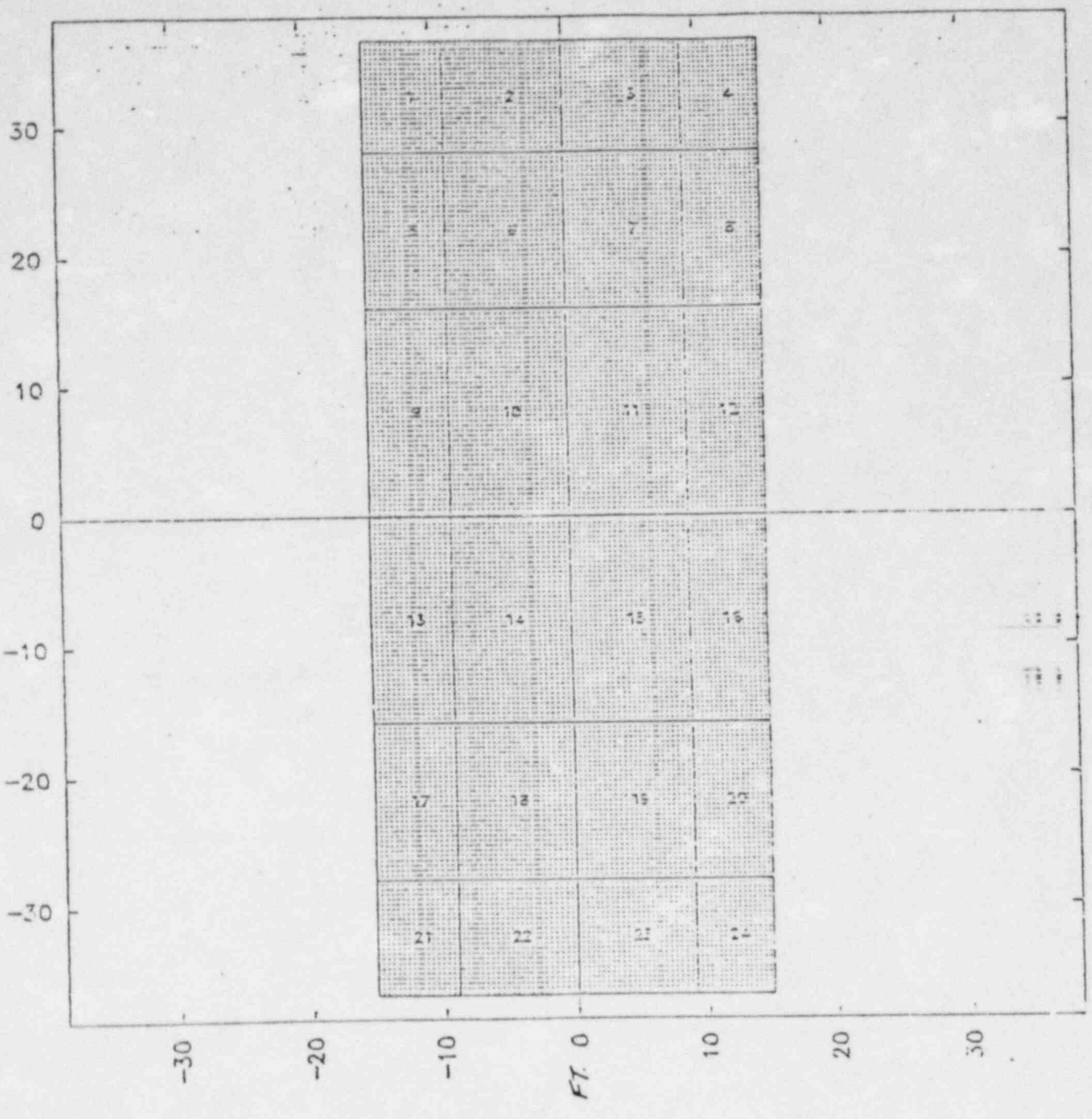

Figure 34. Fuel storage building foundation model B.

DRAFT FOR COMMENT

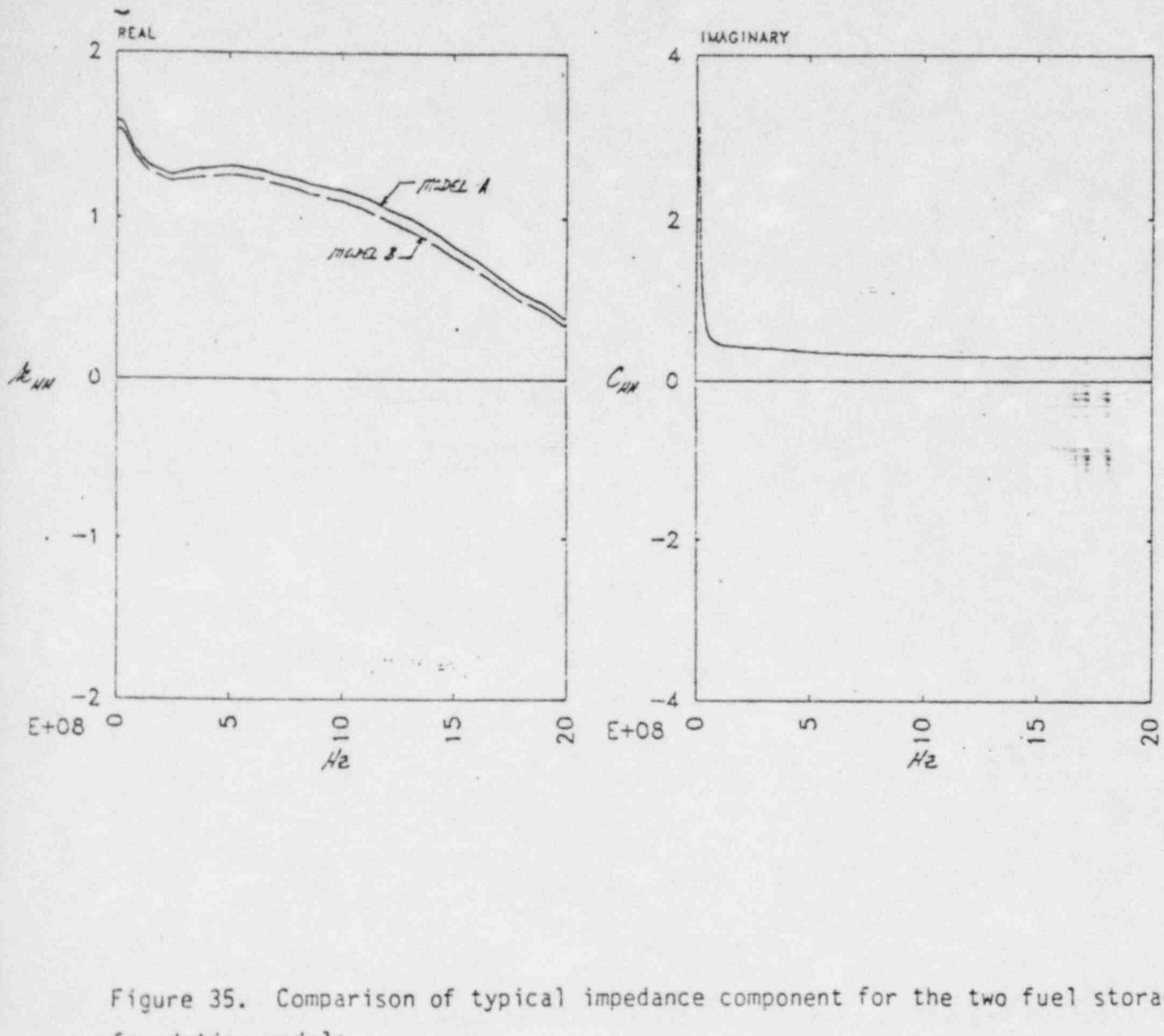

Figure 35. Comparison of typical impedance component for the two fuel storage foundation models.

DRAFT FOR COMMENT

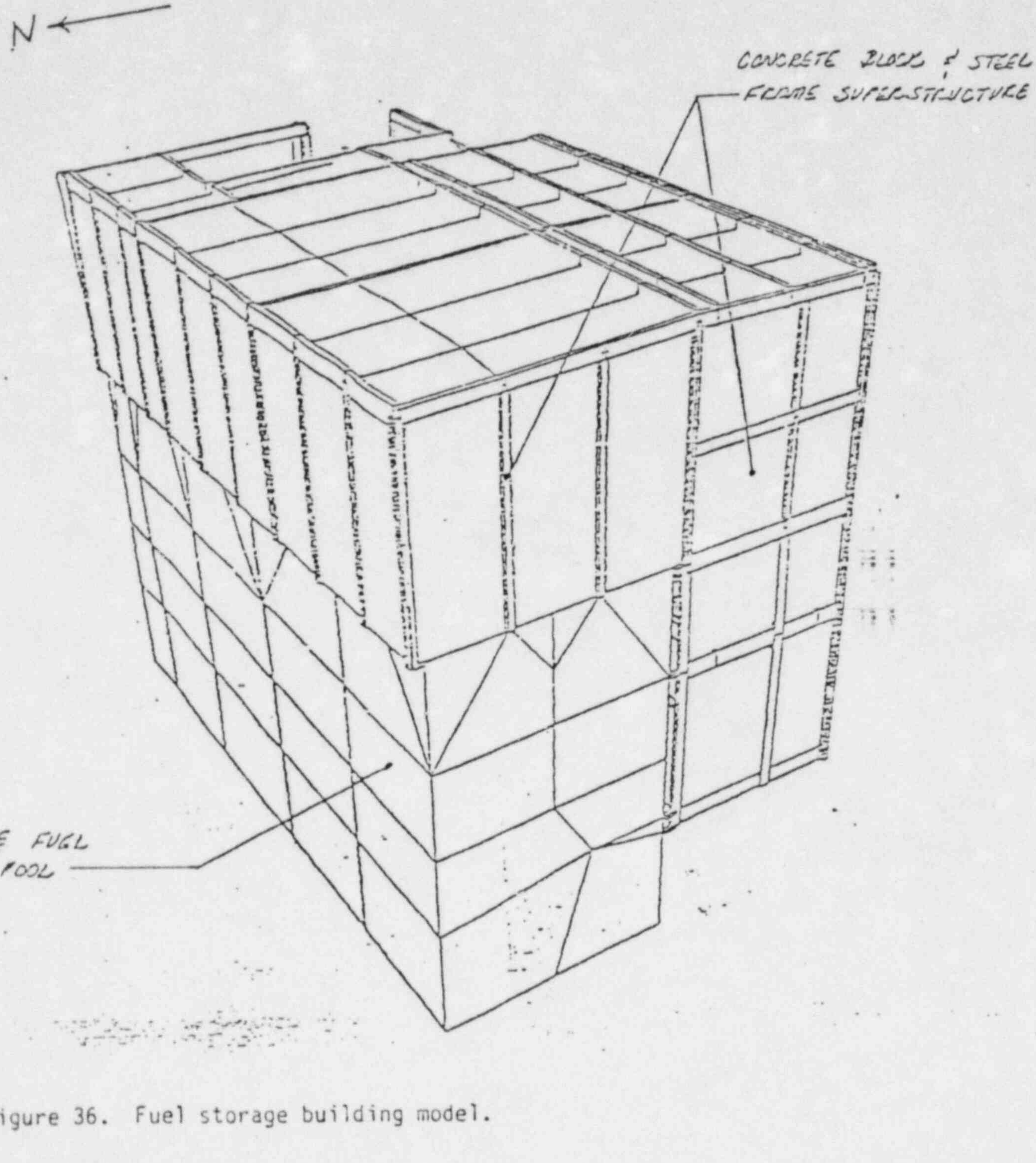

Figure 36. Fuel storage building model.

DRAFT FOR COMMENT

A3.3.4.1 Impedance and Scattering Matrices for the Control-administration Building

The development of SSI models for this structure was not completed at the time the project was terminated.

A3.3.4.2 Structural Model of Control-administration Building

A detailed finite element model of the structure was constructed. Thin plate and shell elements defined the reinforced concrete shear walls and floor slabs. Beam elements modeled the structural steel in the control bay and administration areas. As in the models of the other structures, a combination of beam and plane stress elements were used to characterize the masonry walls. Equipment loads were included either in the form of added masses lumped at nodes or increased element densities.

Figure 37 illustrates the model. Eigenvalue analysis results are listed in Table 13. An initial comparison between these modal data and the frequencies supplied by SCEC/Bechtel indicated significant differences. However, no effort was made to resolve or explain the differences.

Mode Number	Frequency (Hz)	Mass Participation Fraction X	Y	Z
14	7.99	0.4	0.1	16.4
28	10.30	6.2	35.8	0.2
29	10.50	34.4	2.5	0.4
40	14.54	0.7	0.0	25.9
Mass sum of all modes		77.7	77.2	81.0

Table 13. Significant modes of the control-administration building model.

DRAFT FOR COMMENT

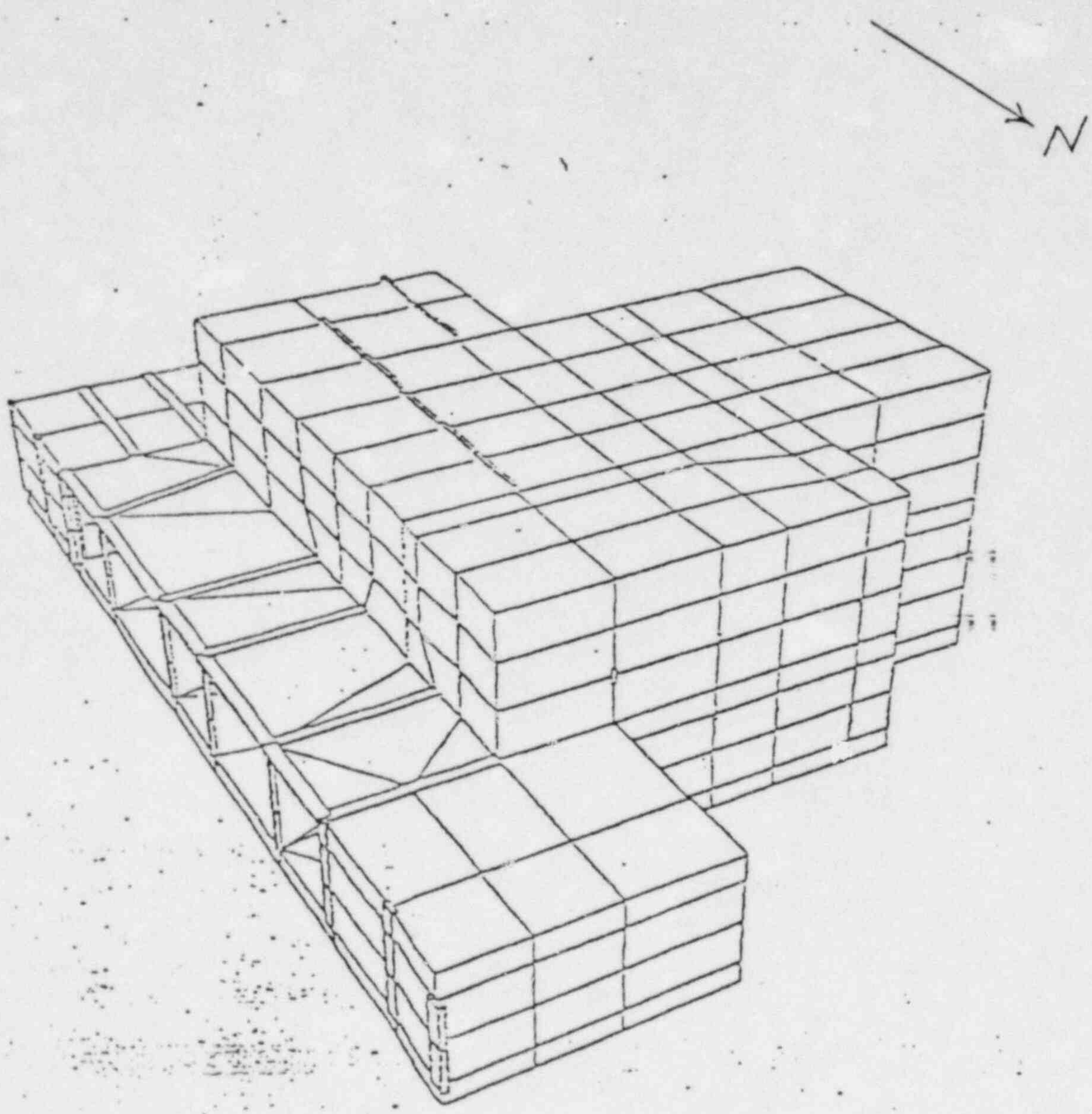

Figure 37. Control-administration building model.

A4 RESPONSE COMPARISON FOR REACTOR BUILDING/CONTAINMENT SPHERE

One major objective of this project was to assess the conservatism in the seismic responses of the SONGS-1 structures and piping systems of the AFWS as calculated by SCEC/Bechtel using design procedures by comparing with those calculated by SMACS. In the SCEC/Bechtel case, a deterministic analysis was performed using analysis procedures and parameter values selected for seismic reevaluation and definition of the design ground response spectra termed SONGS Unit 1 seismic reevaluation spectra, anchored to a 0.67 g zero period acceleration (ZPA). In the SMACS case, three sets of analyses were performed. Each set differed by the definition of the seismic input: SONGS Unit 1 seismic reevaluation spectra; the SONGS Units 2 and 3 design spectra; and the average of the two. All of the spectra were anchored to a 0.67 g ZPA in the horizontal direction and to a 0.45 g ZPA in the vertical direction. Each set contained multiple analyses which permitted incorporation of variability in the seismic input, SSI, and structure characteristics.

The response comparison was only completed for the reactor building/ containment sphere at the time the project was terminated. It is reported here.

A4.1 SCEC/Bechtel Seismic Reevaluation

The seismic reevaluation analysis by SCEC/Bechtel was based on the SONGS-1 seismic reevaluation spectra as described above. Both response spectrum analysis and time history analysis were performed. The former case produced force/moment results, and the latter case produced time histories from which in-structure response spectra were generated. An artificial acceleration time history whose response spectra essentially enveloped the seismic reevaluation ground response spectra was used. Three directions of excitation were considered, each direction analyzed independently, and the results combined by the square root of the sum of the squares (SRSS) method. Noteworthy aspects of the analysis include their SSI model and the use of composite modal damping. Frequency-independent soil springs were used to represent the force-displacement characteristics of the soil. Properties of these soil springs were derived from a detailed finite element analysis of the soil and structure, i.e., an axisymmetric model subjected to circumferential harmonic loadings of $n = 0$ (vertical) and $n = 1$ (horizontal). Composite modal damping techniques yielded damping values near 4 percent of critical for structure modes and significantly higher values for coupled soil-structure modes. The in-structure spectra compared here were peak broadened and smoothed by SCEC/Bechtel.

A4.2 SMACS analysis

The modus operandi of SMACS is to perform repeated deterministic analyses, each analysis simulating an earthquake occurrence. By performing many such analyses and by varying the values of the several input parameters, we incorporate the uncertainty inherent in any deterministic analysis. Variability in the seismic input phase was incorporated by using ensembles of time histories. In the SSI area, soil shear modulus and material damping were varied. In the major structures and subsystems, frequencies and modal damping were our uncertainty parameters. Parameter values for each simulation were sampled from assumed probability distributions according to a Latin hypercube experimental design.

Three sets of SMACS analyses were performed. Each set differed by the definition of the seismic input. In each set, thirty earthquake simulations were considered. The seismic input for each simulation comprised three acceleration time histories (two horizontal and a vertical) acting on the surface of the soil. These artificially generated time histories were described in detail in Section A2 of this appendix. The mean of their response spectra closely fit the target spectra. The resulting mean spectra for the three targets was shown in Fig. 1 of Section A2. Spectral accelerations of the target spectra for selected frequencies are superposed, and the close match can be readily observed.

The structure and SSI models of the reactor building-containment sphere described previously were used in the SMACS analyses. The fixed-base frequencies and an assumed modal damping of 4 percent of critical for the structures comprised the nominal values. The impedances and scattering matrices for the partial spherical foundation, shown in Figs. 16 and 17 of Subsection A3.3.1.1. respectively, which were calculated for equivalent

DRAFT FOR COMMENT

linear soil properties associated with a 0.67 g excitation were termed nominal values. As mentioned above, the parameters were varied in the analysis to incorporate uncertainty. Two cases were considered and itemized in Table 14. Two modeling assumptions were made. The wave propagation mechanism at the site was assumed to be vertically-propagating waves. Structure-to-structure interaction effects between the sphere enclosure building and the reactor building/containment sphere were ignored.

Parameter	Coefficients of Variation Case 1	Case 2
Soil shear modulus	0.7	0.35
Soil damping	1.0	0.50
Structure frequency	0.5	0.25
Structure damping	0.7	0.35

Table 14. Statistical parameters that define the variation of input values.

Note: Values are given for the median and the coefficient of variation (COV). Case 1 reflects a state of maximum uncertainty about the SONGS-1 plant. Case 2 represents a state of significantly greater knowledge.

Variations in this limited number of parameters are intended to represent all sources of variability in each link of the seismic methodology chain (SSI, structure, etc.). For example, by varying soil shear modulus and damping in the SSI link, the uncertainty in the definition of the viscoelastic material constants at a point were represented as were variations due to phenomena not modeled and the perceived accuracy of analysis procedures. Similar comments apply to structure uncertainty parameters. This is discussed in more detail in Ref. 2. To assess the effect of input parameter distributions on the results, two cases were analyzed and are briefly discussed later.

DRAFT FOR COMMENT

A4.3 Response Comparison

Two forms of seismic response were compared: in-structure response spectra in the reactor building, and element stress components in the containment sphere. Seven node points in the reactor building were selected for comparison; three directions of response per node point. Figure 39 shows the points: five nodes on the operating deck (four corners and an interior node); the center of gravity of the foundation; and a node on top of a steam generator compartment. Due to the close similarity in response of the five points on the operating deck, results at only one point are shown here, node 201 at the south-east corner of the operating deck. At all points, response in the two horizontal directions was nearly the same, hence, only north-south (x-direction) and vertical response is included. Figures 40 and 41 show response on the foundation, Figs. 42 and 43 on the operating deck, and Fig. 44 and 45 on the top of the steam generator compartment. These results should be considered more appropriate for evaluation than for design purposes. However, this opinion may change with additional research.

The comparison in Figs. 40-45 is between the mean SMACS response and the SCEC/Bechtel seismic reevaluation values. This comparison is believed to be appropriate because the SMACS seismic input is defined so that its mean corresponds to the target spectra (Fig. 38). In Figs. 40-45, in-structure response spectra due to the SONGS Unit 1 seismic reevaluation spectra are shown with a long segmented curve; those due to SONGS Units 2 and 3 are shown with a solid curve; and the average spectra are shown with a short segmented curve. The spectra due to SCEC/Bechtel seismic reevaluation spectra[13] are overplotted.

It is of interest to examine Figs. 38 and 40-45 which trace response from the free-field ground motion to the foundation to the upper elevations of the structure. Concentrate first on the SMACS results for a specific definition of the seismic input. Comparing Figs. 38 and 40-45, one observes a general reduction in motion from the free-field to the foundation and a subsequent increase in response (albeit small) as one proceeds to the upper elevations. Some observations are in order. In general, the reactor building

162

DRAFT FOR COMMENT

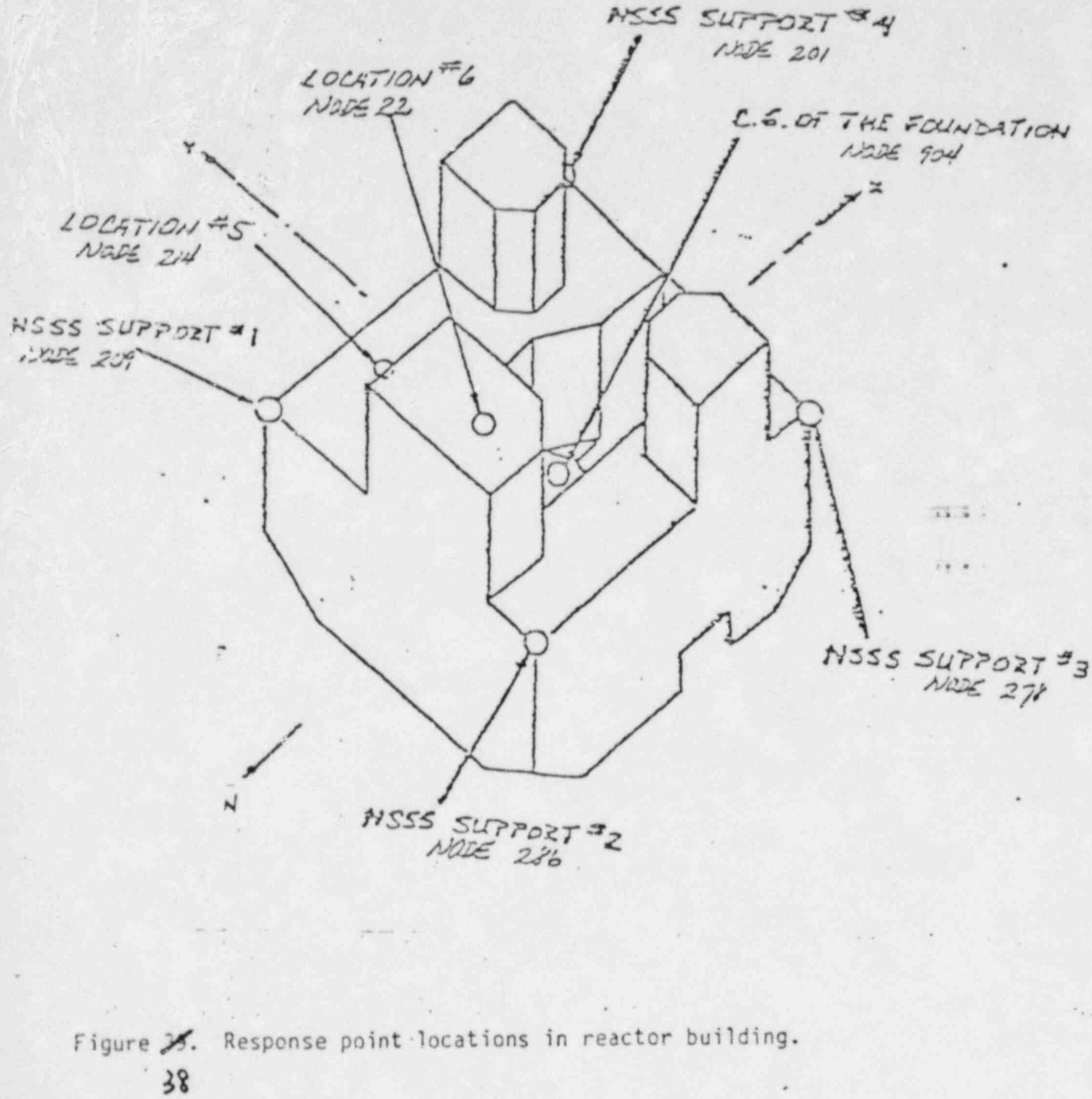

Figure ~~35~~ 38. Response point locations in reactor building.

DRAFT FOR COMMENT

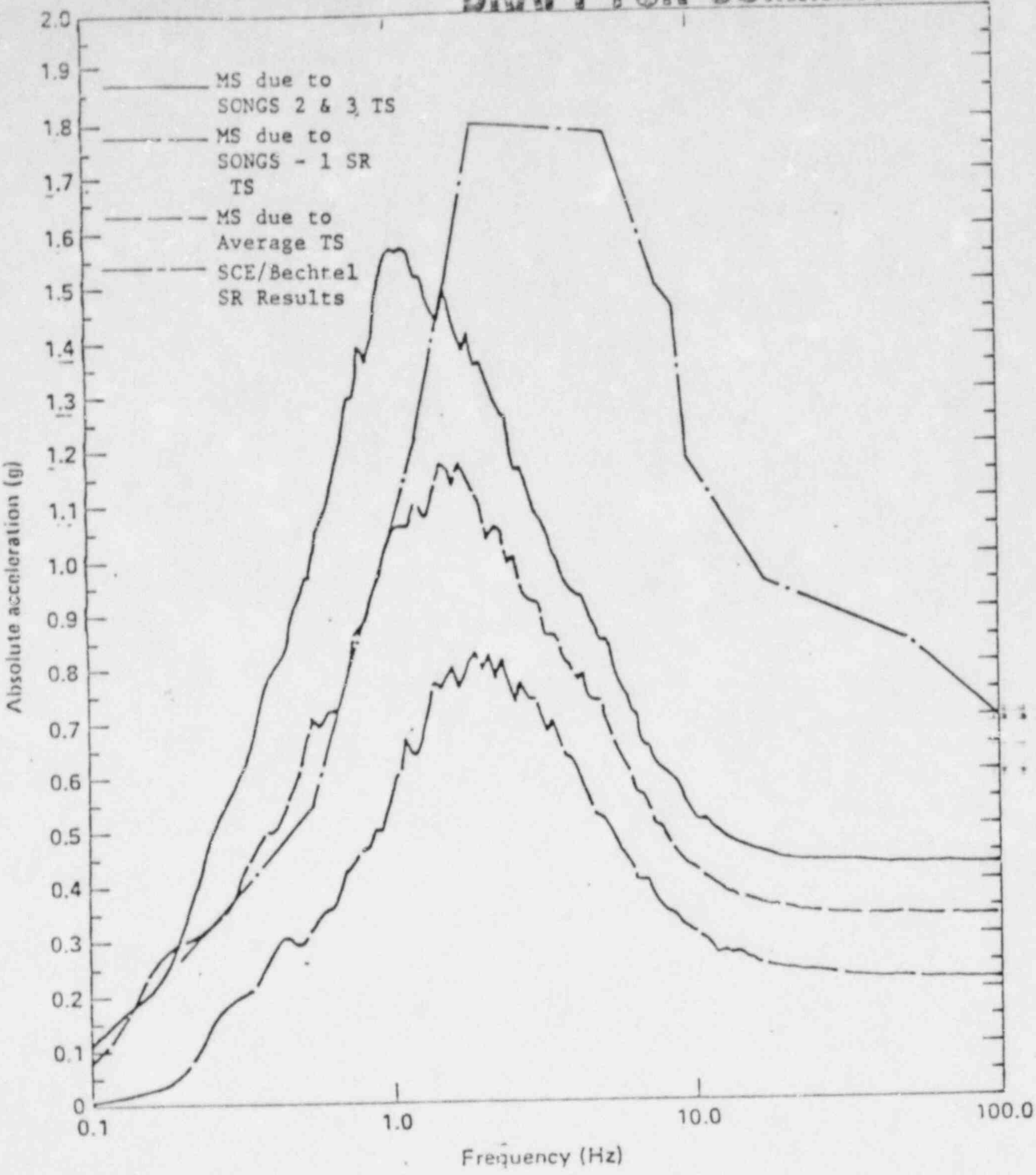

Figure ~~40~~ 39. C G of foundation mean response spectra: N-S direction.

NOTE: MS = Means response

SR = Seismic reevaluation

TS = Target Spectra

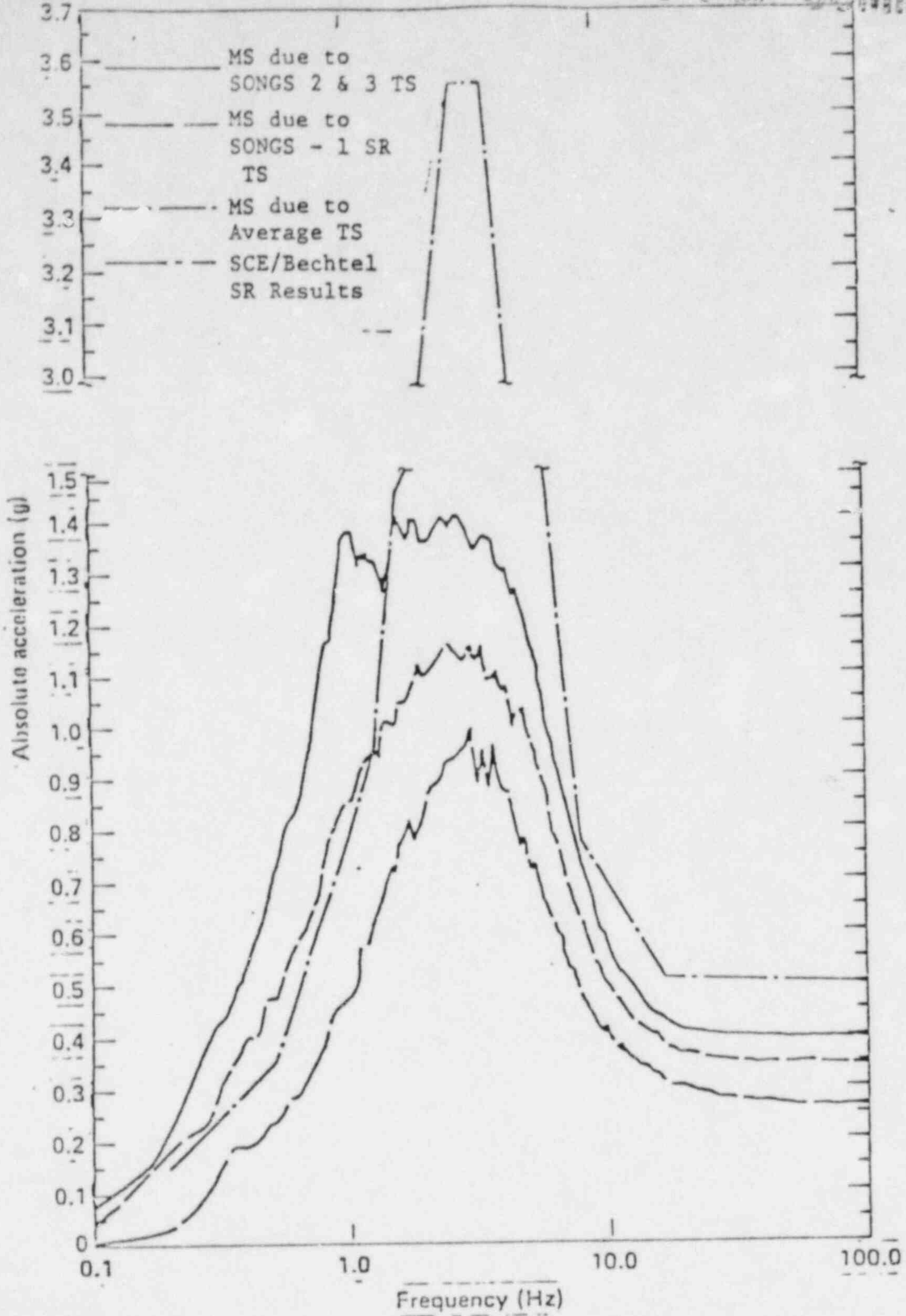

Figure 40. C G of foundation mean response spectra: vertical direction.

NOTE: MS = Means response spectra

SR = Seismic reevaluation

TS = Target spectra

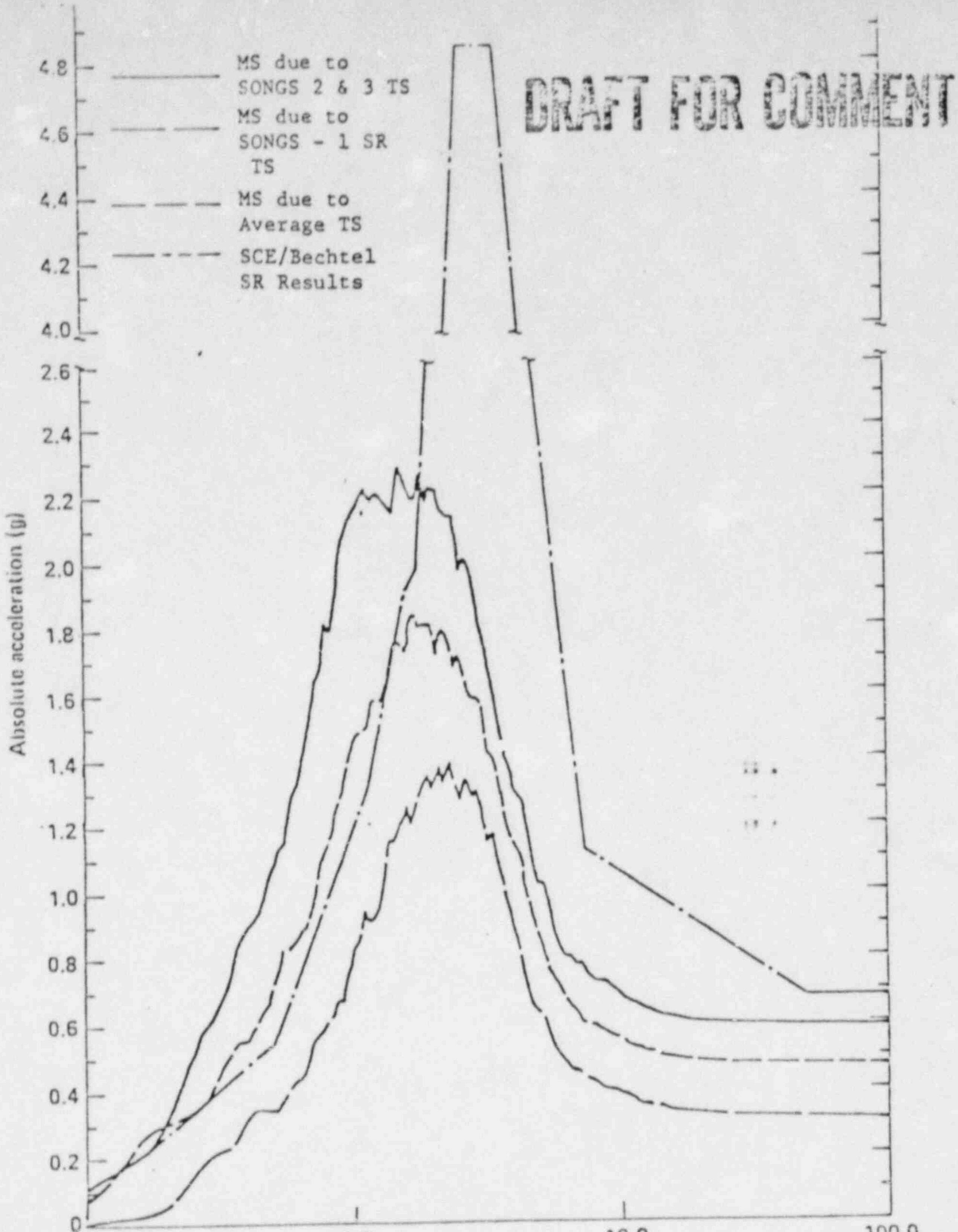

Figure 41. S-E corner of operating deck mean response spectra: N-S direction.

NOTE: MS = Means response spectra

SR = Seismic reevaluation

TS = Target Spectra

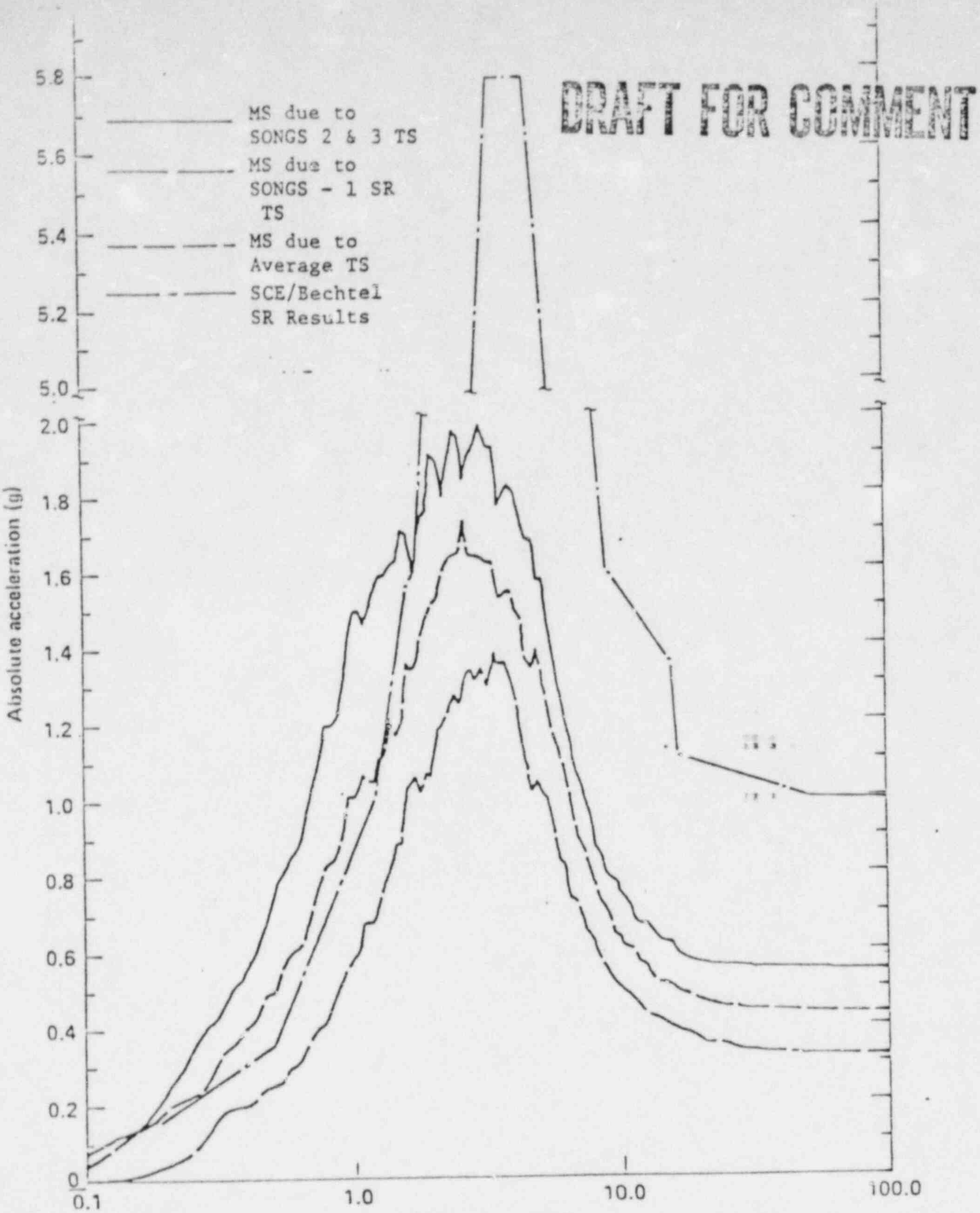

Figure ~~43~~ 42. S-E corner of operating deck mean response spectra: vertical direction.

NOTE: MS = Means response spectra
SR = Seismic reevaluation
TS = Target Spectra

DRAFT FOR COMMENT

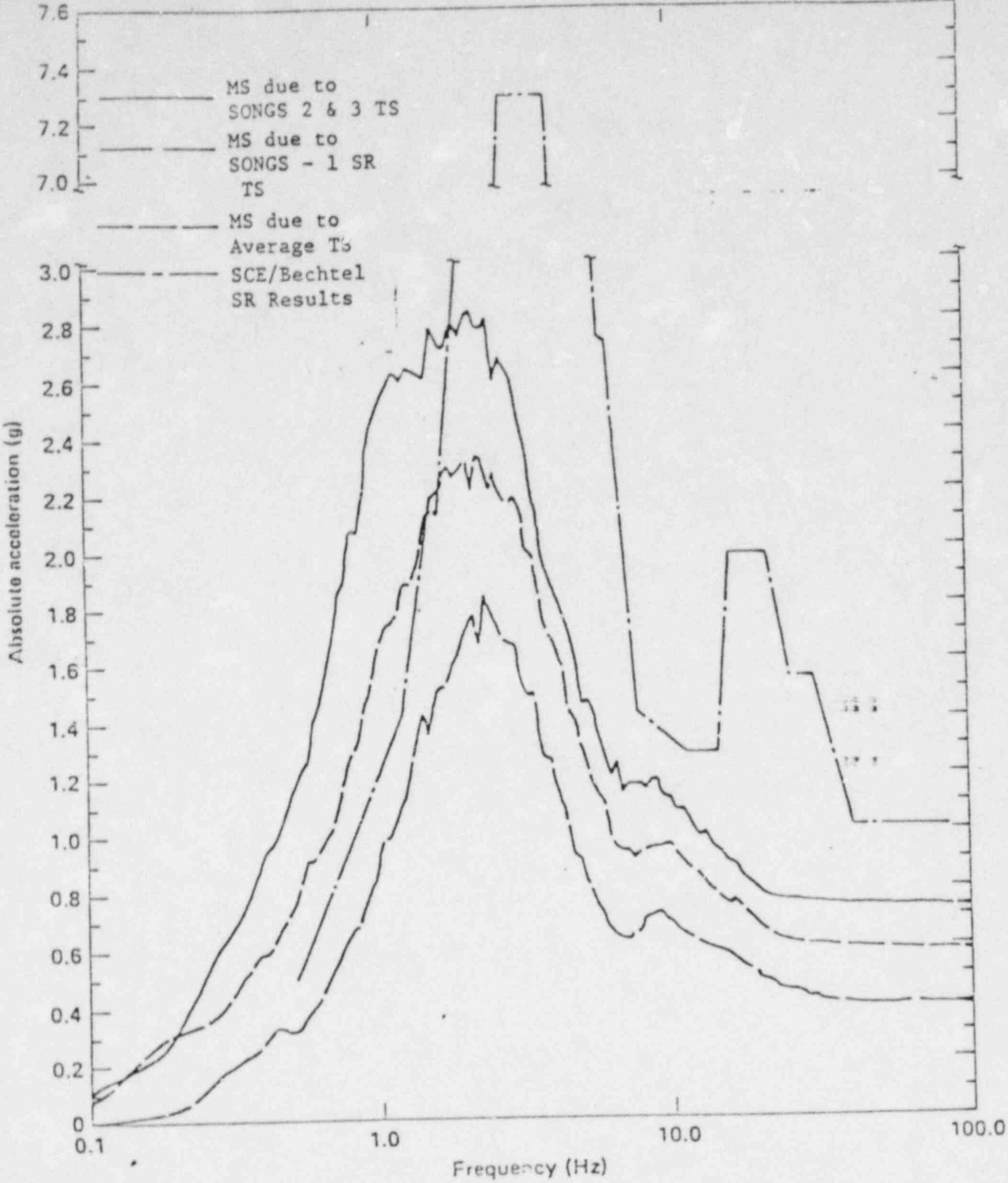

Figure 43. Top of steam generator compartment B - N-S direction.

NOTE: MS = Means response spectra

SR = Seismic reevaluation

TS = Target spectra

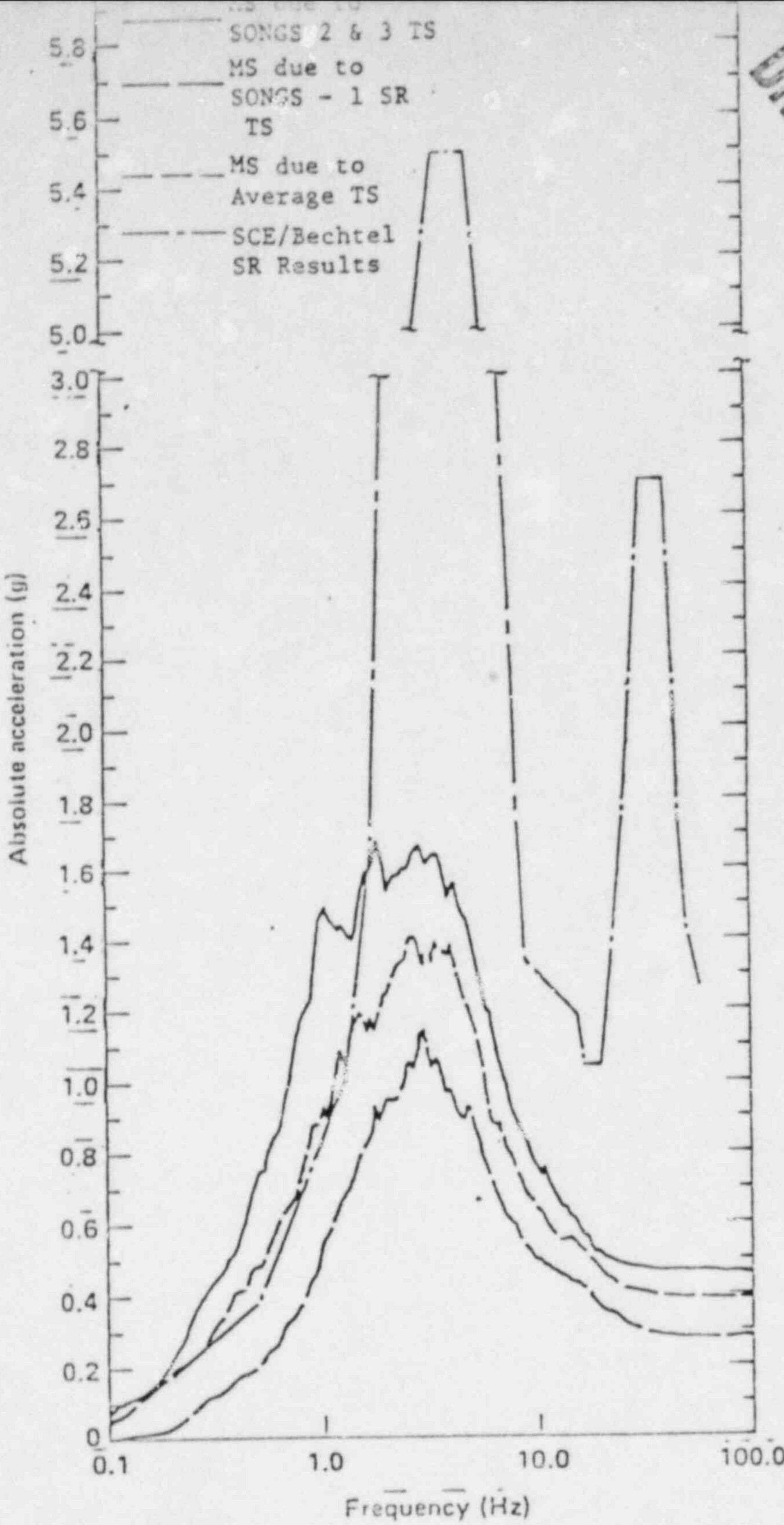

Figure ~~45~~ 46. Top of steam generator compartment B - vertical direction.

NOTE: MS = Means response spectra

SR = Seismic reevaluation

TS = Target Spectra

DRAFT FOR COMMENT

acts similar to a rigid body on a deformable medium due to its relatively high fixed-base frequencies and mass distribution. Hence, dominant overall motion of the reactor building is due to coupled soil-structure response with little structural deformation. Two aspects of the SSI model contribute significantly to the reduction in motion of the foundation and the minimal amplification through the structure: the scattering matrix, and the impedances. The scattering matrix, which accounts for kinematic interaction and in so doing generates foundation input motion from the free-field motion, results in a reduction in horizontal translation and the addition of a rotational component. For this case, the reduction dominates. Our representation of the foundation impedances includes the effects of radiation and material damping. Earlier the equivalent linear soil properties were described. They included a significant amount of soil material damping (near 10% in the upper layers) for a 0.67 g excitation. The combined effect of radiation and material damping for this case is a significant energy dissipation mechanism. Finally, although no eigenvalue extraction of the coupled soil-structure system is performed (due to the frequency dependence of the impedances), one can estimate the frequency of peak response for the nominal soil-structure system by inspecting in-structure response spectra generated for a single broad-band time history and soil-structure parameters held at their nominal values. In so doing, the frequency is estimated to be near 1.8 Hz which has minimal amplification in the target design ground response spectra (especially for the SONGS Unit 1 seismic reevaluation spectra).

Next consider the comparison between the SCEC/Bechtel seismic reevaluation analysis and the SMACS results. The most appropriate comparison is between the SMACS results due to SONGS Unit 1 seismic reevaluation spectra and the SCEC/Bechtel results. This is because the seismic input target spectra are the same for these two cases. To clarify this point, these two results from Fig. 43 are shown in Fig. 45. In Figs. 39 through 45, the SCEC/Bechtel results are observed to envelop those of SMACS over the entire frequency range; in the amplified frequency range by considerable factors. This may be interpreted as an indication of calculational conservatism or margin. If the comparison of these seismic reevaluation results were carried further, for example, to piping moments, this margin is expected to grow by a significant factor. Studies will soon be underway to quantify this estimate for piping moments in another project at LLNL.

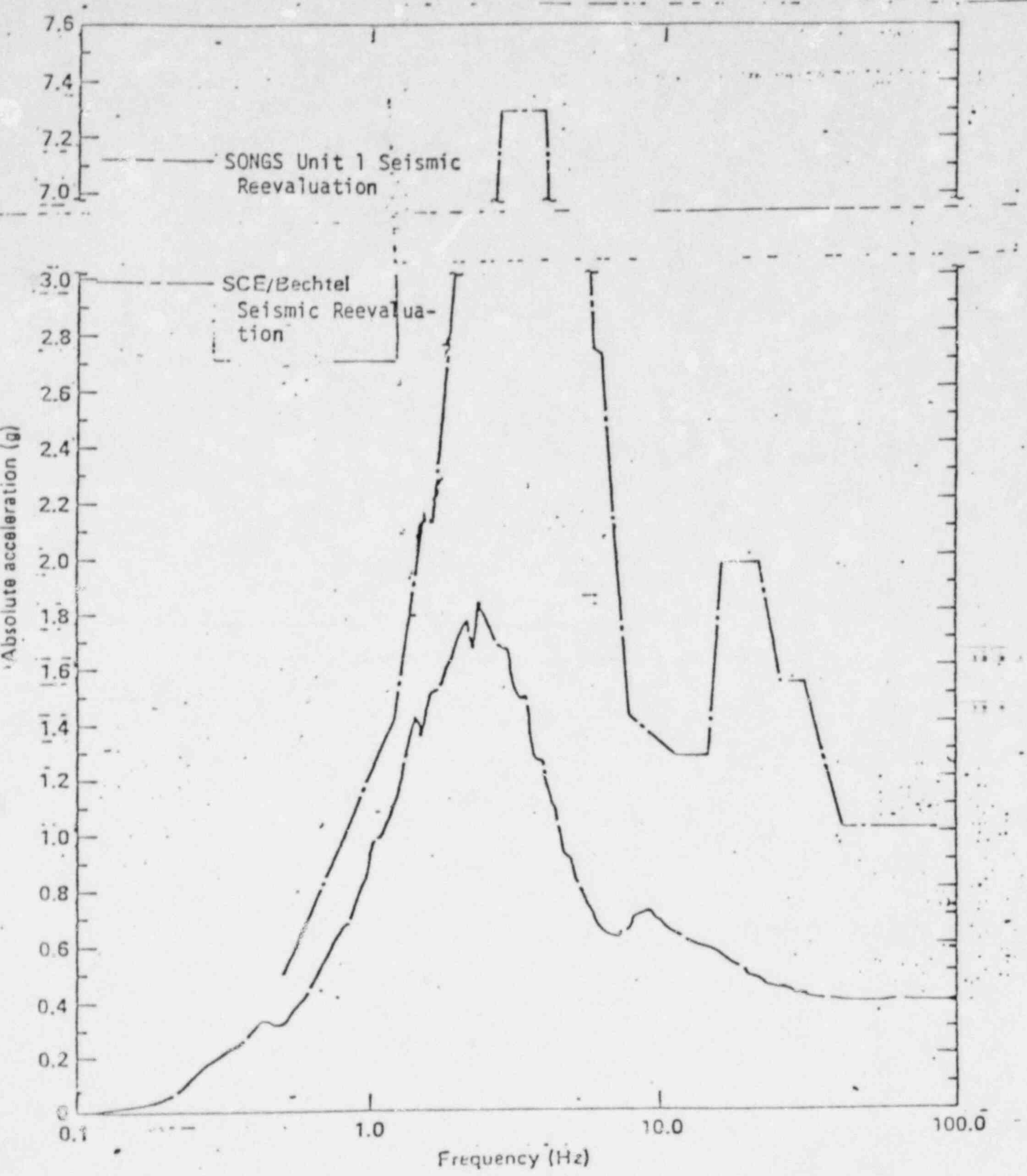

45
Figure 46. Comparison of the mean spectra due to SONGS-1 seismic reevaluation target spectra and the SCEC/Bechtel results (from Fig. 44). 43

DRAFT FOR COMMENT

It is also evident from Figs. 40-45 that significant conservatism in the SCEC/Bechtel results over those due to SMACS exists for both the SONG Units 2 and 3 design spectra and the average spectra in the amplified and higher frequency ranges. In the low frequency range, the SMACS results due to the SONGS Units 2 and 3 design spectra are lower than the SCEC/Bechtel results. This effect may be interpreted as a result of the strong motions in the low frequency range of the SONGS Units 2 and 3 design spectra.

The SMACS results shown are for variations in input parameters corresponding to Case 1 of Table 14. To assess the effect of varying degrees of uncertainty on the mean response, Case 2 (Table 10) was analyzed. A comparison of the mean response for Cases 1 and 2 showed minimal differences.

A comparison of stress components at two locations in the containment shell is shown in Table 15. The two locations are the stiffness discontinuity just above the sand transition zone (grade discontinuity) and a point in the free-standing shell between the foundation and the equator (contintous shell). In all cases, the SCEC/Bechtel results [14] exceeded those computed by SMACS. Again, this can be interpreted as an indication of conservatism or margin. For reasons discussed above, the most appropriate comparison is between the SCEC/Bechtel results and the second column of the three SMACS results, for example, 1172 psi vs. 286 psi, respectively. Finally, Fig. 47 showed a typical cumulative distribution function of the meridian stress of continuous shell due to the SONGS Units 2 and 3 design spectra. The thirty circles represent the calculated responses and the dotted line is a lognormal fit with a median value of 458 psi and a beta of 0.664.

Stress (psi)	Bechtel Seismic Reevaluation Analysis		SONGS-2&3 Spectra SMACS Analysis		SONGS-1 Spectra SMACS Analysis		Average Spectra SMACS Analysis	
	Continuous Shell	Grade Discontinuity	Continous Shell	Grade Discontinuity	Continuous Shell	Grade Discontinuity	Continuous Shell	Grade Discontinuity
Membrane-Long Stress N_θ	1172	2034	553	339	303	187	421	260
Membrane-Merid. Stress N_s	1483	6615	458	661	252	362	350	505
Membrane-Shear Stress $N_{\theta s}$	1517	1849	601	791	332	437	473	622
Bending-Long Stress M_θ/S	115	7922	4	359	2	196	3	274
Bending-Merid. Stress M_s/S	34	2404	14	1180	7	640	10	901
Twist $M_{\theta s}/S$	4	26	*	7	*	4	*	6

Table 15 Response comparison of containment sphere. Stress values from Bechtel seismic reevaluation analysis versus median stress values given by SMACS.

Note: * = negligible

DRAFT FOR COMMENT

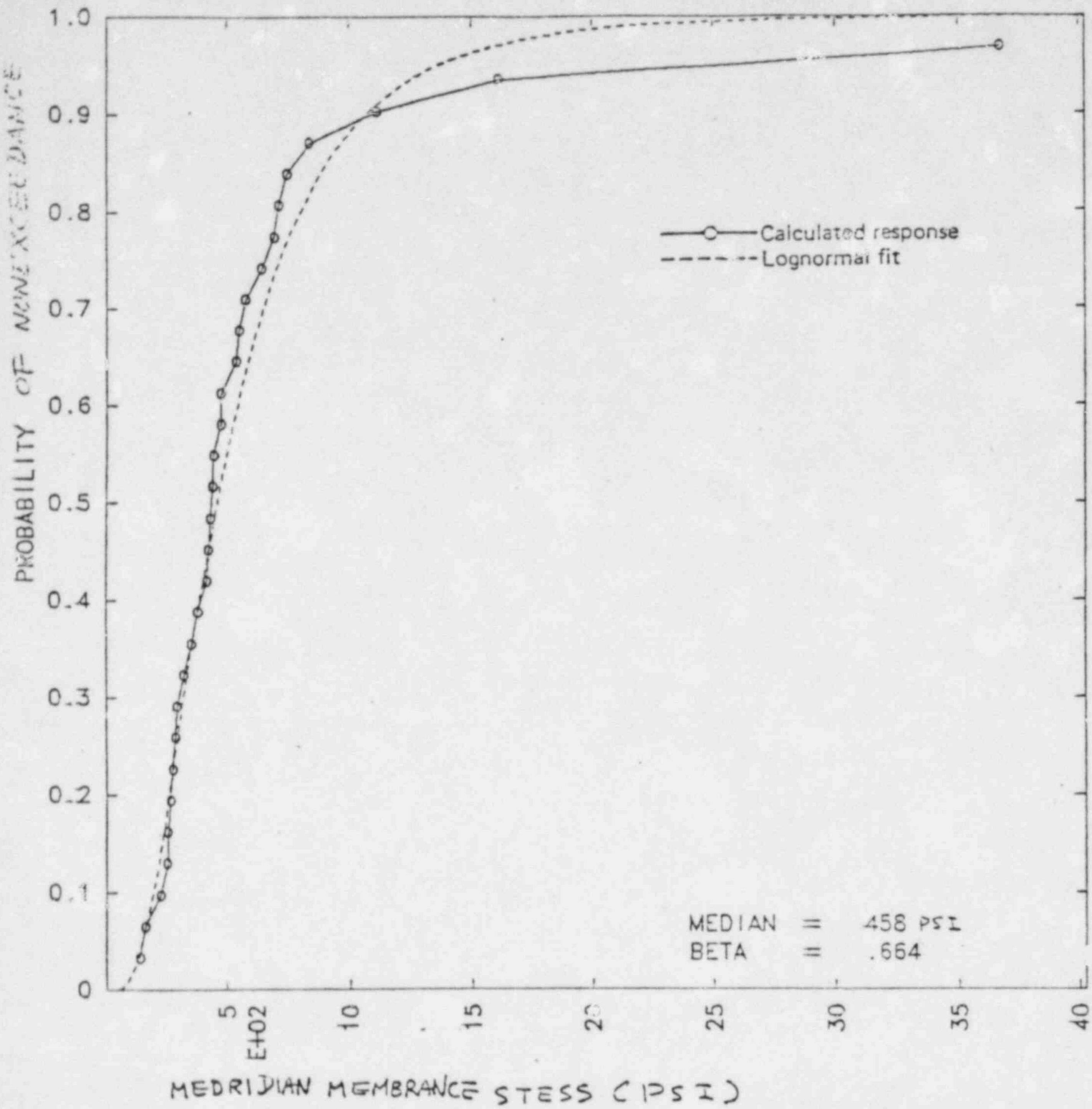

Figure 47. Cumulative distribution function of the meridian membrance stress of continuous shell due to the SONGS - 2&3 design spectra.

A.5 REFERENCES

DRAFT FOR COMMENT

1. D. Gasparini and E. H. Vanmarcke, Simulated Earthquake Motions Compatible with Prescribed Response Spectra, Report 2 of Evaluation of Seismic Safety of Buildings, Department of Civil Engineering, Massachussetts Institute of Technology, Cambridge, Massachussetts, Pub. No. R76-4, (January, 1976).

2. J. J. Johnson, G. L. Goudreau, S. E. Bumpus, O. R. Maslenikov, Seismic Safety Margins Research Program Phase I Final Report - SMACS - Seismic Methodology Analysis Chain with Statistics (Project VIII), Lawrence Livermore National Laboratory, Livermore, Calif., UCRL-53021, NUREG/CR2015, Vol. 9, (July, 1981).

3. Southern California Edison Company, Final Safety Analysis Report (FSAR), San Onofre Nuclear Generating Station Unit 1, NRC Docket 50-206.

4. Southern California Edison Company, Final Safety Analysis Report (FSAR), San Onofre Nuclear Generating Station Units 2 & 3, NRC Docket 50-361 and 50-362.

5. Dames and Moore, "Seismic and Foundation Studies," proposed Unit 2 and 3, San Onofre Nuclear Generating Station, San Onofre, California, for Southern California Edison Co., (April, 1970).

6. Woodward-McNeill and Associates, "Material Properties Studies," San Onofre Nuclear Generating Station, Report Prepared for Southern California Edison Co., (March, 1972).

7. P. B. Schnabel, J. Lysmer, and H. B. Seed, SHAKE--A Computer Program for Earthquake Response Analysis of Horizontally Layered Sites, UCB/EERC 72-12, (December, 1972).

DRAFT FOR COMMENT

8. Westinghouse Electric Corporation letter MA-RCSA-175, from T. A. Christopher to J. E. Dempsey, Bechtel Power Corporation, April 7, 1978.

9. R. L. Iman, W. H. Conover, and J. E. Campbell, "Risk Methodology for Geologic Disposal of Radioactive Waste: Small-Sample Sensitivity Analysis Techniques for Computer Models, with an Application to Risk Assessment," Sandia Laboratories, Albuquerque, N.M., SANMD80-0020, March 1980 (also published as U. S. Nuclear Regulatory Commission NUREG/CR-1397).

10. J. J. Johnson, "A Modified Version of the Structural Analysis Program SAP IV for the Static and Dynamic Response of Linear and Localized Nonlinear Structures," GA-A-14006 REV., (June, 1976).

11. H. L. Wong and J. E. Luco, "Tables of Impedance Functions and Input Motions for Rectangular Foundations," Report no. CE 78-15, University of Southern California, December, 1978.

12. Bechtel Power Corporation letter BPC/SCE-81-169 from A. Sanders, Bechtel Power Corporation, to R. Blaschke, Southern California Edison Company, July 6, 1981.

13. Bechtel Power Corporation letter from A. Sanders, Bechtel Power Corporation, to T. Y. Chuang, Lawrence Livermore National Laboratory, December 9, 1981.

14. Bechtel Power Corporation letter BPC/SCE-81-204 from A. Sanders, Bechtel Power Corporation, to A. Blaschke, Southern California Edison Company, August 7, 1981.

APPPENDIX B

FAULT TREE DEVELOPMENT

This appendix contains the followings:

- o Top levels of the San Onofre Unit 1 AFWS fault tree. (Figure 1)
- o Upper level of development for gate of insufficient flow to the steam generator (SAFA). (Figure 2)
- o Minimal cut sets of order 2 for SONGS-1 AFWS. (Table 1)

The remainings are on file at LLNL. The model includes the AFWS as well as those portions of other systems (condensate storage, auxiliary steam supply, electric power, and service water and fire protection) which interface with the SONGS-1 AFWS. No fault tree analysis of Zion-1 was initiated at the time the project was terminated.

DRAFT FOR COMMENT

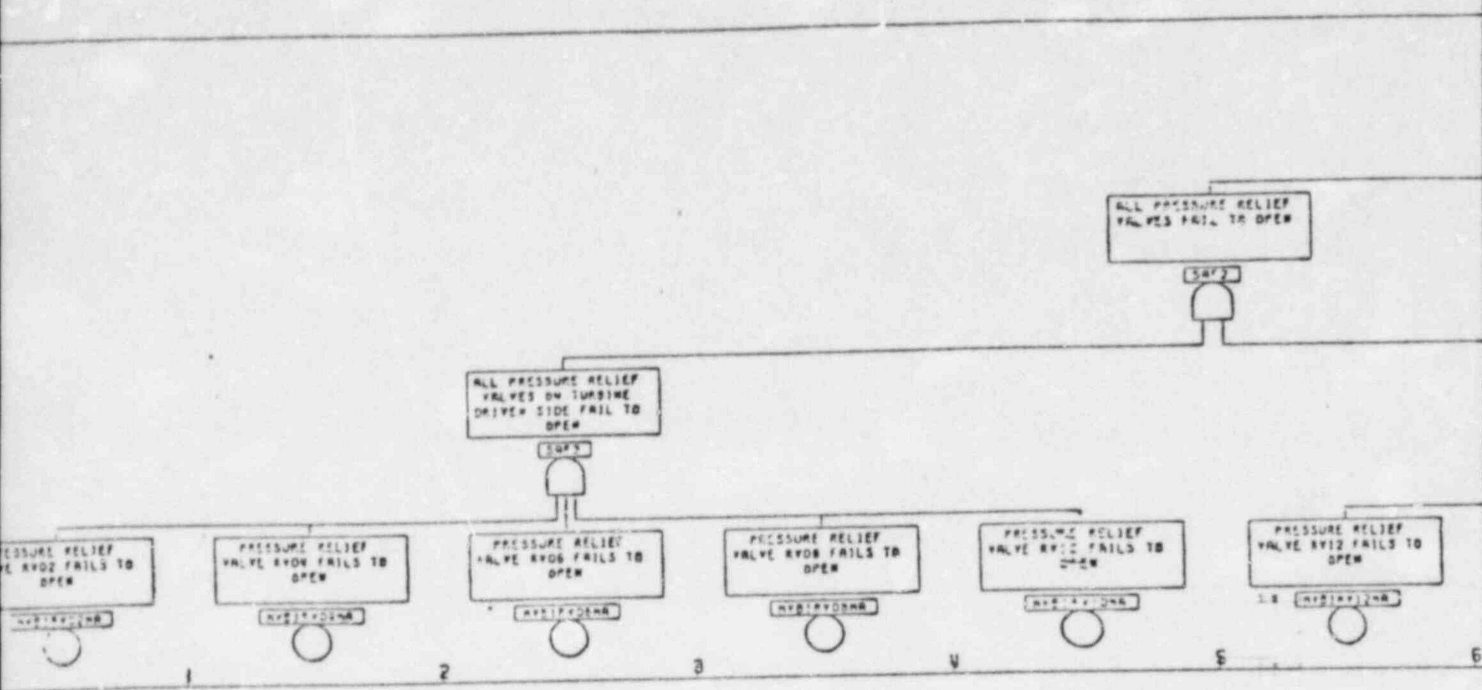

Figure 1. Top level of SONGS-1 AFWS fault tree

DRAFT FOR COMMENT

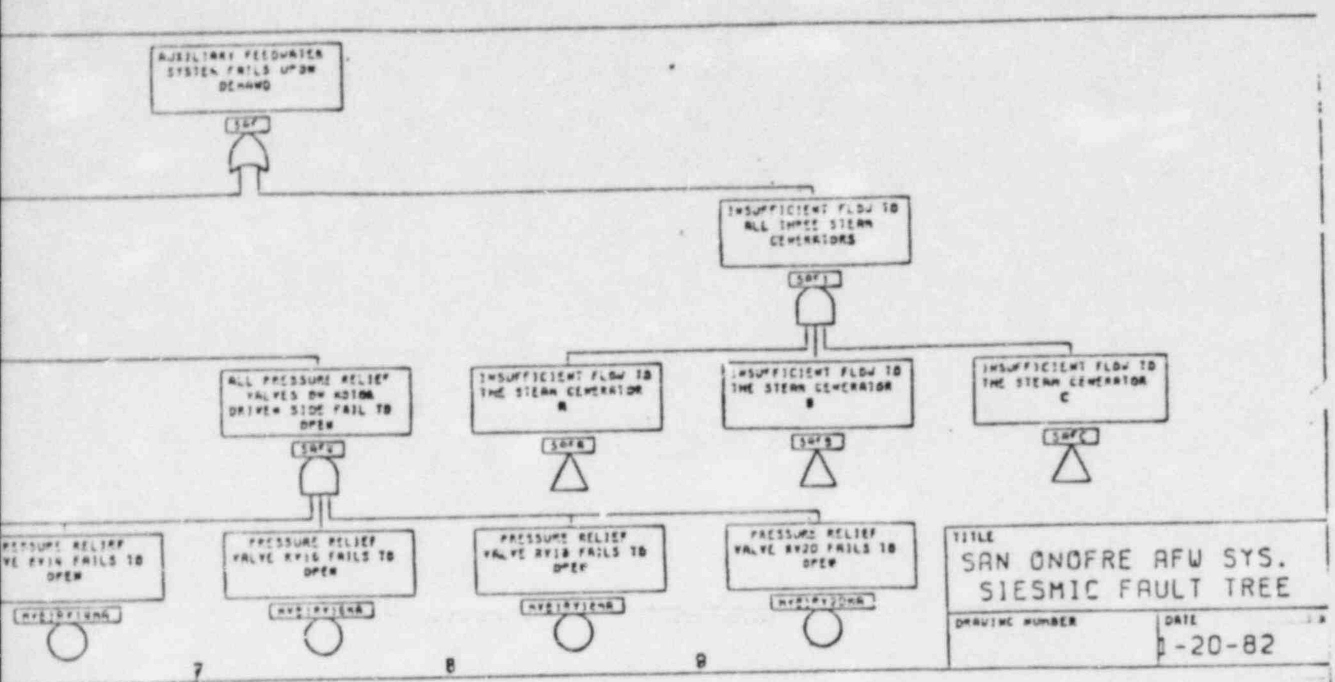

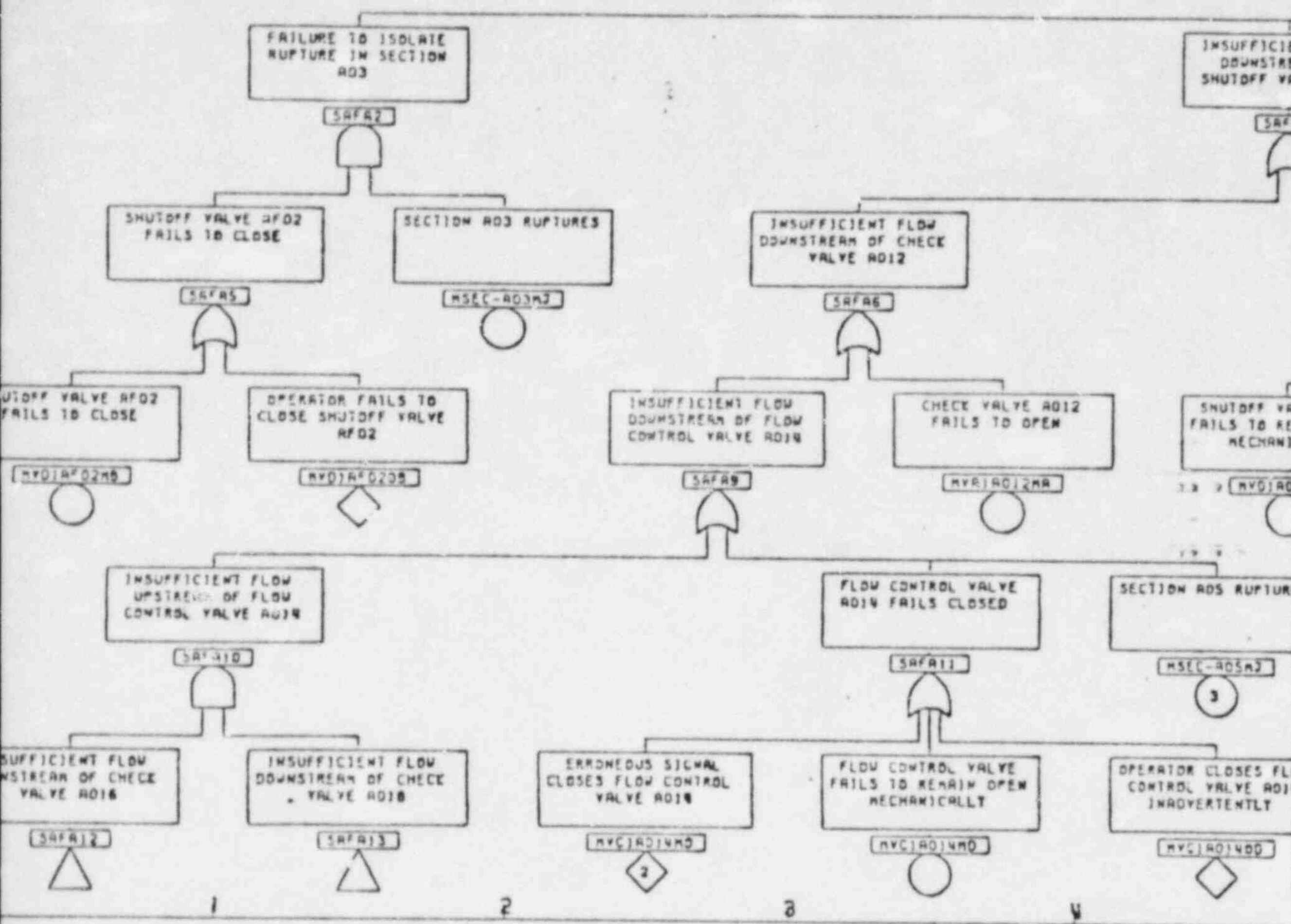

Figure 2. Upper level of development for gate SAF

DRAFT FOR COMMENT

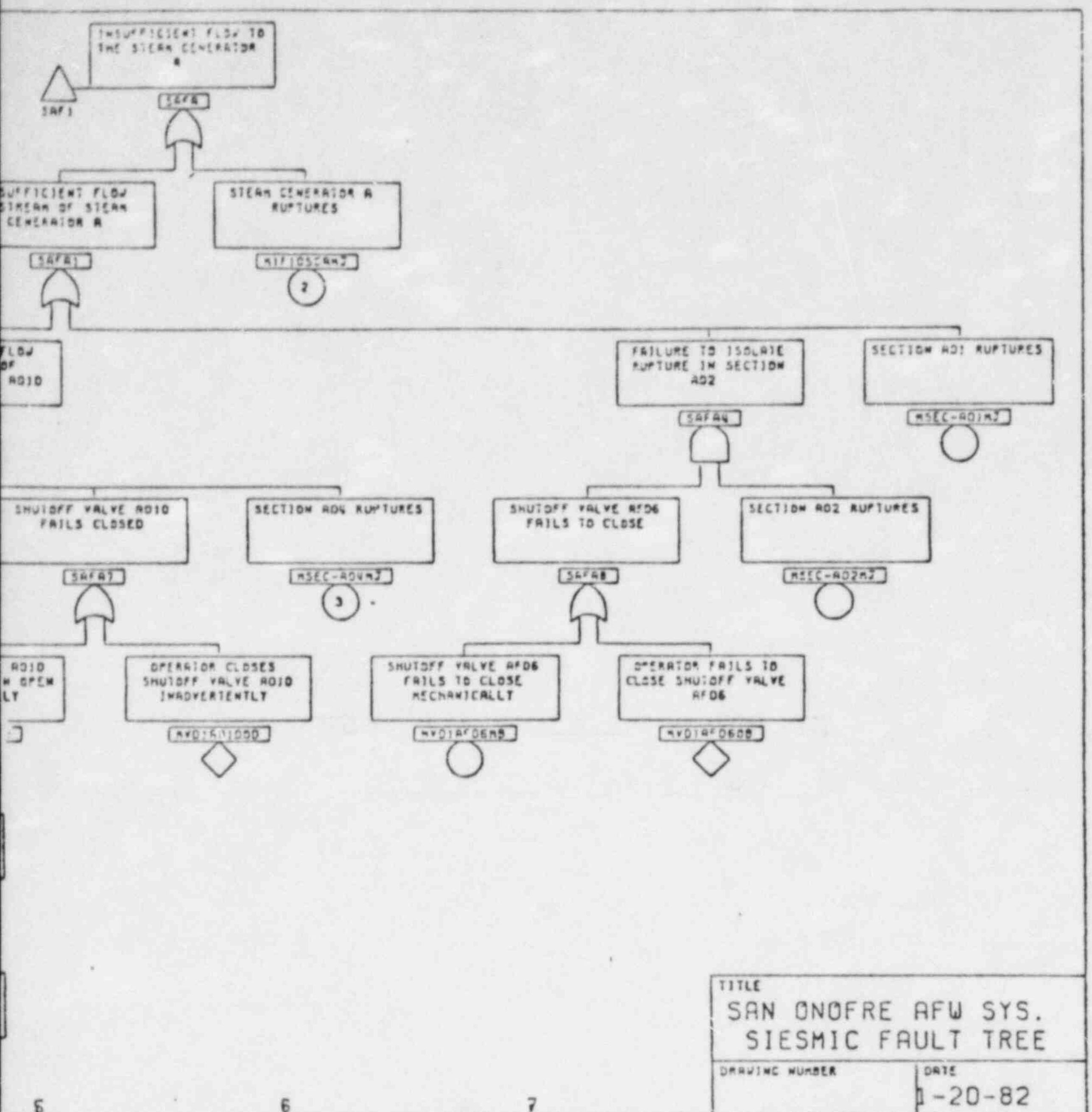

as shown in Figure 1.

```
* TITLE -- SONGS AUX FEED
*KF   --   SYSTEM CODE
* TOP EVENT   --   SAF
* TIME AND DATE OF RUN -- SAT, FEB 06 1982   10:38:14
* MIN CUT SET INFORMATION
* COMPLEMENTED EVENTS ? -- NO
* TOTAL NUMBER OF IMPLICANTS =   6007
*
* ORDER              1        2        3
* NUMBER OF          0      569     5438
* IMPLICANTS
*
```

Table 1. Minimal cut sets of order 2 for SONGS-1 AFWS

MIN CUT SET NO.			MIN CUT SET NO.		
1	MVD1M018OC	SORVALVES	286	MPB1000SME	MVD1M018MC
2	MVD1M018OC	MVG1SS100D	287	MPB1000SME	MVD1M018MB
3	MVD1M018OC	MVG1SS10MO	288	MPB1000SME	MVD1M016OD
4	MVD1M018OC	MVG1SS10MD	289	MPB1000SME	MVD1M016MO
5	MVD1M018OC	MVD1SS120D	290	MPB1000SME	MVD1M016MD
6	MVD1M018OC	MVD1SS12MD	291	MPB1000SME	MVD1M016MA
7	MVD1M018OC	MVD1S018OC	292	MPB1000SME	MVA1M020MA
8	MVD1M018OC	MVD1S018MC	293	MPB1000SME	MSEC.M03MJ
9	MVD1M018OC	MVD1S016OD	294	MPB1000SME	MSEC.M02MJ
10	MVD1M018OC	MVD1S016MO	295	MPB1000SME	MSEC.M01MJ
11	MVD1M018OC	MVD1S016MD	296	MPB1000SME	MSEC.CS6MJ
12	MVD1M018OC	MVD1S016MA	297	MPB1000MOO	SORVALVES
13	MVD1M018MO	SORVALVES	298	MPB1000MOO	MVG1SS100D
14	MVD1M018MO	MVG1SS100D	299	MPB1000MOO	MVG1SS10MO
15	MVD1M018MO	MVG1SS10MO	300	MPB1000MOO	MVG1SS10MD
16	MVD1M018MO	MVG1SS10MD	301	MPB1000MOO	MVD1SS120D
17	MVD1M018MO	MVD1SS120D	302	MPB1000MOO	MVD1SS12MD
18	MVD1M018MO	MVD1SS12MD	303	MPB1000MOO	MVD1S018OC
19	MVD1M018MO	MVD1S018OC	304	MPB1000MOO	MVD1S018MC
20	MVD1M018MO	MVD1S018MC	305	MPB1000MOO	MVD1S016OD
21	MVD1M018MO	MVD1S016OD	306	MPB1000MOO	MVD1S016MO
22	MVD1M018MO	MVD1S016MO	307	MPB1000MOO	MVD1S016MD
23	MVD1M018MO	MVD1S016MD	308	MPB1000MOO	MVD1S016MA
24	MVD1M018MO	MVD1S016MA	309	MPB1000MOO	MVA1S020MA
25	MVD1M018MC	SORVALVES	310	MPB1000MOO	MSEC.SS1MJ
26	MVD1M018MC	MVG1SS100D	311	MPB1000MOO	MSEC.S03MJ
27	MVD1M018MC	MVG1SS10MO	312	MPB1000MOO	MSEC.S02MJ
28	MVD1M018MC	MVG1SS10MD	313	MPB1000MOO	MSEC.S01MJ
29	MVD1M018MC	MVD1SS120D	314	MPB1000MOO	MSEC.CS7MJ
30	MVD1M018MC	MVD1SS12MD	315	MPB1000MOO	MPB1000SOG
31	MVD1M018MC	MVD1S018OC	316	MPB1000MOO	MPB1000SMG
32	MVD1M018MC	MVD1S018MC	317	MPB1000MOO	MPB1000SME
33	MVD1M018MC	MVD1S016OD	318	MPB1000MOG	SORVALVES
34	MVD1M018MC	MVD1S016MO	319	MPB1000MOG	MVG1SS100D
35	MVD1M018MC	MVD1S016MD	320	MPB1000MOG	MVG1SS10MO
36	MVD1M018MC	MVD1S016MA	321	MPB1000MOG	MVG1SS10MD
37	MVD1M018MB	SORVALVES	322	MPB1000MOG	MVD1SS120D
38	MVD1M018MB	MVG1SS100D	323	MPB1000MOG	MVD1SS12MD
39	MVD1M018MB	MVG1SS10MO	324	MPB1000MOG	MVD1S018OC
40	MVD1M018MB	MVG1SS10MD	325	MPB1000MOG	MVD1S018MC
41	MVD1M018MB	MVD1SS120D	326	MPB1000MOG	MVD1S016OD
42	MVD1M018MB	MVD1SS12MD	327	MPB1000MOG	MVD1S016MO
43	MVD1M018MB	MVD1S018OC	328	MPB1000MOG	MVD1S016MD
44	MVD1M018MB	MVD1S018MC	329	MPB1000MOG	MVD1S016MA
45	MVD1M018MB	MVD1S016OD	330	MPB1000MOG	MVA1S020MA
46	MVD1M018MB	MVD1S016MO	331	MPB1000MOG	MSEC.SS1MJ

DRAFT FOR COMMENT

Table 1. Minimal cut sets of order 2 for SONGS-1 AFWS (cont.)

47	MVD1MØ10MB	MVD1SØ16MD
48	MVD1MØ10MB	MVD1SØ16MA
49	MVD1MØ160D	SORVALVES
5Ø	MVD1MØ160D	MVG1SS1ØOD
51	MVD1MØ160D	MVG1SS1ØMO
52	MVD1MØ160D	MVG1SS1ØMD
53	MVD1MØ160D	MVD1SS12OD
54	MVD1MØ160D	MVD1SS12MD
55	MVD1MØ160D	MVD1SØ10OC
56	MVD1MØ160D	MVD1SØ10MC
57	MVD1MØ160D	MVD1SØ160D
58	MVD1MØ160D	MVD1SØ16MO
59	MVD1MØ160D	MVD1SØ16MD
6Ø	MVD1MØ160D	MVD1SØ16MA
61	MVD1MØ16MO	SORVALVES
62	MVD1MØ16MO	MVG1SS1ØOD
63	MVD1MØ16MO	MVG1SS1ØMO
64	MVD1MØ16MO	MVG1SS1ØMD
65	MVD1MØ16MO	MVD1SS12OD
66	MVD1MØ16MO	MVD1SS12MD
67	MVD1MØ16MO	MVD1SØ10OC
68	MVD1MØ16MO	MVD1SØ10MC
69	MVD1MØ16MO	MVD1SØ160D
7Ø	MVD1MØ16MO	MVD1SØ16MO
71	MVD1MØ16MO	MVD1SØ16MD
72	MVD1MØ16MO	MVD1SØ16MA
73	MVD1MØ16MD	SORVALVES
74	MVD1MØ16MD	MVG1SS1ØOD
75	MVD1MØ16MD	MVG1SS1ØMO
76	MVD1MØ16MD	MVG1SS1ØMD
77	MVD1MØ16MD	MVD1SS12OD
78	MVD1MØ16MD	MVD1SS12MD
79	MVD1MØ16MD	MVD1SØ10OC
8Ø	MVD1MØ16MD	MVD1SØ10MC
81	MVD1MØ16MD	MVD1SØ160D
82	MVD1MØ16MD	MVD1SØ16MO
83	MVD1MØ16MD	MVD1SØ16MD
84	MVD1MØ16MD	MVD1SØ16MA
85	MVD1MØ16MA	SORVALVES
86	MVD1MØ16MA	MVG1SS1ØOD
87	MVD1MØ16MA	MVG1SS1ØMO
88	MVD1MØ16MA	MVG1SS1ØMD
89	MVD1MØ16MA	MVD1SS12OD
9Ø	MVD1MØ16MA	MVD1SS12MD
91	MVD1MØ16MA	MVD1SØ10OC
92	MVD1MØ16MA	MVD1SØ10MC
93	MVD1MØ16MA	MVD1SØ160D
94	MVD1MØ16MA	MVD1SØ16MO
95	MVD1MØ16MA	MVD1SØ16MD
96	MVD1MØ16MA	MVD1SØ16MA
97	MVA1SØ2ØMA	MVD1MØ10OC
98	MVA1SØ2ØMA	MVD1MØ10MO
99	MVA1SØ2ØMA	MVD1MØ10MC
1ØØ	MVA1SØ2ØMA	MVD1MØ10MB
1Ø1	MVA1SØ2ØMA	MVD1MØ160D
1Ø2	MVA1SØ2ØMA	MVD1MØ16MO
1Ø3	MVA1SØ2ØMA	MVD1MØ16MD
1Ø4	MVA1SØ2ØMA	MVD1MØ16MA
1Ø5	MVA1MØ2ØMA	SORVALVES
1Ø6	MVA1MØ2ØMA	MVG1SS1ØOD
332	MPB1ØØØHOG	MSEC.SØ3MJ
333	MPB1ØØØHOG	MSEC.SØ2MJ
334	MPB1ØØØHOG	MSEC.SØ1MJ
335	MPB1ØØØHOG	MSEC.CS7MJ
336	MPB1ØØØHOG	MPB1ØØØSOO
337	MPB1ØØØHOG	MPB1ØØØSOG
338	MPB1ØØØHOG	MPB1ØØØSMG
339	MPB1ØØØHOG	MPB1ØØØSME
34Ø	MPB1ØØØHMG	SORVALVES
341	MPB1ØØØHMG	MVG1SS1ØOD
342	MPB1ØØØHMG	MVG1SS1ØMO
343	MPB1ØØØHMG	MVG1SS1ØMD
344	MPB1ØØØHMG	MVD1SS12OD
345	MPB1ØØØHMG	MVD1SS12MD
346	MPB1ØØØHMG	MVD1SØ10OC
347	MPB1ØØØHMG	MVD1SØ10MC
348	MPB1ØØØHMG	MVD1SØ160D
349	MPB1ØØØHMG	MVD1SØ16MO
35Ø	MPB1ØØØHMG	MVD1SØ16MD
351	MPB1ØØØHMG	MVD1SØ16MA
352	MPB1ØØØHMG	MVA1SØ2ØMA
353	MPB1ØØØHMG	MSEC.SS1MJ
354	MPB1ØØØHMG	MSEC.SØ3MJ
355	MPB1ØØØHMG	MSEC.SØ2MJ
356	MPB1ØØØHMG	MSEC.SØ1MJ
357	MPB1ØØØHMG	MSEC.CS7MJ
358	MPB1ØØØHMG	MPB1ØØØSOO
359	MPB1ØØØHMG	MPB1ØØØSOG
36Ø	MPB1ØØØHMG	MPB1ØØØSMG
361	MPB1ØØØHMG	MPB1ØØØSME
362	MPB1ØØØHME	SORVALVES
363	MPB1ØØØHME	MVG1SS1ØOD
364	MPB1ØØØHME	MVG1SS1ØMO
365	MPB1ØØØHME	MVG1SS1ØMD
366	MPB1ØØØHME	MVD1SS12OD
367	MPB1ØØØHME	MVD1SS12MD
368	MPB1ØØØHME	MVD1SØ10OC
369	MPB1ØØØHME	MVD1SØ10MC
37Ø	MPB1ØØØHME	MVD1SØ160D
371	MPB1ØØØHME	MVD1SØ16MO
372	MPB1ØØØHME	MVD1SØ16MD
373	MPB1ØØØHME	MVD1SØ16MA
374	MPB1ØØØHME	MVA1SØ2ØMA
375	MPB1ØØØHME	MSEC.SS1MJ
376	MPB1ØØØHME	MSEC.SØ3MJ
377	MPB1ØØØHME	MSEC.SØ2MJ
378	MPB1ØØØHME	MSEC.SØ1MJ
379	MPB1ØØØHME	MSEC.CS7MJ
38Ø	MPB1ØØØHME	MPB1ØØØSOO
381	MPB1ØØØHME	MPB1ØØØSOG
382	MPB1ØØØHME	MPB1ØØØSMG
383	MPB1ØØØHME	MPB1ØØØSME
384	LVD1FW44OD	MXX1CSØ6MD
385	LVD1FW44OD	MVD1CSØ8OD
386	LVD1FW44OD	MVD1CSØ8MD
387	LVD1FW44OD	MTA1ØCSTMM
388	LVD1FW44OD	MSEC.CS1MJ
389	LVD1FW44OD	MF11ØCSTMK
39Ø	LVD1FW44MD	MXX1CSØ6MD
391	LVD1FW44MD	MVD1CSØ8OD

DRAFT FOR COMMENT

Table I. Minimal cut sets of order 2 for SONGS-1 AFWS (cont.)

108	MVA1M020MA	MVG1SS10MD	393	LVD1FW44MD	MTA10CSTMM
109	MVA1M020MA	MVD1SS120D	394	LVD1FW44MD	MSEC.CS1MJ
110	MVA1M020MA	MVD1SS12MD	395	LVD1FW44MD	MF110CSTMK
111	MVA1M020MA	MVD1S0180C	396	LTA1RSVRMM	MXX1CS06MD
112	MVA1M020MA	MVD1S018MC	397	LTA1RSVRMM	MVD1CS000D
113	MVA1M020MA	MVD1S0160D	398	LTA1RSVRMM	MVD1CS00MD
114	MVA1M020MA	MVD1S016MO	399	LTA1RSVRMM	MTA10CSTMM
115	MVA1M020MA	MVD1S016MD	400	LTA1RSVRMM	MSEC.CS1MJ
116	MVA1M020MA	MVD1S016MA	401	LTA1RSVRMM	MF110CSTMK
117	MVA1M020MA	MVA1S020MA	402	LSEC.F5XMJ	MXX1CS06MD
118	MSEC.SS1MJ	MVD1M0180C	403	LSEC.F5XMJ	MVD1CS000D
119	MSEC.SS1MJ	MVD1M018MO	404	LSEC.F5XMJ	MVD1CS00MD
120	MSEC.SS1MJ	MVD1M018MC	405	LSEC.F5XMJ	MTA10CSTMM
121	MSEC.SS1MJ	MVD1M018MD	406	LSEC.F5XMJ	MSEC.CS1MJ
122	MSEC.SS1MJ	MVD1M0160D	407	LSEC.F5XMJ	MF110CSTMK
123	MSEC.SS1MJ	MVD1M016MO	408	LSEC.F07MJ	MXX1CS06MD
124	MSEC.SS1MJ	MVD1M016MD	409	LSEC.F07MJ	MVD1CS000D
125	MSEC.SS1MJ	MVD1M016MA	410	LSEC.F07MJ	MVD1CS00MD
126	MSEC.SS1MJ	MVA1M020MA	411	LSEC.F07MJ	MTA10CSTMM
127	MSEC.S03MJ	MVD1M0180C	412	LSEC.F07MJ	MSEC.CS1MJ
128	MSEC.S03MJ	MVD1M018MO	413	LSEC.F07MJ	MF110CSTMK
129	MSEC.S03MJ	MVD1M018MC	414	LSEC.F05MJ	MXX1CS06MD
130	MSEC.S03MJ	MVD1M018MD	415	LSEC.F05MJ	MVD1CS000D
131	MSEC.S03MJ	MVD1M0160D	416	LSEC.F05MJ	MVD1CS00MD
132	MSEC.S03MJ	MVD1M016MO	417	LSEC.F05MJ	MTA10CSTMM
133	MSEC.S03MJ	MVD1M016MD	418	LSEC.F05MJ	MSEC.CS1MJ
134	MSEC.S03MJ	MVD1M016MA	419	LSEC.F05MJ	MF110CSTMK
135	MSEC.S03MJ	MVA1M020MA	420	LSEC.F04MJ	MXX1CS06MD
136	MSEC.S02MJ	MVD1M0180C	421	LSEC.F04MJ	MVD1CS000D
137	MSEC.S02MJ	MVD1M018MO	422	LSEC.F04MJ	MVD1CS00MD
138	MSEC.S02MJ	MVD1M018MC	423	LSEC.F04MJ	MTA10CSTMM
139	MSEC.S02MJ	MVD1M018MD	424	LSEC.F04MJ	MSEC.CS1MJ
140	MSEC.S02MJ	MVD1M0160D	425	LSEC.F04MJ	MF110CSTMK
141	MSEC.S02MJ	MVD1M016MO	426	LSEC.F03MJ	MXX1CS06MD
142	MSEC.S02MJ	MVD1M016MD	427	LSEC.F03MJ	MVD1CS000D
143	MSEC.S02MJ	MVD1M016MA	428	LSEC.F03MJ	MVD1CS00MD
144	MSEC.S02MJ	MVA1M020MA	429	LSEC.F03MJ	MTA10CSTMM
145	MSEC.S01MJ	MVD1M0180C	430	LSEC.F03MJ	MSEC.CS1MJ
146	MSEC.S01MJ	MVD1M018MO	431	LSEC.F03MJ	MF110CSTMK
147	MSEC.S01MJ	MVD1M018MC	432	LF11RSVRMK	MXX1CS06MD
148	MSEC.S01MJ	MVD1M018MD	433	LF11RSVRMK	MVD1CS000D
149	MSEC.S01MJ	MVD1M0160D	434	LF11RSVRMK	MVD1CS00MD
150	MSEC.S01MJ	MVD1M016MO	435	LF11RSVRMK	MTA10CSTMM
151	MSEC.S01MJ	MVD1M016MD	436	LF11RSVRMK	MSEC.CS1MJ
152	MSEC.S01MJ	MVD1M016MA	437	LF11RSVRMK	MF110CSTMK
153	MSEC.S01MJ	MVA1M020MA	438	BEC1W1RAMK	SORVALVES
154	MSEC.M03MJ	SORVALVES	439	BEC1W1RAMK	MVG1SS100D
155	MSEC.M03MJ	MVG1SS100D	440	BEC1W1RAMK	MVG1SS10MO
156	MSEC.M03MJ	MVG1SS10MO	441	BEC1W1RAMK	MVG1SS10MD
157	MSEC.M03MJ	MVG1SS10MD	442	BEC1W1RAMK	MVD1SS120D
158	MSEC.M03MJ	MVD1SS120D	443	BEC1W1RAMK	MVD1SS12MD
159	MSEC.M03MJ	MVD1SS12MD	444	BEC1W1RAMK	MVD1S0180C
160	MSEC.M03MJ	MVD1S0180C	445	BEC1W1RAMK	MVD1S018MC
161	MSEC.M03MJ	MVD1S018MC	446	BEC1W1RAMK	MVD1S0160D
162	MSEC.M03MJ	MVD1S0160D	447	BEC1W1RAMK	MVD1S016MO
163	MSEC.M03MJ	MVD1S016MO	448	BEC1W1RAMK	MVD1S016MD
164	MSEC.M03MJ	MVD1S016MD	449	BEC1W1RAMK	MVD1S016MA
165	MSEC.M03MJ	MVD1S016MA	450	BEC1W1RAMK	MVA1S020MA
166	MSEC.M03MJ	MVA1S020MA	451	BEC1W1RAMK	MSEC.SS1MJ

DRAFT FOR COMMENT

Table 1. Minimal cut sets of order 2 for SONGS-1 AFWS (cont.)

DRAFT FOR COMMENT

167	MSEC.M03MJ	MSEC.SS1MJ	452	BECIWIRAMK	MSEC.S03MJ
168	MSEC.M03MJ	MSEC.S03MJ	453	BECIWIRAMK	MSEC.S02MJ
169	MSEC.M03MJ	MSEC.S02MJ	454	BECIWIRAMK	MSEC.S01MJ
170	MSEC.M03MJ	MSEC.S01MJ	455	BECIWIRAMK	MSEC.CS7MJ
171	MSEC.M02MJ	SORVALVES	456	BECIWIRAMK	MPB1000SOO
172	MSEC.M02MJ	MVGISS100D	457	BECIWIRAMK	MPB1000SOG
173	MSEC.M02MJ	MVGISS10MO	458	BECIWIRAMK	MPB1000SMG
174	MSEC.M02MJ	MVGISS10MD	459	BECIWIRAMK	MPB1000SME
175	MSEC.M02MJ	MVDISS120D	460	BEC1008IMJ	SORVALVES
176	MSEC.M02MJ	MVDISS12MD	461	BEC1008IMJ	MVGISS100D
177	MSEC.M02MJ	MVDIS0180C	462	BEC1008IMJ	MVGISS10MO
178	MSEC.M02MJ	MVDIS018MC	463	BEC1008IMJ	MVGISS10MD
179	MSEC.M02MJ	MVDIS0160D	464	BEC1008IMJ	MVDISS120D
180	MSEC.M02MJ	MVDIS016MO	465	BEC1008IMJ	MVDISS12MD
181	MSEC.M02MJ	MVDIS016MD	466	BEC1008IMJ	MVDIS0180C
182	MSEC.M02MJ	MVDIS016MA	467	BEC1008IMJ	MVDIS018MC
183	MSEC.M02MJ	MVAIS020MA	468	BEC1008IMJ	MVDIS0160D
184	MSEC.M02MJ	MSEC.SS1MJ	469	BEC1008IMJ	MVDIS016MO
185	MSEC.M02MJ	MSEC.S03MJ	470	BEC1008IMJ	MVDIS016MD
186	MSEC.M02MJ	MSEC.S02MJ	471	BEC1008IMJ	MVDIS016MA
187	MSEC.M02MJ	MSEC.S01MJ	472	BEC1008IMJ	MVAIS020MA
188	MSEC.M01MJ	SORVALVES	473	BEC1008IMJ	MSEC.SS1MJ
189	MSEC.M01MJ	MVGISS100D	474	BEC1008IMJ	MSEC.S03MJ
190	MSEC.M01MJ	MVGISS10MO	475	BEC1008IMJ	MSEC.S02MJ
191	MSEC.M01MJ	MVGISS10MD	476	BEC1008IMJ	MSEC.S01MJ
192	MSEC.M01MJ	MVDISS120D	477	BEC1008IMJ	MSEC.CS7MJ
193	MSEC.M01MJ	MVDISS12MD	478	BEC1008IMJ	MPB1000SOO
194	MSEC.M01MJ	MVDIS0180C	479	BEC1008IMJ	MPB1000SOG
195	MSEC.M01MJ	MVDIS018MC	480	BEC1008IMJ	MPB1000SMG
196	MSEC.M01MJ	MVDIS0160D	481	BEC1008IMJ	MPB1000SME
197	MSEC.M01MJ	MVDIS016MO	482	BCAIBIAAMJ	SORVALVES
198	MSEC.M01MJ	MVDIS016MD	483	BCAIBIAAMJ	MVGISS100D
199	MSEC.M01MJ	MVDIS016MA	484	BCAIBIAAMJ	MVGISS10MO
200	MSEC.M01MJ	MVAIS020MA	485	BCAIBIAAMJ	MVGISS10MD
201	MSEC.M01MJ	MSEC.SS1MJ	486	BCAIBIAAMJ	MVDISS120D
202	MSEC.M01MJ	MSEC.S03MJ	487	BCAIBIAAMJ	MVDISS12MD
203	MSEC.M01MJ	MSEC.S02MJ	488	BCAIBIAAMJ	MVDIS0180C
204	MSEC.M01MJ	MSEC.S01MJ	489	BCAIBIAAMJ	MVDIS018MC
205	MSEC.CS7MJ	MVDIM0180C	490	BCAIBIAAMJ	MVDIS0160D
206	MSEC.CS7MJ	MVDIM018MO	491	BCAIBIAAMJ	MVDIS016MO
207	MSEC.CS7MJ	MVDIM018MC	492	BCAIBIAAMJ	MVDIS016MD
208	MSEC.CS7MJ	MVDIM018MD	493	BCAIBIAAMJ	MVDIS016MA
209	MSEC.CS7MJ	MVDIM0160D	494	BCAIBIAAMJ	MVAIS020MA
210	MSEC.CS7MJ	MVDIM016MC	495	BCAIBIAAMJ	MSEC.SS1MJ
211	MSEC.CS7MJ	MVDIM016MD	496	BCAIBIAAMJ	MSEC.S03MJ
212	MSEC.CS7MJ	MVDIM016MA	497	BCAIBIAAMJ	MSEC.S02MJ
213	MSEC.CS7MJ	MVDICH040B	498	BCAIBIAAMJ	MSEC.S01MJ
214	MSEC.CS7MJ	MVDICH04MB	499	BCAIBIAAMJ	MSEC.CS7MJ
215	MSEC.CS7MJ	MVAIM020MA	500	BCAIBIAAMJ	MPB1000SOO
216	MSEC.CS7MJ	MSEC.M03MJ	501	BCAIBIAAMJ	MPB1000SOG
217	MSEC.CS7MJ	MSEC.M02MJ	502	BCAIBIAAMJ	MPB1000SMG
218	MSEC.CS7MJ	MSEC.M01MJ	503	BCAIBIAAMJ	MPB1000SME
219	MSEC.CS6MJ	SORVALVES	504	BCAI1125MC	SORVALVES
220	MSEC.CS6MJ	MVGISS100D	505	BCAI1125MC	MVGISS100D
221	MSEC.CS6MJ	MVGISS10MO	506	BCAI1125MC	MVGISS10MO
222	MSEC.CS6MJ	MVGISS10MD	507	BCAI1125MC	MVGISS10MD
223	MSEC.CS6MJ	MVDISS120D	508	BCAI1125MC	MVDISS120D
224	MSEC.CS6MJ	MVDISS12MD	509	BCAI1125MC	MVDISS12MD
225	MSEC.CS6MJ	MVDIS0180C	510	BCAI1125MC	MVDIS0180C
226	MSEC.CS6MJ	MVDIS018MC	511	BCAI1125MC	MVDIS018MC

Table 1. Minimal cut sets of order 2 for SONGS-1 AFWS (cont.)

228	MSEC.CS6MJ	MVD1SØ16MO
229	MSEC.CS6MJ	MVD1SØ16MD
230	MSEC.CS6MJ	MVD1SØ16MA
231	MSEC.CS6MJ	MVD1CSØ40B
232	MSEC.CS6MJ	MVD1CSØ4MB
233	MSEC.CS6MJ	MVA1SØ2ØMA
234	MSEC.CS6MJ	MSEC.SS1MJ
235	MSEC.CS6MJ	MSEC.SØ3MJ
236	MSEC.CS6MJ	MSEC.SØ2MJ
237	MSEC.CS6MJ	MSEC.SØ1MJ
238	MSEC.CS6MJ	MSEC.CS7MJ
239	MSEC.CS5MJ	MVD1CS1ØØB
240	MSEC.CS5MJ	MVD1CS1ØMB
241	MSEC.CS4MJ	MVD1CS16ØB
242	MSEC.CS4MJ	MVD1CS16MB
243	MSEC.CS3MJ	MVD1CS22ØB
244	MSEC.CS3MJ	MVD1CS22MB
245	MPB1ØØØSOO	MVD1MØ18OC
246	MPB1ØØØSOO	MVD1MØ18MO
247	MPB1ØØØSOO	MVD1MØ18MC
248	MPB1ØØØSOO	MVD1MØ18MB
249	MPB1ØØØSOO	MVD1MØ16OD
250	MPB1ØØØSOO	MVD1MØ16MO
251	MPB1ØØØSOO	MVD1MØ16MD
252	MPB1ØØØSOO	MVD1MØ16MA
253	MPB1ØØØSOO	MVA1MØ2ØMA
254	MPB1ØØØSOO	MSEC.MØ3MJ
255	MPB1ØØØSOO	MSEC.MØ2MJ
256	MPB1ØØØSOO	MSEC.MØ1MJ
257	MPB1ØØØSOO	MSEC.CS6MJ
258	MPB1ØØØSOG	MVD1MØ18OC
259	MPB1ØØØSOG	MVD1MØ18MO
260	MPB1ØØØSOG	MVD1MØ18MC
261	MPB1ØØØSOG	MVD1MØ18MB
262	MPB1ØØØSOG	MVD1MØ16OD
263	MPB1ØØØSOG	MVD1MØ16MO
264	MPB1ØØØSOG	MVD1MØ16MD
265	MPB1ØØØSOG	MVD1MØ16MA
266	MPB1ØØØSOG	MVA1MØ2ØMA
267	MPB1ØØØSOG	MSEC.MØ3MJ
268	MPB1ØØØSOG	MSEC.MØ2MJ
269	MPB1ØØØSOG	MSEC.MØ1MJ
270	MPB1ØØØSOG	MSEC.CS6MJ
271	MPB1ØØØSMG	MVD1MØ18OC
272	MPB1ØØØSMG	MVD1MØ18MO
273	MPB1ØØØSMG	MVD1MØ18MC
274	MPB1ØØØSMG	MVD1MØ18MB
275	MPB1ØØØSMG	MVD1MØ16OD
276	MPB1ØØØSMG	MVD1MØ16MO
277	MPB1ØØØSMG	MVD1MØ16MD
278	MPB1ØØØSMG	MVD1MØ16MA
279	MPB1ØØØSMG	MVA1MØ2ØMA
280	MPB1ØØØSMG	MSEC.MØ3MJ
281	MPB1ØØØSMG	MSEC.MØ2MJ
282	MPB1ØØØSMG	MSEC.MØ1MJ
283	MPB1ØØØSMG	MSEC.CS6MJ
284	MPB1ØØØSME	MVD1MØ18OC
285	MPB1ØØØSME	MVD1MØ18MO
512	BCA11125MC	MVD1SØ16OD
513	BCA11125MC	MVD1SØ16MO
514	BCA11125MC	MVD1SØ16MD
515	BCA11125MC	MVD1SØ16MA
516	BCA11125MC	MVA1SØ2ØMA
517	BCA11125MC	MSEC.SS1MJ
518	BCA11125MC	MSEC.SØ3MJ
519	BCA11125MC	MSEC.SØ2MJ
520	BCA11125MC	MSEC.SØ1MJ
521	BCA11125MC	MSEC.CS7MJ
522	BCA11125MC	MPB1ØØØSOO
523	BCA11125MC	MPB1ØØØSOG
524	BCA11125MC	MPB1ØØØSMG
525	BCA11125MC	MPB1ØØØSME
526	BCA11123MC	SORVALVES
527	BCA11123MC	MVG1SS1ØOD
528	BCA11123MC	MVG1SS1ØMO
529	BCA11123MC	MVG1SS1ØMD
530	BCA11123MC	MVD1SS12OD
531	BCA11123MC	MVD1SS12MD
532	BCA11123MC	MVD1SØ18OC
533	BCA11123MC	MVD1SØ18MC
534	BCA11123MC	MVD1SØ16OD
535	BCA11123MC	MVD1SØ16MO
536	BCA11123MC	MVD1SØ16MD
537	BCA11123MC	MVD1SØ16MA
538	BCA11123MC	MVA1SØ2ØMA
539	BCA11123MC	MSEC.SS1MJ
540	BCA11123MC	MSEC.SØ3MJ
541	BCA11123MC	MSEC.SØ2MJ
542	BCA11123MC	MSEC.SØ1MJ
543	BCA11123MC	MSEC.CS7MJ
544	BCA11123MC	MPB1ØØØSOO
545	BCA11123MC	MPB1ØØØSOG
546	BCA11123MC	MPB1ØØØSMG
547	BCA11123MC	MPB1ØØØSME
548	BCA11118MC	SORVALVES
549	BCA11118MC	MVG1SS1ØOD
550	BCA11118MC	MVG1SS1ØMO
551	BCA11118MC	MVG1SS1ØMD
552	BCA11118MC	MVD1SS12OD
553	BCA11118MC	MVD1SS12MD
554	BCA11118MC	MVD1SØ18OC
555	BCA11118MC	MVD1SØ18MC
556	BCA11118MC	MVD1SØ16OD
557	BCA11118MC	MVD1SØ16MO
558	BCA11118MC	MVD1SØ16MD
559	BCA11118MC	MVD1SØ16MA
560	BCA11118MC	MVA1SØ2ØMA
561	BCA11118MC	MSEC.SS1MJ
562	BCA11118MC	MSEC.SØ3MJ
563	BCA11118MC	MSEC.SØ2MJ
564	BCA11118MC	MSEC.SØ1MJ
565	BCA11118MC	MSEC.CS7MJ
566	BCA11118MC	MPB1ØØØSOO
567	BCA11118MC	MPB1ØØØSOG
568	BCA11118MC	MPB1ØØØSMG
569	BCA11118MC	MPB1ØØØSME

DRAFT FOR COMMENT

APPENDIX C

INCOMPLETE TASKS

C1. INTRODUCTION

This appendix contains discussions and results of the tasks pertinent to the San Onofre Nuclear Generating Station Unit 1 (SONGS-1) Auxiliary Feedwater System (AFWS) Project which were incomplete, and had made a significant progress at the time the project was terminated. Section C2 presents the description and results of piping models and the methodology used in response computation. The earthquake occurrence model and the ground motion model are described in Sections C3 and C4, respectively. Section C5 contains the beta-factor of pipe components which relate the fragility of individual piping components to a master pipe component. Finally, the SONGS-1 structural fragility development is briefly outlined in Section C6.

C2. PIPING MODELS

Fourteen dynamic piping models have been generated. The natural frequencies and mode shapes for these fourteen models have been computed by the computer program, SAP4. The pseudostatic mode with multisupport input motion approach was planned for computing the piping responses.

C2.1 PIPING SYSTEM DESCRIPTION

The required piping information on the SONGS Unit 1, AFWS were used to develop the mathematical models for 14 piping systems by the state-of-the-art techniques. Near the completion of the modeling process, some information required for one of the fourteen dynamic piping models (namely, the service water suction lines) was found to be insufficient. Therefore, certain service water piping properties were estimated in order to complete the frequency analysis.

Once the piping models were developed, the pseudostatic-mode method with multisupport input motion will be employed as our analytical method to estimate the piping responses. For a complete description of this analytical method, it is referred to Section 4 of the Volume 6 of the SSMRP Phase I report.[1]

The following piping systems were identified as within the system boundary of the auxiliary feedwater system (AFWS) for the response analysis.

1. Auxiliary Feedwater and Condensate System: Ten models (Figs. 1 through 10) consisting of suction piping that runs from the condensers and condensate storage tank to the auxiliary feedwater (AFW) pumps and discharge piping from the AFW pump to the steam generators.

2. Auxiliary Steam Supply: Two models were generated (Figs. 11 and 12). They are: main steam from the steam generators to the main stop valves and structural anchor of auxiliary steam supply, and the structural anchor to AFW pump turbine. The piping of the main steam was modeled up to and including the first anchor after the downstream check valve.

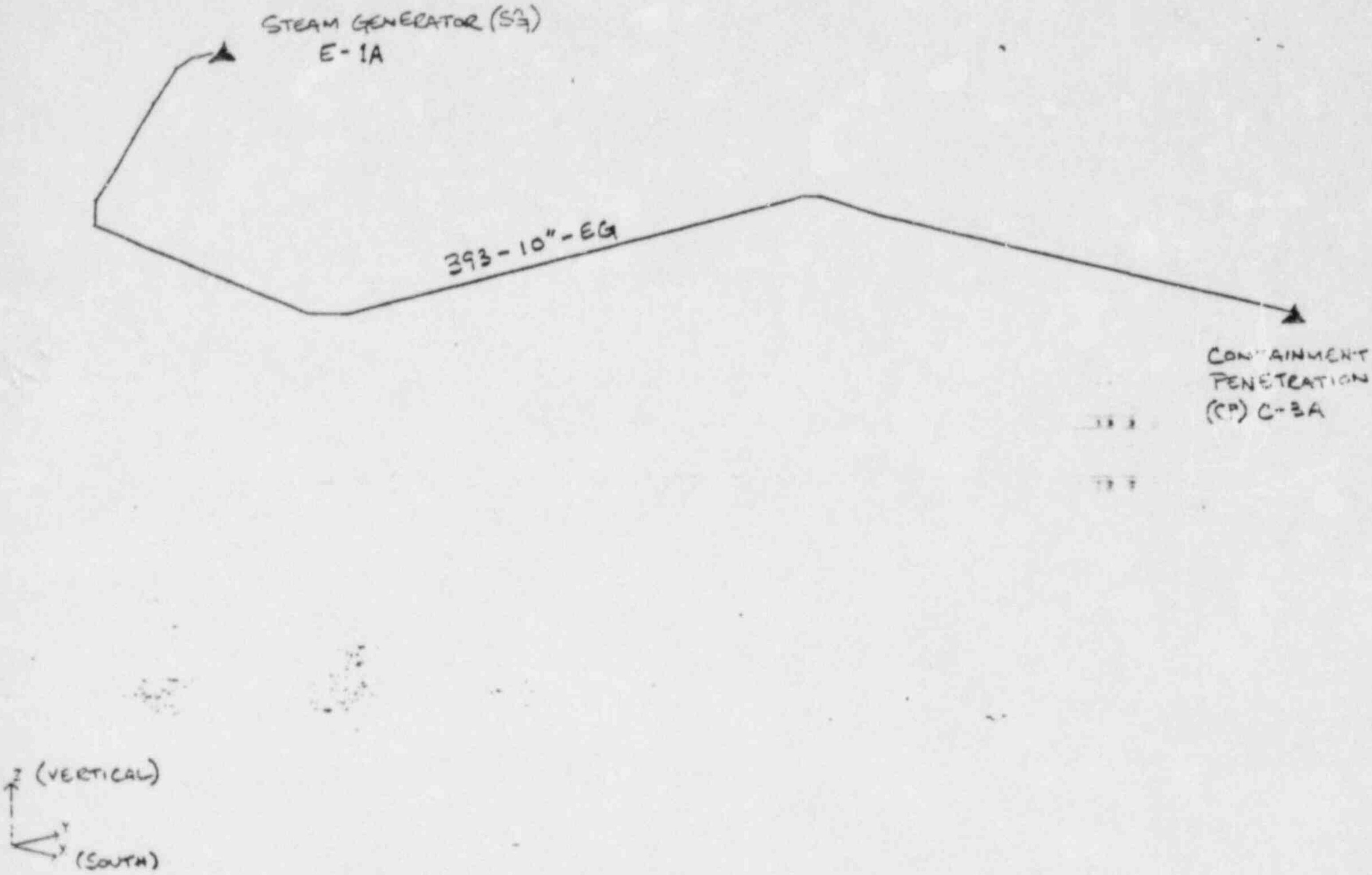

Figure 1. Auxiliary feedwater piping model piping--SG E-1A to CP-3A.

DRAFT FOR COMMENT

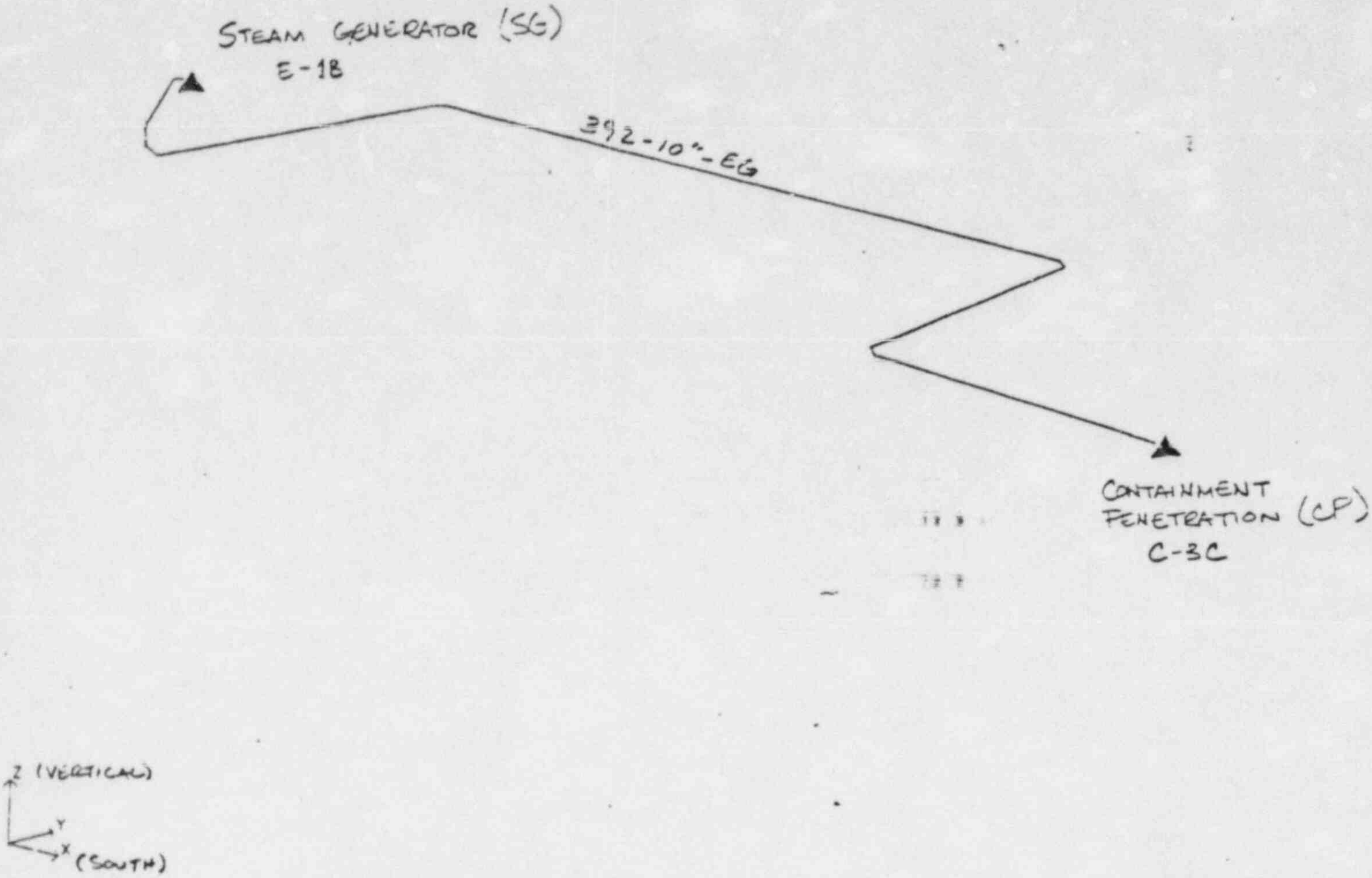

Figure 2. Auxiliary feedwater piping model--SG E-1B to CP C-3C.

DRAFT FOR COMMENT

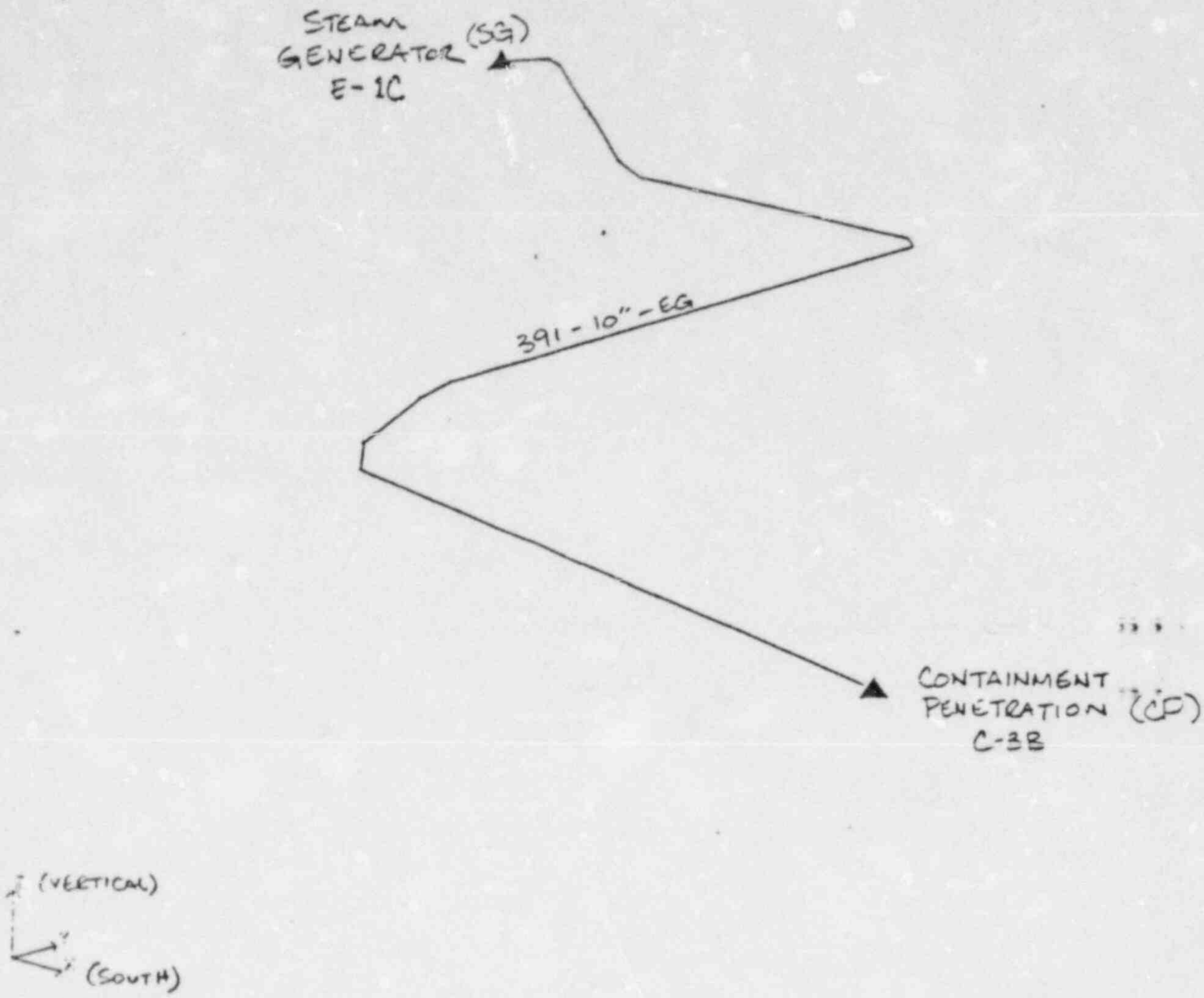

Figure 3. Auxiliary feedwater piping model piping model--SG E-1C to CP C-3B.

DRAFT FOR COMMENT

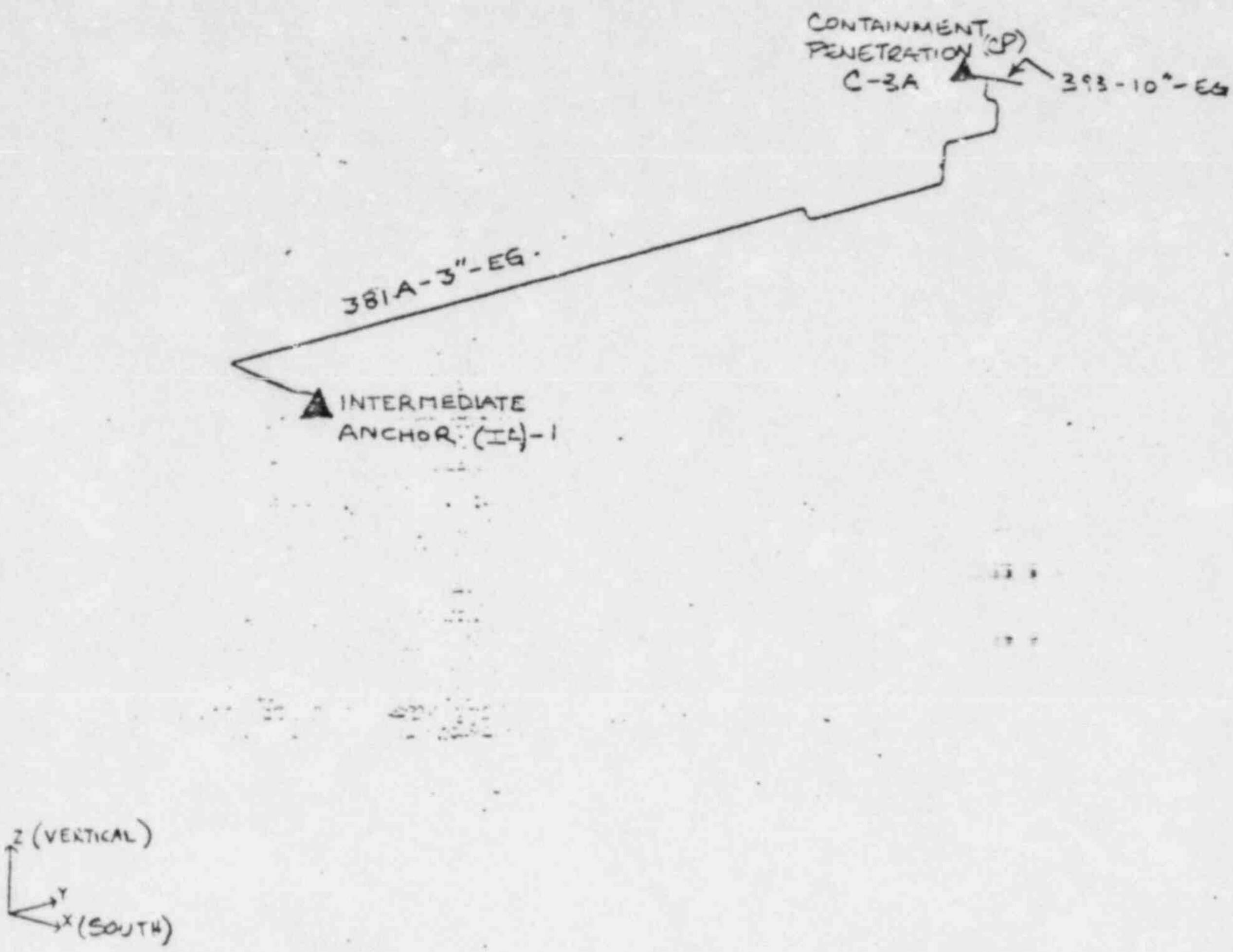

Figure 4. Auxiliary feedwater piping model--CP C-3A to IA-1.

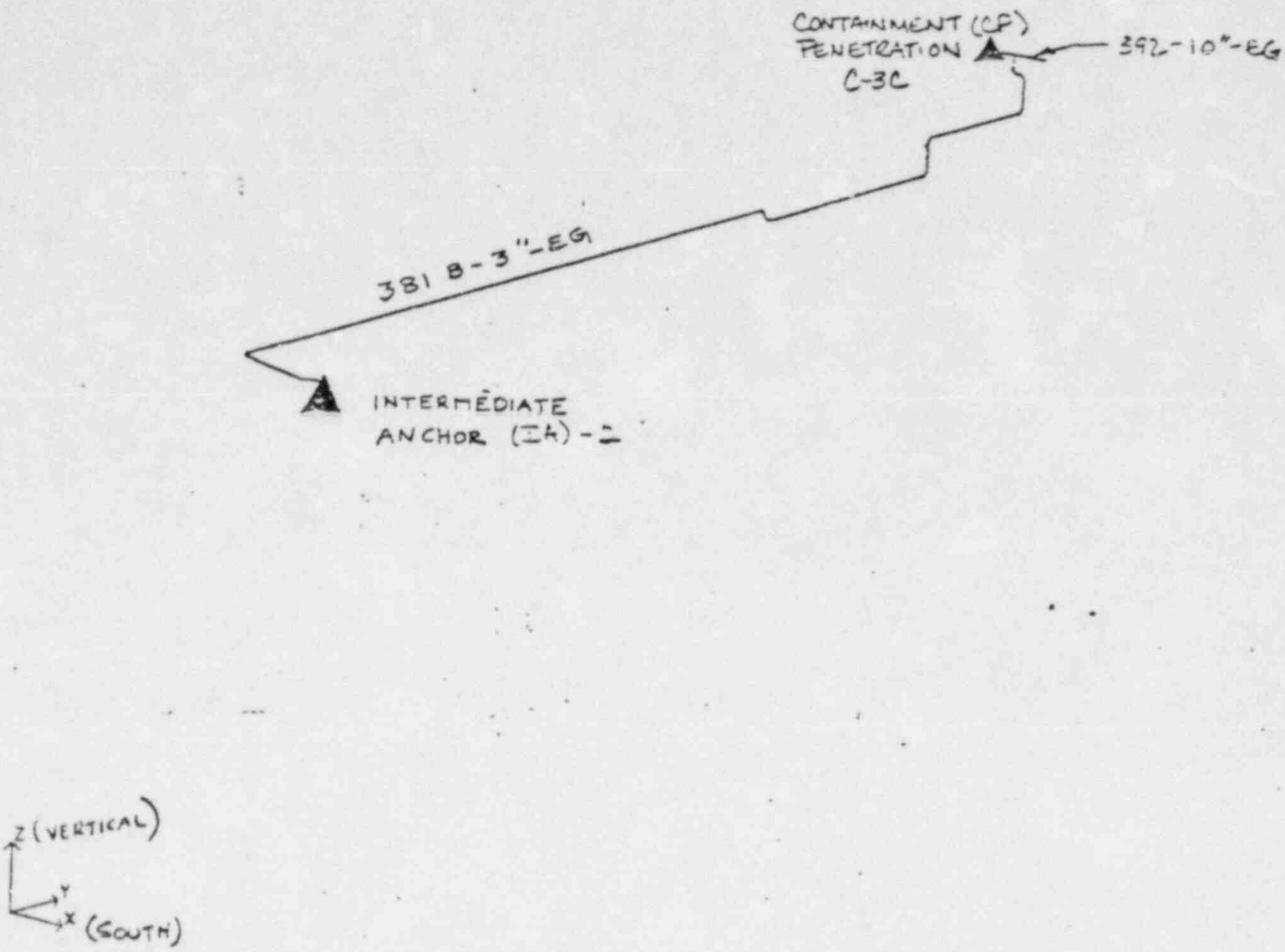

Figure 5. Auxiliary feedwater piping model--CP C-3C to IA-2.

DRAFT FOR COMMENT

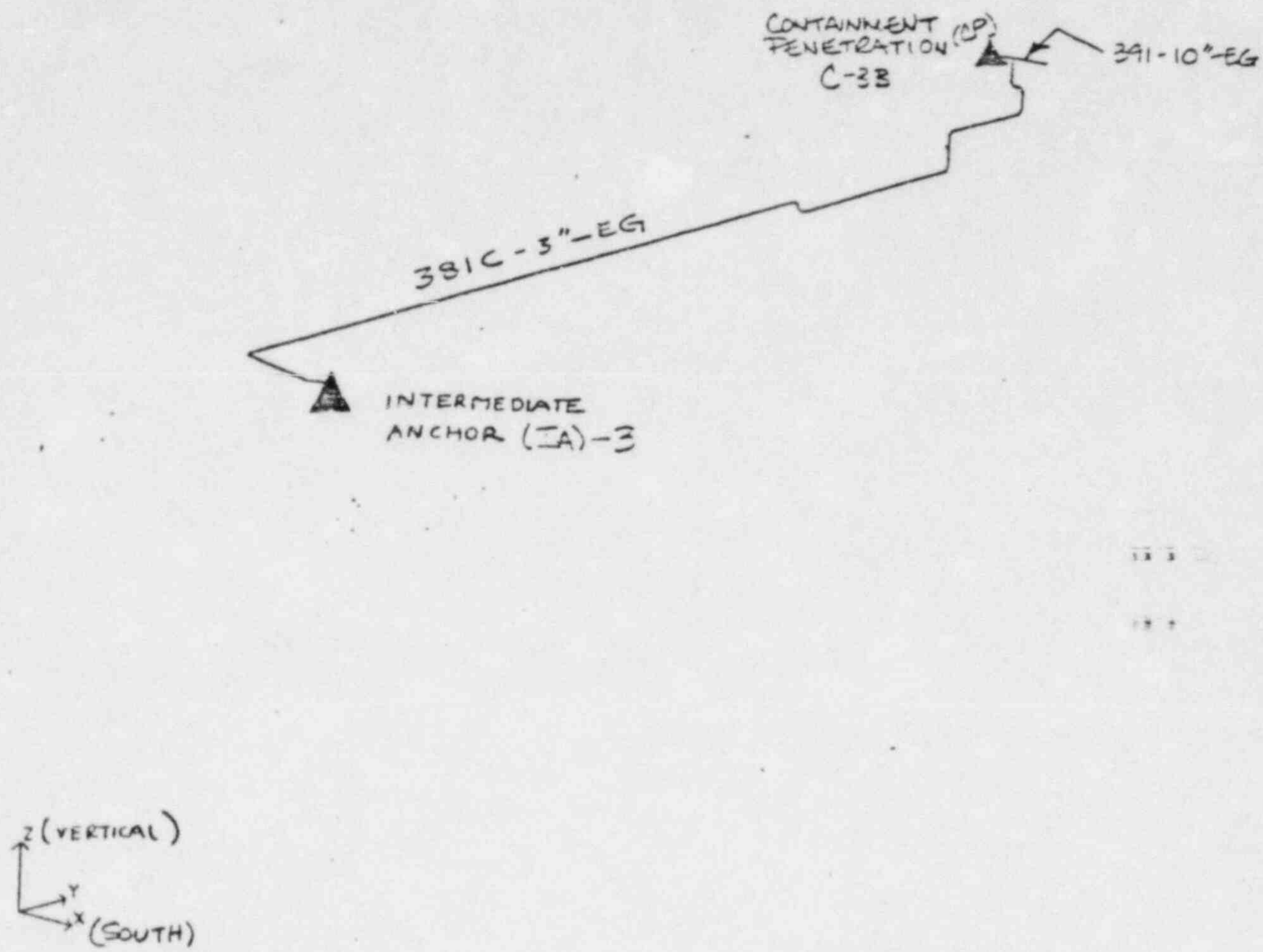

Figure 6. Auxiliary feedwater piping model--CP C-3B to IA-3.

DRAFT FOR COMMENT

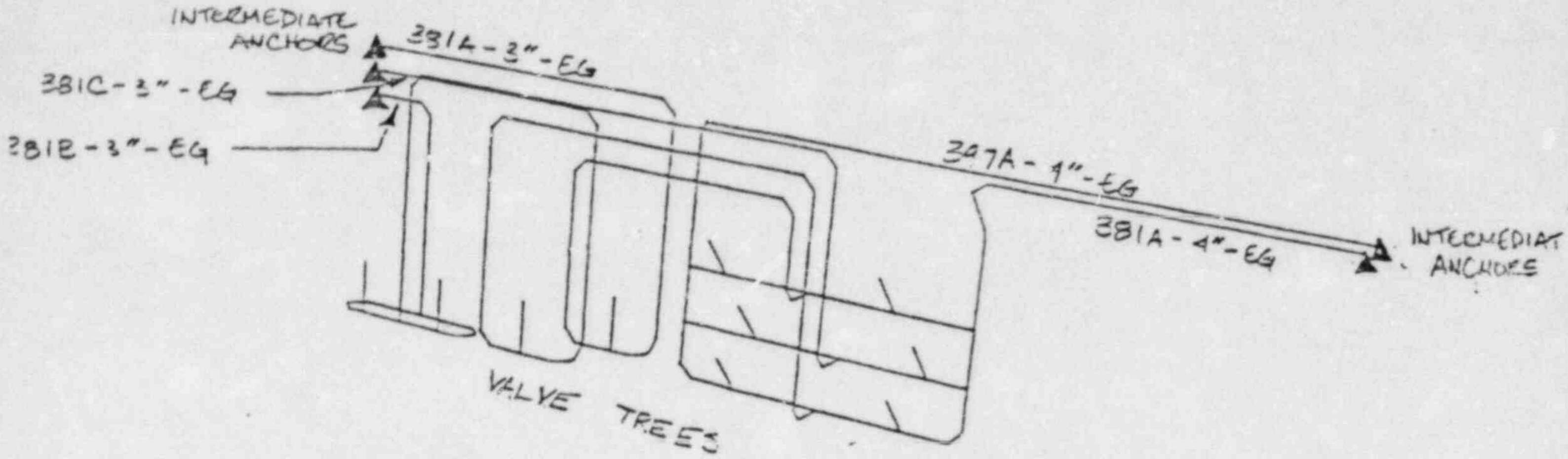

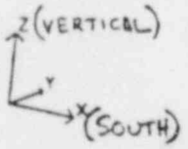

Figure 7. Auxiliary feedwater discharge piping model--valve trees between intermediate anchors.

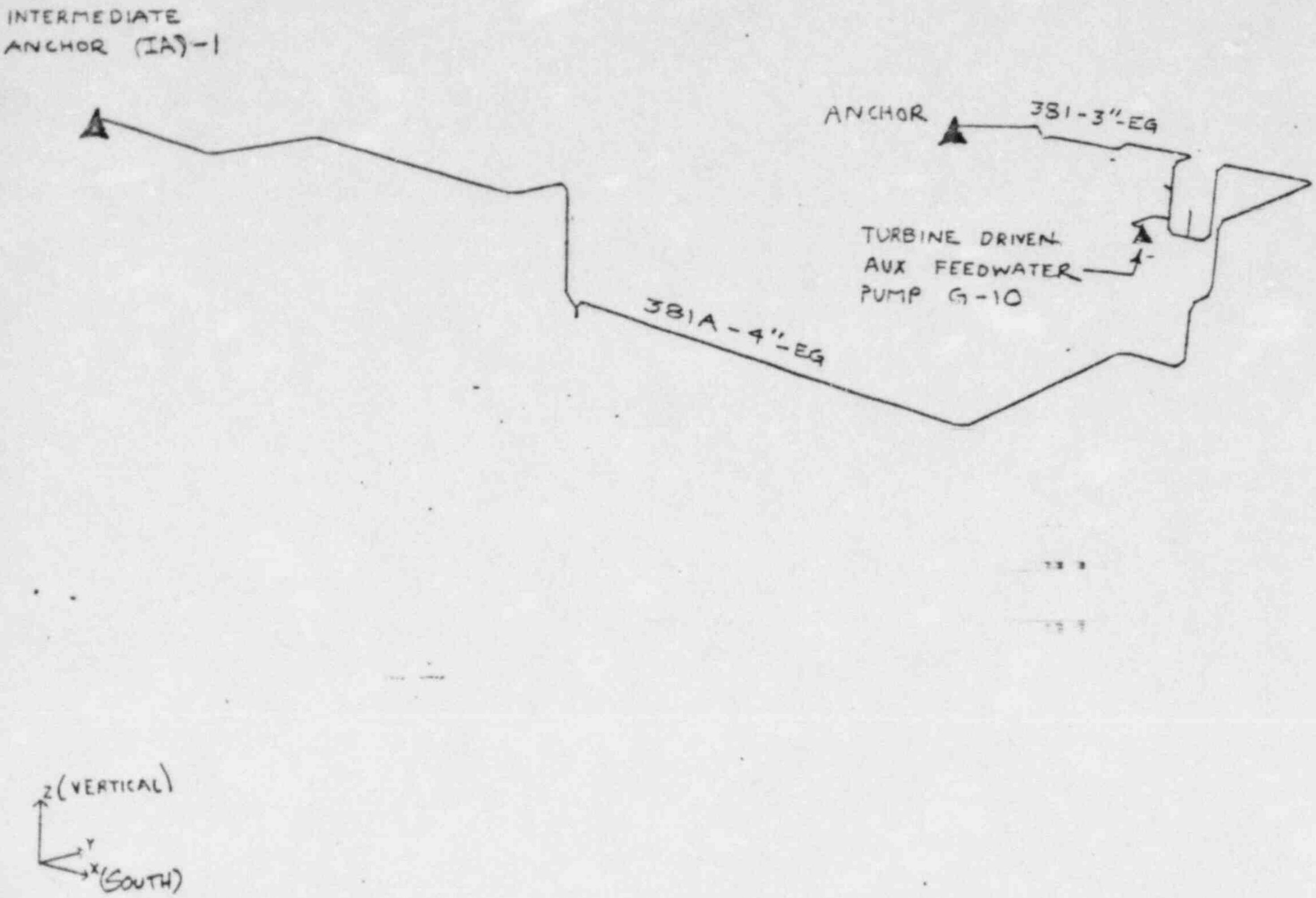

Figure 8. Auxiliary feedwater piping model--IA-1 to AFW pump G-10.

DRAFT FOR COMMENT

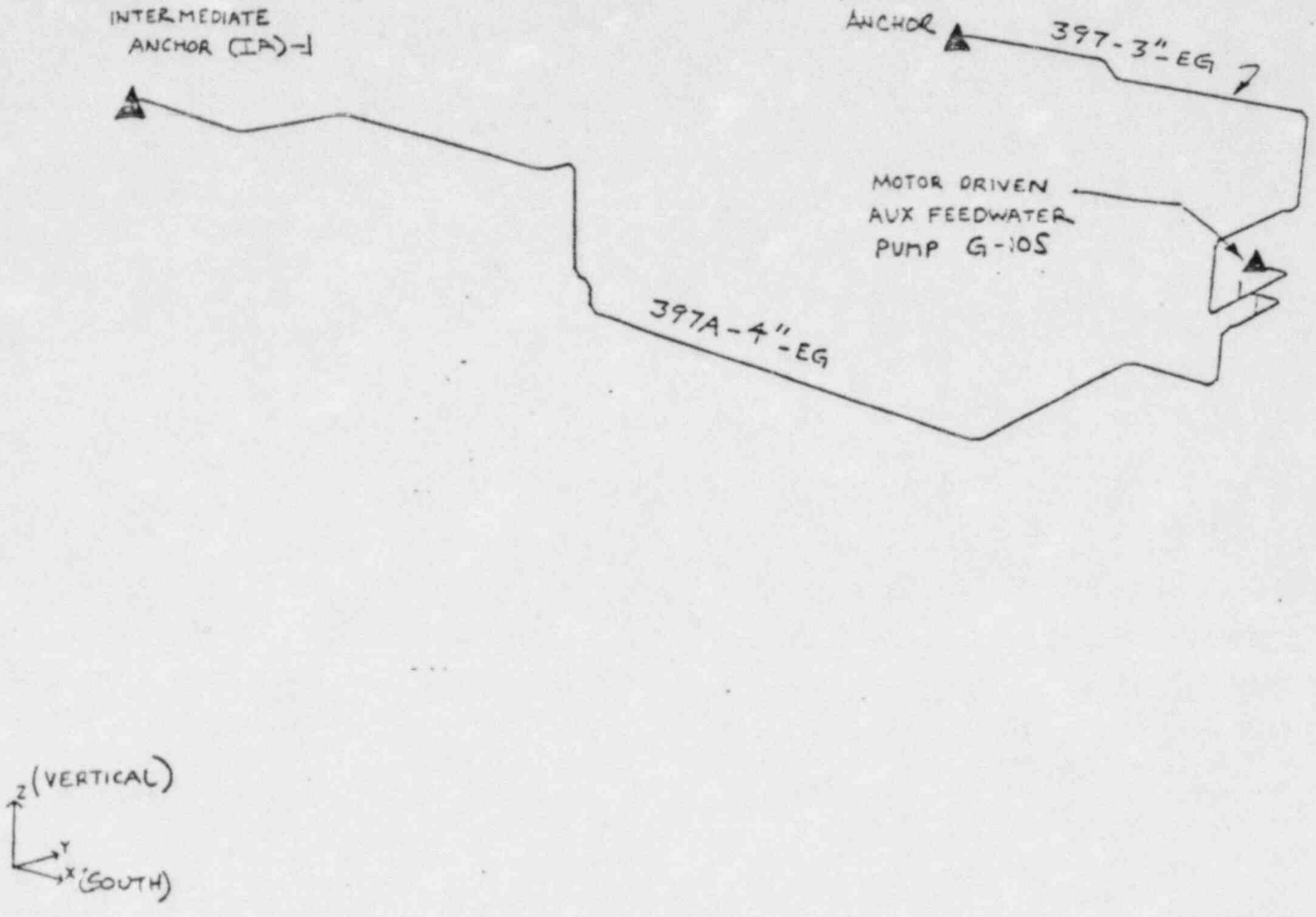

Figure 9. Auxiliary feedwater piping model--IA to AFW pump G-105.

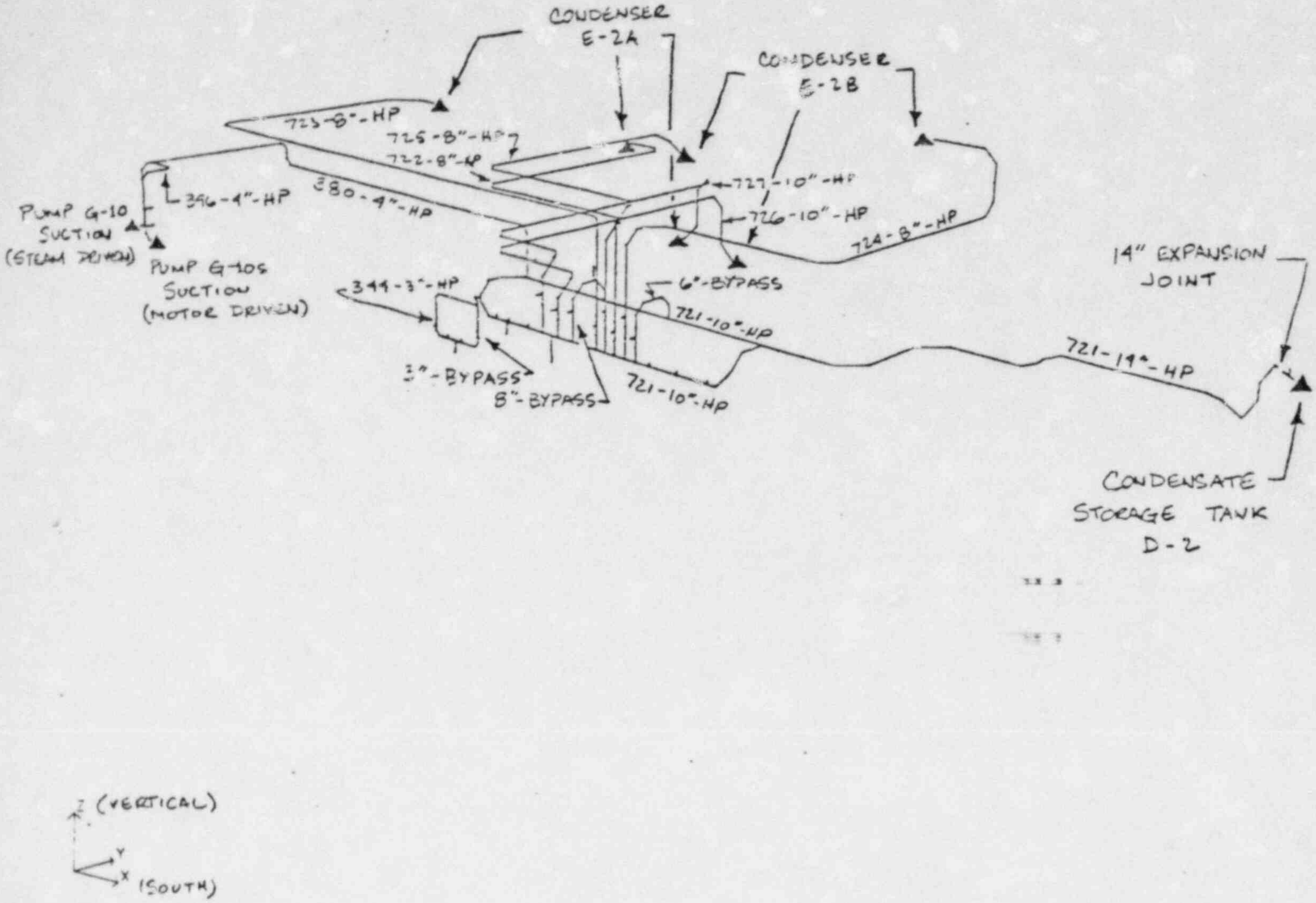

Figure 10. Auxiliary feedwater suction piping model.

DRAFT FOR COMMENT

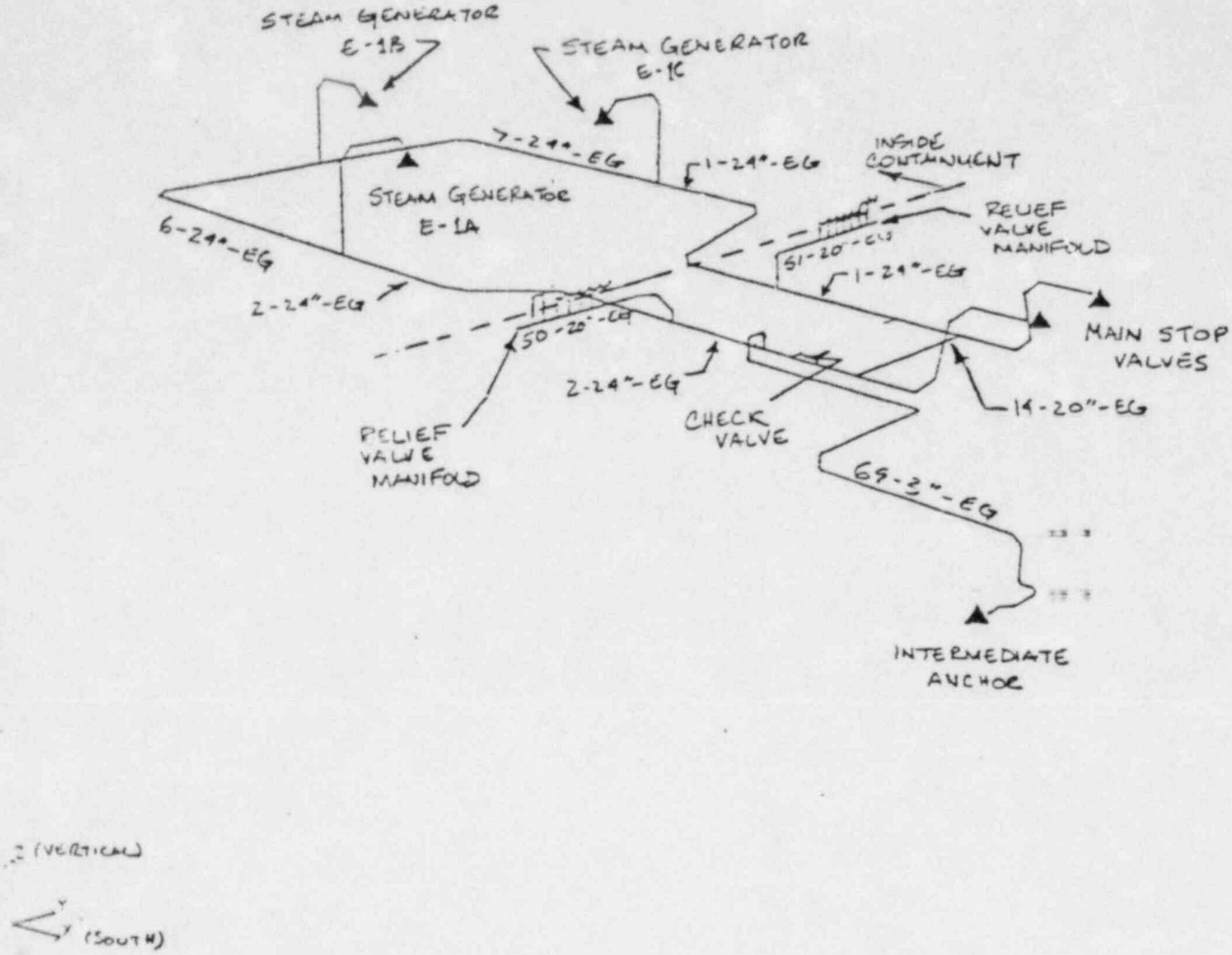

Figure 11. Main steam piping model.

DRAFT FOR COMMENT

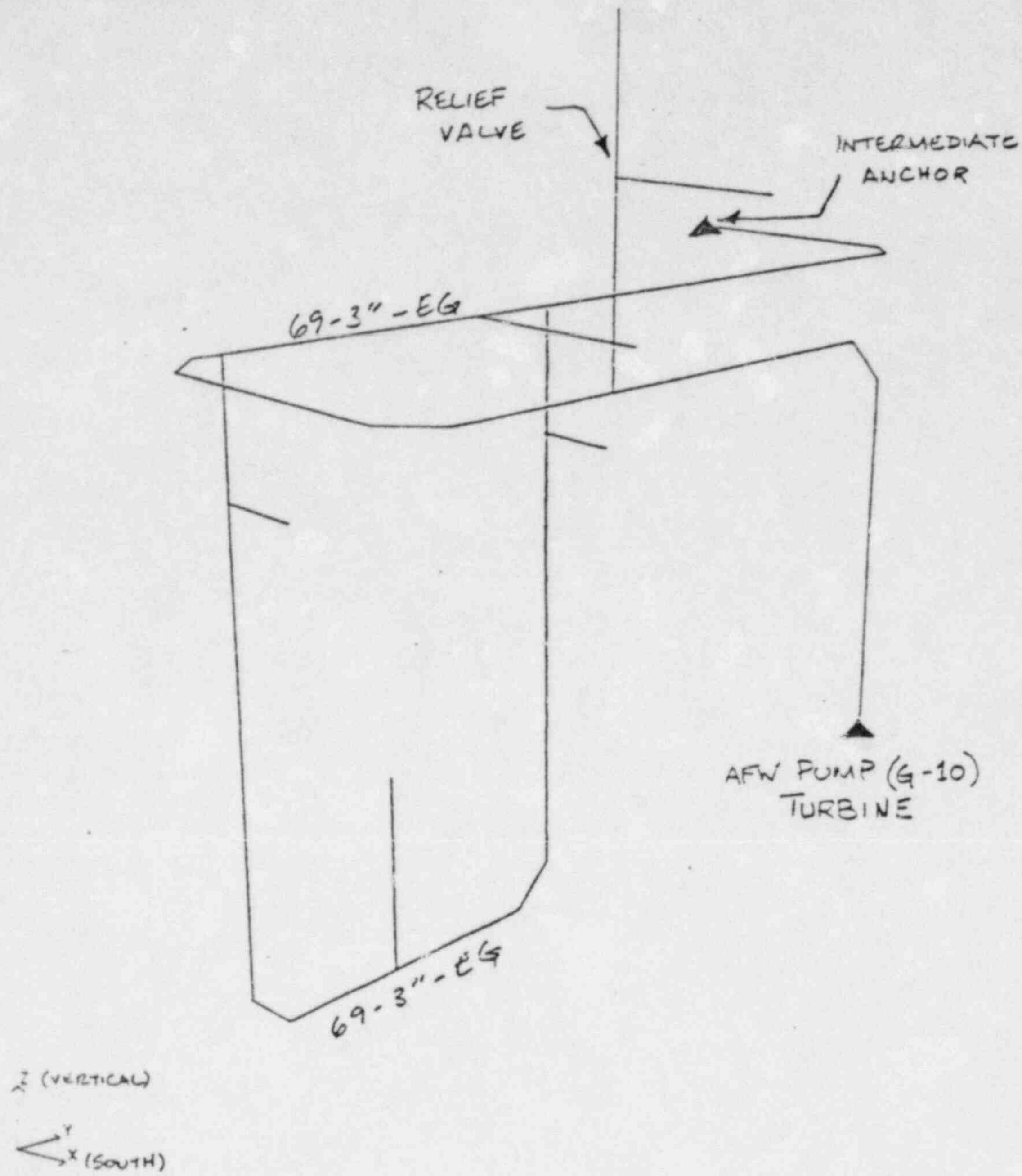

Figure 12. Auxiliary steam supply piping model.

3. <u>Service Water and Fire Protection System</u>: The fire protection system is supplied with water from the service water reservoir by two fire pumps. The service water system also serves as a secondary water supply and path to the auxiliary feedwater system. Two models were created for this system (Figs. 13 and 14). They are the suction and discharge of fire water pumps and runs from the fire water pumps to the service water reservoir and two structural anchors. Note that the piping system of Fig. 14 does not terminate at the service water reservoir. It only extends to an assumed intermediate wall anchor, beyond that point no information was pursued at the time the project was terminated.

The assumptions made in the development of piping models are as follows:

- Piping systems were assumed to be linear elastic.
- Piping supports, including rigid hangers, snubbers, etc. were assumed to be rigid.
- Spring hangers were not included due to their relatively low stiffness compared to the stiffness of other restraints.

The pipe elements of the SAP4 were used to define straight and curved pipes and equipments (if modeled). The boundary elements of SAP4 were used to simulate supports and restraints. The effect of internal pressure on bend flexibility factor was included in the stiffness formulation of the elbow/pipe bend in the SAP4 code.

DRAFT FOR COMMENT

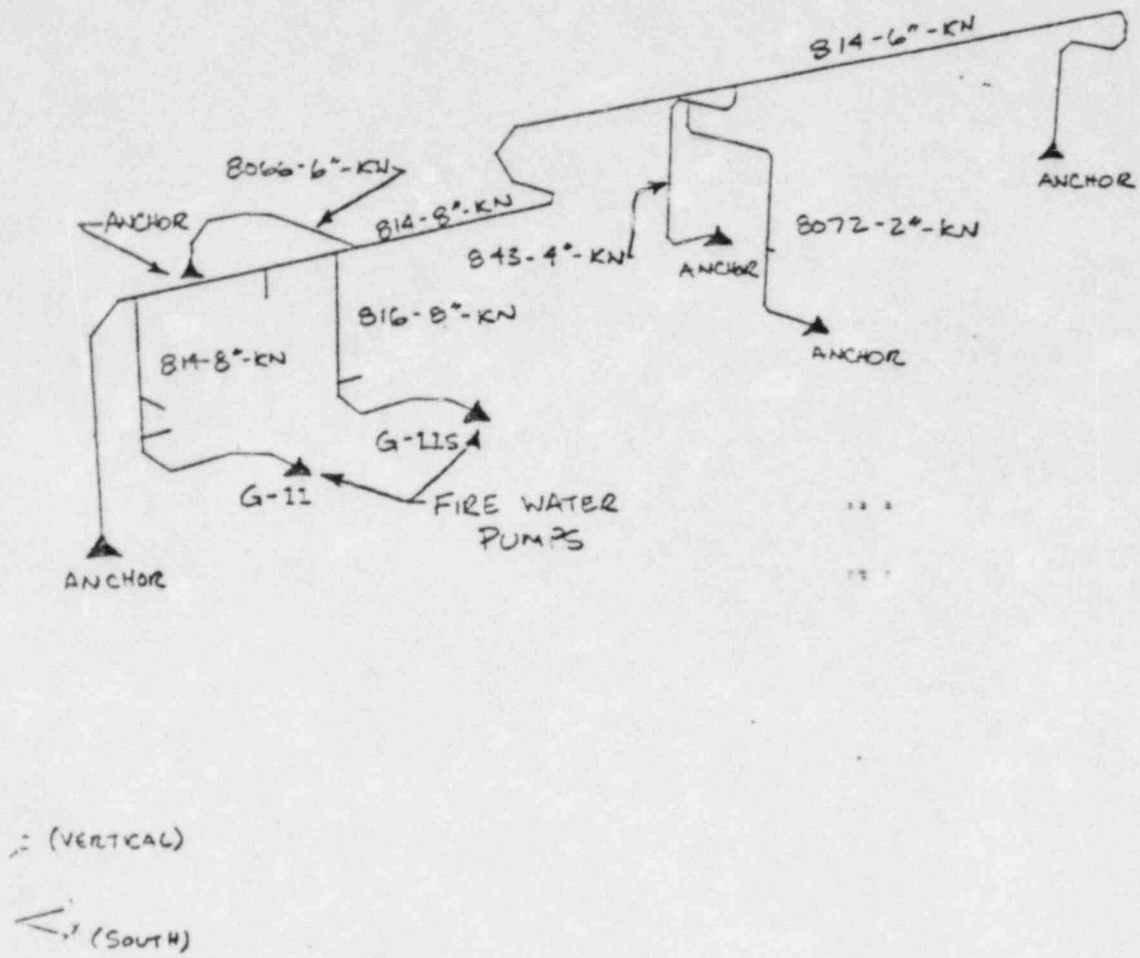

Figure 13. Fire protection discharge piping model.

DRAFT FOR COMMENT

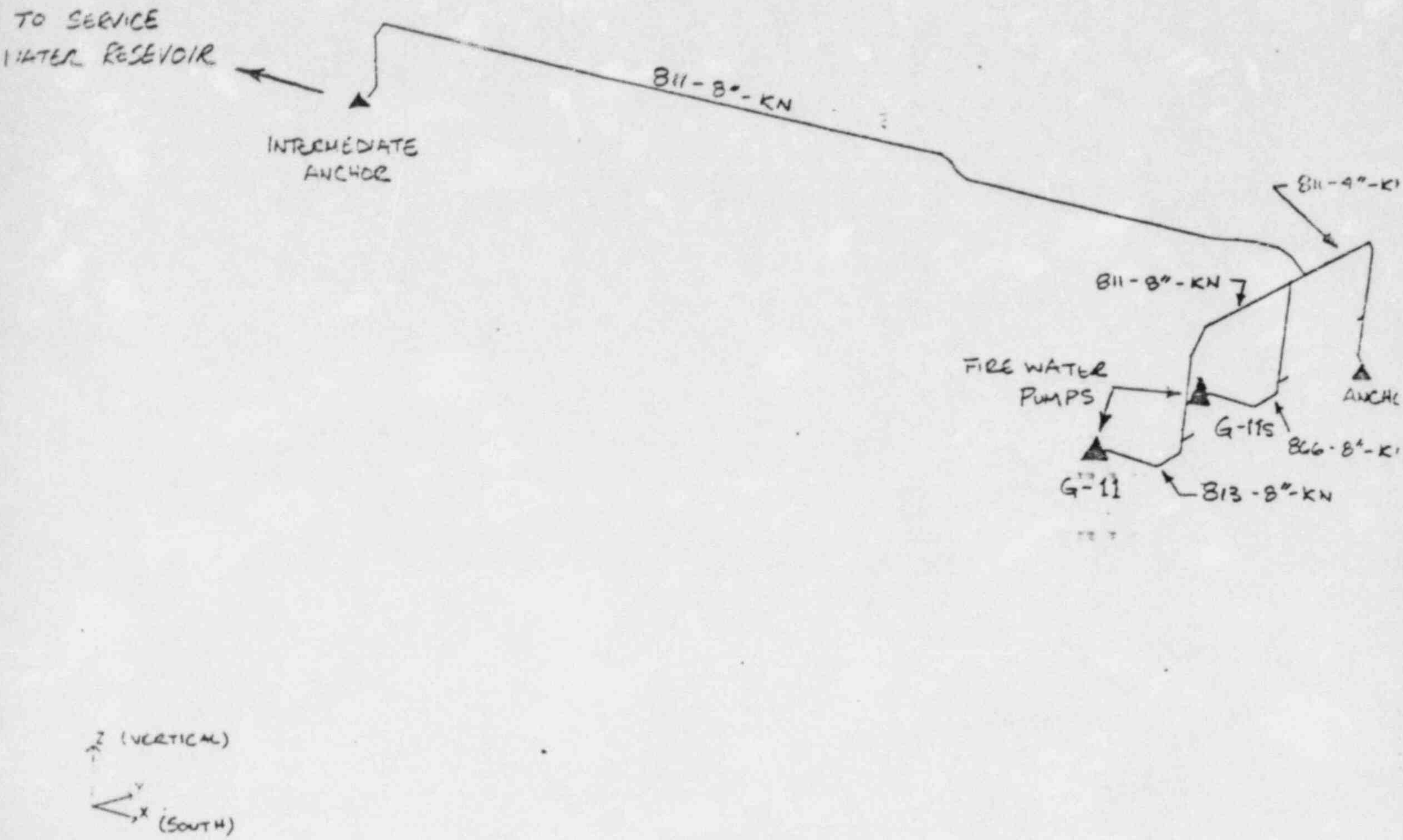

Figure 14. Fire protection suction piping model.

C2.2 TECHNICAL RESULTS

An eigenvalue analysis of the fourteen piping models were completed. Table 1 shows a list of the piping fundamental frequencies. Two piping models require a little more explanation as follows.

1. The main steam piping model (from the steam generators to the main stop valves) has a fundamental frequency of 1.2 Hz. This frequency seems low. However, a more in-depth study showed that this fundamental frequency had occurred at the relief valve manifold where a conglomeration of heavy valves (9 total) are located. By the fact that frequency is inversely proportional to the square root of weight, the calculated fundamental frequency was found to be quite valid.
2. The condensate storage piping model (from the auxiliary feedwater pumps to the condensate storage tank and condensers) contains a section of line which has a fundamental frequency at 1.0 Hz. This is because of the on-line rubber expansion joint (with a relatively low stiffness) is existed in the AFW pumps suction line.

In the next stage of analysis, the critical components are selected to compute piping response. The critical piping components are tees, nozzles, elbows/pipe bends, and etc. The responses of these selected components were intended to be computed by SMACS. Selections of these pipe components were completed for all piping models, however, only the component selection data for seven (out of fourteen) models were completed. They are also shown in Table 1.

DRAFT FOR COMMENT

System	Description	Fundamental Frequency (Hz)	Number of Components Selected	Component Selection Data Complete
Auxiliary Steam Supply	1. Main steam--from steam generators to main stop valves, and structural anchor of auxiliary steam supply.	1.2	133	No
	2. Structural anchor to AFW pump turbine	5.6	22	Yes
Auxiliary Feedwater	3. Steam Generator E-1A to Containment Penetration C-3A	5.5	8	Yes
	4. Steam Generator E-1B to Containment Penetration C-3A	12.6	8	Yes
	5. Steam Generator E-1C to Containment Penetration C-3B	5.6	8	No
	6. Containment Penetration C-3A to Intermediate Anchor-1 (Line No. 381A)	7.8	18	Yes
	7. Containment Penetration C-3C to Intermediate Anchor-2 (Line No. 381B)	12.7	18	Yes
	8. Containment Penetration C-3B to Intermediate Anchor-3 (Line No. 381C)	4.8	18	No
	9. Intermediate Anchors to Intermediate Anchors via the Valve Tree	6.7	76	Yes
	10. Intermediate Anchors to Turbine Driven AFW Pump	8.5	28	No
	11. Intermediate Anchors to Motor Driven AFW Pump	6.8	22	No

Table 1. Pertinent data for the 14 piping models.

DRAFT FOR COMMENT

System	Description	Fundamental Frequency (Hz)	Number of Components Selected	Component Selection Data Complete
Condensate Storage	12. AFW Pumps to Condensate Storage Tank D-2, and Condensers to AFW Pump (AFW Pump Suction)	1.0	71	Yes
Service Water and Fire Protection	13. Fire Water Pumps Discharge	5.3	48	No
	14. Fire Water Pumps Suction	1.4	24	No
TOTAL			502	

Table 1 (Cont.) Pertinent data for the 14 piping models.

DRAFT FOR COMMENT

C3. Earthquake Occurrence Model for the SONGS Site

The region of Southern California and Baja California that adjoins the SONGS site is a highly seismic area. For this region, the methodology for constructing the earthquake occurrence model for the site is divided into the following:

1. Geometric specifications of local seismic regions. This step is based on the geology and historic seismicity of the region. Sources are identified as line sources (faults) or area sources (zones). The largest earthquake associated with each source is established from the historic seismicity and the state-of-the-art knowledge about the geology and the fault-magnitude relationships.
2. Description of past seismicity in terms of earthquake occurrence. The recurrence of earthquakes of various magnitudes is based primarily on the historic seismicity. A straight line or set of straight lines is fitted to the data using regression analysis.

In this manner, the assessment of active faults and maximum credible earthquakes for the Southern California - Northern Baja California region adjoining the SONGS site has been made. The result of this study[2] is being published. The appended tables and figures[2] (maps included) of this study summarized the data and the findings of the supplemental fault maps for Southern California and Northern Baja California adjoining the SONGS site. The best estimates of fault slip-rate and recurrence interval estimates for analysis for determining the slope of the earthquake recurrence relationship in the region were also presented.

C3.1 Regional Setting and Data Base

The regional setting of the SONGS site is summarized in a report by Woodward-Clyde Consultants.[3] Publications on regional seismic, tectonic, and geologic settings can be found in several reports.[4,5,6]

The faults of this region appear to have branching relations between the transverse ranges and the northern San Andreas fault system on the north and the Salton Trough-Gulf of California region on the south. The transverse range province is characterized by thrust or reverse-slip displacement on east-west faults and right-slip offset on northwest-trending faults. The overall model constructed on these interrelationships is generally consistent with fault slip-rate models based on the papers by Anderson[6] and Atwater,[7] and the fault slip-rate data of Woodward-Clyde Consultants.

The Anderson model[6] is based on the continuity of fault slip transferred northwestward on a branching system of faults that originate in the Gulf of California. This general model for the strike-slip faults is used for the analysis. The pattern of faults in this region is shown in Plates 1 and 2 of Ref. 2. The plates are compiled from a variety of sources; the main sources are the fault map of California[8], offshore faults[9,10] and the geologic maps of Baja California.[11,12]

C3.2 Data Base

It is essential that credible seismic hazard analysis has an accurate and current seismicity data base. In the probabilistic seismic hazard analysis, the accurate and current data base is even more essential because earthquakes of all sizes contribute to the hazard.

There are several specific ways in which uncertainty or unreliability in the seismic data base will influence the results of a probabilistic seismic hazard analysis. First, and most important, is the uncertainty in the number of unassociated earthquake events that are contained in the host region (that is the source region containing the site in question). It is generally the case that this so-called background seismicity is a major contributor to the seismic hazard. Second, the uncertainty in the location of events, in particular the larger historical earthquakes, drives uncertainty in the seismic zonation of the area and this in turn drives the uncertainty in the proximity of nearby active source regions. Third, whether for host regions or for other source regions, the historical record provides the only quantitative basis for assessing the frequency of large events in any region. At the probabilities relevant to our study (10^{-3} to 10^{-4}), a credible model for the occurrence of these earthquake events is most significant. In order to develop as consistent and accurate a seismic data base as possible, three individual seismic data bases were integrated into one as shown in Table 2. Emphasis has been given to selected individual bases within the region of southern California and northwestern Mexico.

Base	Time Coverage	Area Coverage
Algermissen	Pre-1900 AD	Entire United States
CDMG*	1900 - 1974	Entire California
USGS**	1974 - 1981	Southern California

Note: *CDMG: California Division of Mines and Geology, Sacramento, CA.
**USGS: United States Geological Survey and California Institute of Technology, Seismological Laboratory, Pasadena, CA.

Table 2. Seismic data bases for the region surrounding the SONGS site.

C3.3 Seismicity and Focal Mechanisms

The regional seismicity provided by the available seismic maps of the Southern California - Baja California regions defines some of the major fault zones. The main continuous or semi-continuous zones include the San Andreas fault system from the Salton Trough northward, most of the San Jacinto fault, and the southern portion of the Elsinore fault zone. The instrumental seismicity record is too brief to confirm many of the major structures defined by the geologic data.

The focal mechanism and geodetic data for Southern California and Northern Baja California are generally consistent with the seismotectonic models of Refs. 2, 3, and 6. Most of the focal mechanisms indicate a north-south orientation for the compression azis, which is consistent with current models for North American and Pacific plate interactions. These data are also compatible with geodetic data for the region.

Aftershock data and the focal mechanism for the main earthquake of the 1933 Long Beach event show a right-slip displacement for a 30 km segment of the Newport-Inglewood section of the Offshore Zone of Deformation (OZD). The section of the OZD south of the 1933 Long Beach earthquake epicenter has been characterized by only minor, scattered historic earthquake activity, although one local zone of activity was recorded in late 1981.

C3.4 Random, "Detection Level", or "Floating" Earthquakes

In seismic or weakly seismic regions, the background earthquake activity includes infrequent events that may not be associated with known surface or subsurface faults. These earthquakes are commonly referred to as "floating earthquakes" and appear to occur in random locations or patterns that do not coincide with apparent faults. The epicentral region is commonly oval in shape and the aftershocks do not follow an elongate or planar distribution. These earthquakes have been referred to as "detection level" earthquakes. The maximum magnitude for this type of earthquake in the eastern and central United States is about 5.75 to 6 for the historic record. The earthquake data[13] compiled by Liu and Kanemori show intraplate earthquakes within many stable parts of the North American plate, in the Atlantic Ocean, and in intraplate settings in other parts of the world. The data show most larger earthquakes of these intraplate settings to have a range in magnitude of 5.8 to 6.4. Accordingly, this range in magnitude appears to be a very conservative estimate for scattered, non-predictable earthquakes in the Southern California region.

C3.4 Determination of Active Faults and Maximum Earthquakes

The evaluation of active faults within the Southern California and Northern Baja California region is at once a problem of detecting, delineating, and defining the character of potential seismogenic faults and assessing their maximum earthquakes. No component of the above three D's (detection, delineation, or definition) is complete for the region surrounding the SONGS site. On the basis of the literature search and the application of the state-of-the-art knowledge about the geology and tectonics of the region, the zones of seismogenic areas associated with active faults and fault zones were established. For the region surrounding the SONGS site, the most probable seismic hazard was determined that it comes from earthquake activities associated with the Offshore Zone of Deformation (OZD).

The determination of maximum credible earthquakes for fault zones can be made either by qualitative or quantitative methods.[2]

Qualitative methods[2, 3, 14] were suggested for estimating the maximum credible earthquake for capable fault zones:

1. Maximum Historic Earthquake Method: This method is for non-representative earthquake, or short earthquake histories.

2. Fault Rupture Length Method: This method is for areas with poor-to-fair field data for total rupture length during paleoseismic earthquakes.

3. Total Displacement Method: This method is for total amount of fault displacement during the present seismotectonic regime.

4. Degree of Deformation Method: This method is for assessing the size or degree of deformation along a fault zone in geologically young materials.

Quantitative measures of fault activity that can provide an estimate of maximum credible earthquakes for a fault include:

1. Maximum Historic Earthquake Method: This method is for faults with a sufficiently long historic record that the maximum credible earthquake has occurred.

2. Total Fault Length Method: Empirical data for strike-slip faults indicate that this method provides an indication of maximum credible earthquakes for strike-slip faults.

3. Fault Segment, or Fractional Rupture Length Method: This method is applicable where there is good structural, stratigraphic and geomorphic data for definition of rupture elements.

4. Fault Movement Magnitude with Fractional Rupture Length Method: This method is combined use of moment magnitude with fractional fault rupture length application.

C3.6 Summary: Maximum earthquake magnitude, fault slip-rate, and recurrence interval

In this subsection, Table 3 summarized the estimated fault slip-rate and recurrence interval estimates for computer analysis for determining b-values and to provide a basis for comparison between geologic and seismologic information on earthquake frequency, maximum earthquake values and recurrence intervals between large earthquakes.

Table 3. Estimated maximum earthquake magnitude, fault slip rate and recurrence interval for zones and faults of the southern California - Baja California region. Superscripts indicate the following references: a. Woodward-Clyde Consultants (1979 and 1980); b. Anderson (1979); c. Slemmons and others, in this report; and d. Shieh (1978).

NO.	ZONE OR FAULT	MAX. MAGNITUDE (Ms)			FAULT SLIP RATES mm/yr			RECURRENCE INTERVAL IN YEARS		
		Low, Max. Historic	Preferred Est.	High	Low	Preferred Est.	High	Shortest	Preferred Est.	Longest
1C	Central San Andreas f.z.	8.25[a]	8.25[c]	8.5[c]	34[a]	37[a]	41[a]	160[d]	160[d]	357[c]
1S*	Southern San Andreas f.z.	6.5[a]	6.9[c]	7.5[b]	15[b]	25[a]	25[a]	10[c]	21[c]	115[c]
2	Transverse Ranges Region	---	---	---	---	---	---	---	---	---
3	San Jacinto f.z.	7.1[a]	7.1[c]	7.5[b]	5[b]	8[a]	15[b]	52[c]	98[c]	344[c]
4	Whitier-Elsinor f.z.	6.0[a]	7.1[c]	8.0[b]	1.8[a]	2.3[a]	2.3[a]	40[c]	342[c]	2539[c]
5	Sierra Juarez-San Pedro Martir f.z.	---	7[c]	7.5[c]	---	---	---	---	---	---
6	Coast Ranges Province	---	---	---	---	---	---	---	---	---
7	Offshore Zone of Deformation: including Newport-Inglewoodw f.z. to Rose Canyon f.z.	6.3[a]	7.0[c]	7.5[b]	0.4[a]	0.5[a]	0.7[c]	235[c]	1294[c]	4300[c]
8	Northwestern Baja California Region	6.8[a]	6.8[c]	7.0[c]	---	---	---	---	---	---
9	Palos Verdes-Coronado Banks f.z.	---	7.0[c]	7.5[b]	0.5[c]	1.0[c]	1.5[c]	431[c]	647[c]	3440[c]
10	San Pedro-San Diego Trough-Coronado Escarpment f.z.	---	6.9[c]	7.5[c]	0.5[c]	1.0[c]	1.5[c]	355[c]	532[c]	3440[c]
11	San Clemente f.z.	---	7.0[c]	8.0[c]	0.5[c]	1.0[c]	1.5[c]	431[c]	647[c]	9141[c]
12	Agua Blanca f.z.	---	7.3	8.0[b]	2.0[c]	2.7[b]	3.5[c]	332[c]	431[c]	2285[c]
13	Southern San Clemente-Maximos-San Isidro f.z.	---	7.0[c]	7.5[c]	2.0[c]	2.7[c]	3.5[c]	185[c]	240[c]	860[c]

* Geologic observations indicates the recurrence intervals to be much too short. Special factors may influence this fault zone.

1. Sources of Data for Table 3

The primary sources of data are the Woodward-Clyde Consultants report,[3] their response in Southern California Edison Company's response to NRC Question 361.45[14], including Tables 361.45-2 and 3, and Anderson's results.[6]

Earthquake Magnitude estimates are for the lowest, generally based on the maximum historic earthquake. The preferred or selected value, is generally based on Plates 1 and 2, the U.S. Nuclear Regulatory Commission's Safety Evaluation Report for San Onofre[15], in NUREG-07-12), or the maximum historic earthquake for cases where it is assumed that the maximum historic magnitude approximates the maximum credible event (for the Central San Andreas fault zone and the San Jacinto fault zone).

The fault slip-rates are based on Woodward-Clyde Consultants[3] and Anderson.[6] The field observations of Sieh[16] are used for fault slip-rate and earthquake recurrence estimates for the Central San Andreas fault zone.

2. Results

The estimation of earthquake recurrence interval is obtained by use of the extreme magnitudes listed under the columns of "MAX. MAGNITUDE (M_S)" and the extreme values under the columns of "FAULT SLIP RATES" for the longest and shortest estimated recurrence intervals between maximum earthquakes. The preferred or selected estimate uses the preferred estimates of these two parts of the table.

The method of estimation of the recurrence interval is obtained by use of the new fault relationships of Slemmons and Chung[17] of the logarithm of maximum fault displacement, $\log D = A + B (M_S)$, where D is in meters and $A = 5.831$ and $B = 0.849$. The maximum displacement is converted to average fault displacement, to obtain the earthquake recurrence interval for a given section of a fault, by the empirical relation that the average displacement is approximately 50 percent of the maximum. No adjustment is made for the fractional length that is involved in the above estimates. Accordingly, the above estimates may be too high by factors of two to four times.

C4 GROUND MOTION MODEL FOR THE SONGS SITE

C4.1 General Form of the Model

The object of ground motion model development is to generate a model of prediction of the maximum peak acceleration which could occur at the SONGS site.

The methodology for developing seismic hazard curves is already well established. Consequently, this imposes the general form of our ground motion model, and by using the now well accepted combination of theoretical considerations and actual earthquake data the ground motion model is finalized.

Following Joyner, et al.[18] and Joyner and Boore[19] we choose the general form of the acceleration to be:

$$y = \frac{k}{r} e^{-qr} \qquad (1)$$

where k is a function of the magnitude M; q is a constant; and r is a measure of the distance from the recording station to some significant point associated with the source. Eq. (1) corresponds to a single point-source geometric spreading with constant - Q anelastic attenuation. Although the rupture surface is not a point source, it is very likely that the maximum peak acceleration can be associated with the rupture of a limited area of the rupture surface, thus the assumption of a point source. Most of the data from earthquakes is at distances greater than 10 km from the fault zone and for magnitudes less than 7. However, as discussed in the section on development of the earthquake occurrence model, the SONGS site is located very close to a major fault zone. This introduces general complications into ground motion modeling. Firstly, good estimates are required for the ground motion very close to the fault zone where there is little data. Secondly, estimates for the ground motion from earthquakes significantly larger than magnitude 7 are also required. Finally, at larger magnitudes (around 7 to 8) various magnitude scales tend to saturate. The scope of work for the SONGS-1 AFWS Project was towards addressing these issues.

In order to improve upon the Joyner - Boore[19] model in the near-field, weighting schemes were introduced and alternative measures of distance were explored. Hopefully, alternative weighting schemes would also lead to an improved capability to predict the ground motion for large magnitude events.

C4.2 The Data

The most complete and representative set of data available at the time of the study was presented in Joyner, et al.[18] This set of data was used, but it was also recognized its limitations with respect to the intended use of the ground motion model. This expansion of the data set has been almost completed at the time the project was stopped. Thus, what follows is only for the Joyner, et. al.[18] data set.

Basically, the data were taken from Ref. 20. The sources for the more recent data include Porter[21], Procella[22], Procella, et al.[23], Brady, et al.[24] and Boore and Procella.[25]

The main limitation in this set of data resides in the fact that the maximum value of both horizontal components was selected as the data point for each recording. This is not current practice in the engineering profession, and it is not realistic since the actual direction of the maximum peak occurs in a random direction. The net effect of this choice (of the maximum component) is a conservative ground motion model. Campbell[26] examined this question for a similar data set and found that when only the maximum component was used, it lead to results that were 13 percent higher on the average than when both components were used.

Another limitation appears, especially among the recent data, when one realizes that some of the data were provided by stations close to the faults. As the stations come closer and closer to the fault, the problem of defining the distance, r, of Eq. (1) becomes more and more difficult. Ideally, one would work with the distance to the point on the rupture that contributes the maximum peak motion, but it would be difficult to determine the location of that point for most earthquakes and practically impossible for past earthquakes. Furthermore, it is not sure that the maximum peak is created by the rupture of a single zone. Joyner, et al.[18] used the closest distance to the surface projection of the fault rupture as the horizontal component of the station distance, and the vertical component is an empirical value which is determined by a minimization process.

Another undesirable aspect of this data set is the uneven (non-uniform) distribution of the data points in the sample space. This is a general characteristic of all earthquake catalogs and has been the reason for many different approaches by researchers. Joyner and Boore[19], Campbell[26], Askins and Cornell.[27] A list of the data set used in our analysis is available in Joyner, et al.[17]

C4.3 Fit of the Ground Motion Model to the Data

Several forms of the general form Eq. 1 were actually studied, but in all cases the type of material (Soil vs. Rock) was neglected as an independent variable since Joyner, et al.[17] have concluded that the ground quality was insignificant.

The regressions performed in the following analyses were all linear regression with independent identically distributed (i.i.d.) residuals.

The various equations considered for the regressions were as follows:

$$\text{Log } a = b_1 + b_2 M + b_3 \text{Log } r + b_4 R \qquad (2)$$

$$\text{Log } a = b_1 + b_2 M + b_3 \text{Log } r \qquad (3)$$

where:

- M has been successively taken as the moment magnitude and the local magnitude.
- r has been successively taken as the distance defined above by Joyner, et al. 1981, and the distance to the center of energy, whenever it was possible to do so.
- b_3 has been set to −1 in a series of calculations, as per Eq. (1), and set free in others.

Two types of regressions-analyses were performed. In the first type, the method developed by Joyner, et al.[18], was exactly duplicated. This method consists of a series of two successive regressions. In the first regression, the quantity $(b_1 + b_2M)$ is lumped into a single value, c_i, constant for each earthquake. That is all data points associated with the i-th earthquake have a constant, c_i, to be determined in the first regression. In the second regression the equation: $b_1 + b_2M$ is fitted to the set of c's as per Eq. (4).

$$c = b_1 + b_2M \tag{4}$$

In their study, Joyner, et al.[18], had first considered a quadratic equation for Eq. (4) but finally concluded that the second degree term in M was insignificant and discarded it. The net result is to actually decouple magnitude from distance. This technique has the effect of weighting equally each earthquake with respect to the determination of the magnitude dependence.

In the second type of regressions, a single regression was performed with several types of weighting to try to alleviate on the one hand, the lack of data in some regions of the sample space, the abundance of it in others, and the paucity of data points associated with some earthquake as opposed to the large number for others (for example, Daly City 1957 vs San Fernando, 1971). In the case of the "earthquake weighting," the weight was simply the inverse of the number of records for a particular earthquake. For the "Distance weighting," the distance axis was divided into four adjacent bands: 0-20 km, 20-100 km, 100-200 km, and greater than 200 km. The weight associated to a data point, a_i, whose distance was in the j-th band (j = 1,2,3,4) was the inverse of the total number of data points whose distance fell into that same band.

Both earthquake and/or distance weighting were analyzed. In the analyses that were performed here with the Joyner, et al.[18] technique, the earthquakes to which only one data point was associated were eliminated, as in the case of the Joyner,[18] study. This then obliged us to perform regression with this same truncated set in the second type of analysis also. Thus, two analyses were performed with the single regression analysis: one with the single record earthquake, and one without.

All the results of these analyses are presented in Tables 4, 5 and 6. They are shown below.

DRAFT FOR COMMENT

Eq form	b_1	b_2	b_3	b_4	σ_1	σ_2	σ
				Moment Mag			
2	-1.02	.249	-1	-.00255	.222	.134	.259
2	-.95	.258	-1.096	-.00209	.222	.134	.259
3	-.56	.231	-1.322	0	.228	.122	.258
				Local Mag			
2	-1.48	.336	-1	-.00299	.216	.142	.259
2	-1.43	.343	-1.075	-.00261	.217	.142	.259
3	-.85	.288	-1.340	0	.226	.125	.258

Distance to Center of Energy

Eq form	b_1	b_2	b_3	b_4	1	2	
				Moment Mag			
2	-1.02	.251	-1.	-.00246	.228	.144	.270
2	-.97	.259	-1.078	-.00209	.228	.144	.270
3	-.59	.236	-1.316	0	.234	.138	.272

σ_1 is the standard deviation of the residuals due to the first regression

σ_2 is the standard deviation of the residuals due to the second regression.

σ is the standard deviation of the residuals after both regressions combined.

The regressions were performed with two alternative definitions of magnitude (i.e., Moment magnitude and local magnitude) and two definitions of distances (i.e., Closest Distance and Distance to Center of Energy).

Table 4. Results for Joyner, et al. - Method Analyses Closest Distance.

Eq. fitted $\text{Log } a = b_1 + b_2M + b_3 \text{ Log } R + b_4R$

Weighting	W W/O	Distance	b_1	b_2	b_3	b_4
W1	W	Closest	-1.82	.462	-1.37	-.000899
W1	W	En. Center	-1.88	.477	-1.39	-.000947
W1	W/O	Closest	-1.69	.427	-1.29	-.00122
W1	W/O	En. Center	-1.75	.448	-1.33	-.0012
W2	W	Closest	-1.68	.437	-1.38	-.000889
W2	W	En. Center	-1.82	.469	-1.39	-.00103
W2	W/O	Closest	-1.58	.371	-1.11	-.00193
W2	W/O	En. Center	-1.73	.406	-1.13	-.00204
W3	W	Closest	-1.24	.327	-1.19	-.00116
W3	W	En. Center	-1.46	.393	-1.29	-.00124
W3	W/O	Closest	-1.18	.313	-1.17	-.00125
W3	W/O	En. Center	-1.41	.381	-1.26	-.00133

Key:
W1 = weighting by No. Recds in R band and No. Recds in R band for each Eq.
W2 = No. of Recds in R band and No. of Recds in Eq.
W3 = No. of Recds in the R band.
W = with the single-record earthquakes
W/O = single-record earthquakes are discarded.

Table 5. Results for the Single Regression Analyses.

Eq Form	W W/O	Distance	b_1	b_2	b_3	b_4	
2	W	Closest	-1.13	.271	-1	-.00207	.246
2	W	Closest	-1.05	.271	-1.071	-.00166	.247
2	W/O	Closest	-1.01	.253	-1.004	-.00191	.230
2	W	En. Center	-1.45	.357	-1.104	-.00213	.254
3	W	Closest	-.72	.251	-1.27	0	.251
3	W	En. Center	-1.07	.342	-1.37	0	.261

For definition of symbols see Table 3.

Table 6. Results for the single regression analyses, without weighting and with Local Magnitude.

C5. BETA-FACTORS FOR PIPE COMPONENTS

Table 7 through 18 contain load scale factors (beta-factors) for use in relating the fragility of individual piping components to the fragility of the master (reference) piping component. A 6 in. schedule 160 carbon-steel butt weld pipe joint represents the master component. The load scale factors are defined as:

$$\text{beta} = \frac{\text{Capacity of reference pipe component}}{\text{Capacity of pipe component under consideration}} \; .$$

The fragility of the master pipe component is represented by a cumulative distribution function of percent probability of failure as a function of resultant moment capacity with log-normal parameters:

$$\text{median} = 2.03 \times 10^5 \text{ ft-lbs}$$

$$\beta = .42$$

DRAFT FOR COMMENT

Table 7 PIPING LOAD SCALE (BETA) FACTORS
SCHEDULE 10 CARBON STEEL

NOMINAL DIAM (IN)	BUTT WELD TEMPERATURE (F) 100	300	500	ELBOW TEMPERATURE (F) 100	300	500	STRAIGHT TEMPERATURE (F) 100	300	500
0.5	577.5000	682.2200	727.6500	666.0500	702.2400	773.8500	358.0500	429.7986	451.1430
0.7	320.7815	357.9391	416.3258	353.0214	385.4464	465.4933	203.8445	225.5016	258.1220
1.0	198.4891	201.8259	252.9043	204.6369	230.7718	298.2911	123.0632	127.1503	156.8007
2.0	44.1418	51.2284	57.9832	63.1126	72.1694	86.4343	27.3679	32.2739	35.9496
3.0	20.8106	24.2424	29.9301	28.6575	36.1959	45.2325	12.9026	15.2727	18.5567
4.0	10.5394	12.3714	14.6939	13.9672	18.7528	22.1447	6.5344	7.7940	9.1102
6.0	4.9677	5.7064	6.5713	6.7301	8.3160	10.0010	3.0800	3.5950	4.0742
8.0	2.6260	2.9189	3.1859	3.8263	5.1873	5.7594	1.6281	1.8389	1.9753
10.0	1.4766	1.5971	1.8143	2.2208	2.9492	3.4441	0.9155	1.0062	1.1249
12.0	1.0534	1.1481	1.3065	1.6366	2.1843	2.5368	0.6531	0.7233	0.8100
14.0	0.7380	0.8111	0.9268	1.1920	1.6053	1.8570	0.4576	0.5110	0.5746
16.0	0.5272	0.5842	0.6658	0.8214	1.0628	1.2156	0.3269	0.3680	0.4128
18.0	0.3717	0.4150	0.4719	0.5585	0.6944	0.7857	0.2305	0.2614	0.2926
20.0	0.2082	0.2342	0.2650	0.3000	0.3579	0.4002	0.1291	0.1475	0.1643
24.0	0.0899	0.1026	0.1154	0.1199	0.1327	0.1455	0.0557	0.0646	0.0715

Table 8. PIPING LOAD SCALE (BETA) FACTORS
SCHEDULE 40 CARBON STEEL

NOMINAL DIAM (IN)	BUTT WELD TEMPERATURE (F) 100	300	500	ELBOW TEMPERATURE (F) 100	300	500	STRAIGHT TEMPERATURE (F) 100	300	500
0.5	385.0000	446.6000	462.0000	423.5000	462.0000	500.5000	238.7000	281.3580	286.4400
0.7	258.3956	299.2544	315.1057	306.5413	337.9985	370.5235	160.2053	188.5303	195.3655
1.0	173.4241	200.5222	214.9169	221.8834	247.2792	274.3011	107.5229	126.3290	133.2485
2.0	35.1890	40.4250	46.5080	60.9070	70.8400	82.3900	21.8172	25.4677	28.8350
3.0	14.7229	16.9133	19.4833	24.2122	31.0721	36.0628	9.1282	10.6554	12.0796
4.0	6.1600	7.0763	8.1620	9.6250	13.6290	15.7850	3.8192	4.4581	5.0604
6.0	2.2715	2.6796	3.1647	3.7730	5.0050	6.3140	1.4083	1.6881	1.9621
8.0	1.1550	1.3706	1.5785	2.0944	3.3572	3.8808	0.7161	0.8635	0.9787
10.0	0.6468	0.7238	0.8932	1.2628	1.9019	2.3177	0.4010	0.4560	0.5538
12.0	0.4464	0.5064	0.6261	0.8984	1.3744	1.6685	0.2768	0.3190	0.3882
14.0	0.3080	0.3542	0.4389	0.6391	0.9933	1.2012	0.1910	0.2231	0.2721
16.0	0.1943	0.2272	0.2798	0.3898	0.5696	0.6790	0.1205	0.1431	0.1735
18.0	0.1226	0.1458	0.1783	0.2377	0.3266	0.3838	0.0760	0.0919	0.1105
20.0	0.0774	0.0936	0.1137	0.1449	0.1873	0.2169	0.0480	0.0590	0.0705
24.0	0.0308	0.0385	0.0462	0.0539	0.0616	0.0693	0.0191	0.0243	0.0286

Table 9. PIPING LOAD SCALE (BETA) FACTORS
SCHEDULE 60 CARBON STEEL

NOMINAL DIAM (IN)	BUTT WELD TEMPERATURE (F) 100	300	500	ELBOW TEMPERATURE (F) 100	300	500	STRAIGHT TEMPERATURE (F) 100	300	500
0.5	370.1923	437.3205	466.4423	426.9551	450.1539	496.0577	229.5192	275.5119	289.1942
0.7	234.2569	255.0316	256.6321	251.5277	274.6306	331.6640	145.2393	160.6699	163.9119
1.0	157.4224	160.0688	200.5793	162.2982	183.0260	236.5757	97.6019	100.8433	124.3592
2.0	28.6990	33.3063	37.6980	41.0330	46.9213	56.1957	17.7934	20.9830	23.3728
3.0	11.0423	12.8633	15.8813	15.2060	19.2060	24.0009	6.8462	8.1039	9.8464
4.0	4.7562	5.5830	6.6311	6.3031	8.4628	9.9935	2.9488	3.5173	4.1113
6.0	1.9825	2.2774	2.6225	2.6858	3.3188	3.9912	1.2291	1.4348	1.6259
8.0	1.0476	1.1645	1.2710	1.5264	2.0694	2.2976	0.6495	0.7336	0.7880
10.0	0.5359	0.5797	0.6585	0.8060	1.0704	1.2500	0.3323	0.3652	0.4083
12.0	0.3691	0.4022	0.4577	0.5733	0.7651	0.8887	0.2288	0.2534	0.2838
14.0	0.2555	0.2808	0.3209	0.4127	0.5558	0.6429	0.1584	0.1769	0.1990
16.0	0.1650	0.1829	0.2084	0.2571	0.3327	0.3805	0.1023	0.1152	0.1292
18.0	0.1025	0.1144	0.1301	0.1540	0.1914	0.2166	0.0635	0.0721	0.0807
20.0	0.0646	0.0726	0.0822	0.0930	0.1110	0.1241	0.0401	0.0457	0.0510
24.0	0.0254	0.0290	0.0326	0.0339	0.0375	0.0411	0.0157	0.0183	0.0202

DRAFT FOR COMMENT

Table 10 PIPING LOAD SCALE (BETA) FACTORS
SCHEDULE 80 CARBON STEEL

NOMINAL DIAM (IN)	BUTT WELD TEMPERATURE (F) 100	BUTT WELD 300	BUTT WELD 500	ELBOW TEMPERATURE (F) 100	ELBOW 300	ELBOW 500	STRAIGHT TEMPERATURE (F) 100	STRAIGHT 300	STRAIGHT 500
0.5	343.7500	406.0834	433.1250	396.4584	418.0000	460.6250	213.1250	255.8125	268.5375
0.7	220.4770	240.0290	279.1831	236.7320	258.4758	312.1544	136.6957	151.2188	173.0935
1.0	141.7779	144.1613	180.6459	146.1692	164.0371	213.0651	87.9023	90.8216	112.0005
2.0	25.3620	29.4336	33.3146	36.2617	41.4653	49.6613	15.7244	18.5432	20.6551
3.0	9.7034	11.3058	13.9585	13.3649	16.8806	21.0950	6.0173	7.1227	8.6543
4.0	4.3441	5.0992	6.0565	5.7570	7.7295	9.1276	2.6933	3.2125	3.7550
6.0	1.7669	2.0296	2.3373	2.3938	2.9579	3.5572	1.0955	1.2786	1.4491
8.0	0.8793	0.9774	1.0668	1.2811	1.7369	1.9284	0.5452	0.6158	0.6614
10.0	0.4641	0.5020	0.5702	0.6980	0.9269	1.0824	0.2877	0.3163	0.3535
12.0	0.3111	0.3390	0.3858	0.4833	0.6450	0.7491	0.1929	0.2136	0.2392
14.0	0.2089	0.2296	0.2623	0.3375	0.4545	0.5257	0.1295	0.1446	0.1626
16.0	0.1331	0.1475	0.1681	0.2074	0.2683	0.3068	0.0825	0.0929	0.1042
18.0	0.0846	0.0945	0.1074	0.1271	0.1581	0.1789	0.0525	0.0595	0.0666
20.0	0.0526	0.0591	0.0669	0.0758	0.0904	0.1011	0.0326	0.0372	0.0415
24.0	0.0208	0.0238	0.0267	0.0278	0.0307	0.0337	0.0129	0.0150	0.0166

Table 11 PIPING LOAD SCALE (BETA) FACTORS
SCHEDULE 120 CARBON STEEL

NOMINAL DIAM (IN)	BUTT WELD TEMPERATURE (F) 100	BUTT WELD 300	BUTT WELD 500	ELBOW TEMPERATURE (F) 100	ELBOW 300	ELBOW 500	STRAIGHT TEMPERATURE (F) 100	STRAIGHT 300	STRAIGHT 500
0.5	320.8334	379.0111	379.0111	370.0278	390.1334	429.9166	198.9167	238.7770	234.9869
0.7	199.3676	217.0482	217.0482	214.0662	233.7282	282.2672	123.6079	136.7404	134.5699
1.0	127.5209	129.6647	129.6647	131.4706	148.2613	191.6396	79.0630	81.6088	80.3921
2.0	20.3731	23.6439	23.6439	29.1289	33.3090	39.8928	12.6313	14.8957	14.6592
3.0	8.2607	9.6229	9.6229	11.3755	14.3678	17.9549	5.1216	6.0624	5.9662
4.0	3.5010	4.2034	4.2034	4.7456	6.3716	7.5241	2.2202	2.6481	2.6061
6.0	1.4425	1.6570	1.6570	1.9543	2.4149	2.9041	0.8944	1.0439	1.0273
8.0	0.6614	0.7351	0.7351	0.9636	1.3064	1.4504	0.4101	0.4631	0.4558
10.0	0.3502	0.3788	0.3788	0.5267	0.6994	0.8167	0.2171	0.2386	0.2349
12.0	0.2302	0.2509	0.2509	0.3576	0.4772	0.5542	0.1427	0.1581	0.1556
14.0	0.1545	0.1698	0.1698	0.2496	0.3360	0.3887	0.0958	0.1070	0.1053
16.0	0.0989	0.1096	0.1096	0.1542	0.1994	0.2282	0.0613	0.0690	0.0680
18.0	0.0621	0.0694	0.0694	0.0933	0.1160	0.1314	0.0385	0.0437	0.0430
20.0	0.0388	0.0437	0.0437	0.0559	0.0668	0.0746	0.0241	0.0275	0.0271
24.0	0.0151	0.0172	0.0172	0.0202	0.0223	0.0245	0.0094	0.0108	0.0107

Table 12 PIPING LOAD SCALE (BETA) FACTORS
SCHEDULE 160 CARBON STEEL

NOMINAL DIAM (IN)	BUTT WELD TEMPERATURE (F) 100	BUTT WELD 300	BUTT WELD 500	ELBOW TEMPERATURE (F) 100	ELBOW 300	ELBOW 500	STRAIGHT TEMPERATURE (F) 100	STRAIGHT 300	STRAIGHT 500
0.5	308.0000	369.6000	404.2500	369.6000	378.8400	423.5000	190.9600	232.8480	250.6350
0.7	191.3501	195.5800	250.8863	184.8000	199.4300	267.5907	118.6371	123.2154	155.5495
1.0	118.8795	103.9500	155.7055	92.4000	106.2600	169.0785	73.7053	65.4085	96.5374
2.0	17.7100	20.7900	23.1000	19.2500	21.3290	26.9500	10.9802	13.0977	14.3220
3.0	6.2370	7.4074	9.9804	6.2370	7.5845	11.1304	3.8669	4.6657	6.1878
4.0	2.9260	3.5169	4.3120	3.0800	3.7499	4.5969	1.8141	2.2169	2.6734
6.0	1.3426	1.5087	1.6996	1.4869	1.6736	1.8719	0.8324	0.9505	1.0538
8.0	0.6160	0.6468	0.6699	0.7178	0.7469	0.7623	0.3819	0.4075	0.4153
10.0	0.3080	0.3234	0.3388	0.3465	0.3696	0.3927	0.1910	0.2037	0.2101
12.0	0.2066	0.2175	0.2284	0.2422	0.2559	0.2694	0.1281	0.1370	0.1416
14.0	0.1386	0.1463	0.1540	0.1694	0.1771	0.1848	0.0859	0.0922	0.0955
16.0	0.0875	0.0923	0.0972	0.1026	0.1076	0.1124	0.0542	0.0581	0.0603
18.0	0.0552	0.0582	0.0613	0.0622	0.0653	0.0684	0.0342	0.0367	0.0380
20.0	0.0348	0.0367	0.0387	0.0377	0.0397	0.0416	0.0216	0.0231	0.0240
24.0	0.0139	0.0146	0.0154	0.0139	0.0146	0.0154	0.0086	0.0092	0.0095

Table 13. PIPING LOAD SCALE (BETA) FACTORS
SCHEDULE 10 STAINLESS STEEL

NOMINAL DIAM (IN)	BUTT WELD TEMPERATURE (F)			ELBOW TEMPERATURE (F)			STRAIGHT TEMPERATURE (F)		
	100	300	500	100	300	500	100	300	500
0.5	750.0000	886.0000	945.0000	865.0000	912.0000	1005.0000	465.0000	558.1800	585.9000
0.7	426.9890	464.8860	540.6828	458.4693	500.5798	604.5368	264.7332	292.6593	335.2233
1.0	257.7781	262.1116	328.4472	265.7622	299.7037	387.3911	159.8224	165.1303	203.6373
2.0	57.3270	66.5304	75.3029	81.9644	93.7265	112.2524	35.5427	41.9142	46.6878
3.0	27.0267	31.4836	38.8703	37.2175	47.0076	58.7435	16.7566	19.8347	24.0996
4.0	13.6875	16.0667	19.0830	18.1392	24.3543	28.7594	8.4862	10.1220	11.8315
6.0	6.4516	7.4109	8.5341	8.7404	10.8000	12.9883	4.0000	4.6689	5.2911
8.0	3.4104	3.7908	4.1375	4.9692	6.7367	7.4798	2.1144	2.3882	2.5652
10.0	1.9176	2.0742	2.3562	2.8842	3.8301	4.4728	1.1889	1.3067	1.4608
12.0	1.3681	1.4911	1.6960	2.1255	2.8367	3.2945	0.8482	0.9394	1.0520
14.0	0.9584	1.0534	1.2036	1.5481	2.0848	2.4117	0.5942	0.6636	0.7462
16.0	0.6847	0.7587	0.8647	1.0667	1.3803	1.5787	0.4245	0.4780	0.5361
18.0	0.4827	0.5390	0.6128	0.7253	0.9018	1.0204	0.2993	0.3396	0.3799
20.0	0.2704	0.3041	0.3442	0.3896	0.4648	0.5198	0.1676	0.1916	0.2134
24.0	0.1167	0.1333	0.1499	0.1557	0.1723	0.1889	0.0724	0.0840	0.0929

Table 14. PIPING LOAD SCALE (BETA) FACTORS
SCHELULE 40 STAINLESS STEEL

NOMINAL DIAM (IN)	BUTT WELD TEMPERATURE (F)			ELBOW TEMPERATURE (F)			STRAIGHT TEMPERATURE (F)		
	100	300	500	100	300	500	100	300	500
0.5	500.0000	580.0000	600.0000	550.0000	600.0000	650.0000	310.0000	365.4000	372.0000
0.7	335.5787	388.6421	409.2282	398.1056	438.9591	481.1994	208.0588	244.8445	253.7215
1.0	225.2261	260.4185	279.1128	288.1602	321.1418	356.2352	139.6402	164.0637	173.0499
2.0	45.7000	52.5000	60.4000	79.1000	92.0000	107.0000	28.3340	33.0750	37.4480
3.0	19.1207	21.9653	25.3030	31.4444	40.3534	46.8348	11.8548	13.8301	15.6879
4.0	8.0000	9.1900	10.6000	12.5000	17.7000	20.5000	4.9600	5.7897	6.5720
6.0	2.9500	3.4000	4.1100	4.9000	6.5000	8.2000	1.8290	2.1924	2.5482
8.0	1.5000	1.7800	2.0500	2.7200	4.3600	5.0400	0.9300	1.1214	1.2710
10.0	0.8400	0.9400	1.1600	1.6400	2.4700	3.0100	0.5208	0.5922	0.7192
12.0	0.5797	0.6576	0.8131	1.1667	1.7850	2.1669	0.3594	0.4143	0.5041
14.0	0.4000	0.4600	0.5700	0.8300	1.2900	1.5600	0.2480	0.2898	0.3534
16.0	0.2524	0.2951	0.3634	0.5062	0.7398	0.8818	0.1565	0.1859	0.2253
18.0	0.1592	0.1893	0.2316	0.3087	0.4242	0.4984	0.0987	0.1193	0.1436
20.0	0.1005	0.1215	0.1477	0.1882	0.2433	0.2817	0.0623	0.0765	0.0916
24.0	0.0400	0.0500	0.0600	0.0700	0.0800	0.0900	0.0248	0.0315	0.0372

Table 15. PIPING LOAD SCALE (BETA) FACTORS
SCHEDULE 60 STAINLESS STEEL

NOMINAL DIAM (IN)	BUTT WELD TEMPERATURE (F)			ELBOW TEMPERATURE (F)			STRAIGHT TEMPERATURE (F)		
	100	300	500	100	300	500	100	300	500
0.5	460.7692	567.9487	605.7692	554.4872	584.6154	644.2308	298.0769	357.8077	375.5769
0.7	304.2297	331.2099	385.2365	326.6594	356.6631	430.7325	188.6224	208.6622	238.8466
1.0	204.4447	207.8816	260.4926	210.7769	237.6961	307.2412	126.7557	130.9654	161.5054
2.0	37.2714	43.2550	48.9585	53.2896	60.9368	72.9814	23.1083	27.2506	30.3543
3.0	14.3407	16.7056	20.6251	19.7481	24.9428	31.1700	8.8912	10.5245	12.7876
4.0	6.1769	7.2506	8.6118	8.1859	10.9906	12.9786	3.8297	4.5679	5.3393
6.0	2.5747	2.9576	3.4058	3.4881	4.3101	5.1834	1.5963	1.8633	2.1116
8.0	1.3605	1.5123	1.6506	1.9824	2.6875	2.9839	0.8435	0.9527	1.0234
10.0	0.6960	0.7528	0.8552	1.0468	1.3901	1.6234	0.4315	0.4743	0.5302
12.0	0.4793	0.5224	0.5944	0.7446	0.9937	1.1541	0.2972	0.3291	0.3685
14.0	0.3318	0.3647	0.4167	0.5360	0.7218	0.8349	0.2057	0.2298	0.2584
16.0	0.2143	0.2375	0.2707	0.3339	0.4321	0.4942	0.1329	0.1496	0.1678
18.0	0.1331	0.1486	0.1689	0.2000	0.2486	0.2813	0.0825	0.0936	0.1047
20.0	0.0839	0.0943	0.1068	0.1208	0.1442	0.1612	0.0520	0.0594	0.0662
24.0	0.0330	0.0377	0.0423	0.0440	0.0487	0.0534	0.0205	0.0238	0.0262

DRAFT FOR COMMENT

Table 16. PIPING LOAD SCALE (BETA) FACTORS
SCHEDULE 80 STAINLESS STEEL

NOMINAL DIAM (IN)	BUTT WELD TEMPERATURE (F) 100	300	500	ELBOW TEMPERATURE (F) 100	300	500	STRAIGHT TEMPERATURE (F) 100	300	500
0.5	445.4286	527.3810	562.5000	514.8810	542.8571	598.2143	276.7857	332.2500	340.7500
0.7	286.3338	311.7270	362.5755	307.4441	335.6829	405.3953	177.5270	196.3880	224.7968
1.0	184.1272	187.2225	234.6051	189.8301	214.0741	276.7079	114.1589	117.9502	145.4552
2.0	32.9376	38.2254	43.2657	47.0931	53.8511	64.4952	20.4213	24.0820	26.0247
3.0	12.6044	14.6829	18.1279	17.3570	21.9228	27.3961	7.8147	9.2502	11.2393
4.0	5.6417	6.6223	7.8656	7.4766	10.0383	11.8540	3.4979	4.1720	4.8767
6.0	2.2947	2.6359	3.0354	3.1088	3.8414	4.6197	1.4227	1.6606	1.8819
8.0	1.1419	1.2693	1.3854	1.6638	2.2557	2.5044	0.7080	0.7997	0.8589
10.0	0.6027	0.6519	0.7405	0.9065	1.2038	1.4057	0.3737	0.4107	0.4591
12.0	0.4040	0.4403	0.5011	0.6277	0.8377	0.9729	0.2505	0.2774	0.3107
14.0	0.2713	0.2982	0.3407	0.4383	0.5902	0.6827	0.1682	0.1879	0.2112
16.0	0.1728	0.1915	0.2183	0.2693	0.3484	0.3985	0.1071	0.1206	0.1353
18.0	0.1099	0.1227	0.1395	0.1651	0.2053	0.2323	0.0681	0.0773	0.0865
20.0	0.0683	0.0768	0.0869	0.0984	0.1174	0.1313	0.0423	0.0484	0.0539
24.0	0.0270	0.0309	0.0347	0.0361	0.0399	0.0438	0.0167	0.0195	0.0215

Table 17. PIPING LOAD SCALE (BETA) FACTORS
SCHEDULE 120 STAINLESS STEEL

NOMINAL DIAM (IN)	BUTT WELD TEMPERATURE (F) 100	300	500	ELBOW TEMPERATURE (F) 100	300	500	STRAIGHT TEMPERATURE (F) 100	300	500
0.5	416.6667	492.2222	492.2222	480.5556	506.6667	558.3333	258.3334	310.1000	305.1778
0.7	250.9189	281.8808	281.8808	278.0080	303.5431	366.5600	160.5297	177.5849	174.7661
1.0	165.6116	168.3957	168.3957	170.7411	192.5471	248.0826	102.6792	106.0893	104.4053
2.0	26.4586	30.7063	30.7063	37.8297	43.2584	51.8088	16.4043	19.3450	19.0379
3.0	10.7282	12.4973	12.4973	14.7734	18.6595	23.3180	6.6515	7.8733	7.7483
4.0	4.6506	5.4590	5.4590	6.1631	8.2748	9.7715	2.8834	3.4392	3.3846
6.0	1.8734	2.1520	2.1520	2.5381	3.1362	3.7716	1.1615	1.3558	1.3342
8.0	0.8589	0.9547	0.9547	1.2514	1.6966	1.8837	0.5325	0.6015	0.5919
10.0	0.4548	0.4919	0.4919	0.6840	0.9083	1.0607	0.2820	0.3099	0.3050
12.0	0.2989	0.3258	0.3258	0.4644	0.6197	0.7198	0.1853	0.2053	0.2020
14.0	0.2006	0.2205	0.2205	0.3241	0.4364	0.5048	0.1244	0.1389	0.1367
16.0	0.1285	0.1424	0.1424	0.2002	0.2590	0.2963	0.0797	0.0897	0.0883
18.0	0.0807	0.0901	0.0901	0.1212	0.1507	0.1706	0.0500	0.0568	0.0559
20.0	0.0504	0.0567	0.0567	0.0726	0.0867	0.0969	0.0312	0.0357	0.0352
24.0	0.0196	0.0224	0.0224	0.0262	0.0290	0.0318	0.0122	0.0141	0.0139

Table 18. PIPING LOAD SCALE (BETA) FACTORS
SCHEDULE 160 STAINLESS STEEL

NOMINAL DIAM (IN)	BUTT WELD TEMPERATURE (F) 100	300	500	ELBOW TEMPERATURE (F) 100	300	500	STRAIGHT TEMPERATURE (F) 100	300	500
0.5	400.0000	480.0000	525.0000	480.0000	492.0000	550.0000	248.0000	302.4000	325.5000
0.7	248.5066	254.0000	325.8264	240.0000	259.0000	347.5204	154.0741	160.0200	202.0124
1.0	154.3889	135.0000	202.2150	120.0000	138.0000	219.5825	95.7211	85.0500	125.3733
2.0	23.0000	27.0000	30.0000	25.0000	27.7000	35.0000	14.2600	17.0100	18.6000
3.0	8.1000	9.6200	12.9615	8.1000	9.8500	14.4551	5.0220	6.0606	8.0361
4.0	3.8000	4.5700	5.6000	4.0000	4.8700	5.9700	2.3560	2.8791	3.4720
6.0	1.7436	1.9593	2.2073	1.9310	2.1735	2.4311	1.0810	1.2344	1.3665
8.0	0.8000	0.8400	0.8700	0.9322	0.9700	0.9900	0.4960	0.5292	0.5394
10.0	0.4000	0.4200	0.4400	0.4500	0.4800	0.5100	0.2480	0.2646	0.2728
12.0	0.2683	0.2825	0.2966	0.3146	0.3323	0.3499	0.1663	0.1780	0.1839
14.0	0.1800	0.1900	0.2000	0.2200	0.2300	0.2400	0.1116	0.1197	0.1240
16.0	0.1136	0.1199	0.1262	0.1333	0.1397	0.1460	0.0704	0.0755	0.0782
18.0	0.0717	0.0756	0.0796	0.0808	0.0840	0.0888	0.0445	0.0476	0.0494
20.0	0.0452	0.0477	0.0502	0.0490	0.0515	0.0540	0.0280	0.0301	0.0311
24.0	0.0180	0.0190	0.0200	0.0180	0.0190	0.0200	0.0112	0.0120	0.0124

DRAFT FOR COMMENT

C6. STRUCTURAL FRAGILITIES

The evaluation of the potential seismic failure modes of a system as complex as those at the SONGS Unit 1 involves consideration of a great many items such as strengths and building response characteristics. In most cases, values of many of the parameters affecting structural seismic capacity levels are not known exactly and substantial dispersion may exist. This dispersion can result from sources of inherent randomness and from uncertainty concerning the values of the sources. Randomness is considered to represent those sources of dispersion which cannot be reduced by additional analysis or more data. Uncertainty can be considered to be the result of lack of knowledge of such parameters as material properties, as well as approximations in analytical modeling.

Structural fragilities are defined by estimated median seismic capacities and their variabilities due to randomness and uncertainty. The median capacities and variabilities account for structural strength and inelastic energy absorption capabilities. Estimation of these quantities is dependent to a significant degree of engineering judgement as well as available test data. To determine the earthquake level at which structural failure occurs, structural capacity is compared to estimates of seismic response which account for damping, modal combination, earthquake directional components, and soil-structue interaction. Structural strength and ductility are assumed to be lognormally distributed since this distribution seems to provide a good representation of the sources of structural variability. The lognormal distribution is also mathematically convenient for definging fragility curves.

SONGS-1 structures included in the fragilities evaluation are: reactor building, containment sphere, sphere enclosure building, control-administration building, diesel generator building, turbine-generator pedestal, north turbine extension, west feedwater heater platform, and the fuel storage building. Structural failure is defined as occurring when inelastic seismic structural deformations are of sufficient magnitude to potentially interfere with the operability of attached equipment. These deformation limits correspond to the onset of significant structural damage. Potential failure modes were identified for each of the SONGS-1 structures included in this study by establishing the seismic load-paths and comparing expected load distributions to available capacities for the elements of each load-path. Particular attention was given to possible weak links and details. The more likely failure modes were screened for more detailed investigation.

Determination of median capacities for fragility curve formulation is dependent on estimates of structural response due to seismic excitation. Final results from the SONGS-1 structure model analyses were not yet available at the time the project was stopped. These analytical results were to provide the correlation between earthquake input and structural failure. Median structure strengths and variabilities for the identified failure modes were only partially completed at the time the project was stopped. These median strengths account for median material properties estimated from actual plant-specific test data where available or by comparison to other data bases. Predictive models derived from actual test data were used whenever possible to estimate median element strengths. These models eliminate design conservatism normally associated with building code requirements. Reference 28 provides more details.

DRAFT FOR COMMENT

REFERENCES

1. L. C. Shieh, T. Y. Chuang, and W. J. O'Connell, Seismic Safety Margins Research Program, Phase I Final Report--Subsystem Response (Project V), Lawrence Livermore National Laboratory report UCRL-53021, Vol. 6., NUREG/CR-2015, Vol. 6., Livermore, CA (July 1981).

2. D. B. Slemmons, P. Omalley, R. A. Whitney, D. H. Chung, and D. L. Bernreuter, Assessment of Active Faults for Maximum Credible Earthquakes of the Southern California - Northern Baja Region, Lawrence Livermore National Report UCID-19125, Livermore, CA (1982).

3. Woodward-Clyde Consultants, "Report of the Evaluation of Maximum Earthquake and Site Ground Motion Parameters Associated with the Offshore Zone of Deformation, San Onofre Nuclear Generating Station," as amended in response to U.S. NRC Question 361.55 (June 1979).

4. Abbott and Elliott, editors, Earthquakes and Other Perils of the San Diego Region (1979).

5. Crowell and Sylvester, editors, Tectonics of the Juncture between the San Andreas Fault System and the Salton Trough, Southeastern California, (1979).

6. Anderson, J. G., "Estimating the Seismicity from Geological Structure for Seismic-Risk Studies," Seismological Society of America Bulletin, b. 69, p. 135-158 (1979).

7. Atwater, Tanya, "Implications of Plate Tectonics for the Cenozoic Tectonic Evolution of Western North America," Geological Society of America Bulletin, v. 81, p. 3513-3536 (1970).

DRAFT FOR COMMENT

8. Jennings, C. W., "Fault Map of California with Locations of Volcanoes Thermal Springs, and Thermal Wells," California Division of Mines and Geology Data Map Series Map No. 1, scale 1:750,000 (1975).

9. Legg, M. R., and Kennedy, M. P., "Faulting Offshore San Diego and Northern Baja California," in Earthquakes and Other Perils of the San Diego Region, Abbott, P. L., and Elliot, W. J., eds., San Diego Association of Geologists for the Geological Society of America, Field Trip Guidebook, p. 29-46, (1979).

10. Green, H. G., Bailey, K. A., Clarke, S. H., Ziony, J. I., and Kennedy, R. P., "Faulting Offshore San Diego and Northern Baja California," in Earthquakes and Other Perils of the San Diego Region, Abbott, P. L., and Elliot, W. J., eds., San Diego Association of Geologists for the Geological Society of America, Field Trip Guidebook, p. 21-28 (1979).

11. Gastile, R. G., Phillips, R. P., and Allison, E. C., "Reconnaissance Geology of the State of Baja California," Geological Society of America Memoir 140, p. 170 with maps (1975).

12. Gastile, R. G., Kies, R., and Melius, D. J., "Active and Potentially Active Faults, San Diego County and Northwesternmost Baja California," in Earthquakes and Other Perils of the San Diego Region, Abbott, P. L., and Elliott, W. J., eds., San Diego Association of Geologists for the Geological Society of America, Field Trip Guidebook, p. 47-60 (1979).

13. Liu, H. L., and Kanamori, H., "Determination of Source Parameters of Mid-Plate Earthquakes from the Waveforms of Body Waves," Seismological Society of America Bulletin, v. 70, p. 1989-2004 (1980).

14. Southern California Edison Company, "Response to US NRC Questions 361.37 through 361.68: San Onofre Nuclear Generating Station Units 2 and 3," (1980).

DRAFT FOR COMMENT

15. U.S. Nuclear Regulatory Commission, Safety Evaluation Report for San Onofre, NUREG-07-12 (1980).

16. Sieh, K. E., "Slip along the San Andreas Fault Associated with the Great 1857 Earthquake," Seismological Society of America Bulletin, v. 68, p. 1421-1448 (1978).

17. D. B. Slemmons and D. H. Chung, Maximum Credible Earthquake Magnitudes for the Calaveras and Hayward Fault Zones, California, Lawrence Livermore National Laboratory Report UCRL-86219 (1982), to be published in Earthquake Hazards in the East Bay Area (in press).

18. Joyner, W. B., Boore, D. M., Procella, R. L., (1981), Peak Horizontal Acceleration and Velocity from Strong-Motion Records Including Records from the 1979 Imperial Valley, California Earthquake. USGS Open-file Report 81-365, March 1981.

19. Joyner, W. B. and Boore, D. M. (1981), Peak Horizontal Acceleration and Velocity from Strong Motion Records Including Records from the 1979 Imperial Valley, California, Earthquake, BSSA 71, pp. 2011-2018.

20. Hudson, Strong Motion Earthquakes, Vol. I, CIT.

21. Porter, L. D. (1978). Compliation of strong-motion records recovered from the Santa Barbara earthquake of August 13, 1978, California Div. Mines and Geol. Prelim. Report 22, p. 43.

22. Procella, R. L., ed. (1979). Seismic Engineering Program Report, U.S. Geol. Surv. Circular 818-A, p. 20.

23. Procella, R. L., Matthiesen, R. B., McJunkin, R. D., and Ragsdale, J. T., (1979). Compilation of strong motion records from the August 6, 1979 Coyote Lake earthquake, U.S. Geol. Surv. Open-File Report 79-385, p. 71.

24. Brady, A. G., Mork, P. N., Perez, V., and Porter, L. D., (1980). Processed data from the Gilroy array and Coyote Creek records, Coyote Lake, California earthquake August 6, 1979, U.S. Geol. Surv. Open-File Report 81-42, p. 171

25. Boore, D. M., and Procella, R. L., (1981). Peak horizontal ground motions from the 1979 Imperial Valley earthquake: comparison with data from previous earthquakes, in The Imperial Valley, California earthquake of October 15, 1979, U.S. Geol. Surv. Prof. Paper, in press.

26. Campbell, K. W., (1981). Near-source attenuation of peak horizontal acceleration, Bull. Seism. Soc. Am., v. 71, pp. 2039-2070.

27. Askins, R. C. and Cornell, A. C., (1979). SHA-based Attenuation Model Parameter Estimation Proceedings, US National Eathquake Engineering Conference, Stanford, CA, August 1979.

28. D. A. Wesley and P. S. Hashimoto, Seismic Structural Fragility Investigation for the San Onofre Nuclear Generating Station, Unit 1, Seismic Safety Margins Research Program, Livermore, CA, UCRL-in print, (1982)